ISSN 1881-7815 Online ISSN 1881-7823

BST BioScience Trends

Volume 13, Number 2
April, 2019

IRCA BSSA

IACMHR

www.biosciencetrends.com

BST
BioScience Trends

ISSN: 1881-7815
Online ISSN: 1881-7823
CODEN: BTIRCZ
Issues/Year: 6
Language: English
Publisher: IACMHR Co., Ltd.

BioScience Trends is one of a series of peer-reviewed journals of the International Research and Cooperation Association for Bio & Socio-Sciences Advancement (IRCA-BSSA) Group and is published bimonthly by the International Advancement Center for Medicine & Health Research Co., Ltd. (IACMHR Co., Ltd.) and supported by the IRCA-BSSA and Shandong University China-Japan Cooperation Center for Drug Discovery & Screening (SDU-DDSC).

BioScience Trends devotes to publishing the latest and most exciting advances in scientific research. Articles cover fields of life science such as biochemistry, molecular biology, clinical research, public health, medical care system, and social science in order to encourage cooperation and exchange among scientists and clinical researchers.

BioScience Trends publishes Original Articles, Brief Reports, Reviews, Policy Forum articles, Case Reports, News, and Letters on all aspects of the field of life science. All contributions should seek to promote international collaboration.

Editorial Board

Editorial Office

Pearl City Koishikawa 603,
2-4-5 Kasuga, Bunkyo-ku, Tokyo 112-0003, Japan
Tel: +81-3-5840-8764 Fax: +81-3-5840-8765
E-mail: office@biosciencetrends.com

BioScience Trends

Editorial and Head Office

Pearl City Koishikawa 603, 2-4-5 Kasuga, Bunkyo-ku,
Tokyo 112-0003, Japan

Tel: +81-3-5840-8764, Fax: +81-3-5840-8765
E-mail: office@biosciencetrends.com
URL: www.biosciencetrends.com

Editorial Board Members

Policy Forum

110 - 116 **Driving factors and mode transformation regarding health technology assessment (HTA) in China: Problems and recommendations.**
Haiyin Wang, Chunlin Jin, Fei Bai, Xia Lin, Liang Fang, Hui Sun, Wendi Cheng, Peipei Song

Review

117 - 129 **Chinese herbal medicine for acute upper respiratory tract infections and reproductive safety: A systematic review.**
Zengshu Huang, Xinyao Pan, Jing Zhou, Wing Ting Leung, Chuyu Li, Ling Wang

Original Article

130 - 135 **IPS-1 polymorphisms in regulating interferon response in HBV infection.**
Kehui Liu, Liwen Chen, Gangde Zhao, Zhujun Cao, Fengdi Li, Lanyi Lin, Chuanwu Zhu, Qing Xie, Yumin Xu, Shisan Bao, Hui Wang

136 - 144 **A Clinical scoring model to predict mortality in HIV/TB coinfected patients at end stage of AIDS in China: An observational cohort study.**
Zhe Zhang, Ling Xu, Xiaoli Pang, Yongqin Zeng, Yiwei Hao, Yu Wang, Liang Wu, Guiju Gao, Di Yang, Hongxin Zhao, Jiang Xiao

145 - 151 **Methanol extract of *Lonicera caerulea* var. *emphyllocalyx* fruit has antibacterial and anti-biofilm activity against *Streptococcus pyogenes in vitro*.**
Masaaki Minami, Hiroshi Takase, Mineo Nakamura, Toshiaki Makino

152 - 159 **Sperm DNA fragmentation valued by SCSA and its correlation with conventional sperm parameters in male partner of recurrent spontaneous abortion couple.**
Minmin Yuan, Liqing Huang, Wing Ting Leung, Mingyan Wang, Yi Meng, Zengshu Huang, Xinyao Pan, Jing Zhou, Chuyu Li, Yizhen Sima, Lan Wang, Yanzhi Zhang, Chunmei Ying, Ling Wang

160 - 167 **Daucosterol induces autophagic-dependent apoptosis in prostate cancer *via* JNK activation.**
Ping Gao, Xiaopeng Huang, Tingting Liao, Guangsen Li, Xujun Yu, Yaodong You, Yuxing Huang

168 - 175 **Predictive value of some pro-oxidants in type 2 diabetes mellitus with vascular complications.**
Petia Goycheva, Galina Nikolova, Mariana Ivanova, Todor Kundurdzhiev, Veselina Gadjeva

176 - 181 **Preoperative albumin-bilirubin grade combined with aspartate aminotransferase-to-platelet count ratio index predict outcomes of patients with hepatocellular carcinoma within Milan criteria after liver resection.**
Hongmei Luo, Chuan Li, Liping Chen

182 - 188 **Treatment modalities and relative survival in patients with brain metastasis from colorectal cancer.**
Xingang Lu, Yibo Cai, Liang Xia, Haixing Ju, Xin Zhao

189 - 196 **A selective oral vasopressin V2-receptor antagonist for patients with end-stage liver disease awaiting liver transplantation: a preliminary study.**
Sho Kiritani, Junichi Kaneko, Yoichi Miyata, Masaru Matsumura, Nobuhisa Akamatsu, Takeaki Ishizawa, Junichi Arita, Sumihito Tamura, Norihiro Kokudo, Kiyoshi Hasegawa

Brief Report

197 - 203 **Design, synthesis and biological evaluation of 4-piperidin-4-yltriazole derivatives as novel histone deacetylase inhibitors.**
He Miao, Jianjun Gao, Zishuo Mou, Baolei Wang, Li Zhang, Li Su, Yantao Han, Yepeng Luan

204 - 211 **Circular RNA profiling reveals circRNA1656 as a novel biomarker in high grade serous ovarian cancer.**
Yan Gao, Chuanqi Zhang, Yisi Liu, Min Wang

212 - 215 **Living donor liver transplantation for a patient with a history of total gastrectomy.**
Keita Shimata, Tomoaki Irie, Masashi Kadohisa, Seiichi Kawabata, Sho Ibuki, Yasuko Narita, Hidekazu Yamamoto, Yasuhiko Sugawara, Taizo Hibi

Guide for Authors

Copyright

Policy Forum

DOI: 10.5582/bst.2019.01100

Driving factors and mode transformation regarding health technology assessment (HTA) in China: Problems and recommendations

Haiyin Wang[1,§], Chunlin Jin[1,§], Fei Bai[2], Xia Lin[2], Liang Fang[1], Hui Sun[1], Wendi Cheng[1], Peipei Song[1,3,*]

[1] *Shanghai Health Development Research Center (Shanghai Medical Information Center), Shanghai, China;*
[2] *Medical Administration Center of National Health Commission, Beijing, China;*
[3] *National Center for Global Health and Medicine, Tokyo, Japan.*

Summary **As the reform of Chinese medical and health undertakings has advanced (since 2015), the admission, pricing and payment policies regarding the new health technologies of China have undergone significant changes, and health technology assessment (HTA) has gradually become one of the current reform and research hotspots in China. Based on the perspective of HTA driving factors and the development mode, this paper proposes a two-stage mode of HTA development in China, namely, the mode driven by the management of new heath technology admission and another one driven by new health technology pricing and medical insurance payment. In addition, the paper also proposes the challenges that HTA faces in China under the current mode, including the development system, process standard, data mechanism, and policy application. Besides, recommendations are provided for the further development of HTA construction in China, including strengthening the development system of regional HTA centers, formulating HTA process guidance, building a database, improving evaluation quality and intensifying policy integration.**

Keywords: Health technology assessment, China, driving factors, development mode, issues, recommendations

1. Introduction

Health technology assessment (HTA) is a comprehensive policy research method for systematically evaluating the characteristics, effects and impacts of health technologies. HTA's main goal is to support decision making regarding health technology management (*1*). After more than 40 years of development, health technology assessment has been widely adopted by countries around the world, especially in most middle- and high-income countries where formal HTA procedures have been established. The application areas of HTA include fundraising and planning, pricing and payment, clinical guidelines, and service quality (*2,3*). In recent years, HTA has been widely developed and applied in Thailand, South Korea, Vietnam, and Chinese Taipei in Asia (*4*). HTA has also played an important role in the allocation and management of health technology resources.

China introduced HTA in the 1990s under the support of key decision makers from the Chinese Ministry of Health followed by the development and application in Chinese academic and research institutions (*5*). However, overall, HTA in China is still in slow development and has not been incorporated into policy procedures, with only a small number of studies being translated into policy decisions (*6*), which lags far behind European and neighboring countries and regions. The main problems faced by HTA in China include a lack of legal support, national HTA centers, relevant process mechanisms, discipline talents and funding inputs (*7*). Since 2015, with the advancement of China's medical insurance payment methods and the reform of the compensation mechanism of public hospitals (*8,9*). HTA has been applied for the first time in such fields as price negotiation regarding high-priced

Released online in J-STAGE as advance publication April 20, 2019.

[§]These authors contributed equally to this work.

**Address correspondence to:*
Dr. Peipei Song, Shanghai Health Development Research Center (Shanghai Medical Information Center), 1477 Beijing Road (west), Shanghai, China.
E-mail: songpeipei@shdrc.org

drugs in China, centralized procurement of high-value consumables and evaluation of new technologies, which has enabled HTA in China to enter a new development stage.

New health technologies refer to new technologies that have entered the market while not yet entering the pricing directory and reimbursement payments and include drugs, equipment and surgical plans. Access, payment and pricing of new health technologies are all important application areas of HTA. In recent years, China has undergone significant changes in the admission, payment and pricing management modes of new health technologies, such as accelerating the admission and adjustment of the directory of new health technologies, liberalizing the price control over some new health technologies and empowering public hospitals to take charge of the admission of new health technologies. These policy changes are highly consistent with the development of HTA in China in recent years, which suggests that the admission, payment and pricing of China's medical technologies may be the key driving factors for the development of HTA in China.

With the admission, payment and pricing management policies regarding new health technologies as the entry point, this paper analyzes the key elements driving the development of HTA and their respective development characteristics before and after the changes of such policies. This paper also summarizes the development rules and modes of HTA in China and the current development of HTA in China and proposes corresponding reform suggestions in the hope of providing empirical support for the development of HTA in China and other Asian countries and regions.

2. Driving factors and development modes of HTA in China

Since 2015, the strategy for admission of new health technologies to public hospitals in China has transformed from admission granted by the government and based on grades and categories (Grade-I technologies are subject to the management of hospitals themselves, and Grade-II and Grade-III are subject to provincial and national examination and approval, respectively; the grading of technologies is mainly based on such issues as difficulty, risks and ethics) to "instant admission without forbiddance" (public hospitals can independently determine the admission of new health technologies beyond the restriction list formulated by the central government) (*10*). In addition, the management subject of new health technologies has also transformed from the government to public hospitals. Furthermore, the pricing of new health technologies in China has also been gradually liberalized. In 2015, the Chinese government canceled pricing on a majority of drugs, and new medical service projects also adopted a strategy "integrating adjustment and liberalization" (adjustment of medical service prices and liberalization of the pricing on certain medical service prices) (*11,12*). For example, the prices of new medical services in such areas as Beijing and Guangzhou were independently formulated by the hospitals in those cities. At the same time, the medical insurance payment mode in China was also gradually transformed from payment by items to payment by diseases (*13*).

From the perspective of driving factors, driving forces and content characteristics of HTA in China, the development of HTA in China can be divided into two stages based on the driving factors. The first stage is the period from 1993 to 2015, during which the main driving factor was the management of the admission of clinical new health technologies; the main driving force was the Ministry of Health of the People's Republic of China. The second stage is the period from 2015 to the present, during which the main driving factors are the adjustment of the directory of medical insurance drugs and the negotiation-based pricing on drugs and high-value consumables; the main driving departments are the China Human Resources Security Bureau and the China Development and Reform Commission (adjusted as the China Medical Insurance Bureau subjected to 2018 institutional reform).

2.1. *Mode driven by the management of admission of new health technologies*

The main driving force for the development of HTA at this stage is the management of health technology admission, during which the Ministry of Health of the People's Republic of China, according to the *Measures for Management and Application of Clinical New Technologies* issued in 2009, assumed responsibility for the evaluation on Grade-III technologies, which mainly involve such contents as safety, effectiveness, risks and ethical social impacts. At the same time, the management of admission configuration was also adopted for large-scale equipment, and the Ministry of Health of China conducted HTA for Grade-A equipment, which was mainly involved in economic evaluation and effect evaluation. Therefore, at this stage, the Department of Science and Education and other departments of the Ministry of Health of the People's Republic of China actively promoted the pilot project and selected key technologies and equipment for technology assessment every year. These cover such new medical technologies as assisted reproductive technology, newborn screening and cervical cancer screening and such large-scale equipment such as gamma knife, MRI and Leonardo's robot (*14*).

Under this mode, HTA mainly focuses on the safety, effectiveness, and feasibility of new medical technologies and the qualification of relevant

institutions. In addition, most research focuses on the concept of HTA and relevant domestic and international development experience. A system evaluation is the main method that was adopted with cost-effectiveness and other health economic evaluation methods being less frequently used (*15*). In April 2011, the *Guideline for Pharmacoeconomics Evaluation in China* was issued and showed a basic failure in incorporating pharmacoeconomic research into the decision-making scope of the government for applications not being compulsorily required by the state or recommended by the government (*16*).

Under this mode, HTA research institutions are mainly colleges and universities with only a few governmental HTA centers. For example, 4 national HTA institutions were established in the 1990s, and another 5 were established by 2015, of which only 3 belonged to the government (*17*) (Table 1).

2.2. *Mode driven by new health technology pricing and medical insurance payment*

At this stage, the main driving forces for the development of HTA are medical insurance payments and negotiation-based pricing. During this time, the government liberalized the pricing of medicines and the admission of medical technologies and the Ministry of Human Resources and Social Security and the National Health Commission of the People's Republic of China explored the adjustment on the directory of medical insurance medicines and introduced HTA evidence in pricing negotiation regarding costly medicines and high-value consumables (Table 2). Meanwhile, the implementation of HTA in the procurement of consumables for medical devices is also under exploration in hospitals (*18*).

At this stage, HTA focuses on the cost-effectiveness, budget influence and payment standard of medical technologies. For example, during the initial negotiation on the pricing of 44 medicines implemented in 2017, the Ministry of Human Resources and Social Security of the People's Republic of China based on the extensive collection of information with regard to such aspects as the efficacy, prices, economy and medical insurance payments of negotiating medicines and referencing ones, established two assessment expert panels for an assessment measurement perspective of two aspects, namely, the economy of medicines and the affordability of medical insurance funds. Based on the assessment results of the two expert panels, the working group finally determined the expected medical insurance payment standard according to established principles (*19*) (Figure 1).

At this stage, HTA institutions and networks acquire a further development. For example, in 2016, the China Health Policy and Technology Assessment Research

Table 1. HTA institutions under the new medical technology admission management mode

Year	Place	Name
1993	Beijing	China Medicinal Biotechnology Association.
1994	Shanghai	Key HTC Laboratory of the Department of Health in Fudan University.
1994	Beijing	Assessment and Transformation Research Office of the Health Economics Institute of the Ministry of Health of the People's Republic of China.
1999	Chengdu	Chinese Cochrane Center (West China University of Medical Sciences).
2002	Shanghai	Pharmacoeconomics Evaluation and Research Center of Fudan University.
2004	Shanghai	EBM (evidence-based medicine) Center of Fudan University.
2005	Lanzhou	EBM Center of Lanzhou University.
2007	Beijing	Health Policy and Technology Assessment Research Office of National Health Development Research Center of China.
2011	Shanghai	Shanghai HTA Research Center.

HTA, health technology assessment.

Table 2. HTA applications in China since 2015

Year	Published by	Policy practices	HTA applications
2017	Ministry of Human Resources and Social Security of the People's Republic of China.	Adjustment on the directory of medical insurance medicines in 2017.	Compare similar medicines following the principle of pharmacoeconomics and preferentially select medicines whose clinical necessity, safety and effectiveness as well as reasonable pricing are fully proved.
2017	Ministry of Human Resources and Social Security of the People's Republic of China.	Negotiation on the pricing of 44 original medicines.	HTA was determined as optional submission material for the first time.
2017	National Health Commission of the People's Republic of China.	Negotiation on the pricing of 4 high-value consumables.	Submit HTA evaluation materials.
2018	National Medical Insurance Administration.	Negotiation on the pricing of 17 anti-cancer medicines to be incorporated in the scope of medical insurance.	HTA was determined as optional submission material.

HTA, health technology assessment.

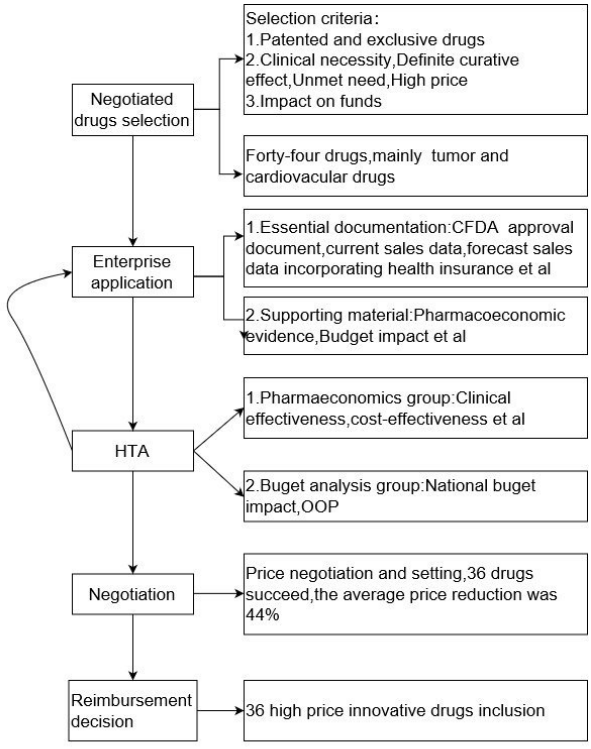

Figure 1. Negotiations on the pricing of 44 medicines by the Ministry of Human Resources and Social Security of the People's Republic of China in 2017.

Network was established under the guidance of the Health Development Research Center of the National Health of Family Planning Commission of the People's Republic of China. In total, 37 relevant institutions applied to join; in 2017, the HTA research center was established in Hubei Province and Peking University; in 2018, the National Integrated Assessment Center on Medicines and Health Technologies was established under the approval of the National Health Commission of the People's Republic of China, which marked the formal establishment of the state-level HTA center in China (*20*) (Table 3).

At this stage, HTA was also gradually clarified in policy and legal documents. In 2016, the five ministries and commissions (including the National Health and Family Planning Commission and the Ministry of Science and Technology) jointly issued the *Guiding Opinions on Comprehensively Promoting Health-related Science and Technology Innovations* and the *Guiding Opinions on Strengthening the Transfer and Transformation of Health-related Science and Technology Achievements*. It was stated that "we should establish an HTA system, formulate the opinions on the implementation of HTA, develop evidence-based medicine, and strengthen health technology assessment" (*21*). The Basic Law of Medical Health, which was drawn up in 2017, has HTA incorporated into the scope of the draft legislation. In the *Guiding Opinions on the Reform and Improvement of the Comprehensive*

Table 3. Establishment of HTA institutions in China since 2016

Year	Place	Name
2016	Beijing	China Health Policy and Technology Assessment Research Network.
2017	Wuhan	Hubei HTA Research Center.
2017	Chengdu	IDEAL China Center.
2017	Beijing	Health Policy and Technology Assessment Center in Peking University Health Science Center.
2018	Beijing	National Integrated Assessment Center on Medicines and Health Technologies.

HTA, health technology assessment.

Supervision System of the Medical and Health Industry promulgated by the State Council in 2018, it is proposed that full play be given to the decision-making support role of HTA in clinical admission, standardized application, disuse and elimination of medical technologies, drugs and medical devices (*22*). The reform plan of the National Medical Security Administration newly established in 2018 proposes to carry out and organize the economic evaluation on health. In addition, the guidance opinions on promoting the HTA work organized by the Department of Science and Education of the National Health of the People's Republic of China, is under formulation and involves establishing and perfecting the HTA organization and team, establishing a topic selection mechanism and assessment process, methodology and evaluation results as a releasing mechanism for HTA, and promoting the transformation and application of HTA achievements.

3. Problems remaining from the development of HTA in China and corresponding development recommendations

The key driving factors of HTA in China have transformed from admission management to payment and pricing of health technologies followed by the gradual transformation of HTA research to decision-making applications; from safety and effectiveness to cost-effectiveness and budget impact analysis and from the institutional individual development to national system construction, the development characteristics of HTA in China have undergone great changes. Although HTA in China has made progresses in many aspects since 2015, it still faces some key problems and challenges that have not been solved to date (Figure 2).

3.1. *Under unbalanced development, HTA in China is in urgent need of system construction*

The provinces, municipalities directly under the central government and autonomous regions in China are responsible for setting the prices of medical services and the formulation of a medical insurance directory. However, the development of HTA in different regions

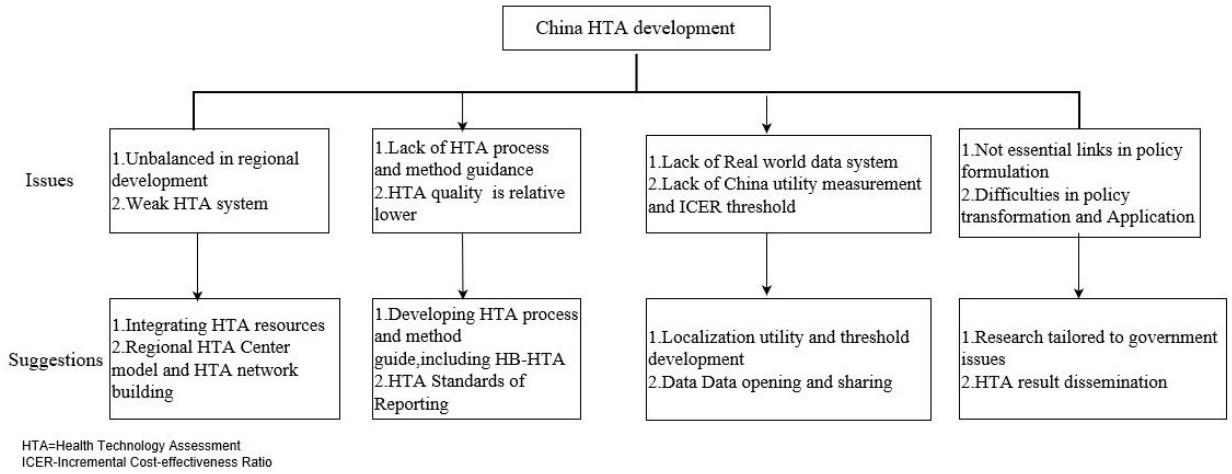

Figure 2. Problems existing in the development of HTA in China and corresponding countermeasures.

is significantly unbalanced. Existing HTA institutions are mainly concentrated in economically developed regions, and there is a large gap between central and western regions in the development and application of HTA concepts (*23*). HTA at the hospital level is mainly implemented in such developed regions as Shanghai and Beijing and is still in the preliminary exploration stage (*24-26*). Therefore, it is not mature to construct a national, provincial and hospital HTA system in the short term. At the current stage, it is suggested to fully integrate existing resources, such as enterprises, public hospitals, research institutions and universities, to guide all parties in understanding and applying HTA and form a good HTA development environment. Thus, a national HTA development system based on regional HTA centers should be gradually established to form a development system featured by the linkage of HTA in national centers, regional centers and hospitals and the sharing of resources among all stakeholders, including medical security bureaus and health commissions.

3.2. *Imperfect HTA application mechanism entails the development of Chinese HTA processes and methods*

Currently, the imperfection of the HTA application mechanism is mainly reflected in the lack of norms for HTA evidence submission in price negotiation and medical insurance payments (*27*), such as a lack of clear definitions and evaluation standards for HTA data submitted by enterprises. The state has not promulgated HTA processes and norms for reference in China, and there are few domestic studies on this aspect (*28*). Existing HTA centers in China are less experienced in the establishment of process systems and expert evaluation mechanisms for topic selection, assessment and evaluation, and the research quality of the evaluation of health economics is relatively low (*29*). It is suggested that China accelerated the construction of the HTA evaluation process and method guidelines, including two dimensions, namely, hospital HTA to form a referable practice mode, improve the transparency and objectivity of HTA, and ensure the quality of HTA research.

3.3. *Lack of an HTA data support system entails strengthening the construction of data collection and sharing mechanisms for HTA in China*

Presently, it is difficult to obtain and share real world data between public hospitals in China (*30*). Research on the life quality of people suffering diseases in China, especially the health utility values of various disease states, are currently an urgent need. Localized utility measurement tools and transformation need to be developed, and there are few studies on the threshold setting based on different populations in different regions of China (*31*). Improvement of the localization of life quality tools and utility transformation tools in China strengthening the construction of data opening and the sharing mechanism in different regions and public hospitals, building an HTA sharing database, and forming a timely and high-quality data guarantee system is recommended.

3.4. *Lack of HTA research and decision-making practice transformation channels entails the enhancement of policy integration*

HTA research in China has not become a necessary part of policy making to date; for example, it is still uncommon to see the application of HTA in decision making regarding medicines and other health technologies (*32*). The policy transformation capability of HTA research is relatively weak with only 30-40% of HTA research published in journal articles and submitted to relevant policy makers, and the government also has limited access to HTA evidence (*33*). Reliance on national and provincial HTA platforms to strengthen topic selection, focus on the key demands of price and

payment, conduct HTA based on problem-oriented entrustment, improve decision-making transformation and application and implementation of monitoring and assessment is recommended.

4. Conclusion

The driving factors for the development of HTA in China have undergone important changes, which makes the dominant development mode of HTA in China transform from technology admission to medical insurance payment and pricing. The transformation of admission, payment and pricing policies regarding new health technologies is an important driving factor for HTA reform in China. HTA in China is moving toward policy application under many challenges, such as the HTA development system, HTA process and methodology, data and standard development, and policy transformation channel, which are all core issues in the development solution for HTA in China. On the basis of China's practical environment, HTA in China needs to establish an integrated development strategy, collect resources from public hospitals, enterprises, universities and research institutions, and establish a decision-making mechanism and environment based on HTA and thus promote and develop HTA in China.

Acknowledgements

This study was supported by the "Fourth Round of Shanghai Three-year Action Plan on Public Health Discipline and Talent Program: Evidence-based Public Health and Health Economics" (No. 15GWZK0901).

References

1. International Network of Agencies for Health Technology Assessment. Resources for health technology assessment. *http://www.inahta.org/wp-content/themes/inahta/img/AboutHTA_Resources_for_HTA.pdf* (accessed January 2, 2019).
2. World Health Organization. 2015 report of global survey on health technology assessment by national authorities. *http://www.who.int/health-technology-assessment/en/* (accessed January 3, 2019).
3. Minamikawa K, Okumura A, Kokudo N, Kono K. Regulation on introducing process of the highly difficult new medical technologies: A survey on the current status of practice guidelines in Japan and overseas. BioSci Trends. 2018; 12:560-568.
4. Kennedy-Martin T, Mitchell BD, Boye KS, Chen W, Curtis BH, Flynn JA, Ikeda S, Liu L, Tarn YH, Yang BM, Papadimitropoulos E. The health technology assessment environment in mainland China, Japan, South Korea, and Taiwan—implications for the evaluation of diabetes mellitus therapies. Value Health Reg Issues. 2014; 3:108-116.
5. Chen Y, Banta D, Tang Z. Health technology assessment development in China. Int J Technol Assess Health Care. 2009; 25 Suppl 1:202-209.
6. Liu W, Shi L, Pong RW, Dong H, Mao Y, Tang M, Chen Y. Determinants of knowledge translation from health technology assessment to policy-making in China: From the perspective of researchers. PLoS One. 2018; 13:e0190732.
7. Wang HY, He D, Wang XJ, Feng ZY, Chen MX, Yang XJ, Jin CL. Progress and recommendations for international and domestic application of health technology assessment. Chinese Journal of Health Policy. 2014; 7:19-23. (in Chinese)
8. Dou GS, Wang Q, Ying XH. Reducing the medical economic burden of health insurance in China: Achievements and challenges. BioSci Trends. 2018; 12:215-219.
9. Zhao CR, Wang C, Shen CW, Wang Q. China's achievements and challenges in improving health insurance coverage. Drug Discov Ther. 2018; 12:1-6.
10. National Health Committee of the People's Republic of China. Management of clinical application of medical technology. *http://www.nhc.gov.cn/fzs/s3577/201809/e61d0999c95d4eb7b8a6658bf6af149c.shtml* (accessed January 8, 2019) (in Chinese)
11. National Development and Reform Commission. Circular on issuing opinions on promoting drug price reform. *http://jgs.ndrc.gov.cn/zcfg/201505/t20150505_748205.html* (accessed January 12, 2019) (in Chinese)
12. National Development and Reform Commission. Opinions on reforming price management of medical services. *http://shs.ndrc.gov.cn/zcyj/200704/t20070419_130540.html* (accessed January 16, 2019) (in Chinese)
13. General Office of the State Council. Guiding opinions of the General Office of the State Council on further deepening the reform of the payment mode of basic medical insurance. *http://www.gov.cn/zhengce/content/2017-06/28/content_5206315.htm* (accessed January 20, 2019) (in Chinese)
14. National Health Commission. Division of Science and Education convening the selection meeting of health technology assessment in 2014. *http://www.nhc.gov.cn/qjjys/s3582/201407/895c2a7037a441e982f779c77c6a07f2.shtml* (accessed January 22, 2019) (in Chinese)
15. Mu Y, Zhen T, He Y, Gu JL, Song KN, Wang N, Zhao W. Comparative Analysis on Health Technology Assessment Study in China and Abroad. Journal of Medical Informatics. 2017; 38:14-18. (in Chinese)
16. Guan H, Yue X, Wu J. Applications and challenges of guidelines for pharmacoeconomic evaluation in China. Chin Pharm J. 2017; 52:1188-1193.
17. Chen Y, He Y, Chi X, Wei Y, Shi L. Development of health technology assessment in China: New challenges. Biosci Trends. 2018; 12:102-108.
18. Yang H. Application of hospital-based health technology assessment in the management of medical disposable materials. Chin Med Dev. 2017; 32:123-126. (in Chinese)
19. Ministry of Human Resources and Social Security. Xu Yanjun introduced the situation of negotiation of medical insurance drug catalogue. *http://www.mohrss.gov.cn/yiliaobxs/YILIAOBXSgongzuodongtai/201707/t20170728_274815.html* (accessed January 25, 2019). (in Chinese)
20. National Health Commission. Notice on the work of the National Center for the Comprehensive Evaluation of Drugs and Health Technologies undertaken by the Health Development Research Center of the National Health and

Family Planning Commission. *http://www.nhc.gov.cn/qjjys/s7946/201810/8446e74c71fb4db5811ab8aed59c7d6d.shtml* (accessed January 25, 2019). (in Chinese)
21. National Health Commission. Guidance on strengthening the transfer and transformation of scientific and technological achievements in health. *http://www.gov.cn/xinwen/2016-10/12/content_5117948.htm* (accessed February 1, 2019). (in Chinese)
22. General Office of the State Council. Guidance of the General Office of the State Council on reforming and perfecting the comprehensive supervision system of the medical and health industry. *http://www.gov.cn/zhengce/content/2018-08/03/content_5311548.htm* (accessed February 3, 2019). (in Chinese)
23. Mao Y, Chen Y, Tang M, Liu W. Health technology assessment institutions in China: A cross-sectional study. Chinese Health Quality Management. 2015; 22:77-80. (in Chinese)
24. Zhan Z, Fan R, Cheng X. Application of hospital-based health technology assessment in medical equipment configuration management of our hospital. China Medical Devices. 2018; 33:170-172,177. (in Chinese)
25. Fu Q, Ji C, Xu C, Yao C, Ma Y, Ai H. Mini-HTA index system and evaluation method study in medical institutions. Hospital Administration Journal of Chinese People's Liberation Army. 2018; 5:131-134. (in Chinese)
26. Yang J, Jin W, Zhang H. Analysis and discussion of the application of mini-HTA in medical device evaluation in the hospital. China Medical Devices. 2016; 31:77-9. (in Chinese)
27. Li H, Liu GG, Wu J, Wu JH, Dong CH, Hu SL. Recent pricing negotiations on innovative medicines pilot in China: Experiences, implications, and suggestions. Value Health Reg Issue. 2018; 15:133-137.
28. Wang HY, Zhang XX, Fang L, Jin CL. Health technology assessment process and normative research in China. Chinese Health Quality Management. 2016; 23:60-63. (in Chinese)
29. Zhang R, Modaresi F, Borisenko O. Health economic evaluations of medical devices in the People's Republic of China: A systematic literature review. Clinicoecon Outcomes Res. 2015; 7:195-204.
30. Sun X, Tan J, Tang L, Guo JJ, Li X. Real world evidence: Experience and lessons from China. BMJ. 2018; 360:j5262.
31. Luo N, Liu G, Li M, Guan H, Jin X, Rand-Hendriksen K. Estimating an EQ-5D-5L value set for China. Value Health. 2017; 20:662-669.
32. Zhen X, Sun X, Dong H. Health technology assessment and its use in drug policies in China. Value Health Reg Issues. 2018; 15:138-148.
33. Wei Y, Pong RW, Shi L, Ming J, Tang M, Mao Y, Liu W, Chen Y. Perceptions of health technology assessment knowledge translation in China: A qualitative study on HTA researchers and policy-makers. International Journal of Healthcare Technology and Management. 2017; 16:44-58.

(Received March 28, 2019; Revised April 16, 2019; Accepted April 18, 2019)

Review

DOI: 10.5582/bst.2018.01298

Chinese herbal medicine for acute upper respiratory tract infections and reproductive safety: A systematic review

Zengshu Huang[1,2,3,§], Xinyao Pan[1,2,3,§], Jing Zhou[1,2,3], Wing Ting Leung[1,2,3], Chuyu Li[1,2,3], Ling Wang[1,2,3,*]

[1] *Laboratory for Reproductive Immunology, Hospital & Institute of Obstetrics and Gynecology, Shanghai Medical College, Fudan University, Shanghai, China;*
[2] *The Academy of Integrative Medicine, Fudan University, Shanghai, China;*
[3] *Shanghai Key Laboratory of Female Reproductive Endocrine-related Diseases, Shanghai, China.*

Summary **Acute upper respiratory tract infections (AURTIs) are common and self-limited in people with normal immunity but sometimes lead to poor clinical outcomes under specific conditions such as pregnancy if not treated appropriately. Chinese herbal medicines (CHM), which are widely used to treat AURTIs, have proven to be effective in preclinical and clinical studies. This review focuses on the bioactivities of typical CHM and the adverse reactions they cause, and especially issues with reproductive safety when treating AURTIs. The main mechanisms for clinical efficacy may include anti-viral, anti-bacterial, anti-inflammatory, antipyretic, and immunomodulatory action as indicated by preclinical evidence. Most clinical trials indicate that CHM shortens the natural course of AURTIs and that it relieves related symptoms such as a fever, headaches, coughing, myalgia, a cold, sore throat, and a nasal obstruction. However, some CHM have a range of adverse effects and potentially affect reproduction from endocrinal secretion to embryo development while others do not. Therefore, clinical adverse reactions and preclinical studies on the toxicity of CHM are discussed. More reliable evidence is required to conclude that CHM are efficacious and safe for pregnant women with AURTIs. This review should help to promote advances in the research on and development of CHM as alternative treatments for AURTIs and offer insight into strategies to manage the safety of CHM during clinical use.**

Keywords: Chinese herbal medicine, acute upper respiratory tract infections, efficacy, reproductive safety, mechanism

1. Introduction

Acute upper respiratory tract infections (AURTIs) refer to infections that involve tonsillitis, pharyngitis, laryngitis, sinusitis, otitis media, and the common cold. Viruses are the pathogens that most often cause AURTIs, while bacteria, fungi, and helminths are far less common. Human rhinoviruses are the most prominent causes (*1*), but other viruses such as adenovirus and influenza virus and bacteria have also been implicated. Symptoms manifest as sneezing, nasal congestion, a sore throat, coughing, a fever, and headaches, with varying degrees of severity. Most AURTIs are mild and self-limited. Occasionally, they can lead to poor clinical outcomes, and their complications may threaten the health of the infected. Severe consequences tend to occur in people with a specific level of immunity, such as pregnancy.

Pregnant women with AURTIs usually face more problems such as a higher risk of severe clinical outcomes and more limitations on medication they can take. Western medicines are commonly used to treat pregnant women with AURTIs, but there are questions about their safety due to adverse reactions. Ibuprofen

Released online in J-STAGE as advance publication March 31, 2019.

[§]These authors contributed equally to this work.

**Address correspondence to:*
Dr. Ling Wang, Obstetrics & Gynecology Hospital of Fudan University, 419 Fangxie Road, Shanghai 200011, China.
E-mail: Dr.wangling@fudan.edu.cn

is a popular fever and pain reliever but contraindicated in pregnant women (*2*). Potential fetal defects prevent doctors from prescribing dextromethorphan, an antitussive component added to common cold medications, to pregnant women. Perceiving Chinese herbal medicines (CHM) to be less toxic, pregnant women in China tend to choose CHM when given the choice between Western medicine and CHM. According to China: *2015 Expert consensus on the standardization of common cold medicines for special populations*, CHM are largely marketed as over-the-counter medicines (*2*). Having analyzed a total of 33 Chinese patent medicines (CPMs) listed in the 2012 China National Essential Drug List for the treatment of the common cold, Chen *et al*. concluded that CPMs had a potential positive effect on the cure rate of the common cold (*3*). Numerous clinical trials have indicated that CHM are efficacious in treating AURTIs, but their mechanisms of action and the adverse reactions they cause remain unclear. Greater efficacy and unknown toxicity underscore the significance of proper use of CHM in light of special situations such as pregnancy.

This review describes well-known herbs and traditional Chinese herbal preparations, it explains their main role in treating AURTIs, and it summarizes advances in the study of their efficacy and safety, and especially in terms of reproductive safety.

2. Mechanisms by which CHM treat AURTIs

2.1. *Anti-viral action*

The viral replication cycle includes attachment, penetration, transcription, protein synthesis, assembly, and release (*4*). These steps provide strategies to screen for CHM that prevent or control infections of the respiratory tract with viruses (Table 1). As an example, researchers searching for influenza neuraminidase (NA) inhibitors found that Forsythiae *Fructus*, *Lonicera japonica*, and *Scutellaria baicalensis* displayed exceptional performance (*5,6*). *Radix Isatidis* inhibits the hemagglutinin (HA) of the influenza virus in the early stages (*7*) and then retains the influenza viral ribonucleoprotein (vRNP) complex in the nucleus (*8*), thereby blocking viral replication.

2.2. *Anti-bacterial action*

CHM tends to act to prevent bacterial growth or to reduce the possibility of sepsis. The mechanisms are complicated and unclear but probably relate to microbial enzymes or other interactions that inactivate microbial adhesins. As an example, phenolic compounds of *Lonicera japonica* have bacteriostatic activity (*9*) that affects a broad spectrum of bacteria, including *Bacillus cereus* and *Staphylococcus aureus* (*10*), by damaging the cytoplasmic membrane.

2.3. *Anti-inflammatory action*

Symptoms of AURTIs are associated with viral replication and the related cytokine cascade response. In addition to direct antiviral action, CHMs often target multiple components of the inflammatory response to decrease production of pro-inflammatory mediators and recruitment of leukocytes. *Lonicera japonica* attenuates the expression of TNF-a, IL-6, and iNOS *via* down-regulation of nuclear factor-κB (NF-κB) pathways, and it enhances the expression of IL-10 by increasing Sp1 phosphorylation (*11*). *Forsythiae Fructus* suppresses the activation of mitogen-activated protein kinase (MAPK) and NF-κB pathways to decrease the production of TNF-a, IL-1β, IL-6, and myeloperoxidase (MPO) (*12*). *Flos Lonicera*, *Forsythia Fructus*, and *Radix Platycodon* combinations have synergistic anti-inflammatory action by alleviating pathological changes in the respiratory system and by reducing inflammatory cytokines in bronchoalveolar lavage fluid (BALF) (*13*).

2.4. *Antipyretic action*

A fever, a common feature of infectious diseases, serves as a defense response to pathogens as well as injuries to vital organs. The mechanism of fever onset is acknowledged to be sequential production of complement and prostaglandin E2 (PGE_2), followed by the subsequent transfer of pyrogenic cytokines peripherally and centrally (*14*). The efficacy of volatile oils, crucial to the treatment of fever with *Radix Bupleuri*, has been verified in a rat model of fever. This action might be associated with declining cAMP in the hypothalamus and arginine vasopressin (AVP) in the ventral septal area (*15*). Interestingly, another well-known antipyretic herb, *Folium Mori*, has potent synergistic action by relieving fever and inflammation when combined with *Flos Chrysanthemi* in a proportion of only 1:1 (*16*).

2.5. *Immunomodulatory action*

Host innate and adaptive immune responses to pathogens play a role throughout the course of AURTIs. Overreaction of the host immune response may also lead to tissue damage and multi-organ injuries, which in turn may cause related diseases (*4*). CHM are able to optimize host-pathogen immune responses of patients with AURTIs. As an example, the supplement of Bu-Zhong-Yi-Qi-Tang (BZYQT) after intranasal vaccination against influenza increases the virus-specific IgA and IgG antibody titers in the nasal cavity and sera by enhancing upper respiratory mucosal and systemic immunity (*17*). Interferon-a (IFN-α) increases in the BALF of mice. The stimulation

Table 1. The methodologies and findings of studies on CHM for treatment of AURTIs

Pharmacological effect	Name	Components	Materials	Methods	Mechanism of action
Anti-viral					
Viral attachment inhibitors	*Andrographis paniculata*	14-a-lipoyl andrographolide	MDCK cells, BALB/c mice	NR uptake assay, plaque reduction assay, MTT assay, IC_{50}, HAI assay	Directly interferes with HA of influenza A binding to RBC surface receptors (*72*)
Viral entry/uncoating inhibitors	*Radix Isatidis*	Clemastanin B	MDCK, HEp-2, LLC-MK2, VERO-E6 and MRC-5 cells	MTT assay, plaque assay, $TCID_{50}$, IC_{50}, fluorescence microscopy, virus resistance assay	Targets influenza A endocytosis, uncoating, *etc.* (*8*)
	Ephedrae herba	Tannin	MDCK cells	Virus growth assay, vital fluorescence staining, MTT assay	Inhibitory effect on the acidification of endosomes and lysosomes, interferes with viral uncoating (*73*)
Biological synthesis inhibitors	*Cinnamomi cortex*	Trans-cinnamaldehyde	MDCK cells, ICR female mice	Virus growth assay, RT-PCR, MTT assay, protein synthesis assay	Inhibits viral protein synthesis at the post-transcriptional level (*74*)
Biological synthesis & assembly inhibitors	*Rhizoma Polygoni Cuspidati*	Resveratrol	MDCK and NCL-H292 cells, BALB/c mice	Immunoblotting, RT-PCR, glutathione assay, immune-fluorescence	Retains vRNPs of influenza A in cell nuclei and reduces expression of late viral proteins related to the inhibition of protein kinase C activity (*75*)
Assembly inhibitors	*Forsythia suspense*	Forsythoside A	MDCK cells, Human blood macrophages, BALB/c mice	HPLC, ICC, western blot, transmission electron microscopy	Suppresses the expression of M1 protein of influenza A (*76*)
Budding inhibitors	*Scutellaria baicalensis*	Baicalein, baicalin, chrysin and apigenin	MDCK cells	Plaque inhibition assay, fingerprint analysis, NA enzymatic activity, MTT assay, RT-PCR, molecular docking	NA specific inhibitor (*6*)
	Lonicera japonica	chlorogenic acid and phenolic acids		UPLC-Q-TOF-MS/MS, HPLC-MSn, NA assay, fluorometric assay	NA inhibitory activity (*5*)
Anti-bacterial	*Radix Isatidis*	Syringic acids, salicylic acid, and benzoic acid	Escherichia coli	Microcalorimetry and molecular structure analysis	Syringic acid - potent antibacterial effect due to the different phenyl ring (*77*)
	Lonicera japonica	Phenolic compounds (3,5-bis-O-caffeoyl quinic acid)		MS analysis, chromatographic analysis, disk agar diffusion assay	Counters S. aureus and E. coli related to iron deprivation or hydrogen binding to vital proteins (*9*)
Anti-inflammatory	*Forsythia suspense*	Phillyrin	RAW264.7 murine macrophage cell line	MTT assay, western blot, RT-PCR, Nitrite assay, BCA protein assay, ELISA, fluorescence microscopy	Anti-inflammatory action by suppressing LPS-induced activation of JAK-STATs and p38 MAPKs signaling pathways and production of ROS in macrophage cells (*78*)
	Radix Bupleuri	Saikosaponin a and d	Male BALB/c mice, RAW264.7 murine macrophage cell line	MTT assay, Nitrite assay, western blot, RT-PCR, ELISA, Immunoblotting	Potent anti-inflammatory activity through inhibitory effects on NF-κB activation and thereby on iNOS, COX-2 and pro-inflammatory cytokines (79)

Abbreviations: HA: hemagglutination; HAI: hemagglutination inhibition, $TCID_{50}$: 50% tissue culture infective dose; NR: neutral red; NA: neuraminidase; MTT: 3-(4,5-dimethylthiazol-2-Yl)-2,5-diphenyltetrazolium bromide; IC_{50}: median inhibitory concentration; MS: mass spectrometry; HPLC: high-performance liquid chromatography ; GC: gas chromatography; EMSA: electrophoretic mobility shift assay; BCA: bicinchoninic acid; cAMP: cyclic adenosine monophosphate; AVP: arginine vasopressin; vRNPs: viral ribonucleoproteins; LPS: lipopolysaccharide; RANTES: regulated upon activation, normal T cell expressed and secreted ; HUVEC: human umbilical vein endothelial cell; ELISA: enzyme-linked immunospot assay; RT-PCR: real time-PCR; ICC: immunocytochemistry; MDCK cells: monolayers of dog kidney cells; MIP-1: macrophage inflammatory protein-1;ROS: reactive oxygen species; iNOS: inducible nitric oxide synthase; COX-2: cyclooxygenase-2; MAPK: mitogen-activated protein kinases; PI3K: phosphatidylinositol 3 kinase: JAK: Janus kinases; STATs: signal transducer and activator of transcription proteins; *S. aureus*: *Staphylococcus aureus*; *E. coli*: *Escherichia coli*.

Table 1. The methodologies and findings of studies on CHM for treatment of AURTIs (continued)

Pharmacological effect	Name	Components	Materials	Methods	Mechanism of action
Anti-pyretic	*Radix Bupleuri*	Water extract, volatile oil, saponin	Male Wistar rats	Rectal temperature assay, ELISA	Adjusts synthesis and exudation of cAMP from the hypothalamus and AVP in the ventral septal area (*15*)
Immunomodulatory	*Andrographis paniculata*	Andrographolide	Primary mouse peritoneal macrophages from C57BL/6 mice, female BALB/c mice	MTT assay, ELISA, western blot, flow cytometry, RT-PCR	Modulates innate and adaptive immune responses by regulating macrophage phenotypic polarization and antigen-specific antibody production *via* MAPK and PI3K signaling pathways (*80*)
	Houttuynia cordata	Polysaccharides	Human PBMCs	BCA protein assay, FT-IR, ^{1}H and ^{13}C NMR spectroscopy, ELISA	Enhances innate immune responses through activation of TLR-4 on the cell membrane of dendritic cells and macrophages secreting IL-ß, MIP-1, and RANTES (*81*)

Abbreviations: HA: hemagglutination; HAI: hemagglutination inhibition, $TCID_{50}$: 50% tissue culture infective dose; NR: neutral red; NA: neuraminidase; MTT: 3-(4,5-dimethylthiazol-2-Y1)-2,5-diphenyltetrazolium bromide; IC_{50}: median inhibitory concentration; MS: mass spectrometry; HPLC: high-performance liquid chromatography ; GC: gas chromatography; EMSA: electrophoretic mobility shift assay; BCA: bicinchoninic acid; cAMP: cyclic adenosine monophosphate; AVP: arginine vasopressin; vRNPs: viral ribonucleoproteins; LPS: lipopolysaccharide; RANTES: regulated upon activation, normal T cell expressed and secreted ; HUVEC: human umbilical vein endothelial cell; ELISA: enzyme-linked immunospot assay; RT-PCR: real time-PCR; ICC: immunocytochemistry; MDCK cells: monolayers of dog kidney cells; MIP-1: macrophage inflammatory protein-1;ROS: reactive oxygen species; iNOS: inducible nitric oxide synthase; COX-2: cyclooxygenase-2; MAPK: mitogen-activated protein kinases; PI3K: phosphatidylinositol 3 kinase: JAK: Janus kinases; STATs: signal transducer and activator of transcription proteins; *S. aureus*: *Staphylococcus aureus*; *E. coli*: *Escherichia coli*.

of both IFN-α production and antibody responses are possible explanations for the effect of BZYQT on "cold syndrome" (*17*).

3. CHM in the treatment of AURTIs

3.1. *Single herbs*

Frequently, the CHM that combat AURTIs are formulations rather than a single medicine, except for a few medicines such as *Andrographis paniculate*. According to a general search of a Chinese database, *Flos Lonicerae Japonicae*, *Scutellaria baicalensis*, *Houttuynia cordata*, *Flos Chrysanthemi*, *Patrinia Herbae*, *Forsythia suspense*, *Radix Isatidis*, *Radix Bupleuri*, *Ephedra Herbae*, *Radix Glycyrrhizae*, *Ziziphus jujube*, *Rhizoma Polygoni Cuspidati*, *Folium Mori*, *Radix Platycodon*, and *Radix Puerariae* are usually included in those formulations. A brief outline of the active component, pharmacological effect, and toxicity of the most commonly used single herbs is shown in Table 2

3.2. *CHM preparations*

Single Chinese herbs have proven ability to combat AURTIs. The synergistic effect of different individual herbs in traditional herbal formulations further enhances bioavailability and counteracts drug toxicity when combined with "monarch," "minister," "assistant," and "guide" components. Today, traditional herbal formulations are transformed into Chinese medicines through use of modern advanced pharmaceutical technology. This review provides evidence of the efficacy and safety of typical preparations in managing AURTIs (Table 3).

3.2.1. *Ge-gen-tang*

Ge-gen-tang (GGT) is a CHM formulation consisting of *Puerariae Radix* (Ge-gen), Ephedrae *Herba* (Ma-huang), *Cinnamomi Ramulus* (Gui-zhi), *Paeoniae Radix* (Bai-shao), *Glycyrrhizae Radix et Rhizoma preparata* (Zhi-gan-cao), *Zingiberis Rhizoma Recens* (Sheng-jiang), and *Jujubae Fructus* (Da-zao) (*18*). GGT is of a great value in treating the common cold, fever, influenza, and even diarrhea in eastern Asia.

3.2.1.1. *Clinical findings*

A multicenter double-blind, parallel group, randomized controlled trial (RCT) of 240 patients with a cold in mainland China indicated that the GGT mixture is safe and efficacious (*19*). However, a study in Japan found that it did not significantly prevent the progression of cold symptoms (*20*). A point worth noting is that a study in Taiwan found that women who take GGT for relief

Table 2. The various active components, preparations, mechanism, and toxicity of single Chinese herbs to treat AURTIs

Single herb	Active component	Preparation	Mechanism of action	Toxicity
Lonicera japonica (*82*)	Organic acids (chlorogenic acid and caffeic acid), flavones (luteolin and hyperoside), essential oils, saponins, *etc*.	Shuang-huang-lian Oral Liquid, Yin-huang Granules, Yin-qiao-san, Xiao-yin-pian, Qin-re-jie-du Oral Liquid	Anti-viral, anti-bacterial, anti-inflammatory, anti-pyretic, and anti-oxidative action	Contraceptive action in mice, dogs and monkeys; No oral acute and subacute toxicities in rats
Andrographis paniculate (*83*)	Diterpenoids (deoxyandrographolide, andrographolide and neoandrographolide), flavonoids, xanthones, *etc*.	Kan Jang, KalmCold, Andrographis paniculata Tablet, Andrographolide sodium bisulfite Injection	Anti-viral, anti-bacterial, anti-inflammatory, and immunomodulatory action	Possible contraceptive action but still controversial; oral acute toxicity:> 17 g/kg, LD_{50}; testicular toxicity:> 1 g/kg, LD_{50}; genotoxicity:5 g/kg, LD_{50}
Radix Scutellariae (*84*)	Flavonoids (baicalin, wogonin, wogonoside, baicalein and oroxylin A), *etc*.	Shuang-huang-lian Oral Liquid, Compound Houttuynia cordata Granules, Compound Honeysuckle Granules	Anti-viral, anti-allergy, anti-inflammatory, anti-oxidative, and immunomodulatory action	Not toxic to normal cells in animals and humans but toxic to malignant cells
Houttuynia cordata (*85*)	Flavonoids (quercitrin, hyperoside and afzelin), alkaloids, volatile oils, organic acids (chlorogenic acid), *etc*.	Yu Jin Injection, Compound Houttuynia cordata Granules	Anti-viral, anti-bacterial, anti-inflammatory, anti-pyretic, anti-allergy, anti-oxidative, and immunomodulatory action	Not toxic *in vitro* or *in vivo*
Forsythia suspense (*12*)	Lignans (phillyrin), phenylethanoid glycosides (forsythiaside), flavonoids (rutin, quercetin and forsythoneoside), *etc*.	Yin-qiao-san, Lian-qiao Drink, Ling-qiao-jie-du Pillule, Shuang-huang-lian Oral Liquid, Vitamin C Yin-qiao Tablets	Anti-viral, anti-bacterial, anti-inflammatory, anti-oxidative, and anti-allergy action	Forsythiaside is cytotoxic and has acute toxicity in mice
Herba Ephedra (*86*)	Alkaloids (ephedrine), tannin, flavanols, flavones, carboxylic acids, volatile terpenes, *etc*.	Ma-huang-tang, Ma-xing-shi-gan-tang, Xiao-qing-long-tang	Anti-viral, anti-bacterial, anti-inflammatory, anti-pyretic, and antitussive action	Activation of sympathetic and central nervous systems (insomnia, palpitation, rapid pulse, elevation of blood pressure, and dysuria) and hepatotoxicity
Rhizoma Polygoni Cuspidati (*87*)	Quinones (emodin), stilbenes (resveratrol and polydatin), flavonoids (rutin and quercetin), *etc*.	Shu-feng-jie-du Capsules, Re-yan-ning Granules	Anti-viral, anti-bacterial, anti-inflammatory, anti-oxidative, cardioprotective, and estrogenic action	Contraindicated for pregnant women; Lack of relative systematic toxicity and safety evaluation but few evaluations of adverse reactions (no systemic anaphylaxis or passive skin allergy (5.6 mg/kg) in rabbits)

Table 3. The use of CHM in AURTIs on the basis of clinical findings

Group		Sample Size		Patients characteristics		Evaluation index	Outcome	Adverse events	
T	C	T	C	T	C			T	C
MXSGT+ symptomatic treatments (*34*)	symptomatic treatments	55	45	Pregnancy flu Gestational week: < 28 w Age: 25.22 ± 3.88 y		Duration of fever, symptom alleviation time, threatened abortion rate, maternal delivery, fetal development	MXSGT helps reduce the duration of fever, alleviate the duration of symptoms, and reduce the duration of hospitalization with no adverse reactions in pregnant women.	None	None
Shu-feng-jie-du Capsules (*88*)	Placebo	120	120	AURTIs ("wind-heat syndrome") M/F: 45/75 Age:34.83 ± 10.95 y	M/F: 44/76 Age:34.60 ± 11.40 y	Total scores of diseases, antifebrile effective rate, TCM symptom scores before and after treatment, cure rate, total effective rate, laboratory indexes	SFJDC is efficacious in treating AURTIs with "wind-heat syndrome."	None	None
Re-du-ning Injection (*49*)	Oseltamivir	24	22	Pandemic influenza M/F: 12/12 Age: 37.9 ± 13.9 y	M/F: 7/15 Age: 38.4 ± 14.5 y	The median fever alleviation time, clearance time and total scores of influenza symptoms	RDN Injections have a similar effect to oseltamivir in reducing the duration of influenza illness.	Transfusion reaction (1), blood leukocyte (1)	Blood leukocyte (1)
Lian-hua-qing-wen Capsules (*45*)	Oseltamivir	122	122	AURTIs ("wind-cold syndrome") M/F: 64/58 Age: 21.5 ± 5.9 y	M/F: 63/59 Age: 21.4 ± 3.9 y	The median duration of viral shedding, symptom scores, individual symptom alleviation time, the duration of illness, the defervescence time	Compared to oseltamivir, LHQWC has a similar therapeutic effectiveness in terms of reducing the duration of illness and the duration of viral shedding.	No	Nausea and vomiting (4)
Ban-lan-gen Granules + oseltamivir (*7*)	Oseltamivir	128	107	Influenza A (H1N1) M/F: 91/37 Age: 18-45 y	M/F: 78/29 Age: 16-52 y	The temperature period, clinical symptoms, blood routine, viral test and length of stay	Oseltamivir phosphate combined with Ban-lan-gen granules performs better than oseltamivir phosphate alone in the treatment of influenza A (H1N1).	Nausea and vomiting (2), diarrhea (1), dizziness (1), rash (1)	Nausea and vomiting (2), diarrhea (2), headache (1), rash (1)
Andrographis paniculata (KalmCold) (*89*)	Placebo	112	110	Uncomplicated URTIs M/F: 5/37; Age: 34.36 ± 0.97 y	M/F: 68/42 Age: 32.42 ± 1.1 y	Severity of 9 symptoms of common cold and overall symptoms (VAS,0 ± 100)	KalmCold™ treatment significantly decreases all symptom scores except for earache whereas in the placebo group the symptoms are either unchanged or exacerbated after day 3.	Diarrhea (3), vomiting (1), epistaxis (1), urticaria (1)	Diarrhea (1), vomiting (1), moderate rigor (1)
Zheng-chai-hu Granules (*90*)	Qing-re-ling Granules	115	115	Exogenous fever ("wind-cold syndrome") M/F: 83/32 Age: 35 ± 9 y	M/F: 8/27 Age: 32 ± 8 y	Cure rate, symptoms scores, total effective rate	Zheng Chai-hu group has better improvement of chief symptoms (fever, cough, sore throat etc.) than Qing-re-ling group.	None	None

Abbreviations: AURTIs: acute upper respiratory tract infections; TCM: traditional Chinese medicine; T: Treatment group, C: Control group; M/F: male/female.

of respiratory discomfort are unexpectedly exposed to phytoestrogen generated by *Ge gen* (*21*). Nearly 5% of female users of Chinese medicines consumed cumulative doses of *Ge gen* above 60 g (*21*). Since little is known about the action of phytoestrogenic herbs in female patients, physicians need to be aware of threats to the female endocrine system when prescribing such herbs.

3.2.1.2. *Mechanism of action*

GGT stimulates the airway epithelium to secrete IFN-β to counteract a viral infection before and after that infection, but it is more effective before infection (*22*). It disrupts influenza virus replication by directly blocking the virus-induced phosphatidylinositol 3-kinase (PI3K)/Akt signaling pathway, which in turn causes retention of vRNPs in the nucleus (*23*). Promotion of the phagocytic activity of macrophages and an increase in the level of IL-12 in BALF contribute to a reduction in the virus yields as well (*24*).

3.2.2. *Shuang-huang-lian*

The Shuang-huang-lian (SHL) formulation, which consists of *Lonicera japonica* (Jin-yin-hua), *Scutellaria baicalensis* (Huang-qin), and *Forsythia suspense* (Lian-qiao), generally has a satisfactory curative effect on AURTIs (*25*) and influenza (*26*) according to a large amount of laboratory and clinical data.

3.2.2.1. *Clinical findings*

A systematic review that evaluated the SHL injection (SHLI) in treating AURTIs concluded that it had potentially reduced the course of disease and relieved some cold symptoms like a fever and coughing (*25*). However, the poor methodology of the reviewed studies and poor reporting preclude reaching any definite conclusions on its clinical effectiveness. In another systematic review in 2016 that involved 21 studies (2,914 participants), meta-analysis revealed that SHLI was more efficacious at treating AURTIs than Western medicines (*27*).

3.2.2.2. *Mechanism of action*

SHL is reported as an effective agent against adenovirus and influenza virus (*26*). Human adenovirus III (HAdV3), a common pathogen causing AURTIs, is inhibited by SHL in a dose- and time-dependent manner, from viral attachment and internalization to replication, and is accompanied by a high level of IFN-α expression (*28*). In addition, SHL effectively attenuates lipopolysaccharide (LPS)-induced secretion of proinflammatory cytokines and oxidative stress by suppressing the p38- and ERK1/2-mediated AP-1 pathway in alveolar macrophages. Together, the reduction in neutrophil infiltration and excessive levels of inflammatory mediators alleviate pulmonary cellular injury (*29*). Screening of SHL *in vitro* revealed that chlorogenic acid is the main bioactive ingredient that specifically binds to β2-adrenoceptor (*30*), which participates in smooth muscle relaxation and bronchodilation.

3.2.3. *Ma-xing-shi-gan-tang*

Ma-xing-shi-gan-tang (MXSGT) is a decoction consisting of *Herba Ephedra* (Ma-huang), *Semen Armeniacae Amarum* (Ku-xin-ren), *Radix Glycyrrhizae* (Gan-cao), and *Gypsum Fibrosum* (Shi-gao). Although MXSGT and Ma-huang-tang (MHT) differ in only one herb, both are conventional formulations for sweating, asthma, and febrile diseases such as influenza-like illness (*31,32*). The corresponding "syndromes" (exogenous diseases) they treat according to traditional Chinese medicine (TCM) differ substantially.

3.2.3.1. *Clinical findings*

In an RCT involving 410 patients in 11 hospitals in 4 provinces of China, oseltamivir and MXSGT - Yin-qiao-san (MXSGT-YQS), alone and in combination, reduced the duration of fever and effectively lowered severity scores for other symptoms in patients with an H1N1 influenza infection (*33*). Another RCT involving 100 patients was conducted to observe the effect of MXSGT in treating influenza during pregnancy (*34*). The control group (n = 55) received symptomatic treatment and/or intravenous penicillin (8×10^6 U) for 3 days if infected. The treatment group (n = 45) received MXSGT in addition to the same treatment as that of the control group. Flu therapy was more efficacious when combined with MXSGT, and the treatment group also had a lower threatened abortion rate than that of the control group. Follow-up of the treatment group revealed no adverse pregnancy outcomes while results for the control group were lost. Although there were significant differences between the two groups, this RCT did not constitute sufficient evidence.

3.2.3.2. *Mechanism of action*

MXSGT acts in several ways against human influenza A viruses *in vitro* by: 1) reducing viral uptake through damage of the viral ultrastructure; 2) inhibiting viral entry by inactivation of the PI3K/Akt signaling pathway; and 3) impairing the synthesis of both viral RNA and protein (*35*). Its extract relieves hyperthermic syndrome in rats *via* the synergic effects of *Gypsum* and *Ephedra* and through the modulation of PGE_2 synthesis in the hypothalamus-adrenal gland axis (*36*). Early on, MXSGT has anti-inflammatory action by

inhibiting neutrophil infiltration into the airway. It further attenuates lung microvascular hyperpermeability and decreases the number of leukocytes adhering to lung venules (*37*). Moreover, the antitussive action of MXSGT is dose-dependent property; it suppresses bronchial contractions induced by acetylcholine/histamine (*36*).

3.2.4. *Shu-feng-jie-du Capsules*

Shu-feng-jie-du Capsules (SFJDC) have been extensively used to treat AURTIs and acute lung injury (ALI) for over 30 years in China. The capsules consist of 8 herbs: *Rhizoma Polygoni Cuspidati* (Hu-zhang), *Fructus Forsythiae* (Lian-qiao), *Radix Isatidis* (Ban-lan-gen), *Radix Bupleuri* (Chai-hu), *Herba Patriniae* (Bai-jiang-cao), *Herba Verbenae* (Ma-bian-cao), *Rhizoma Phragmitis* (Lu-gen), and *Radix Glycyrrhizae* (Gan-cao) (*38*).

3.2.4.1. *Clinical findings*

A multicenter, open-label phase IV clinical trial on SFJDC found that they were efficacious in treating AURTIs ("wind-heat syndrome"), with 0.03% of patients suffering an adverse drug reaction (ADR) (*39*). After 3 days of treatment, the cure rate was 40.23% and the total efficacy was 87.40%. The median time for onset and duration of defervescence were 4.50 hours and 20.00 hours, respectively (*39*). According to an RCT, SFJDC alleviate acute suppurative tonsillitis, with a shorter duration of fever and pharyngeal purulence, greater shrinkage of the tonsils, and greater safety (*40*).

3.2.4.2. *Mechanism of action*

In vitro, SFJDC repress H1N1 (*41*), respiratory syncytial virus (RSV), coxsackie virus B3 (CoxB3), and herpes simplex virus 1 (HSV-1); SFJDC are less potent than ribavirin but also less cytotoxic (*42*). SFJDC are far more potent than Qing-kai-ling granules but weaker than ceftriaxone sodium injection in fighting 6 different bacteria (42). SFJDC protect against ALI by suppressing the MAPK/NF-κB pathway *in vivo* (*43*). Proteomic analysis of a rat model of LPS-induced ALI revealed that the anti-inflammatory and immunomodulatory actions of SFJDC are the results of action on the core regulator protein AKT1 in five respects: 1) NF-κB/Nrf2 in the oxidative stress response; 2) the MAPK (ERK1/2 and JNK) signaling pathway; 3) p53/Bcl-2/Caspase in apoptosis; 4) AKT1/SOCS1 in negative feedback to TLR4 signaling; 5) and AKT/mTOR signaling (*38*).

3.2.5. *Other preparations*

A number of new compound preparations that are derived from traditional formulations have come onto the market. Lian-hua-qing-wen Capsules (LHQWC) are an example that was developed from two conventional CHM formulae - MXSGT and YQS. LHQWC provide broad-spectrum protection against influenza viruses by restricting viral proliferation in the early stages, with an IC_{50} ranging from 0.35 mg/mL to 2 mg/mL, and by efficiently blocking the nuclear export of vRNP (*44*). In addition, a virus-induced inflammatory reaction is alleviated by suppression of the NF-kB signaling pathway in a dose-dependent manner (*44*). In a double-blind RCT involving 244 patients with influenza A, LHQWC performed similar to oseltamivir in reducing the duration of illness and viral shedding and in relieving the severity of illness and symptoms including fever, cough, sore throat, and fatigue (*45*).

Re-du-ning injection (RDNI) is another modern patent CHM prepared with an extract purified from *Artemisia annua* (Qing-hao), *Gardenia jasminoides Ellis* (Zhi-zi), and Flos Lonicerae (Jin-yin-hua). Previous studies indicated that RDNI inhibits human rhinovirus *in vitro* in three ways: inactivating the virus, interfering with viral proliferation, and blocking the interaction of infected cells (*46*). In addition to regulation of the host defense system (*47*), it has antipyretic action by reducing cAMP in the hypothalamus and MPO in the lungs of mice (*48*). Moreover, it shortens the clinical course of influenza, it alleviates fever, it reduces fever clearance time, and it alleviates all influenza symptoms (*49*). An RDNI infusion may be an effective alternative for treatment of influenza in adults, possibly with fewer adverse effects than oseltamivir (*49*). However, the clinical use of RDNI needs to be monitored to preclude off-label use, especially overdosing, improper dilution and over-indication (*50*).

4. Adverse reactions and reproductive safety

4.1. *General adverse reactions to CHM*

The reasons why adverse reactions to CHM occur vary from inherent herbal toxicity, excessive doses of herbs, drug-herb interactions, anaphylaxis to co-existing diseases (*51*). Surprisingly, allergic reactions (skin itch, dermatitis and anaphylactic shock) occur in most cases of adverse reactions to CHM (*52*). ADR reports that are related to CHM injections account for > 50% of all ADR reports related to CHM, and the percentage has been rising annually (*53*). Considerable attention is paid to the hepatic damage caused by CHM, but different organs may be affected (Tables 2 and 3). Some herbs may have no direct toxicity but cause harmful drug interactions, which are mainly associated with cytochrome P450(CYP)-linked drug metabolism. If CHM are used with other drugs, their curative effect might be hampered or their toxicity increased, or both.

One herb can sometimes have multiple impacts in terms of adverse reactions. As an example, oral intake of andrographolide extracted from *Andrographis paniculata* likely leads to reduced metabolic activity of intestinal CYP3A4 (*54*) and induces nephrotoxicity associated with activation of oxidative and endoplasmic reticulum stress (*55*).

4.2. *Reproductive safety of CHM*

In addition to considering general adverse reactions, more attention needs to be paid to the reproductive safety of pregnant women. There is no doubt that pregnancy is a dynamic process for both the mother and fetus. This complicated situation requires the consideration of the continued health of the mother, embryo-fetal development, and prenatal growth during different gestational stages. The placenta, a key avenue for the maternal-fetal transfer of substances, has alterations in transport proteins (*56*) and expression of biotransformation enzymes (*57*). Consequently, drug permeability, metabolism, and clearance differ from the early to late period (*58*). As an example, chemicals like chlorinated insecticides, probably used to farm herbs, affect oxytocin, testosterone, oestradiol, and prostaglandin secretion of ovarian and uterine cells, interfering with fertilization as well as with myometrial contractions (*59*). Accordingly, the reproductive organs could be affected by contaminated CHM.

Temporal variations in pharmacokinetics (PK) and pharmacodynamics (PD) during gestation are not limited to the reproductive system. A previous study found that gestation influences the systematic PK profile of certain Chinese herbs such as *Puerariae Radix* (puerarin), with different levels during different stages in pregnant rats (*60*). Dynamic changes in CYP-mediated drug metabolism in the body of pregnant women have also been reported (*61*). Much more should be known about the reproductive safety of CHM. This can be achieved by monitoring the magnitude of variations in physiologic and morphological parameters of the reproductive system and all relevant changes related to drug therapy during pregnancy that may affect maternal-fetal health.

4.3. *Status of research*

In fact, most clinical studies of CHM preparations for treatment of AURTIs exclude pregnant women, who are not often exposed to the uncertain safety risks of medicines in clinical trials in order to avoid further complications. As a consequence, there is a lack convincing clinical evidence of the reproductive safety of many CHM preparations. There are only a few studies of clinical outcomes of use of single herbs and preparations by pregnant women (*34*) and studies of reproductive toxicity (*62*).

As an example, no study has examined the toxicity of a daily dose (6-15 g) of *Forsythiae Fructus* thus far (Pharmacopoeia Commission of the PRC, 2015). Administration of forsythoside gelsiccation powder to SD rats yielded negative results in terms of teratogenicity (*63*). However, one of the active constituents of *Forsythiae Fructus*, forsythiaside, caused acute toxicity in mice (IC_{50} = 1.98 g/kg) (*12*).

The metabolic process of a single herb and be determined and its target organ can be identified, but studying adverse reactions to preparations is much more difficult due to the multiple components and targets involved. Preparations intensify or diminish the toxicity of single herbs. According to a cytotoxicity assay, SHL is slightly less toxic than a mixture of its active ingredients - chlorogenic acid, baicalin, and forsythia glycosides A (*28*).

Adverse reactions to SHL have often been studied. Of the different dosage forms such as oral liquids, granules, and injections, SHLI caused most cases of adverse reactions (*64*). According to a systematic review (*64*), ADRs caused by SHLI are mainly skin allergic reactions and gastrointestinal reactions. Involved systems or organs are, in decreasing order: the skin, the digestive system, general reactions, the respiratory system, and other systems or organs. In addition, there is an increased risk of ADRs induced by combining SHLI and other drugs, and especially antibiotics. Nearly all cases of death were caused by anaphylactic shock (*65*) induced by C5 activation and the subsequent release of histamine, which is largely due to chlorogenic acid (*66*).

In 2018, China's State Food and Drug Administration announced the prohibition of the use of SHLI by children under 4 years of age and pregnant women, but instructions on other dosage forms still indicate that use of SHLI by pregnant or nursing women should be under a physician's direction. Clearly, in-depth studies on the reproductive safety of SHL need to continue in light of previous studies. In addition to its indication for AURTIs, one herb in SHL, *Radix Scutellariae*, is listed as an herb for prevention of miscarriage. Baicalin, one of its active components, has anti-abortifacient action (*67*), and it reverses trophoblast apoptosis in the treatment of preeclampsia (*68*). However, several individual cases of hepatotoxicity after taking *Radix Scutellariae* have been reported (*69*). Moreover, a study of SHL as a frozen powder provided evidence that baicalein and baicalin exchange can occur in the maternal-fetal interface but that it does not affect the contractile activity of human uterine smooth muscle strips *in vitro* (*70*). A later study indicated weak toxicity to the maternal side of the placental barrier with no toxicity to the fetal side *in vitro* (*71*). Although the toxicological and protective roles of the placental barrier with respect to drug detoxification and transporter-controlled protection of the fetus have been

intensively examined (*57*), little work has been done to elucidate the detailed mechanism at the molecular biological level.

5. Conclusion

There is no doubt that CHM play important roles in treating AURTIs by controlling and preventing those infections, limiting the economic burden in comparison to oseltamivir, and benefiting patients with poor tolerance to Western medicines in clinical practice. More advanced technology and strategies allow identification of active CHM and CHM-derived compounds from a vast body of traditional CHM *via* high-throughput screening, and they allow determination of the mechanisms by which CHM treat AURTIs (*4*). Nonetheless, some problems still limit the use of CHM to treat AURTIs, such as inconsistent clinical efficacy and the insufficient evaluation of safety.

Since there are still many herbs and preparations for treatment of AURTIs with either contradictory results or no systematic evaluation of efficacy and safety, and especially reproductive safety, attention must be paid to conducting more well-designed clinical trials and studies to help avoid the misuse of CHM. Although some single herbs or formulations are cited as suitable for pregnant women, more reliable evidence combining preclinical and clinical data should be obtained. In-depth research at the molecular level is needed to reveal underlying pharmacological mechanisms of efficacy and reproductive safety. Moreover, the range of teratogenicity testing should be extended to fertility, sexual maturity, and even organ changes in pregnancy.

Patients may have reduced tolerance and, therefore, more toxicity studies should be conducted on both normal and ill subjects. Given differences between animals and humans, more clinical studies on the safety of CHM during pregnancy are required before CHM can ultimately be used clinically. These efforts may help to formulate strategies to prevent ADRs by adding antagonist drugs or by optimizing the dose, thus minimize risk and maximizing benefit for the mother and fetus in clinical settings.

Acknowledgements

This work was supported by grants from the National Natural Science Foundation of China (no. 31571196 to Ling Wang and no. 30801502 to Ling Wang), the Program to Guide Medicine ("Yixueyindao") of the Shanghai Municipal Science and Technology Commission (no. 18401902200 to Ling Wang and no. 15401932200 to Ling Wang), the Shanghai Program for Support of Leading Disciplines-Integrative Medicine (no. 20180101 and no. 20150407), the Research Foundation ("CR Sanjiu") of Obstetrics & Gynecology committee of Chinese Association of Integrated Traditional Chinese and Western Medicine (CR1901FC01 to Ling Wang), the Shanghai Committee of the China Democratic League (no. 02054 to Ling Wang), the FY2008 JSPS Postdoctoral Fellowship for Foreign Researchers (P08471 to Ling Wang), and the Shanghai Pujiang Program (no. 11PJ1401900 to Ling Wang).

References

1. Passioti M, Maggina P, Megremis S, Papadopoulos NG. The common cold: Potential for future prevention or cure. Curr Allergy Asthma Rep. 2014; 14:413.
2. China: Expert consensus on the standardization of common cold medicines for special populations. International Journal of Respiration. 2015;35:1-5. (in Chinese)
3. Chen W, Liu B, Wang LQ, Ren J, Liu JP. Chinese patent medicines for the treatment of the common cold: A systematic review of randomized clinical trials. BMC Complementary Altern Med. 2014; 14:273-280.
4. Li T, Peng T. Traditional Chinese herbal medicine as a source of molecules with antiviral activity. Antiviral Res. 2013; 97:1-9.
5. Gamaleldin Elsadig Karar M, Matei MF, Jaiswal R, Illenberger S, Kuhnert N. Neuraminidase inhibition of dietary chlorogenic acids and derivatives - Potential antivirals from dietary sources. Food Funct. 2016; 7:2052-2059.
6. Hour MJ, Huang SH, Chang CY, Lin YK, Wang CY, Chang YS, Lin CW. Baicalein, ethyl acetate, and chloroform extracts of Scutellaria baicalensis inhibit the neuraminidase activity of pandemic 2009 H1N1 and seasonal influenza A viruses. Evid Based Complement Alternat Med. 2013; 2013:750-803.
7. Tu B, Nie W, Ding PP, Li FY, Chen WW, Zhou ZP, Zhang X, Fan R, Huo DD, Zhao M. Efficacy of treatment of influenza A (H1N1) with oseltamivir phosphate and isatis root granules. Medical Journal of the Chinese People's Armed Police Forces. 2013; 24:465-467+470. (in Chinese)
8. Yang Z, Wang Y, Zheng Z, Zhao S, Zhao J, Lin Q, Li C, Zhu Q, Zhong N. Antiviral activity of Isatis indigotica root-derived clemastanin B against human and avian influenza A and B viruses *in vitro*. Int J Mol Med. 2013; 31:867-873.
9. Xiong J, Li S, Wang W, Hong Y, Tang K, Luo Q. Screening and identification of the antibacterial bioactive compounds from Lonicera japonica Thunb. leaves. Food Chem. 2013; 138:327-333.
10. Shan B, Cai YZ, Brooks JD, Corke H. The *in vitro* antibacterial activity of dietary spice and medicinal herb extracts. Int J Food Microbiol. 2007; 117:112-119.
11. Kao ST, Liu CJ, Yeh CC. Protective and immunomodulatory effect of flos Lonicerae japonicae by augmenting IL-10 expression in a murine model of acute lung inflammation. J Ethnopharmacol. 2015; 168:108-115.
12. Wang Z, Xia Q, Liu X, Liu W, Huang W, Mei X, Luo J, Shan M, Lin R, Zou D, Ma Z. Phytochemistry, pharmacology, quality control and future research of Forsythia suspensa (Thunb.) Vahl: A review. J Ethnopharmacol. 2018; 210:318-339.

13. Li YH, Zheng FJ, Huang Y, Zhong XG, Guo MZ. Synergistic anti-inflammatory effect of Radix Platycodon in combination with herbs for cleaning-heat and detoxification and its mechanism. Chin J Integr Med. 2013; 19:29-35.
14. Roth J, Blatteis CM. Mechanisms of fever production and lysis: Lessons from experimental LPS fever. Compr Physiol. 2014; 4:1563-1604.
15. Jin GT, Li B, Wang SR. Experimental study on material basis, efficacy and mechanism of antipyretic effect of Bupleuri Radix. Journal of Chengdu University of Traditional Chinese Medicine. 2013; 36:28-30. (in Chinese)
16. Qin XJ, Ma C. Experimental study on pyretolysis mechanism of compatible application of Folium Mori and Flos Chrysanthemi. Journal of New Chinese Medicine. 2013; 45:133-135.
17. Kiyohara H, Nagai T, Munakata K, Nonaka K, Hanawa T, Kim SJ, Yamada H. Stimulating effect of Japanese herbal (kampo) medicine, hochuekkito on upper respiratory mucosal immune system. Evid Based Complement Alternat Med. 2006; 3:459-467.
18. Yan Y, Chai CZ, Wang DW, Yue XY, Zhu DN, Yu BY. HPLC-DAD-Q-TOF-MS/MS analysis and HPLC quantitation of chemical constituents in traditional Chinese medicinal formula Ge-Gen Decoction. J Pharm Biomed Anal. 2013; 80:192-202.
19. Song HN, Mao ZF, Han DF, Xiang N, Li RL. Randomized double-blind controlled trial on Gegentang mixture in treatment of cold. Clinical Focus. 2005; 20:313-315.
20. Kitamura H, Urano H, Ara T. Preventive effects of a Kampo medicine, Kakkonto, on inflammatory responses via the suppression of extracellular signal-regulated kinase phosphorylation in lipopolysaccharide-treated human gingival fibroblasts. ISRN Pharmacol. 2014; 2014:1-7.
21. Wu CT, Tzeng JN, Lai JN, Tsan SH, Wang JD. Prescription profile of Chinese herbal products containing coumestrol, genestein, and/or daidzein among female users: An analysis of national health insurance data in Taiwan between 1997 and 2007. Chin Med. 2012; 7:22.
22. Chang JS, Wang KC, Shieh DE, Hsu FF, Chiang LC. Ge-Gen-Tang has anti-viral activity against human respiratory syncytial virus in human respiratory tract cell lines. J Ethnopharmacol. 2012; 139:305-310.
23. Wu MS, Yen HR, Chang CW, Peng TY, Hsieh CF, Chen CJ, Lin TY, Horng JT. Mechanism of action of the suppression of influenza virus replication by Ko-Ken Tang through inhibition of the phosphatidylinositol 3-kinase/Akt signaling pathway and viral RNP nuclear export. J Ethnopharmacol. 2011; 134:614-623.
24. Cheng HM, Li CC, Chen CY, Lo HY, Cheng WY, Lee CH, Yang SZ, Wu SL, Hsiang CY, Ho TY. Application of bioactivity database of Chinese herbal medicine on the therapeutic prediction, drug development, and safety evaluation. J Ethnopharmacol. 2010; 132:429-437.
25. Zhang H, Chen Q, Zhou W, Gao S, Lin H, Ye S, Xu Y, Cai J. Chinese medicine injection shuanghuanglian for treatment of acute upper respiratory tract infection: A systematic review of randomized controlled trials. Evid Based Complement Alternat Med. 2013; 2013:987-326.
26. Shen SY, Liu JH, Tian YR, Guo J, Feng JZ, Liu SD, Zeng XJ, Dong XH, Long M. Antiviral activity of shuanghuanglian tablet against influenza A1 virus FM1 and adenovirus ADV3 in mice. China Practical Medicine. 2008; 3:50-52.
27. Wu JR, Zhang D, Zhang XM, Zhang B. Systematic review of Shuanghuanglian injection in the treatment of acute upper respiratory infection. Chinese Journal of Pharmacoepidemiology. 2016; 25:269-274. (in Chinese)
28. Ma Q, Liang D, Song S, Yu Q, Shi C, Xing X, Luo JB. Comparative study on the antivirus activity of Shuang-Huang-Lian injectable powder and its bioactive compound mixture against human adenovirus III *in vitro*. Viruses. 2017; 9:79-91.
29. Fang L, Gao Y, Liu F, Hou R, Cai RL, Qi Y. Shuang-huang-lian attenuates lipopolysaccharide-induced acute lung injury in mice involving anti-inflammatory and antioxidative activities. Evid Based Complement Alternat Med. 2015; 2015:283939.
30. Wang J, Li FW, Zeng KZ, Li Q, Zhao XF, Zheng XH. Bioactive compounds of Shuang-Huang-Lian prescription and an insight into its binding mechanism by beta2 -adrenoceptor chromatography coupled with site-directed molecular docking. J Sep Sci. 2017; 40:4357-4365.
31. Ma CH, Ma ZQ, Fu Q, Ma SP. Ma Huang Tang ameliorates asthma though modulation of Th1/Th2 cytokines and inhibition of Th17 cells in ovalbumin-sensitized mice. Chin J Nat Med. 2014; 12:361-366.
32. Wang JW, Chiang MH, Lu CM, Tsai TH. Determination the active compounds of herbal preparation by UHPLC-MS/MS and its application on the preclinical pharmacokinetics of pure ephedrine, single herbal extract of Ephedra, and a multiple herbal preparation in rats. J Chromatogr B Analyt Technol Biomed Life Sci. 2016; 1026:152-161.
33. Wang C, Cao B, Liu QQ, *et al*. Oseltamivir compared with the Chinese traditional therapy maxingshigan-yinqiaosan in the treatment of H1N1 influenza: A randomized trial. Ann Intern Med. 2011; 155:217-225.
34. Hu JM, Yan JY, Cheng GZ, Wang HH, Feng CB, Zhao AX. Clinical research for Maxingshigan decoction on treating pregnancy influenza. Chinese Medicine Modern Distance Education of China. 2012; 10:80-81. (in Chinese)
35. Hsieh CF, Lo CW, Liu CH, Lin S, Yen HR, Lin TY, Horng JT. Mechanism by which ma-xing-shi-gan-tang inhibits the entry of influenza virus. J Ethnopharmacol. 2012; 143:57-67.
36. Lin YC, Chang CW, Wu CR. Antitussive, anti-pyretic and toxicological evaluation of Ma-Xing-Gan-Shi-Tang in rodents. BMC Complement Altern Med. 2016; 16:456-464.
37. Ma LQ, Pan CS, Yang N, Liu YY, Yan L, Sun K, Wei XH, He K, Xiao MM, Fan JY, Han JY. Posttreatment with Ma-Xing-Shi-Gan-Tang, a Chinese medicine formula, ameliorates lipopolysaccharide-induced lung microvessel hyperpermeability and inflammatory reaction in rat. Microcirculation. 2014; 21:649-663.
38. Tao Z, Meng X, Han YQ, Xue MM, Wu S, Wu P, Yuan Y, Zhu Q, Zhang TJ, Wong CCL. Therapeutic mechanistic studies of ShuFengJieDu capsules in an acute lung injury animal model using quantitative proteomics technology. J Proteome Res. 2017; 16:4009-4019.
39. Xu YL, Zhang HH, Xue YL, YANG JS, Zhou XM, Mao B, Fan FY, Jin WL, Liu FY, Tian ZJ, Xing ZH. Phase IV clinical trial of Shufeng Jiedu Capsules in the treatment of 2031 cases of acute upper respiratory infection of wind-heat syndrome. China Journal of Traditional Chinese Medicine and Pharmacy. 2016; 32:353-355. (in Chinese)
40. Yang X, Yang XW. Observation on efficacy of Shufengjiedu capsules in treatment of acute suppurative

tonsillitis. Evaluation and Analysis of Dug-Use in Hospitals of China. 2017; 17:57-59. (in Chinese)
41. Liu Y, Shi H, Jin YH, Gao YJ, Shi YJ, Liu FZ, Guo SS, Cui XL. Experimental pharmacodynamic research *in vivo* of Shufengjiedu capsule on treatment and prevention of influenza. World Journal of Integrated Traditional and Western Medicine. 2010; 5:107-110. (in Chinese)
42. Lv WW, Zhu TN, Qiu H, Hu T, Huang SH. Pharmacodynamic study on antiviral and antibacterial effects of Shufeng Jiedu capsules *in vitro*. Traditional Chinese Drug Research & Clinical Pharmacology. 2013; 24:234-238. (in Chinese)
43. Tao Z, Gao J, Zhang G, Xue M, Yang W, Tong C, Yuan Y. Shufeng Jiedu Capsule protect against acute lung injury by suppressing the MAPK/NF-kappaB pathway. Biosci Trends. 2014; 8:45-51.
44. Ding Y, Zeng L, Li R, Chen Q, Zhou B, Chen Q, Cheng PL, Yutao W, Zheng J, Yang Z, Zhang F. The Chinese prescription lianhuaqingwen capsule exerts anti-influenza activity through the inhibition of viral propagation and impacts immune function. BMC Complement Altern Med. 2017; 17:130.
45. Duan ZP, Jia ZH, Zhang J, Liu S, Chen Y, Liang LC, Zhang CQ, Zhang Z, Sun Y, Zhang SQ, Wang YY, Wu YL. Natural herbal medicine Lianhuaqingwen capsule anti-influenza A (H1N1) trial: A randomized, double blind, positive controlled clinical trial. Chin Med J (Engl). 2011; 124:2925-2933.
46. Feng GZ, Zhou F, Huang M, Yao K. Inhibitory effects of Reduning injection on human rhinoviruses *in vitro*. Journal of China Pharmaceutical University. 2008; 39:262-266. (in Chinese)
47. Zhang X, Gu J, Cao L, Li N, Ma Y, Su Z, Ding G, Chen L, Xu X, Xiao W. Network pharmacology study on the mechanism of traditional Chinese medicine for upper respiratory tract infection. Mol Biosyst. 2014; 10:2517-2525.
48. Tang LP, He RR, Li YF, Li HB, Yao XS, Hiroshi K, Xiao W. Study on antipyretic effect of Reduning injection on lipopolysaccharide-induced fever rats. China Journal of Chinese Materia Medica. 2013; 38:2374-2377. (in Chinese)
49. Liu Y, Huang Y, Wei B, Liu X, Zhang Y, Huang X, Tan Y, Sun Z. Efficacy and safety of clearing heat and detoxifying injection in the treatment of influenza: a randomized, double-blinded, placebo-controlled trial. Evid Based Complement Alternat Med. 2014; 2014:1-8.
50. Li YR, Sun SG. Revaluating the rationality and safety of Reduning injections in clinical use: An integrated approach. Chinese Journal of Clinical Pharmacology. 2015; 31:569-572. (in Chinese)
51. Ko R. A U.S. perspective on the adverse reactions from traditional Chinese medicines. J Chin Med Assoc. 2004; 67:109-116.
52. Shaw D. Toxicological risks of Chinese herbs. Planta Med. 2010; 76:2012-2018.
53. Li H, Wang S, Yue Z, Ren X, Xia J. Traditional Chinese herbal injection: Current status and future perspectives. Fitoterapia. 2018; 129:249-256.
54. Qiu F, Hou XL, Takahashi K, Chen LX, Azuma J, Kang N. Andrographolide inhibits the expression and metabolic activity of cytochrome P450 3A4 in the modified Caco-2 cells. J Ethnopharmacol. 2012; 141:709-713.
55. Gu LL, Zhang XY, Xing WM, Xu JD, Lu H. Andrographolide-induced apoptosis in human renal tubular epithelial cells: Roles of endoplasmic reticulum stress and inflammatory response. Environ Toxicol Pharmacol. 2016; 45:257-264.
56. Anderson GD. Pregnancy-induced changes in pharmacokinetics: A mechanistic-based approach. Clin Pharmacokinet. 2005; 44:989-1008.
57. Pavek P, Smutny T. Nuclear receptors in regulation of biotransformation enzymes and drug transporters in the placental barrier. Drug Metab Rev. 2014; 46:19-32.
58. Myllynen P, Vahakangas K. Placental transfer and metabolism: An overview of the experimental models utilizing human placental tissue. Toxicol In Vitro. 2013; 27:507-512.
59. Wrobel MH, Mlynarczuk J. Chlorinated insecticides (toxaphene and endrin) affect oxytocin, testosterone, oestradiol and prostaglandin secretion from ovarian and uterine cells as well as myometrial contractions in cow *in vitro*. Chemosphere. 2018; 198:432-441.
60. Cao L, Pu J, Cao QR, Chen BW, Lee BJ, Cui JH. Pharmacokinetics of puerarin in pregnant rats at different stages of gestation after oral administration. Fitoterapia. 2013; 86:202-207.
61. Tracy TS, Venkataramanan R, Glover DD, Caritis SN, National Institute for Child H, Human Development Network of Maternal-Fetal-Medicine U. Temporal changes in drug metabolism (CYP1A2, CYP2D6 and CYP3A Activity) during pregnancy. Am J Obstet Gynecol. 2005; 192:633-639.
62. Zhao J, Wen LZ, Chen SH, Ling XZ. Effects of Chinese medicine Jinyebaidu Granules on immunity and genitality of pregnant mice. Chinese Traditional Patent Medicine. 2003; 25:130-133. (in Chinese)
63. Zhu J, Qiu J, Zhu Y, MA XL, Wan X, Zhang T. Teratogenicity of forsythoside gelsiccation powder in SD rats. Chinese Journal of New Drugs. 2008; 17:570-573. (in Chinese)
64. Wang L, Cheng L, Yuan Q, Cui X, Shang H, Zhang B, Li Y. Adverse drug reactions of Shuanghuanglian injection: A systematic review of public literatures. J Evid Based Med. 2010; 3:18-26.
65. Wang HS, Cheng F, Shi YQ, Li ZG, Qin HD, Liu ZP. Hypotensive response in rats and toxicological mechanisms induced by shuanghuanglian, an herbal extract mixture. Drug Discov Ther. 2008; 6:339-343.
66. Gao Y, Hou R, Han Y, Fei Q, Cai R, Qi Y. Shuang-Huang-Lian injection induces an immediate hypersensitivity reaction *via* C5a but not IgE. Sci Rep. 2018; 8:3572-3582.
67. Ma AT, Zhong XH, Liu ZM, Shi WY, Du J, Zhai XH, Zhang T, Meng LG. Protective effects of baicalin against bromocriptine induced abortion in mice. Am J Chin Med. 2009; 37:85-95.
68. Wang YH, Song J, Dong JP, Yang TT, Hao M. Effects of baicalin on mitochondria apoptotic pathway of trophoblast cells in a preeclampsia rat model. Chinese Journal of Perinatal Medicine. 2016; 12:933-939. (in Chinese)
69. Teschke R, Wolff A, Frenzel C, Schulze J. Review article: Herbal hepatotoxicity--An update on traditional Chinese medicine preparations. Aliment Pharmacol Ther. 2014; 40:32-50.
70. Li HJ, Song DR. Effect of shuanghuanglian freeze-dried powder on the contraction of isolated human uterine smooth muscle in pregnancy. Lishizhen Medicine and Materia Medica Research. 2017; 28:772-773. (in Chinese)
71. Song DR, Zhang W, Zhao LY, Guo J, Li HJ, Du WX.

Evaluation of embryo toxicity of Shuanghuanglian based on human placental barrier model. Chinese Journal of Pharmacology and Toxicology. 2017; 31:649-654. (in Chinese)
72. Chen JX, Xue HJ, Ye WC, Fang BH, Liu YH, Yuan SH, Yu P, Wang YQ. Activity of andrographolide and its derivatives against influenza virus *in vivo* and *in vitro*. Biol Pharm Bull. 2009; 32:1385-1391.
73. Mantani N, Andoh T, Kawamata H, Terasawa K, Ochiai H. Inhibitory effect of Ephedrae herba, an oriental traditional medicine, on the growth of influenza A/PR/8 virus in MDCK cells. Antiviral Res. 1999; 44:193-200.
74. Hayashi K, Imanishi N, Kashiwayama Y, Kawano A, Terasawa K, Shimada Y, Ochiai H. Inhibitory effect of cinnamaldehyde, derived from Cinnamomi cortex, on the growth of influenza A/PR/8 virus *in vitro* and *in vivo*. Antiviral Res. 2007; 74:1-8.
75. Palamara AT, Nencioni L, Aquilano K, De Chiara G, Hernandez L, Cozzolino F, Ciriolo MR, Garaci E. Inhibition of influenza A virus replication by resveratrol. J Infect Dis. 2005; 191:1719-1729.
76. Law AH, Yang CL, Lau AS, Chan GC. Antiviral effect of forsythoside A from Forsythia suspensa (Thunb.) Vahl fruit against influenza A virus through reduction of viral M1 protein. J Ethnopharmacol. 2017; 209:236-247.
77. Kong WJ, Zhao YL, Shan LM, Xiao XH, Guo WY. Thermochemical studies on the quantity-antibacterial effect relationship of four organic acids from Radix Isatidis on *Escherichia coli* growth. Biol Pharm Bull. 2008; 31:1301-1305.
78. Pan XL, Cao X, Li N, Xu YM, Wu QY, Bai J, Yin ZM, Luo L, Lan L. Forsythin inhibits lipopolysaccharide-induced inflammation by suppressing JAK-STAT and p38 MAPK signalings and ROS production. Inflamm Res. 2014; 63:597-608.
79. Lu CN, Yuan ZG, Zhang XL, Yan R, Zhao YQ, Liao M, Chen JX. Saikosaponin a and its epimer saikosaponin d exhibit anti-inflammatory activity by suppressing activation of NF-kappaB signaling pathway. Int Immunopharmacol. 2012; 14:121-126.
80. Wang W, Wang J, Dong SF, Liu CH, Italiani P, Sun SH, Xu J, Boraschi D, Ma SP, Qu D. Immunomodulatory activity of andrographolide on macrophage activation and specific antibody response. Acta Pharmacol Sin. 2010; 31:191-201.
81. Cheng BH, Chan JY, Chan BC, Lin HQ, Han XQ, Zhou X, Wan DC, Wang YF, Leung PC, Fung KP, Lau CB. Structural characterization and immunomodulatory effect of a polysaccharide HCP-2 from Houttuynia cordata. Carbohydr Polym. 2014; 103:244-249.
82. Shang XF, Pan H, Li MX, Miao XL, Ding H. Lonicera japonica Thunb.: Ethnopharmacology, phytochemistry and pharmacology of an important traditional Chinese medicine. J Ethnopharmacol. 2011; 138:1-21.
83. Hossain MS, Urbi Z, Sule A, Hafizur Rahman KM. Andrographis paniculata (Burm. f.) Wall. ex Nees: A review of ethnobotany, phytochemistry, and pharmacology. Scientific World Journal. 2014; 2014:1-28.
84. Li-Weber M. New therapeutic aspects of flavones: The anticancer properties of Scutellaria and its main active constituents Wogonin, Baicalein and Baicalin. Cancer Treat Rev. 2009; 35:57-68.
85. Shingnaisui K, Dey T, Manna P, Kalita J. Therapeutic potentials of Houttuynia cordata Thunb. against inflammation and oxidative stress: A review. J Ethnopharmacol. 2018; 220:35-43.
86. Al-Salihi, Bahia. Ma Huang (Ephedrae Herba): Setting the record straight. Journal of Chinese Medicine 2016;18-30.
87. Peng W, Qin RX, Li XL, Zhou H. Botany, phytochemistry, pharmacology, and potential application of Polygonum cuspidatum Sieb.et Zucc.: A review. J Ethnopharmacol. 2013; 148:729-745.
88. Xu YL, Xue YL, Zhang HH, Lv FY, Tian ZJ, Xing ZH, LiangJin W, Li XY. Clinical observation on treatment of acute upper respiratory infection of Wind-heat Syndrome with Shufeng Jiedu capsules: A randomize-controlled double-blind test. Journal of Traditional Chinese Medicine. 2015; 56:676-679. (in Chinese)
89. Saxena RC, Singh R, Kumar P, Yadav SC, Negi MP, Saxena VS, Joshua AJ, Vijayabalaji V, Goudar KS, Venkateshwarlu K, Amit A. A randomized double blind placebo controlled clinical evaluation of extract of Andrographis paniculata (KalmCold) in patients with uncomplicated upper respiratory tract infection. Phytomedicine. 2010; 17:178-185.
90. Yu DC, Chen B. Clinical observation of exogenous fever cured by Zheng Chai Hu instant granules. Guide of China Medicine. 2008; 6:124-125. (in Chinese)

(Received December 17, 2018; Revised March 11, 2019; Accepted March 12, 2019)

Original Article

DOI: 10.5582/bst.2018.01304

IPS-1 polymorphisms in regulating interferon response in HBV infection

Kehui Liu[1,2,§], Liwen Chen[1,§], Gangde Zhao[2,§], Zhujun Cao[1], Fengdi Li[1], Lanyi Lin[1], Chuanwu Zhu[3], Qing Xie[1], Yumin Xu[1,*], Shisan Bao[4,*], Hui Wang[1,*]

[1] *Department of Infectious Diseases, Rui Jin Hospital, Shanghai Jiao Tong University School of Medicine, Shanghai, China;*
[2] *Department of Infectious Diseases, Rui Jin Hospital North, Shanghai Jiao Tong University School of Medicine, Shanghai, China;*
[3] *Department of infectious Diseases, The Fifth People's Hospital of Suzhou, The Affiliated Infectious Diseases of Soochou University, Suzhou, China;*
[4] *Discipline of Pathology, School of Medical Sciences and The Bosch Institute, The University of Sydney, Sydney, NSW, Australia.*

Summary **Single nucleotide polymorphisms (SNP) influence the outcome of antiviral therapy in chronic hepatitis B patients. Interferon β promoter stimulator 1 polymorphisms (IPS-1) regulate interferon (IFN) mediated viral clearance in hepatitis B virus (HBV) infection. In our study, HepG2 and HepG2.2.15 were transfected with different SNP genotype expression vectors of IPS-1 (wild-type, rs17857295, rs7262903 and rs7269320). The production of IPS-1 and IFN were evaluated in these transfected cells. IPS-1 in the HepG2.2.15 cells transfected with rs17857295 or rs7262903 was 37% or 31% lower than that with wild-type transfection ($p < 0.001$). IFN-β in rs17857295 or rs7262903 transfected HepG2.2.15 cells was 5.4 or 3.7 fold higher than that of wild-type transfection ($p < 0.0001$). IPS-1 in rs7269320 SNP transfected HepG2.2.15 cells was 40% lower than that of wild-type transfection ($p < 0.0001$); no significantly different IFN-β was observed between rs7269320 SNP and wild-type transfections. IFN-β expression was > 2 fold higher in rs17857295 transfected HepG2.2.15 cells than HepG2 cells ($p < 0.001$). The data suggests that host HBV viral clearance is stronger in IPS-1 rs17857295 or rs7262903 SNP genotype patients than wild-type patients. Relatively weak inducible IFN-β production in HBV infected patients with IPS-1 rs7269320 SNP or wild-type may contribute to chronic virus infection.**

Keywords: IPS-1, single nucleotide polymorphism, hepatitis B virus, interferon response, chronic HBV infection

1. Introduction

Chronic hepatitis B (CHB) is still a major challenge to clinicians, due to its serious clinical complications with huge financial and psychological burdens (*1,2*). The precise pathogenesis of CHB is not fully clear, especially the host immunity in CHB viral clearance, and subsequent chronicity, despite decades of extensive research (*3*).

Single nucleotide polymorphism (SNP) is a polymorphism at the genome level, due to a single nucleotide missense mutation (*4*). Missense mutation of a single nucleotide in genetic code leads to the change of the sequence of bases, and transforms the amino acid sequence of the corresponding protein, influencing the structure and function of proteins. SNP is an important biological genetic marker, causing a biological genetic trait change. SNPs determine the effect of drug therapy and/or disease susceptibility in different genetic backgrounds, which may also contribute to different host immunities, especially antiviral immunity (*5*).

Host antiviral innate immunity is initiated *via* viral

Released online in J-STAGE as advance publication March 29 2019.

[§]These authors contributed equally to this work.

**Address correspondence to:*
Drs. Hui Wang and Yumin Xu, Department of Infectious Diseases, Rui Jin Hospital, Shanghai Jiao Tong University School of Medicine, Shanghai 200025, China.
E-mail: wanghuirj@163.com (HW); xym121@163.com (YX)

Dr. Shisan Bao, Discipline of Pathology, School of Medical Sciences and Bosch Institute, University of Sydney, Sydney, NSW 2006, Australia.
E-mail: bob.bao@sydney.edu.au

pathogen-associated molecular patterns (PAMP), such as viral double-stranded RNA(dsRNA). All RNA and most DNA viruses, including HBV (*6*), generate dsRNA molecules at the transcription or replication level. Retinoic acid inducible gene-I (RIG-I) and melanoma differentiation-associated gene 5 (MDA5) are very important pattern recognition receptors (PRRs) *in vivo* (*7*). RIG-I/MDA5 signaling pathway plays an important role in host recognition and clearance of the virus infection process (*8*). After binding to dsRNA, RIG-I transforms into an open conformation, translocates onto mitochondria, and interacts with the downstream adaptor to induce the production of interferon (IFN) and inflammatory factors *via* IRF3/7 and NF-κB pathways. IFN-β promoter stimulator 1 (IPS-1), an essential adaptor protein in the RIG-I/MDA5 anti-viral pathway, plays an important role in the cell recognition and the induce process of IFN-β during viral infection (*9-12*). Upregulation of IPS-1 results in increased production of IFN-β, which finally prevents viral entry (*9,12*). RIG-I mediated antiviral immunity and its downstream signaling pathway have been well illustrated in hepatitis C virus (HCV) infection (*13*). Following HBV stimulation, MDA5 activates innate immune signaling to suppress hepatitis B virus (HBV) replication (*14*). IFN inhibits HBV replication *via* the MDA5/IPS-1 pathway, but patients display different prognosis to HBV infection.

Studies on genetics determine susceptibility of HBV infection and subsequent chronicity has been well documented in families of segregation analysis or twin studies (*15,16*). SNP of IL28B is responsible for the therapeutic outcomes following PEG-IFN plus ribavirin treatment in chronic viral hepatitis C (CHC) (*17*). It has been demonstrated that three SNPs upstream of IL28B (rs12979860 CC, rs12980275 AA, and rs8099917 TT) are highly associated with HCV recovery, but inversely with HBV (*18*). Recent study of polymorphisms near IL28B (rs12980275AA, rs12979860 CC) have also demonstrated an association with serologic response to PEG-IFN in HBeAg+ CHB patients (*19*). Interestingly, IL28B rs12979860 CC genotype do not contribute to the outcome of HBV infection (*20*). HLA-DPA1 rs3077G/G is associated with HBeAg seroconversion and combined response rates at 6 months of the reply in $HBeAg^+$ CHB patients with IFN, suggesting HLA-DPA1 contributes to IFN-induced HBeAg seroconversion (*21*). Our previously published data demonstrates that polymorphisms in IPS-1 (rs2464 CC) are independently associated with response to PEG-IFN among Chinese $HBeAg^+$ CHB patients (*22*). The data from ourselves and others illustrates that different proteins regulated by SNPs contribute to HBV viral clearance and subsequent disease outcome *via* host antiviral immunity in response of interferon. However, it was still unclear whether SNP of IPS-1 polymorphisms influences IFN response in HBV infection.

2. Materials and Methods

2.1. *Cell lines and Culture*

HepG2 and HBV-replication-stable HepG2.2.15 cell lines were maintained in our laboratory, which were obtained from the Chinese Academy of Sciences (*23-25*). HEK293T cells, obtained from American Type Culture Collection, were used as a transfection positive control (*26*). HepG2, HepG2.2.15 and HEK293T cells were cultured in DMEM medium, supplemented with 10% fetal bovine serum at 37°C (Life Technologies, Carlsbad, CA), in a humidified atmosphere containing 5% CO_2.

2.2. *Site-directed Mutagenesis*

The sequences containing IPS-1 cDNA (FL18489) based on a human cDNA library were inserted into pCMV-SPORT6 plasmid, and then transfected into *E. coli* for amplification. The correct clone was confirmed with sequencing, and used as positive control. Primers were designed including the whole ORF sequences of IPS-1, joining enzyme loci Bgl II and Cal I at the both ends, respectively. In addition, KOZAK was also added as protection. The sequence of these two strains of primers were as follows: IPS-1seq-sense: ACCAGATCTGCCACCATGCCGT TTGCTGAAGACAAGACC; IPS-1seq-antisense: ATTGTCGACCTAGTGCAGACGCCGCCGGTA. IPS-1 cDNA fragment, inserted into pRRL-cPPT-PGK-eGFP-WPRE plasmid (Addgene#12252), was amplified for final identification.

Three point mutations, identified from each sequence of IPS-1 cDNA, were localized at the position of the SNPs of interest (Supplement Figure S1, *http://www.biosciencetrends.com/action/getSupplementalData.php?ID=40*). We used site-directed mutagenesis to obtain the wild-type vector of IPS-1 and other different expression vectors of SNP genotype. The primers for site-directed mutagenesis are listed in Supplement Table S1 (*http://www.biosciencetrends.com/action/getSupplementalData.php?ID=40*). PCR was performed as follows: 94°C for 2 minutes, then 25 cycles at 94°C for 15 seconds, 56°C for 30 seconds, 68°C for 1 minute, and 68°C for 9 minutes.

2.3. *qRT-PCR*

HEK293T, HepG2 and HepG2.2.15 cells were transfected with human wild-type IPS-1 or different IPS-1 SNP genotypes (rs17857295, rs7262903 or rs7269320), respectively in triplicate plates. RNA was extracted from individual treated cells, using Trizol (Life Technologies, Carlsbad, CA). cDNA was generated from 1μg total RNA, using the RevertAid™ Reverse Transcriptase kit (Thermo Fisher Scientific, Waltham, MA). The forward and reverse primers for pgRNA are listed in Supplement

Table S2 (*http://www.biosciencetrends.com/action/getSupplementalData.php?ID=40*). qRT-PCR was performed as follows: 95°C for 2 minutes, then 40 cycles at 95°C for 15 seconds, 60°C for 20 seconds, 72°C for 20 seconds, and 39 cycles at 72°C for 30 seconds.

2.4. *Western Blot*

Protein was extracted from these treated cells after lysing with RIPA buffer (Abcam, Cambridge, UK) for Western blot. Electrophoresis was performed after protein quantification using BCA kit (Abcam, Cambridge, UK). The blots were blocked and labeled with primary antibodies (rabbit anti-human IPS-1, Millipore, Darmstadt, Germany) overnight. Membranes were incubated with secondary antibody (goat anti-rabbit-HRP, Amersham Pharmacia Biotech, Saclay, France). The signal was developed and imaged using ImageQuant™ LAS 4000 (Fujifilm, Tokyo, Japan).

2.5. *Statistical analysis*

All data were expressed as the mean ± standard deviation (SD). Two-tailed Student's *t*-test and one-way ANOVA were used for data analysis. All statistical analyses were performed using the SPSS for Windows, Version 19.0 (SPSS Inc., Chicago, IL). Differences were considered statistically significant at $P < 0.05$.

3. Results

3.1. *Construction of recombinant mammalian expressing vector with different IPS-1 SNP genotypes*

It was confirmed that constructions of recombinant mammalian expressing vector carried IPS-1 wild-type or other SNP genotypes (rs17857295, rs7262903 or rs7269320), by sequencing (Figure 1). Furthermore, to verify the ability to express IPS-1 properly, HEK293T cells (GFP gene contained in pRRL-cPPT-PGK-eGFP-WPRE plasmid) were transfected with the vectors, which carried wild-type or different IPS-1 SNPs. Thus GFP production in the cells indicates successful and stable transfection. IPS-1 mRNA from the wild-type or SNP mutated gene type transfected cells were significantly higher than that of mock transfected cells ($p < 0.05$) (Figure 2), confirming the vector plasmids were successfully generated with correct sequence.

3.2. *IPS-1 polymorphisms in HBV infection*

Subsequently, to determine the relationship between SNPs and IPS-1 expression during HBV infection in hepatocytes, HepG2 or HepG2.2.15 cells were transfected with the vectors containing IPS-1 SNPs or wild-type genotypes, respectively. IPS-1 gene

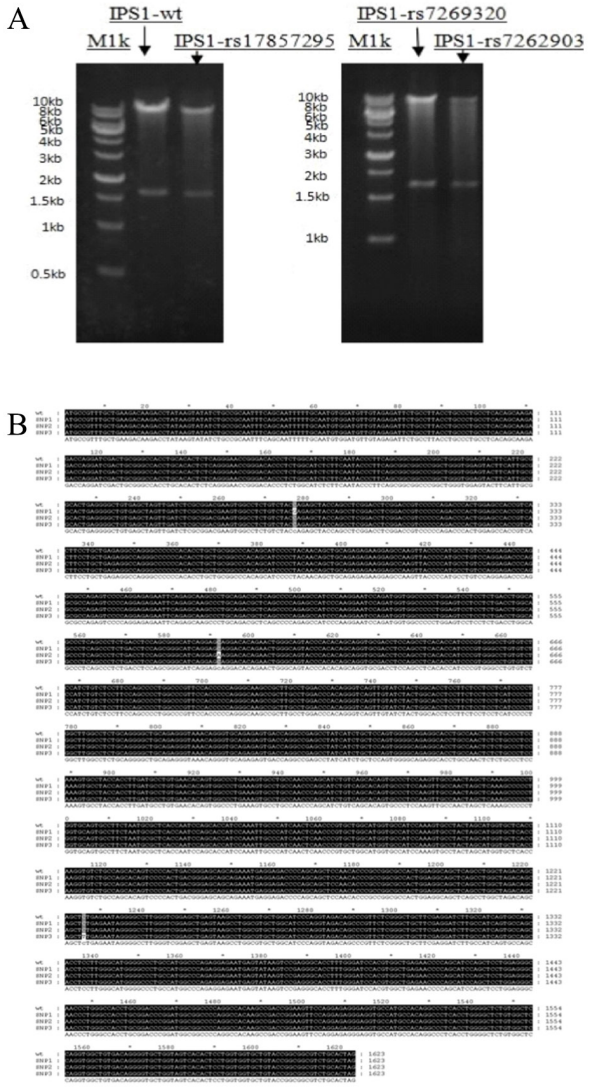

Figure 1. Construction of recombinant mammalian expressing vector with different IPS-1 SNP genotypes. (A). Incision enzyme digestion of different IPS-1 genotype plasmids; **(B).** Sequencing of different IPS-1 genotype plasmids (wt: IPS-1 wildtype, SNP1: rs17857295, SNP2: rs7269320, SNP3: rs7262903).

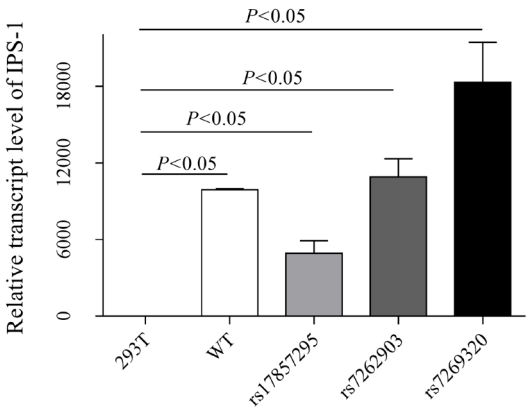

Figure 2. The expression of IPS-1 mRNA in different IPS-1 SNP genotype plasmids transfected 293T cells.

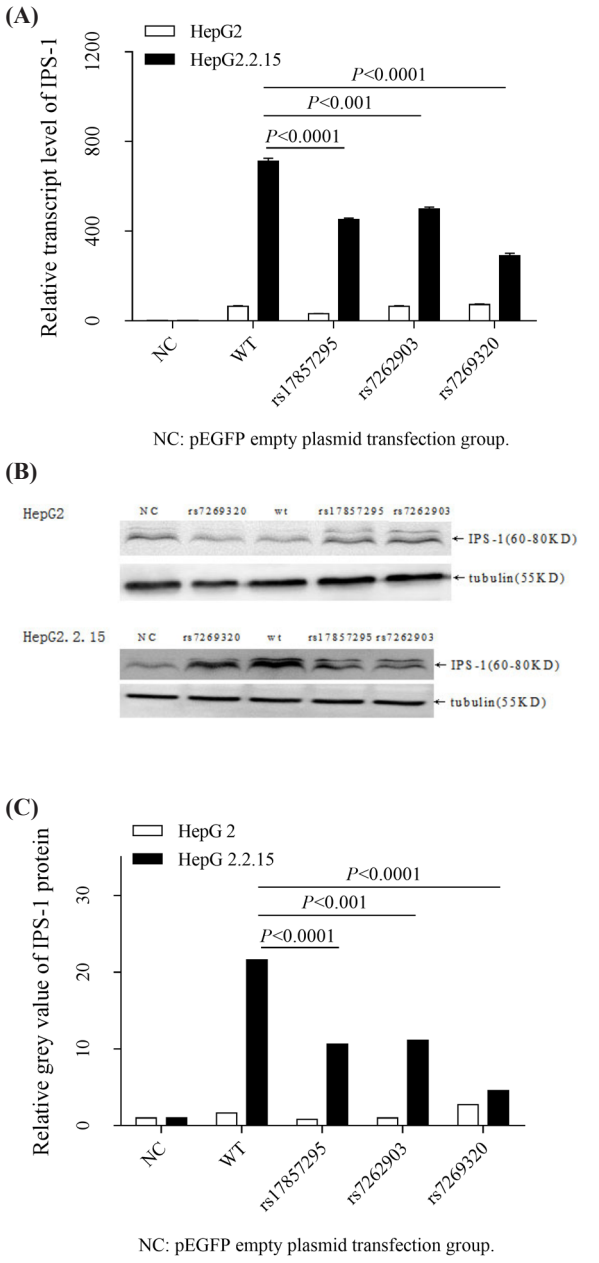

Figure 3. The expression of IPS-1 in different IPS-1 genotype plasmids transfected HepG2 or HepG2.2.15 groups. (A). The expression of IPS-1 mRNA in different IPS-1 genotype plasmids transfected HepG2 or HepG2.2.15 groups. **(B).** Western Blot detect different IPS-1 genotype plasmids transfected HepG2 or HepG2.2.15 groups. **(C).** The analysis of grey value among different IPS-1 genotype plasmids transfected HepG2 or HepG2.2.15 groups.

was significantly higher in the cells transfected with these three different IPS-1 SNPs or wild-type than the mock transfected group ($p < 0.05$). IPS-1 mRNA level in HepG2.2.15 cells transfected with wild-type, rs17857295, rs7262903, rs7269320 was 11, 14, 8 or 4 fold higher than HepG2 cells ($p < 0.05$). In contrast, IPS-1 mRNA level was 37%, 31%, 40% lower in the HepG2.2.15 cells transfected with IPS-1 rs17857295, rs7262903 or rs7269320 ($p < 0.05$) SNP genotypes than wild genotype transfection group (Figure 3A).

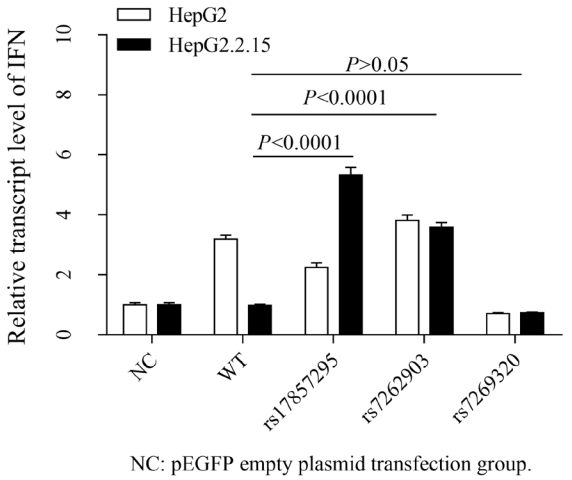

Figure 4. The expression of IFN-β in different IPS-1 genotype plasmids transfected HepG2 or HepG2.2.15 groups.

To confirm if the modification of IPS-1 was consistent between mRNA and protein, Western blot was conducted, demonstrating that IPS-1 was reduced by 49%, 52%, or 21% in the HepG2.2.15 cells transfected with rs17857295, rs7262903 or rs7269320 than that of wild-type transfection ($p < 0.05$) (Figure 3B and 3C). Interestingly, IPS-1 protein was 13, 13, 11, or 2 fold higher in HepG2.2.15 cells than in HepG2 cells with different transfection, *i.e.* wild-type, rs17857295, rs7262903, rs7269320 (Figure 3C).

3.3. *IPS-1 SNP polymorphisms regulate interferon response in HBV infection*

To determine the role of IPS-1 SNP polymorphisms in regulating interferon response in HBV infection, IFN-β mRNA level was detected after the vectors containing these three different IPS-1 SNPs or wild-type genotypes transfected into HepG2 or HepG2.2.15 cells. In HepG2.2.15 cells, IFN-β expression in IPS-1 wild-type vector transfected group had no obvious change compared to pEGFP empty control group. IFN-β mRNA level was 5.4 or 3.7 fold higher in the transfected HepG2.2.15 cells with IPS-1 rs17857295 or rs7262903 SNP genotypes than wild genotype transfected group ($p < 0.0001$). In IPS-1 rs7269320 SNP genotypes transfected groups, IFN-β expression had no obvious change compared to wild-type group. In addition, in IPS-1 rs17857295 genotype vectors transfected groups, the IFN-β mRNA level in HepG2.2.15 cells was > 2 fold higher than that in HepG2 cells ($p < 0.001$) (Figure 4).

4. Discussion

Following transfection of rs17857295 or rs7262903 in the HBV carried hepatocytes, IPS-1 was suppressed, but IFN-β was up-regulated compared to that with

wild-type transfection. IPS-1, but not IFN-β, was suppressed in the HBV carried hepatocytes transfected with rs7269320 SNP compared to that with wild-type transfection. IFN-β was higher in rs17857295 transfected HBV carried hepatocytes than in non-HBV carried hepatocytes.

IPS-1 plays a critical role in the RIG-I signaling pathway, leading to IFN-β activation in cells following viral stimulation (*9-11*). However, viruses may still circumvent IFN initiated host response *via* an unknown mechanism in susceptible individuals (*14,27*), resulting in chronic viral infection. Lin *et al*. (*28*) demonstrated that HCV protease NS3-4A inhibits IFN-β production *via* degrading IPS-1 protein. However, the effect of IPS-1 SNP polymorphism during HBV infection is still unclear. Among 29314bp DNA sequences within IPS-1 gene, 229 SNPs loci have been discovered. Considering the effects on the protein structure and function, we focused on the missense coding SNP (cSNP) sites within the IPS-1 gene. Three out of 12 missense cSNP sites show a mutation frequency which is > 1%, including rs17857295 in exon 3 (446 g>C, Q93E), rs7262903 in exon 5 (761 a>C, Q198K) and rs7269320 in exon 7 (1395 t>C, S409F). The encoding amino acids of rs17857295 loci is in the connection position between CARD structure domain and a proline rich area (Pro-rich), suggesting this SNP is closely related to the IPS-1function (*29*).

In the current study, IPS-1 was significantly higher in the wild type or SNPs transfected HBV carried hepatocytes (HepG2.2.15 cells) than that in non-HBV carried hepatocytes (HepG2 cells), suggesting that IPS-1 production is responding to HBV infection in the hepatocytes. Our data is in line with our previously published data in macrophages, IPS-1 in macrophages from CHB patients is significantly higher than that of good health controls following vesicular stomatitis virus stimulation (*26*).

Furthermore, IPS-1 was suppressed in any of the SNPs transfected (rs17857295, rs7262903 or rs7269320) HBV carried hepatocytes compared to that transfected with wild type. In contrast, IFN-β was substantially higher in the rs17857295 or rs7262903 SNP transfection HBV carried hepatocytes than that of the wild type transfected group. This is consistent with our previous finding that IPS-1 in macrophages from CHB patients is significantly higher than that of good health controls or acute hepatitis B, following vesicular stomatitis virus stimulation, inversely correlated with IFN-β production (*26*). Our current finding suggests that increased IPS-1 production from the virus stimulation in HBV carried hepatocytes is due to compensation for compromised IPS-1 function, and possibly due to interference from HBV infection. This is supported by the finding that HBx protein of HBV interferes the ubiquitination of IPS-1 to restrain the RIG-I pathway of innate immunity (*30*). However the underlying mechanisms leading to compromised IPS-1 function still remain to be explored.

Such findings invite speculation that the viral infection signals are delivered more effectively in rs17857295 and/or rs7262903 SNP transfected HBV viral carried hepatocytes compared with wild-type transfected ones, contributing to IFN-β mediated anti-viral immunity. In addition, IFN-β from rs17857295 transfected HBV carried hepatocytes was significantly higher than from non-HBV carried hepatocytes. No significantly different IFN-β production was detected between HBV carried and non-HBV carried hepatocytes following wild-type transfection, suggesting IPS-1 rs17857295 SNP may play an important role in host resistance to HBV challenge. Moreover, there was no significantly different IFN-β between wild type and rs7269320 SNP transfection, suggesting rs7269320 mutation may not be a critical factor or may be compensated by other factors in the viral host. The precise underlying mechanism will be determined in the future.

There are some limitations in our current study: First, the current study was mainly focused on basic virology. Thus future experiments may focus more on clinical research. Second, more downstream pathways of IPS-1 in RIG-I will be explored in the future. Third, in our current experiment there was correlated up-regulation of IPS-1 and IFN-β, but the viral load wasn't determined at the same time. However it is well known that IFN-β is responsible for viral clearance. Thus it invites speculation that IPS-1 rs17857295 or rs7262903 SNP genotype might contribute to viral clearance. The precise correlation between IPS-1 and viral clearance will be determined in our future study.

In conclusion, rs17957295 and rs7262903 IPS-1 SNP genotypes may contribute to viral clearance, especially rs17857295 SNP genotypes, in comparison with the wild-type or rs7269320 SNP genotypes in HBV infected patients.

Acknowledgements

This work was supported by grants from the National Natural Science Foundation of China [81570560; 81670569]; Technology Supporting Project of the Science and Technology Commission Shanghai Municipality [16411960300]; Suzhou Clinical Medicine Expert Team Introduced Project [SZYJTD201717]; The Shanghai key project of Integrated Traditional Chinese and Western Medicine [ZY (2018-2020)-FWTX-3001] and The Medical Science Research Foundation [YWJKJJHKYJJ-B17503].

References

1. Chen CJ, Yang HI, Su J, Jen CL, You SL, Lu SN, Huang GT, Iloeje UH, Group R-HS. Risk of hepatocellular

carcinoma across a biological gradient of serum hepatitis B virus DNA level. JAMA. 2006; 295:65-73.
2. Sarin SK, Kumar M, Lau GK, *et al*. Asian-Pacific clinical practice guidelines on the management of hepatitis B: A 2015 update. Hepatol Int. 2016; 10:1-98.
3. Morikawa K, Shimazaki T, Takeda R, Izumi T, Umumura M, Sakamoto N. Hepatitis B: Progress in understanding chronicity, the innate immune response, and cccDNA protection. Ann Transl Med. 2016; 4:337.
4. Collins FS, Patrinos A, Jordan E, Chakravarti A, Gesteland R, Walters L. New goals for the U.S. Human Genome Project: 1998-2003. Science. 1998; 282:682-689.
5. Moudi B, Heidari Z, Mahmoudzadeh-Sagheb H. Impact of host gene polymorphisms on susceptibility to chronic hepatitis B virus infection. Infect Genet Evol. 2016; 44:94-105.
6. Patel N, White SJ, Thompson RF, Bingham R, Weiss EU, Maskell DP, Zlotnick A, Dykeman E, Tuma R, Twarock R, Ranson NA, Stockley PG. HBV RNA pre-genome encodes specific motifs that mediate interactions with the viral core protein that promote nucleocapsid assembly. Nat Microbiol. 2017; 2:17098.
7. Beachboard DC, Horner SM. Innate immune evasion strategies of DNA and RNA viruses. Curr Opin Microbiol. 2016; 32:113-119.
8. Kell AM, Gale M, Jr. RIG-I in RNA virus recognition. Virology. 2015; 479-480:110-121.
9. Kawai T, Takahashi K, Sato S, Coban C, Kumar H, Kato H, Ishii KJ, Takeuchi O, Akira S. IPS-1, an adaptor triggering RIG-I- and Mda5-mediated type I interferon induction. Nat Immunol. 2005; 6:981-988.
10. Meylan E, Curran J, Hofmann K, Moradpour D, Binder M, Bartenschlager R, Tschopp J. Cardif is an adaptor protein in the RIG-I antiviral pathway and is targeted by hepatitis C virus. Nature. 2005; 437:1167-1172.
11. Seth RB, Sun L, Ea CK, Chen ZJ. Identification and characterization of MAVS, a mitochondrial antiviral signaling protein that activates NF-kappaB and IRF 3. Cell. 2005; 122:669-682.
12. Xu LG, Wang YY, Han KJ, Li LY, Zhai Z, Shu HB. VISA is an adapter protein required for virus-triggered IFN-beta signaling. Mol Cell. 2005; 19:727-740.
13. Yang DR, Zhu HZ. Hepatitis C virus and antiviral innate immunity: Who wins at tug-of-war? World J Gastroenterol. 2015; 21:3786-3800.
14. Lu HL, Liao F. Melanoma differentiation-associated gene 5 senses hepatitis B virus and activates innate immune signaling to suppress virus replication. J Immunol. 2013; 191:3264-3276.
15. Thursz M. Genetic susceptibility in chronic viral hepatitis. Antiviral Res. 2001; 52:113-116.
16. Akcay IM, Katrinli S, Ozdil K, Doganay GD, Doganay L. Host genetic factors affecting hepatitis B infection outcomes: Insights from genome-wide association studies. World J Gastroenterol. 2018; 24:3347-3360.
17. Ge D, Fellay J, Thompson AJ, Simon JS, Shianna KV, Urban TJ, Heinzen EL, Qiu P, Bertelsen AH, Muir AJ, Sulkowski M, McHutchison JG, Goldstein DB. Genetic variation in IL28B predicts hepatitis C treatment-induced viral clearance. Nature. 2009; 461:399-401.
18. Kim SU, Song KJ, Chang HY, Shin EC, Park JY, Kim DY, Han KH, Chon CY, Ahn SH. Association between IL28B polymorphisms and spontaneous clearance of hepatitis B virus infection. PloS One. 2013; 8:e69166.
19. Sonneveld MJ, Wong VW, Woltman AM, Wong GL, Cakaloglu Y, Zeuzem S, Buster EH, Uitterlinden AG, Hansen BE, Chan HL, Janssen HL. Polymorphisms near IL28B and serologic response to peginterferon in HBeAg-positive patients with chronic hepatitis B. Gastroenterology. 2012; 142:513-520 e511.
20. Martin MP, Qi Y, Goedert JJ, Hussain SK, Kirk GD, Hoots WK, Buchbinder S, Carrington M, Thio CL. IL28B polymorphism does not determine outcomes of hepatitis B virus or HIV infection. J Infect Dis. 2010; 202:1749-1753.
21. Tseng TC, Yu ML, Liu CJ, Lin CL, Huang YW, Hsu CS, Liu CH, Kuo SF, Pan CJ, Yang SS, Su CW, Chen PJ, Chen DS, Kao JH. Effect of host and viral factors on hepatitis B e antigen-positive chronic hepatitis B patients receiving pegylated interferon-alpha-2a therapy. Antivir Ther. 2011; 16:629-637.
22. Wang H, Wu H, Bao S, Xiang X, Zhao G, Liu K, Li F, Xu Y, An B, Zhou H, Lu J, Xie Q. Association of IPS1 polymorphisms with peginterferon efficacy in chronic hepatitis B with HBeAg-positive in the Chinese population. Infect Genet Evol. 2015; 31:161-168.
23. Sells MA, Chen ML, Acs G. Production of hepatitis B virus particles in Hep G2 cells transfected with cloned hepatitis B virus DNA. Proc Natl Acad Sci U S A. 1987; 84:1005-1009.
24. Dong C, Qu L, Wang H, Wei L, Dong Y, Xiong S. Targeting hepatitis B virus cccDNA by CRISPR/Cas9 nuclease efficiently inhibits viral replication. Antiviral Res. 2015; 118:110-117.
25. Wang H, Liu K, Fang BAM, Wu H, Li F, Xiang X, Tang W, Zhao G, Lin L, Bao S, Xie Q. Identification of acetyltransferase genes (HAT1 and KAT8) regulating HBV replication by RNAi screening. Cell Biosci. 2015; 5:66.
26. Zhao G, An B, Zhou H, Wang H, Xu Y, Xiang X, Dong Z, An F, Yu D, Wang W, Bao S, Xie Q. Impairment of the retinoic acid-inducible gene-I-IFN-beta signaling pathway in chronic hepatitis B virus infection. Int J Mol Med. 2012; 30:1498-1504.
27. Randall RE, Goodbourn S. Interferons and viruses: An interplay between induction, signalling, antiviral responses and virus countermeasures. J Gen Virol. 2008; 89:1-47.
28. Lin R, Lacoste J, Nakhaei P, Sun Q, Yang L, Paz S, Wilkinson P, Julkunen I, Vitour D, Meurs E, Hiscott J. Dissociation of a MAVS/IPS-1/VISA/Cardif-IKKepsilon molecular complex from the mitochondrial outer membrane by hepatitis C virus NS3-4A proteolytic cleavage. J Virol. 2006; 80:6072-6083.
29. Potter JA, Randall RE, Taylor GL. Crystal structure of human IPS-1/MAVS/VISA/Cardif caspase activation recruitment domain. BMC Struct Biol. 2008; 8:11.
30. Kumar M, Jung SY, Hodgson AJ, Madden CR, Qin J, Slagle BL. Hepatitis B virus regulatory HBx protein binds to adaptor protein IPS-1 and inhibits the activation of beta interferon. J Virol. 2011; 85:987-995.

(Received December 27, 2018; Revised March 11, 2019; Accepted March 14, 2019)

Original Article

DOI: 10.5582/bst.2018.01309

A Clinical scoring model to predict mortality in HIV/TB co-infected patients at end stage of AIDS in China: An observational cohort study

Zhe Zhang[1,2,§], Ling Xu[3,§], Xiaoli Pang[1,2], Yongqin Zeng[4], Yiwei Hao[5], Yu Wang[1,2], Liang Wu[1,2], Guiju Gao[1,2], Di Yang[1,2], Hongxin Zhao[1,2,*], Jiang Xiao[1,2,*]

[1] *Clinical and Research Center of Infectious Diseases, Beijing Ditan Hospital, Capital Medical University, China;*
[2] *The National Clinical Key Department of Infectious Diseases, Beijing Ditan Hospital, Capital Medical University, China;*
[3] *Department of Infectious Diseases, Peking Union Medical College Hospital, Chinese Academy of Medical Science & Peking Union Medical College, Beijing, China;*
[4] *Clinical and Research Center of Infectious Diseases, Beijing Ditan Hospital, Health Science Center, Beijing University, China;*
[5] *Division of Medical Records and Statistics, Beijing Ditan Hospital, Capital Medical University, China.*

Summary **We construct and validate a non-invasive clinical scoring model to predict mortality in HIV/TB patients at end stage of AIDS in China. There were 1,007 HIV/TB patients admitted to Beijing Ditan Hospital from August 2009 to January 2018 included in this study, who were randomly assigned to form derivation cohort and validation cohort. A clinical scoring model was developed based on predictors associated with mortality identified with Cox proportional hazard models. The discrimination and accuracy of model were further validated using the area under the ROC curves. The derivation and validation cohort consisted of 807 and 200 patients in 8:2 ratio, respectively. In derivation cohort, anemia (HGB < 90g/L), tuberculous meningitis, severe pneumonia, hypoalbuminemia, unexplained infections or space-occupying lesions, and malignancies remained independent risk factors of mortality in HIV/TB co-infected patients, and included in this clinical scoring model. The model indicated good discrimination, including AUC = 0.858 (95% CI: 0.782-0.943) in the derivation cohort, and AUC = 0.867 (95% CI: 0.832-0.902) in validation cohort, respectively. The predicted scores were categorized into two groups to predict the mortality: low-risk (0-2 points with mortality with 3.6-9.1%) and high-risk (4-16 points with mortality with 26.42-74.62%), in which 54.55% and 74.62% of patients with score of 5 to 11 and 12-16 were died among high-risk group. Kaplan-Meier curve indicated a significant difference in the cumulative mortality in the two groups by log-rank test ($p < 0.001$). A clinical scoring model to assess the prognosis in HIV/TB patients at end stage of AIDS was constructed based on simple laboratory and clinical features available at admission, which may be an easy-to-use tool for physicians to evaluate the prognosis and treatment outcome in HIV/TB co-infected patients. The model was also applicable for predicting the death of end-stage HIV/TB patients within a 12 months period after discharge.**

Keywords: HIV, TB, mortality, risk score, China

Released online in J-STAGE as advance publication March 29, 2019.

[§]These authors contributed equally to this work.
******Address correspondence to:*
Dr. Jiang Xiao and Dr. Hongxin Zhao, Clinical and Research Center of Infectious Diseases, Beijing Ditan Hospital, Capital Medical University, Jingshun East Street, Chaoyang District, Beijing 100015, China.
E-mail: shawjiang@163.com (JX) and 13911022130@163.com (HXZ)

1. Introduction

Mycobacterium Tuberculosis was the most important opportunistic pathogen in HIV/AIDS patients, and epidemiological data from World Health Organization (WHO) indicated that 12% of tuberculosis (TB) patients occurred in HIV/AIDS population (*1*). In sub-Sahara countries, the prevalence of HIV/TB co-infection was much higher and 80% of TB patients were found in

people living with HIV (*1*). Our previous study also indicated that TB infection was the most predominant opportunistic infection and prevalence was 32.5% in HIV-infected population in China (*2*).

It was reported that (*3*) synergic interaction was found in HIV/TB co-infection and TB infection promoted HIV-associated immunosuppression, which enhanced mortality in HIV/TB co-infected population. Although different guidelines were established to improve the principle for treatment outcome and prognosis in HIV/TB co-infected patients, TB was the most common cause of death in HIV-infected population. Epidemiological investigation indicated that overall mortality was 15.92% in HIV/TB co-infected patients in China (*4*).

Although previous studies (*5*) indicated that, in HIV/TB co-infected patients in China, some risk factors, including timely diagnosis of TB, optimization of timing of initiation of antiretroviral therapy, and tuberculous meningitis were associated with mortality, it was rarely reported that a standardized clinically scoring model was developed to assess the prognosis of HIV/TB co-infected patients at end stage of AIDS in China. Some literature reported (*6*) that at least a clinical scoring model was currently developed to predict mortality in HIV/TB co-infected patients, but complicated formula and calculation were required in this scoring model. Therefore, development of a clinically scoring model was badly in need for clinicians due to higher mortality, which helped to determine the prognosis and treatment outcome in HIV/TB co-infected patients at end stage of AIDS in China.

2. Patients and Methods

2.1. *Ethical consideration*

This observational study was carried out in Beijing Ditan Hospital based on principles of Declaration of Helsinki, and it was approved by ethical review committee of the hospital. Medical informed consent was waived due to anonymously using clinical information which was summarized from medical records.

2.2. *Study population*

We reviewed 1,070 HIV/TB co-infected patients at end stage of AIDS admitted to Beijing Ditan Hospital, the largest referral hospital for HIV/AIDS population in China, from August 2009 to January 2018. We excluded foreigners, those aged less than 18 years old, the ones who had baseline data missing, and those diagnosed as old tuberculosis (Figure 1). The patients received 12-month follow-up after discharge. Electronic medical records were reviewed and abstracted to develop a standardized clinically scoring model to determine the prognosis and treatment outcome in HIV/TB co-infected patients at end stage of AIDS.

2.3. *Diagnosis and treatment*

Diagnosis of active tuberculosis diseases in HIV-infected patients was based on *Guidelines for Prevention and Treatment of Opportunistic Infections*

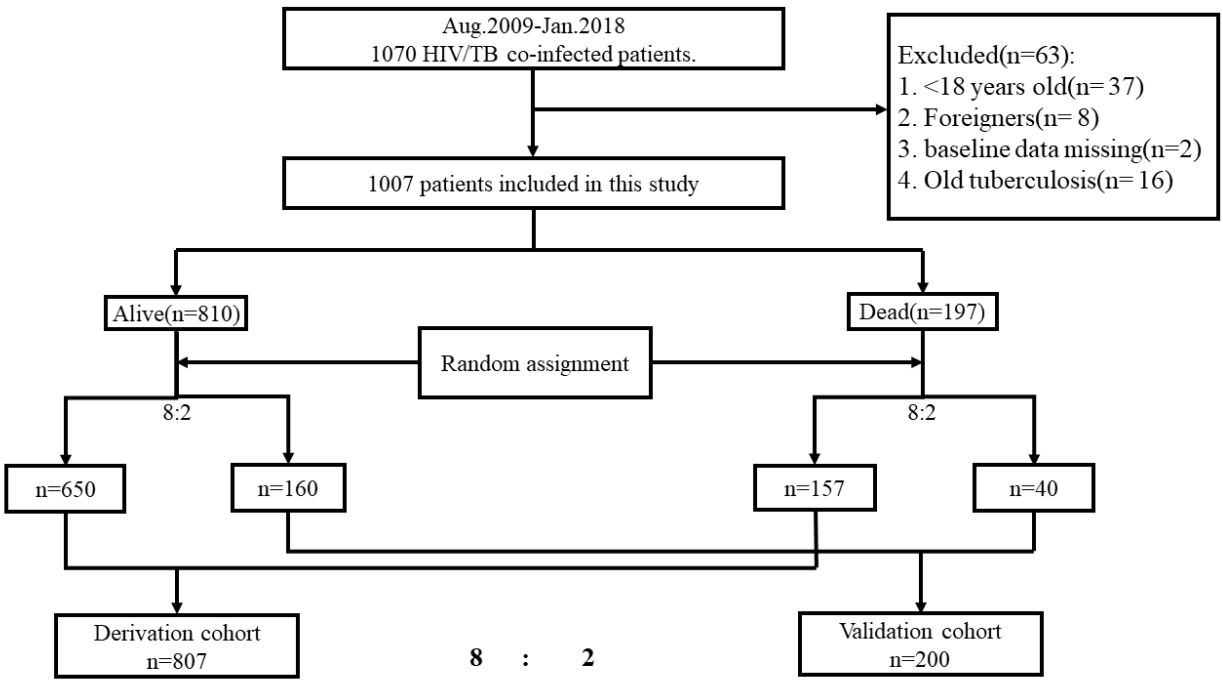

Figure 1. Flow chart of study population and random assignment with ratio of 8:2.

in HIV-Infected Adults and Adolescents recommended by U.S. Center for Disease Control and Prevention (CDC) (*7*). Etiologic diagnosis in HIV-infected patients with suspected active tuberculosis was based on culture and isolation of *Mycobacterium Tuberculosis* in different samples, including sputum,bronochoalveolar lavage fluid (BALF), pleural effusion, ascites and cerebrospinal fluid (CSF). Gene-X-Pert and nucleic acid amplification were also applied in above samples to provide rapid diagnosis of tuberculosis infection. interferon-γ releasing assay (IGRA) was also screened in blood samples in patients with suspected active tuberculosis with related clinical manifestations. Pathological examination of acid-fast bacilli (AFB) was conducted in BALF, pleural effusion, ascites, CSF and samples of lymph nodes or surgical resection.

Anti-tuberculosis treatment was based on guideline recommended by U.S. CDC (*7*), including intensive phase with isoniazid, rifampin, ethambutol and pyrazinamide and continuation phase with isoniazid and rifampin. Adjunctive corticosteriod was also used in patients with HIV-related TB involving central nervous system or pericardium.

Beside active tuberculosis diseases, other opportunistic infections (OIs) in HIV/TB co-infected patients at end stage of AIDS were diagnosed and managed in accordance with *Guidelines for Prevention and Treatment of Opportunistic Infections in HIV-Infected Adults and Adolescents* recommended by U.S. CDC (*7*). The malignant lymphoma and non-AIDS-defining malignancies were diagnosed based on pathological and imaging diagnosis, and managed according to *HIVBOOK* edited by Christian Hoffmann (*8*).

Antiretroviral therapy was recommended to HIV/TB co-infected patients at end stage of AIDS based on Chinese *National free HIV antiretroviral treatment handbook* and preferred regimen was tenofovir (TDF), lamivudine (3TC), plus efavirenz (EFV) (*9*).

2.4. *Data collection and definitions*

Demographic data included age and gender, and clinical data collected in this study included HIV transmission routes, ART initiation or not, duration of active ART initiation, documented opportunistic infections, malignant lymphoma, non-AIDS-defining malignancies. Laboratory tests were performed for baseline CD4, albumin as well as hemoglobin (HGB) levels after admission.

Primary treatment outcome was documented either survival or death when HIV/TB co-infected patients left hospital. Patients who survived when discharged received 12-month follow-up, and the date of last known alive was documented in electronical medical records base on records of last follow-up. The morality in this study was a cumulative measure with a risk period of 12 months after discharge, *i.e.*, dead cases within the 12 months after discharge were calculated.

In HIV/TB co-infected patients at end stage of AIDS, Unexplained infections was diagnosed based on compatible clinical symptoms and intensive pathogenic investigation of OIs without identifying pathogens, and unexplained space-occupying lesions was diagnosed on basis of clinical symptoms and results of Computerized tomography (CT) or magnetic resonance imaging(MRI) scan but lack of pathological diagnosis of biopsy.

Severe pneumonia was diagnosed based on the presence of severe acute respiratory failure and/or septic shock with organ system dysfunction due to different etiologies or pathogens (*10*).

2.5. *Statistical analysis*

Statistical analysis was conducted with SPSS 20.0 (SPSS Institute, Chicago IL, USA). Clinical data were evaluated with percentages for categorical variables and chi-square test or Fisher exact test was used for categorical variables.

Cox proportional hazard models were used to assess the predictors associated with mortality in HIV/TB co-infected patients at end stage of AIDS in the cohort. Univariate Cox proportional hazard models were firstly used to determine the association of the variables with mortality in HIV/TB co-infected patients, and multivariate Cox proportional hazard models were subsequently run and univariate factors with $p < 0.1$ were included into a forward stepwise multivariate Cox proportional hazard model. The integer scores were converted by rounding the hazard ratios (HRs) of the predictors. For example, the HR of 2.110 associated with tuberculous meningitis was equal to 2 points and the final score was the sum of these values. The clinical scoring model was validated in derivation and validation cohort, Receiver operating characteristics (ROC) curves were plotted and the area under curve (AUC) was evaluated in this study. The correlation between clinical scoring model and prognosis was plotted based on cumulative mortality according to scores. Log-rank testing was conducted to evaluate difference in cumulative mortality between the low-level and high-level scores.

Alpha was set to 0.05 with two-side, with 95% confidence intervals. $P < 0.05$ was considered significant.

3. Results

3.1. *Patients characteristics*

From August 2009 to January 2018, 1,070 HIV-infected patients at end stage of AIDS were diagnosed as tuberculosis infection and 1,007 patients were enrolled in this study after excluding those not meeting inclusion criteria, in which 810 were alive and 197 were dead after 12-month follow-up. Random assignment in 8:2 ratio was conducted in alive group (650 and 160 cases)

Table 1. Baseline characteristics of HIV/TB patients at end-stage of AIDS in the study cohort

Variables		Total n = 1007	Derivation cohort n = 807	Validation cohort n = 200	p value
Age (years)	< 50	820 (81.4%)	665 (82.4%)	155 (77.5%)	0.110
	≥ 50	187 (18.6%)	142 (17.6%)	45 (22.5%)	
Gender	Female	902 (89.6%)	716 (88.7%)	186 (93%)	0.076
	Male	105 (10.4%)	91 (11.3%)	14 (7%)	
Transmission route	Homosexual	752 (74.7%)	609 (75.5%)	143 (71.5%)	0.421
	Heterosexual	147 (14.6%)	112 (13.9%)	35 (17.5%)	
Laboratory results	Blood transfusion	108 (10.7%)	86 (10.6%)	22 (11%)	
	HGB > 90g/L	722 (71.7%)	585 (72.5%)	137 (68.5%)	0.262
	HGB ≤ 90g/L	285 (28.3%)	222 (27.5%)	63 (31.5%)	
	ALB > 30g/L	679 (67.4%)	552 (68.4%)	127 (63.5%)	0.185
	ALB ≤ 30g/L	328 (32.6%)	255 (31.6%)	73 (36.5%)	
	CD4 > 100cells/uL	288 (28.6%)	231 (28.6%)	57 (28.5%)	0.972
	CD4 ≤ 100cells/uL	719 (71.4%)	576 (71.4%)	143 (71.5%)	
ART prior to admission	Yes	411 (40.8%)	324 (40.1%)	87 (43.5%)	0.388
	NO	596 (59.2%)	483 (59.9%)	113 (56.5%)	
Tuberculosis					
Pulmonary tuberculosis	Yes	754 (74.9%)	594 (73.6%)	160 (80%)	0.062
	NO	253 (25.1%)	213 (26.4%)	40 (20%)	
Tuberculous pleuritis	Yes	213 (21.2%)	172 (21.3%)	41 (20.5%)	0.801
	NO	794 (78.8%)	635 (78.7%)	159 (79.5%)	
Tuberculous peritonitis	Yes	69 (6.9%)	54 (6.7%)	15 (7.5%)	0.685
	NO	938 (93.1%)	753 (93.3%)	185 (92.5%)	
Tuberculous meningitis	Yes	125 (12.4%)	100 (12.4%)	25 (12.5%)	0.967
	NO	882 (87.6%)	707 (87.6%)	175 (87.5%)	
Opportunistic Infections					
PCP	Yes	134 (13.3%)	117 (14.5%)	17 (8.5%)	0.025
	NO	873 (86.7%)	690 (85.5%)	183 (91.5%)	
CMV pneumonitis	Yes	52 (5.2%)	42 (5.2%)	10 (5%)	0.907
	NO	955 (94.8%)	765 (94.8%)	190 (95%)	
Cryptococcal pneumonitis	Yes	9 (0.9%)	7 (0.9%)	2 (1%)	0.858
	NO	998 (99.1%)	800 (99.1%)	198 (99%)	
Fungal pneumonia	Yes	91 (9%)	66 (8.2%)	25 (12.5%)	0.056
	NO	916 (91%)	741 (91.8%)	175 (87.5%)	
Severe pneumonia	Yes	30 (3%)	27 (3.3%)	3 (1.5%)	0.169
	NO	977 (97%)	780 (96.7%)	197 (98.5%)	
MAC	Yes	63 (6.3%)	51 (6.3%)	12 (6%)	0.867
	NO	944 (93.7%)	756 (93.7%)	188 (94%)	
CMV retinitis	Yes	54 (5.4%)	46 (5.7%)	8 (4%)	0.339
	NO	953 (94.6%)	761 (94.3%)	192 (96%)	
Penicilliosis	Yes	21 (2.1%)	19 (2.4%)	2 (1%)	0.230
	NO	986 (97.9%)	788 (97.6%)	198 (99%)	
Invasive fungal infections	Yes	32 (3.2%)	25 (3.1%)	7 (3.5%)	0.772
	NO	975 (96.8%)	782 (96.9%)	193 (96.5%)	
CMV neurologic diseases	Yes	13 (1.3%)	7 (0.9%)	6 (3%)	0.017
	NO	994 (98.7%)	800 (99.1%)	194 (97%)	
Cryptococcal meningitis	Yes	42 (4.2%)	34 (4.2%)	8 (4%)	0.893
	NO	965 (95.8%)	773 (95.8%)	192 (96%)	
Cerebral Toxoplasmosis	Yes	16 (1.6%)	12 (1.5%)	4 (2%)	0.603
	NO	991 (98.4%)	795 (98.5%)	196 (98%)	
Unexplained infections or space-occupying lesions	Yes	103 (10.2%)	83 (10.3%)	20 (10%)	0.905
	NO	904 (89.8%)	724 (99.7%)	180 (90%)	
Malignancies	Yes	27 (2.7%)	20 (2.5%)	7 (3.5%)	0.423
	NO	980 (97.3)	787 (97.5%)	193 (96.5%)	

Note: ART:antirretroviral therapy; PCP:pneumocystis pneumonia; CMV: cytomegalovirus; MAC: Mycobacterium avium complex.

and dead group (157 and 40 cases) respectively to form derivation cohort (n = 807) and validation cohort (n = 200) in 8:2 ratio (Figure 1). The demographic, clinical and laboratory characteristics of these patients were detailed in Table 1, and there was no significant difference between characteristics in derivation and validation cohort.

3.2. *Development of clinical scoring model of mortality in HIV/TB co-infected patients at end stage of AIDS*

Univariate Cox proportional hazard models were used to identify the predictor associated with mortality in derivation cohort, revealing significant difference in anemia (HGB < 90g/L), tuberculous meningitis, severe

Table 2. Risk factors for mortality rate by Cox proportional hazard regression in HIV/TB patients and hazard rate and integer risk scores

Items		Unadjusted HR (95% CI)	*p* value	Adjusted HR (95% CI)	*p* value	Predictive Score
Anemia (HGB < 90g/L)		1.872 (1.361-2.578)	< 0.001	1.726 (1.224-2.435)	0.002	2
Tuberculous meningitis		2.524 (1.751-3.637)	< 0.001	2.110 (1.399-3.181)	< 0.001	2
Severe pneumonia		6.914 (4.388-10.895)	< 0.001	4.841 (3.002-7.806)	< 0.001	5
Hypoalbuminemia		2.281 (1.665-3.125)	< 0.001	2.062 (1.446-2.939)	< 0.001	2
Unexplained infections or space-occupying lesions		8.542 (6.177-11.813)	< 0.001	7.485 (5.341-10.489)	< 0.001	7
Malignancies		5.576 (3.214-9.674)	< 0.001	4.866 (2.785-8.502)	< 0.001	5
Overall risk level	Mortality					Total score
Low risk	3.6-9.1%					0-2
High risk	26.42-74.62%					4-16

pneumonia, hypoalbuminemia, unexplained infections or space-occupying lesions, and malignancies ($p < 0.05$, Table 2 and Table S1, *http://www.biosciencetrends.com/action/getSupplementalData.php?ID=41*). These variables were entered into a forward stepwise multivariate Cox proportional hazard model, and results indicated that anemia (HGB < 90g/L) ((multivariate-adjusted hazard ratios (HRs)1.726, 95% confidence intervals (CIs) 1.224, 2.435, $p = 0.002$), Tuberculous meningitis (HR: 2.110, 95% CI: 1.399, 3.181, $p < 0.001$), severe pneumonia (HR: 4.841, 95% CI: 3.002, 7.806, $p < 0.001$), hypoalbuminemia (HR: 2.062, 95% CI: 1.446-2.939, $p < 0.001$), unexplained infections or space-occupying lesions (HR: 7.485, 95% CI: 5.341-10.489, $p < 0.001$), and malignancies (HR: 4.866, 95% CI: 2.785-8.502, $p < 0.001$) remained independent risk factors of mortality at 12-month follow-up in HIV/TB co-infected patients at end stage of AIDS. In Table 2, we can find that predictive score of each predictor, including anemia (HGB < 90g/L), tuberculous meningitis, severe pneumonia, hypoalbuminemia, unexplained infections or space-occupying lesions, and malignancies, was 2, 2,5, 2, 7 and 5, respectively.

There was very good conformity between the points and the predictor. The sum of scores from each of the six predictors ranged from 0 to 16 (Table 2). At the cut-off point of 3 matching the maximum Youden index determined by receiver operating curve analysis, the sensitivity and specificity for mortality in HIV/TB co-infected patients were 79.6% and 82.9%, respectively.

Weighted points were assigned to above 6 predictors with linear transformation of their relevant regression coefficient and a clinical score of mortality for individual HIV/TB co-infected patients at end stage of AIDS was calculated using following formula (*11*):

Prognostic score =
2 × [Anemia (HGB < 90g/L)]
+ 2 × [Tuberculous meningitis]
+ 5 × [Severe pneumonia]
+ 2 × [Hypoalbuminemia]
+ 7 × [Unexplained infections or space-occupying lesions]
+ 5 × [Malignancies]

Based on this formula, each patient in HIV/TB co-infected patients had a prognostic score of mortality, and we found that the sum of scores from each of the six predictors ranged from 0 to 16 (Table 2) in this study, and no one had score 1 or 3 according to predictive score of each predictor (Table 2) and the sum of scores from each of the six predictors.

3.3. *Validation of the clinical scoring model*

The potence of the clinical scoring model to predict mortality at 12-month follow-up in HIV/TB co-infected patients at end stage of AIDS was assessed using the area under the ROC curves with the validation cohort. The area under the ROC curves was 0.858 (95% CI: 0.782-0.943) in the derivation cohort, while the area under the ROC curves in validation cohort was 0.867 (95% CI: 0.832-0.902), which indicated that this clinical scoring model may be useful in predicting mortality at 12-month follow-up in HIV/TB co-infected patients (Figure S1, *http://www.biosciencetrends.com/action/getSupplementalData.php?ID=41*).

3.4. *Correlation between the clinical scoring model and mortality in HIV/TB co-infected patients at end-stage of AIDS*

All patients in this study were pooled to further assess the correlation between the clinical scoring model and mortality in HIV/TB co-infected patients at end-stage of AIDS. The score was categorized into two groups with low risk (scoring 0-2) and high risk (scoring 4-16) of mortality based on the maximum Youden index determined by receiver operating curve analysis. We found that patients with higher scores had higher mortality. Among patients with score of 0, 3.6% had died at 12-month follow-up, as compared to 9.1% of patients with score of 2, 26.42% of patients with score of 4, 54.55% and 74.62% of patients with score of 5 to 11 and 12-16, respectively (Figure 2). For the summed clinical scores of 0-2 and 4-16, the mortality at 12-month follow-up was 3.6-9.1% and 26.42-74.62%, respectively (Table 2). Furthermore, Kaplan-

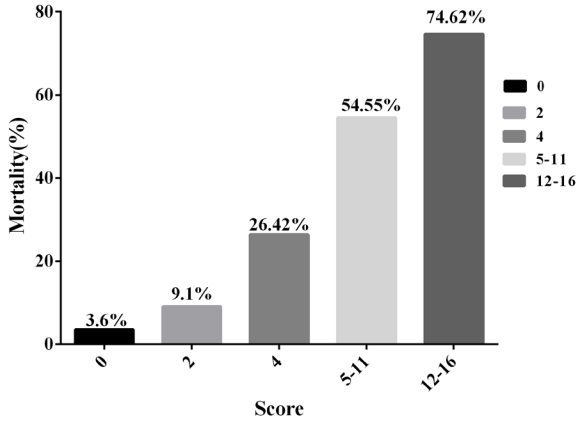

Figure 2. Percentage of mortality of HIV/TB co-infected patients according to the score. The integer scores were converted by rounding the hazard ratios of the predictors and the final score was the sum of these values. Patients were divided into 5 groups according to their baseline levels. Among patients with score of 0, 3.6% had died at 12-month follow-up, as compared to 9.1% of patients with score of 2, 26.42% of patients with score of 4, 54.55% and 74.62% of patients with score of 5 to 11 and 12-16, respectively.

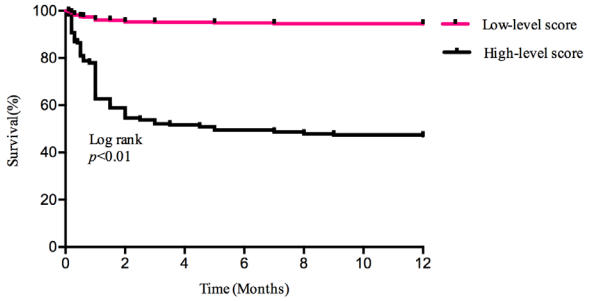

Figure 3. Kaplan-Meier survival curve of HIV/TB co-infected patients between groups of low-level and high-level scores.

Meier curve indicated a significant difference in the cumulative mortality between low-level scores and high-level scores groups (0-2 and 4-16) at 12-month follow-up by log-rank test ($p < 0.001$) (Figure 3), which demonstrated that the model may be useful in predicting mortality in HIV/TB co-infected patients at end-stage of AIDS.

4. Discussion

This predictive model was constructed based on the derivation and the validation cohorts, in which risk factors were found and their risk scores were evaluated based on multivariate Cox proportional hazard model, and a predictive model was developed in the derivation cohort, and the predictive model was further assessed using the area under the ROC curves in the validation cohort.

Routinely and preferably, a simple random sampling should have been applied to the whole sample of 1,007 patients, with 4:1 ratio for the derivation and validation cohorts, and it should meet a prerequisite: there was no significant difference in outcome status (alive vs. dead) between derivation and validation cohorts (*12*), which may experience multiple round random sampling to meet the prerequisite. In this study, we simplified the random sampling processes based on randomly stratifying sampling: random assignment in 8:2 ratio was conducted in alive group (650 and 160 cases) and dead group (157 and 40 cases) respectively to form derivation cohort ($n = 807$) and validation cohort ($n = 200$) in 8:2 ratio (Figure 1), which indicated that there was no significant difference in outcome status between two cohorts and selection bias were reduced to the utmost.

It was reported that several TB predictive scoring models were previously established (*6,11*), but some reason limited their application in specific context in China. HIV infection was reported to be the most important risk factor for mortality in several TB predictive scoring models, but they were not involved in end-stage AIDS patients, who were prone to be complicated by different opportunistic infection, malignancies and co-morbidities. Nguyen *et al*. (11) reported prognostic score model to predict mortality during TB treatment in HIV/TB co-infected patients in high-income countries, but this model had never been validated in China, which has completely different clinical features and healthcare conditions in HIV/TB co-infected population in China.

In China, although availability of potent free antiretroviral regimens has had the most profound influence on opportunistic infections or malignancies-related mortality (*9*), opportunistic infections and AIDS-related malignancies continued to cause morbidity and mortality due to unaware of their HIV status in Chinese HIV-infected population (*2*). These patients sought medical attention so late that their health condition had entered end-stage of AIDS due to severe immunosuppression when HIV infection was diagnosed. Our previous study indicated that (*2*), in HIV/AIDS patients with severe immunosuppression, the same pathogen can co-infected different organs or systems, such as *Mycobacterium Tuberculosis* which can infect nervous, respiratory, lymph, and digestive system, while different pathogens can infect same organ or system, such as respiratory system which can be co-infected with bacteria, virus and invasive fungi. Some pathogens and space-occupying lesions were also found to be difficult to be diagnosed etiologically in end-stage AIDS patients, which increased degree of difficulty of etiologic diagnosis in clinical practice. In HIV/TB co-infected patients at end-stage of AIDS, we also highlighted different clinical complications, including AIDS-defining illnesses (including opportunistic infections and AIDS-related malignancies) and non-AIDS-defining malignancies, resulted in clinical

deterioration or even death in these patients.

TB disease is an important OI and AIDS-defining illness, it can occur at any CD4 cell counts, and its risk increases with progressive immunodeficiency. In this study, we found that TB disease was diagnosed in 28.6% of patients with CD4 > 100 cells/uL and 71.4% of patients with CD4 < 100cells/uL, respectively, which indicated that TB disease was diagnosed in HIV-infected patients with any CD4 cell counts in our cohort, and was more prone to occur in patients with lower CD4 levels. This clinical scoring model was constructed based on this cohort, which indicated that it can be used not only in patients with higher CD4 levels but also in patients with lower CD4 levels. In this study, the majority of TB disease occurred in HIV-infected patients with lower CD4 levels, who were prone to be complicated with different OIs or malignancies, which were common clinical features in HIV-infected patients with end-stage of AIDS in China (*2*). This clinical scoring model was used in HIV/TB co-infected patients at end stage of AIDS, which indicated its advantage in HIV/TB co-infected patients at end stage of AIDS in China.

The result in this study demonstrated that HIV/TB patients with hypoalbuminemia or anemia had significantly higher mortality. Hypoalbuminemia and anemia were commonly treated as marker of malnutrition, and it was associated with wasting and was considered as indicators of increased severity of OIs, which increased risk of mortality in HIV/TB patients (*13,14*).

Tuberculous meningitis was the most severe complication in individuals infected with *Mycobacterium Tuberculosis*, which killed or disabled half of these patients. TB meningitis was also found as a predictor of mortality in our clinical scoring model, which was consistent with some literature found in PubMed (*11,15,16*), and helped remind physicians of this severe complication in HIV/TB co-infected patients.

We found that unexplained infections or space-occupying lesions were another important risk factor of mortality in HIV/TB patients. Some studies demonstrated that some fatal infections or malignancies cannot be determined until at autopsy (*17*). Obscurely etiologic diagnosis increased risk of mortality and it was important to improve pathogenic and pathological diagnosis in HIV-infected patients with unexplained infections or space-occupying lesions.

Malignancies were another important risk factor of mortality in our clinical scoring model. Malignancies were caused based on immunosuppression, life-style and co-infections (HBV, HCV, or HPV) (*18,19*), which indicated that earlier initiation of HAART, healthy life-style, cancer screening and identification of co-infected pathogens would favorably improve prognosis of HIV-infected patients.

Severe pneumonia, which was caused by co-infections with pneumocystis pneumonia (PCP), cytomegalovirus, and invasive fungi, besides tuberculosis, in this study, was required invasive mechanical ventilation earlier admitting to Intensive Care Units (ICU). Several studies demonstrated that severe pneumonia was an important cause of death in patients later admitted to ICU (*10,20*) which was consistent with our result in this study, and helped remind physicians of earlier admitting to ICU to receive mechanical ventilation.

Several important variables having significance in univariate analyses such as CD4 cell count, pulmonary tuberculosis, PCP and fungal pneumonia were also included into a forward stepwise multivariate Cox proportional hazard model, but we cannot make conclusion that lower CD4 levels and some OIs, such as pulmonary tuberculosis, PCP and fungal pneumonia, were associated with mortality of HIV/TB co-infected patients at end stage of AIDS.

It was reported that lower CD4 levels was associated with mortality in HIV/AIDS patients (*21*), but we failed to demonstrate the conclusion in our cohort. Luo *et al*. (*22*) reported that lower CD4 level was not a predictor for predicting mortality in HIV/AIDS patients with OIs in Shanghai, China. The phenomenon may be due to following reasons: First, the majority of patients had lower CD4 levels on admission, and some patients maybe had died prior to arriving at hospital. Our model indicated that CD4 < 100cells/uL was found in 71.4% of HIV/TB co-infected patients at end-stage of AIDS. Second was associated with inherent biases in studies based on retrospective and observational data. Third, Revimohan *et al*. (*23*) reported that, in HIV/TB co-infected patients, early immunologic response, but not pre-ART CD4 counts was associated with early mortality.

Pulmonary tuberculosis was the most common OI in HIV-infected patients at end stage of AIDS, but we did not find that it was an independent predictor of mortality in HIV-infected patients with end-stage of AIDS, which was consistent with some reports about risk factors of mortality in HIV/AIDS patients with OIs (*22,24,25*). In this study, all of patients were diagnosed as tuberculosis, in which 74.9% of patients had pulmonary tuberculosis, which may explain why it was not significant difference among those who were dead in this study. Although pulmonary tuberculosis was not an independent risk factor of mortality in HIV/TB co-infected patients at end stage of AIDS, TB was still an important OI and active TB screening was necessary for HIV-infected patients.

This clinical scoring model indicated several advantages: First, the model was constructed based on HIV/TB infected patients at end-stage of AIDS in China, which was currently the most predominant clinical characteristics in Chinese HIV/AIDS patients. Second, the model used randomized assignment from

large cohort of HIV/TB co-infected patients and received accurate assessment of different predictors. Third, 6 predictors used in the model were common in clinical practice, and model was easy to use in routine clinical practice without complicated calculation. Fourth, the model could help physicians determine the prognosis of HIV/TB co-infected patients, especially for end-stage AIDS patients with tuberculosis.

The study also had some limitations: First, there were potential inherent biases in a retrospective study. Second, the conclusion was made in single center, which should be further validated prior to be generalizable to different hospitals in China.

In conclusion, a clinical scoring model to assess the prognosis in HIV/TB patients at end stage of AIDS was constructed based on simple laboratory and clinical features available at admission, which may be an easy-to-use tool for physicians to evaluate the prognosis and treatment outcome in HIV/TB co-infected patients. The model was also applicable for predicting the death of end-stage HIV/TB patients within a 12 months period after discharge.

Acknowledgements

We acknowledge the work of HIV health care providers for their diagnosis, nursing and treatment of HIV/AIDS patients in Ditan Hospital.

Support for this work was provided by: (1) Healthcare Talent Training Program in Beijing Health System (grant 2015-3-105); (2) the National natural Science Fund *The study of T-cell repertoire diversity in AIDS patients based on the restoration of thymic function (grant 81371804)*; (3) Project from Beijing Municipal Committee of Science & Technology *The study of HIV/HBV co-infection (grant D161100000416004)*; (4) Project for Capital Characteristics *The study for blood concentration of efavirenz influenced by rifampin in HIV/TB co-infected patient (grantZ171100001017053)*; (5) The Thirteen-fifth Key Project *The Study of Construction of Representative areas for Prevention and Therapy of Fatal Infectious Diseases such AIDS & Viral Hepatitis in Chaoyang District, Beijing (grant 2017ZX10105005-002-001)*; (6) The Thirteen-fifth Key Project *The study for strategies to control non-AIDS-associated diseases in HIV/AIDS patients receiving long-term HAART (grant 2017ZX10202101-004).*

The funders had no role in study design, data collection and analysis, decision to publish, or preparation of the manuscript.

References

1. WHO 2010. Global Tuberculosis Control. WHO report 2010. whqlibdoc. *who.int/publications/2010/9789241564069_eng.pdf*. (accessed December 15, 2018)
2. Xiao J, Gao G, Li Y, Zhang W, Tian Y, Huang Y, Su W, Han N, Yang D, Zhao H. Spectrums of opportunistic infections and malignancies in HIV-infected patients in tertiary care hospital, China. PLoS One. 2013; 8:e75915.
3. Toossi Z. Virological and immunological impact of tuberculosis on human immunodeficiency virus type 1 disease. J Infect Dis. 2003; 188:1146-1155.
4. Xiao J, Du S, Tian Y, Su W, Yang D, Zhao H. Causes of death among patients infected with HIV at a tertiary care hospital in China: An observational cohort study. AIDS Res Hum Retroviruses. 2016; 32:782-790.
5. Ji YJ, Liang PP, Shen JY, Sun JJ, Yang JY, Chen J, Qi TK, Wang ZY, Song W, Tang Y, Liu L, Zhang RF, Shen YZ, Lu HZ. Risk factors affecting themortalityofHIV-infected patients with pulmonary tuberculosis in the cART era: A retrospective cohort study in China. Infect Dis Poverty. 2018; 7:25.
6. Pefura-Yone EW, Balkissou AD, Poka-Mayap V, Fatime-Abaicho HK, Enono-Edende PT, Kengne AP. Development and validation of a prognostic score during tuberculosis treatment. BMC Infect Dis. 2017; 17:251.
7. Panel on Opportunistic Infections in HIV-Infected Adults and Adolescents. Guidelines for the prevention and treatment of opportunistic infections in HIV-infected adults and adolescents: Recommendations from the centers for disease control and prevention, the National Institutes of Health, and the HIV Medical Association of the Infectious Diseases Society of America. Available: *http://aidsinfo.nih.gov/contentfiles/lvguidelines/adult_oi.pdf*. (accessed December 15, 2018)
8. Hoffmann C, Jurgen K. Eds., HIVBOOK2010. Medizin Fokus Verlag. 2010.
9. Zhang F, editor. National free HIV antiretroviral treatment handbook. 3rd ed. Beijing, China: People's Medical Publishing House (Chinese). 2012. (in Chinese)
10. Lim WS, Baudouin SV, George RC, Hill AT, Jamieson C, Le Jeune I, Macfarlane JT, Read RC, Roberts HJ, Levy ML, Wani M, Woodhead MA; PneumoniaGuidelines Committee of the BTS Standards of Care Committee. BTS guidelines for the management of community acquired pneumonia in adults: Update 2009. Thorax. 2009; 64 Suppl 3:iii1-55.
11. Nguyen DT, Graviss EA. Development and validationof aprognosticscore to predict tuberculosismortality. J Infect. 2018; 77:283-290.
12. Geng M, Li Y, Gao F, Sun L, Yang X, Wang R, Chen J, Zhang Q, Wan G, Wang X. A scoring model predicts hepatitis B e antigen seroconversion in chronic hepatitis B patients treated with nucleos(t)ide analogs: Real-world clinical practice. Int J Infect Dis. 2017; 62:18-25.
13. Robson SC, White NW, Aronson I, Woollgar R, Goodman H, Jacobs P. Acute phase response and the hypercoagulable state in pulmonary tuberculosis. Br J Haematol. 1996; 93:943-949.
14. Sudfeld CR, Isanaka S, Aboud S, Mugusi FM, Wang M, Chalamilla GE, Fawzi WW. Association of serum albumin concentration with mortality, morbidity, CD4 T-cell reconstitution among tanzanians initiating antiretroviral therapy. J Infect Dis. 2013; 207:1370-1378.
15. Thao LTP, Heemskerk AD, Geskus RB, *et al*. Prognostic Models for 9-MonthMortalityinTuberculous Meningitis. Clin Infect Dis. 2018; 66:523-532.
16. Nguyen DT, Jenkins HE, Graviss EA. Prognostic score to predict mortality during TB treatment in TB/HIV co-infected patients. PLoS One. 2018; 13:e0196022.
17. Cox JA, Lukande RL, Lucas S, Nelson AM, Van

Marck E, Colebunders R. Autopsy causes of death in HIV-positive individuals in sub-Saharan Africa and correlation with clinical diagnoses. AIDS Rev. 2010; 12:183-194.
18. Smith CJ, Ryom L, Weber R, *et al*. Trends in underlying causes of death in people with HIV from 1999 to 2011 (D:A:D): A multicohort collaboration. Lancet. 2014; 384:241-248.
19. Worm SW, Bower M, Reiss P, *et al*. Non-AIDS definingcancersin the D:A:D Study – time trends and predictors of survival: A cohort study. BMC Infect Dis. 2013; 13:471.
20. Ferrer M, Travierso C, Cilloniz C, Gabarrus A, Ranzani OT, Polverino E, Liapikou A, Blasi F, Torres A. Severe community-acquired pneumonia: Characteristics and prognostic factors in ventilated and non-ventilated patients. PLoS One. 2018; 13:e0191721.
21. Álvarez Barreneche MF, Restrepo Castro CA, Hidrón Botero A, Villa Franco JP, Trompa Romero IM, Restrepo Carvajal L, Eusse García A, Ocampo Mesa A, Echeverri Toro LM, Porras Fernández de Castro GP, Ramírez Rivera JM, Agudelo Restrepo CA. Hospitalization causes and outcomes inHIVpatients in the late antiretroviral era in Colombia. AIDS Res Ther. 2017; 14:60.
22. Luo B, Sun J, Cai R, Shen Y, Liu L, Wang J, Zhang R, Shen J, Lu H. Spectrum of opportunistic infections and risk factors for in-hospital mortality of admitted AIDS patients in Shanghai. Medicine (Baltimore). 2016; 95:e3802.
23. Ravimohan S, Tamuhla N, Steenhoff AP, *et al*. Early immunologic failure is associated with early mortality among advanced HIV-infected adults initiating antiretroviral therapy with active tuberculosis. J Infect Dis. 2013; 208:1784-1793.
24. Pang W, Shang P, Li Q, Xu J, Bi L, Zhong J, Pei X. Prevalence of Opportunistic Infections and Causes of Death among Hospitalized HIV-Infected Patients in Sichuan, China. Tohoku J Exp Med. 2018; 244:231-242.
25. Shahrin L, Leung DT, Matin N, Pervez MM, Azim T, Bardhan PK, Heffelfinger JD, Chisti MJ. Characteristics and predictors of death among hospitalized HIV-infected patients in a low HIVprevalence country: Bangladesh. PLoS One. 2014; 9:e113095.

(Received December 30, 2018; Revised February 23, 2019; Accepted March 21, 2019)

Original Article

DOI: 10.5582/bst.2019.01005

Methanol extract of *Lonicera caerulea* var. *emphyllocalyx* fruit has antibacterial and anti-biofilm activity against *Streptococcus pyogenes in vitro*

Masaaki Minami[1,*], Hiroshi Takase[2], Mineo Nakamura[3], Toshiaki Makino[4]

[1] *Department of Bacteriology, Graduate School of Medical Sciences, Nagoya City University, Nagoya, Aichi, Japan;*
[2] *Core Laboratory, Graduate School of Medical Sciences, Nagoya City University, Nagoya, Aichi, Japan;*
[3] *Nakamura Pharmacy, Sapporo, Hokkaido, Japan;*
[4] *Department of Pharmacognosy, Graduate School of Pharmaceutical Sciences, Nagoya City University, Nagoya, Aichi, Japan.*

Summary ***Streptococcus pyogenes*** **causes several infectious diseases such as tonsillitis, cellulitis, and streptococcal toxic shock syndrome. As antibiotics are used for the general treatment of *S. pyogenes* infection, cases of treatment failure due to drug-resistant bacteria have increased. *Lonicera caerulea* var. *emphyllocalyx* (LCE) has been used as a folk medicine in northern Japan (Hokkaido). In this study, we investigated the antibacterial effect of methanol extracts of the fruit, stem, and leaf of LCE (LCEEs) against *S. pyogenes* using disk diffusion assay. As LCEE (fruit) had the strongest antibacterial activity among the three LCEEs, we focused on functional analysis of antibacterial effects of LCEE (fruit). LCEE (fruit) suppressed the growth of *S. pyogenes* in a dose-dependent manner. Morphological analysis by transmission electron microscopy demonstrated that LCEE (fruit) damaged the shape of *S. pyogenes*. Microplate and confocal laser microscopy analysis showed that biofilm formation was also suppressed by LCEE (fruit) in a dose-dependent manner. To further evaluate the surface structure of these biofilms, we performed hydrophobic analysis, which demonstrated that LCEE (fruit) reduced the hydrophobicity of the bacterial surface structure. Our data demonstrated that LCEE (fruit) had anti-bacterial and anti-biofilm effects on *S. pyogenes in vitro*, suggesting that the direct anti-bacterial effects of the LCEE (fruit) may be useful for treatment of local *S. pyogenes* infection.**

Keywords: *Lonicera caerulea* var. *emphyllocalyx*, fruit, *Streptococcus pyogenes*, anti-bacterial effect, anti-biofilm effect

1. Introduction

Streptococcus pyogenes is a common gram-positive virulent bacterium (*1*). Because *S. pyogenes* contains various virulent factors such as streptolysin O, streptolysin S, NADase, and SpeB protease, it causes various types of infectious diseases such as pharyngitis, tonsillitis, nephritis, cellulitis, and necrotizing fasciitis (*1*). Because the antibiotic resistance rate of *S. pyogenes* has been gradually increasing worldwide (*2,3*), identification of novel anti-*S. pyogenes* therapies is of great importance.

Lonicera caerulea var. *emphyllocalyx* (LCE) belongs to the honeysuckle family (Caprifoliaceae) and the honeysuckle genus, which is best-known for having edible berries (*4*). LCE is distributed in northern temperate zones such as the northern part of Japan (Hokkaido) and the northern part of the Eurasian continent (*4*). LCE is cultivated commercially in Japan, Canada, and Russia (*4*).

LCE berries contain several beneficial phytochemicals, including carbohydrates, lipids, proteins, sugar, organic acids, vitamins, and mineral such as iron, magnesium, phosphorus, calcium, and potassium (*5*). They also

Released online in J-STAGE as advance publication April 16, 2019.

*Address correspondence to:
Dr. Masaaki Minami, Department of Bacteriology, Graduate School of Medical Sciences, Nagoya City University, 1 Kawsumi, Mizuho-ku, Nagoya 467-8601, Japan.
E-mail: minami@med.nagoya-cu.ac.jp

contain phenolic acid, anthocyanins such as cyanidin 3-*O*-glucoside, flavonoids, and caffeic acid (*5*). LCE berries have anti-tumorigenic, antimicrobial, anti-inflammatory, and anti-mutagenic properties (*6*).

In Japanese traditional Kampo medicine and traditional Chinese medicine, the flower bud, stem, and leaf of *Lonicera japonica* are formulated into prescriptions for treatment of febrile common cold (*7*), joint pain (*8*), and severe viral diseases (*9,10*). In their countries of origin, honeysuckle plants have also been used as folk medicines, and fresh honeysuckle fruit juice has been used as a general strengthening drink and as a treatment for tonsillitis (*11*).

Owing to the increasing interest in the use of plants belonging to the honeysuckle family as herbal products, various studies have investigated the therapeutic effects of honeysuckle berries for prevention of a range of diseases (*12-14*). However, the mechanisms of action of honeysuckle berries has not been characterized. In this study, we hypothesized that LCE, a plant belonging to the *Lonicera* genus, may exert anti-microbial activity. Furthermore, we evaluated whether LCE is a novel candidate agent for anti-*S. pyogenes* therapy.

2. Materials and Methods

2.1. *Preparation of samples*

LCE was harvested in a field located in Atsuma-Town, Hokkaido, northern part of Japan. Voucher specimens were kept at the Department of Pharmacognosy, Graduate School of Pharmacognosy, Nagoya City University. Six hundred thirty-three grams of the fruit (fresh), 5.6 g of the leaf (dried), and 20.9 g of the stem (dried) were soaked in 2 L, 500 mL, and 500 mL of MeOH (Fujifilm Wako Pure Chemical, Osaka, Japan), respectively, and allowed to incubate for 72 h at room temperature. Following paper filtration, equal amounts of MeOH were added to the residues, and the mixtures were allowed to incubate for 72 h. After filtration, each filtrate was combined, evaporated under reduced pressure, and then lyophilized. The weights of the LCE extracts (LCEEs) after lyophilization were 79.8 g (fruit), 1.33 g (leaf), and 0.686 g (stem). The extraction efficiencies were 12.6% (fruit), 23.8% (leaf), and 3.28% (stem). LCEEs of fruit, leaf, and stem were dissolved and suspended at a concentration of 200 mg/mL in water, 40% DMSO(Fujifilm Wako Pure Chemical), and 20% DMSO, respectively, and stored at –20°C.

Chromatographic signatures of LCEE (fruit) were created as follows. Ten milligrams of LCEE (fruit) was suspended in 1 mL of MeOH and centrifuged at $1.5 \times 10^3 \times g$ for 5 min. Twenty-five microliters of the supernatant was injected onto an HPLC with the following operating conditions: system: Shimadzu LC-$10A_{VP}$; column: TSK-GEL ODS-80_{TS} (4.6 × 250 mm, Tosoh, Tokyo); mobile phase: 0.05 M AcOH-$AcONH_4$ buffer (pH 3.6) (Fujifilm Wako Pure Chemical)/CH_3CN (Fujifilm Wako Pure Chemical) 90:10 (0 min) – 45:55 (40 min), linear gradient; flow rate: 1.0 mL/min; column temperature: 40°C; and detection wavelength: 245-600 nm using a photodiode array detector (Figure 1). Cyanidin 3-*O*-glucoside was purchased from Tokiwa Phytochemical (Sakura, Japan). LCEE (fruit) (5 µg) and cyanidin 3-*O*-glucoside (28.8, 57.5, and 115 ng) were injected onto the HPLC system described above, and absorbance was monitored at 520 nm. The retention time of cyanidin 3-*O*-glucoside was 9.0 min. The range of cyanidin 3-*O*-glucoside was calibrated by analyzing peak response using the least-squares method (r^2 = 0.997), and the concentration of cyanidin 3-*O*-glucoside in LCEE (fruit) was calculated as 1.12% (w/w).

2.2. *Bacterial strains*

S. pyogenes 1529 was isolated from a patient with

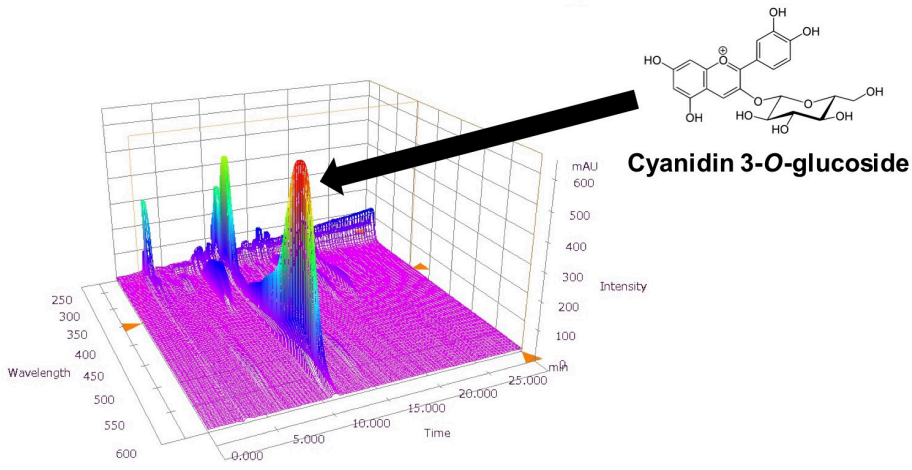

Figure 1. 3D-HPLC profile of LCEE (fruit). Fingerprint analysis of LCEE (fruit) was conducted as described in the Materials and Methods section. Cyanidin 3-*O*-glucoside was identified by comparison with the retention time and UV spectrum of its standard.

streptococcal toxic shock in Japan (*15*). A fresh colony was inoculated overnight on Trypticase soy agar with 5% sheep blood (Nippon Becton Dickinson Co., Ltd., Tokyo, Japan) and cultured for 16 h at 37°C in an atmosphere of 5% CO_2. The bacteria were harvested, centrifuged, and resuspended in sterile phosphate-buffered saline (0.15 M, pH 7.2, PBS) (Fujifilm Wako Pure Chemical). Bacterial density was determined by measuring the absorbance at 600 nm (A_{600}). The bacterial suspension was then diluted with PBS to 1.0×10^9 colony forming units (CFU)/mL using a standard growth curve to determine bacterial concentration from A_{600} values.

2.3. *Disk diffusion assay*

Disk diffusion assay was performed with some modifications (*3*). Sterile paper disks (GE healthcare Japan, Tokyo, Japan) were impregnated with LCEEs (7.5 mg/disk) and dried at room temperature. Kirby-Bauer Disk 'EIKEN' containing penicillin G (10 U = 6 μg/disk) (Eiken Kagaku, Tokyo, Japan) was used as a positive control. *S. pyogenes* colonies cultured overnight on Trypticase soy agar with 5% sheep blood were collected into Todd Hewitt broth (Difco Laboratories Inc., Detroit, MI, USA). 1.0×10^9 CFU/mL of *S. pyogenes* was inoculated on another Trypticase soy agar plate with 5% sheep blood. The paper disks were placed on the plates and were incubated at 37°C in a 5% CO_2 atmosphere for 24 h. Inhibitory zone diameters were measured.

2.4. *Evaluation of growth in vitro*

S. pyogenes (1×10^6 CFU) was cultured in Todd Hewitt broth with 0.3% yeast extract (Difco) (THY broth) and LCEE (fruit) at 37°C in an atmosphere of 5% CO_2 for 24 h. Turbidity was estimated by measuring the absorbance at 600 nm.

2.5. *Biofilm assay*

Biofilm assay was performed with some modifications (*16*). Overnight cultures of *S. pyogenes* (1×10^6 CFU) were seeded onto 96-well polystyrene plates (Thermo Fisher Scientific, MA, USA), which were then incubated in THY broth with or without LCEE (fruit) at 37°C for 48 h. After removal of the media, the plates were washed three times with PBS, and adherent bacteria were stained with 0.2% safranin red (Fujifilm Wako Pure Chemical) at room temperature for 10 min, after which, they were gently washed three times with PBS. Each biofilm was quantitated by measuring the absorbance at 490 nm (A_{490}). Wells incubated without bacteria were used as blanks. The absorbance of blank wells was subtracted from the test values. For confocal microscopic observations, *S. pyogenes* was grown on glass coverslips in 24-well polystyrene plates (Thermo Fisher Scientific) at 37°C for 48 h. After removing the media, the wells were washed three times with PBS and stained with fluorescein isothiocyanate isomer (FITC) (Fujifilm Wako Pure Chemical). Images were collected using an LSM 510 confocal laser microscope (Carl Zeiss, Oberkochen, Germany). Three-dimensional images were created from Z-stack images using Imaris software (Carl Zeiss).

2.6. *Bacterial morphological investigation*

Bacterial morphological analysis using transmission electron microscopy (TEM) JEM1011J (JEOL, Tokyo, Japan) was performed with slight modifications (*17*). *S. pyogenes* strains treated with LCEE were cultured in THY broth for 24 h. For negative staining, approximately one drop of the bacterial culture was applied onto a 300-mesh carbon formvar copper grid (Nisshin EM, Tokyo, Japan). Excess solution was removed and negative staining was performed using 2% phosphotungstic acid (PTA) (Fujifilm Wako Pure Chemical). The samples were visualized using transmission electron microscopy. Digital images were collected using a Mega View Slow-scan camera (JEOL).

2.7. *Analysis of cell surface hydrophobicity*

Cell surface hydrophobicity was evaluated using the hexadecane method with a minor modification (*16*). *S. pyogenes* treated with LCEE (fruit) was grown to the exponential phase and suspended in PBS, and A_{600} was adjusted to 1.0. After addition of 200 μL of n-hexadecane (Fujifilm Wako Pure Chemical) to 2 mL of bacterial suspensions in glass tubes, the A_{600} value of the lower aqueous phase was measured. Then, the tubes were vigorously vortexed for 2 min, followed by 10 min of incubation at room temperature to allow for phase separation, and the A_{600} value of the lower aqueous phase was measured. Hydrophobicity was calculated using the following equation: percent hydrophobicity = $[1 - (A_{600}$ after vortex/A_{600} before vortex$)] \times 100$.

2.8. *Statistical analysis*

Statistical analysis was performed using Student's *t*-test for two groups, and Bonferroni-Dunnett's multiple comparison *t*-test to evaluate differences among multiple groups. *P*-values less than 0.05 were considered statistically significant.

3. Results

3.1. *Evaluation of growth inhibitory effect of LCEE (fruit) against S. pyogenes in vitro*

We evaluated the antibacterial activities of the three LCEEs (fruit, leaf, and stem) by Kirby-Bauer disk diffusion assay (Figure 2). Treatment with each

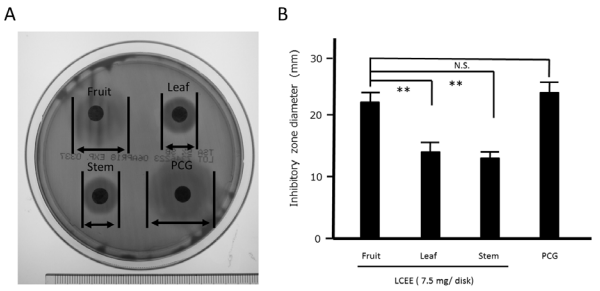

Figure 2. Antibacterial activities of the extracts of fruit, leaf, and stem of LCE (LCEEs). (A) Paper disks, 12 cm in diameter, containing 7.5 mg/disk of LCEEs (fruit, leaf, and stem) or 6 μg/disk of penicillin G (PCG) were placed on *S. pyogenes* cultured on trypticase soy agar with 5% sheep blood, and incubated for 24 h. Arrows show the inhibitory zones resulting from LCEEs or PCG. **(B)** The sizes of the inhibitory zones were measured. Data were expressed as mean ± S.D. (n = 6). N.S. not significant, *p < 0.05 and **p < 0.01 by Bonferroni-Dunnett's multiple t-test.

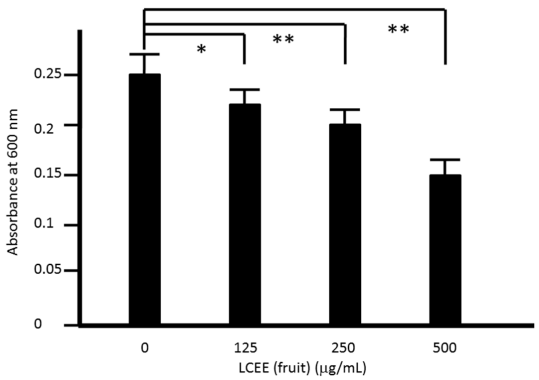

Figure 3. Bacterial growth inhibitory activity of LCEE (fruit). Numerical values represent extract concentrations. LCEE (fruit) was added in Todd Hewitt broth, and growth of *S. pyogenes* was measured for 24 h at 600 nm. Data were expressed as mean ± S.D. (n = 6). *p < 0.05 and ** < 0.01 by Bonferroni-Dunnett's multiple t-test.

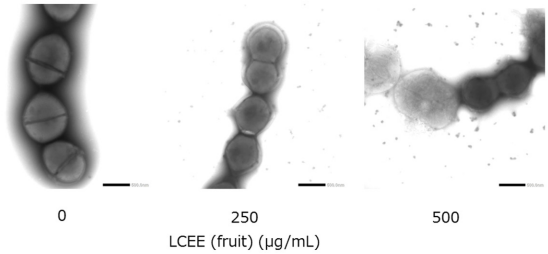

Figure 4. Morphological change of *S. pyogenes* treated with LCEE (fruit). Representative electron microscopy image of *S. pyogenes* cultured for 24 h with or without LCEE using negative staining.

LCEE on trypticase soy agar with 5% sheep blood inhibited bacterial growth by forming inhibitory zones (Figure 2A). Each LCEE showed significant antibacterial activity against the *S. pyogenes* 1529 strain. In particular, LCEE (fruit) showed the strongest antibacterial activity among the three LCEEs (p < 0.01), as evidenced by the largest inhibitory zone observed for this extract (Figure 2B). There were no significant differences in inhibitory zone sizes between 7.5 mg/disk of LCEE (fruit) and 6 μg/disk of penicillin G. Thus, we focused on analysis of LCEE (fruit) in further investigations because LCEE (fruit) had the greatest antibacterial effect among the three LCEEs. Using the liquid dilution method to evaluate antibacterial activity, bacterial growth inhibition by LCEE was measured after 24 h. As a result, we confirmed that LCEE (fruit) had inhibited *S. pyogenes* growth after 24 h in a concentration-dependent manner (Figure 3).

3.2. *Bacterial morphological investigation*

To confirm whether bacterial growth inhibition by LCEE was due to growth arrest or morphological disruption, we performed morphological analysis of *S. pyogenes* treated with LCEE (fruit). Negative staining analysis revealed that the shape of the bacterial cells became irregular in response to LCEE treatment. Local collapse of bacterial cell walls occurred in response to 250 μg/mL LCEE, and cell membrane irregularity and thinning occurred in response to 500 μg/mL LCEE. Finally, the cells collapsed and the bacterial contents were released into the extracellular environment. This morphological change occurred in a concentration-dependent manner (Figure 4).

3.3. *Biofilm analysis by microplate assay and confocal laser scanning microscopy*

Bacteria form biofilms to protect themselves from external stimuli (*16*). To evaluate whether LCEE (fruit) could inhibit biofilm formation, *S. pyogenes* was grown in THY broth with LCEE (fruit), and the ability to form biofilm on polystyrene plates was assessed using safranin red staining. Bacterial biofilms not exposed to LCEE were stained deep red. In contrast, formation of biofilms was suppressed by LCEE treatment, resulting in thinning of the red staining. Thus, a significant inhibitory effect of LCEE on *S. pyogenes* biofilm formation was observed after 48 h (p < 0.01) (Figure 5A). Next, we evaluated absorbance of safranin red to quantify bacterial biofilms. LCEE (fruit) at concentrations above 125 μg/mL significantly inhibited *S. pyogenes* biofilm formation (p < 0.01) (Figure 5B). Thus, we confirmed that LCEE (fruit) inhibited biofilm formation in a concentration-dependent manner. To confirm the results obtained using safranin red staining, *S. pyogenes* biofilms treated/untreated with LCEE (fruit) for 48 h were stained with FITC dye and visualized using confocal laser scanning microscopy (Figure 5C). The obtained Z-stack images were converted into three-dimensional images. The biofilms formed by the control showed a multi-layered surface-adhered cluster reflecting a mature biofilm. In contrast, the LCEE (fruit)-treated strains showed a lack of biofilm extracellular matrix. Overall, the findings from safranin red staining and microscopic three-dimensional

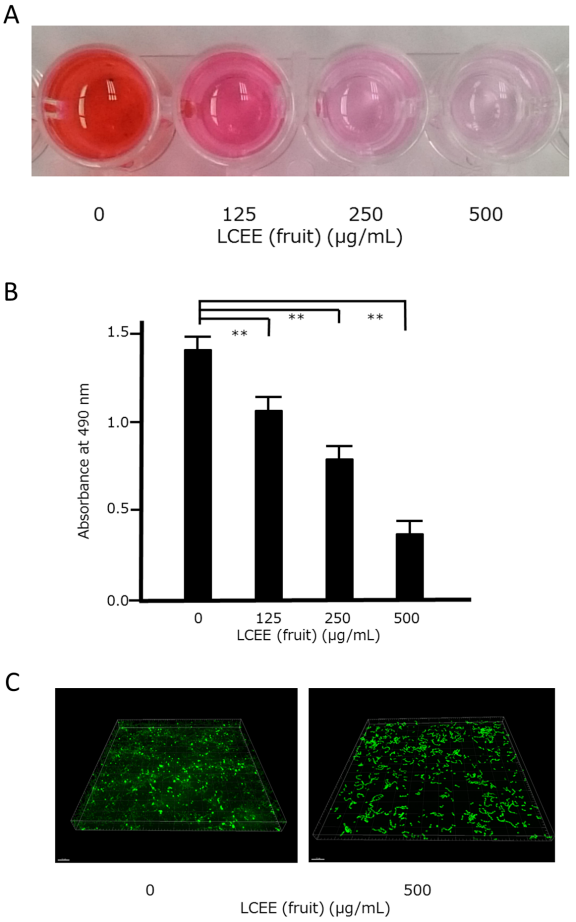

Figure 5. LCEE (fruit) inhibited *S. pyogenes* biofilm formation. (A) Image of a microplate. **(B)** *S. pyogenes* was cultured for 48 h with or without LCEE (fruit), and anti-biofilm activity of LCEE was quantified by safranin red adsorption at 490 nm. Data shown represent the mean ± S.D. ($n = 6$). $^{**}p < 0.01$ by Bonferroni-Dunnett's multiple *t*-test. **(C)** 3D analysis of biofilm formation of *S. pyogenes* treated with LCEE (fruit). Bacteria were cultured with LCEE (fruit) under static conditions at 37°C for 48 h in THY. Biofilms were stained with FITC. Three-dimensional images were reconstructed from confocal optical sections using Imaris software.

observations were consistent in showing that LCEE (fruit) inhibited biofilm formation.

3.4. *Bacterial cell surface hydrophobicity*

Based on the observation that LCEE altered bacterial morphology, we hypothesized that LCEE influenced bacterial surface hydrophobicity. As bacterial cell surface hydrophobicity affects the formation of bacterial biofilms (*16*), we evaluated the hydrophobicity of the strains using the n-hexadecane method. Surface hydrophobicity was markedly reduced in *S. pyogenes* treated with LCEE compared to that of the untreated group ($p < 0.01$) (Figure 6).

4. Discussion

In this study, we demonstrated that LCEE (fruit)

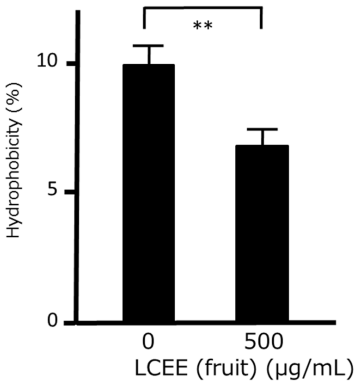

Figure 6. Hydrophobicity of *S. pyogenes* treated with LCEE (fruit). Cell surface hydrophobicity of *S. pyogenes* treated/untreated with LCEE (fruit) in the exponential phase (A_{600} of 1.0) was determined. The value of the control strain was set at 100%. Data shown represent the mean ± S.D. ($n = 6$). $^{**}p < 0.01$ by Student's *t*-test.

showed antibacterial and anti-biofilm activities. LCEE (fruit) inhibited bacterial growth and biofilm formation, and caused bacterial collapse in concentration-dependent manners. Adhesion to host tissues and biofilm formation are important steps in bacterial infections (*16*). A previous study showed that LCEE (fruit), which is rich in polyphenols, suppressed biofilm formation of *Staphylococcus epidermidis*, *Enterococcus faecalis*, and *Streptococcus mutans* (*18*). This study did not include *S. pyogenes* (*18*). Anthocyanins and proanthocyanidins have antibacterial properties and can inhibit adhesion of bacteria to mucosal membranes (*19*). Although organic acids such as succinic, malic, lactic, tartaric, citric, and acetic acid exerted antibiotic activity against streptococci, synthetic mixtures of organic acids tested at the concentrations found in wine had greater antibacterial activity than the beverages, indicating that in wine, mixed organic acids are inhibited by other components (*20*). Since wine is made directly from fruit, the antimicrobial effects of the organic acids in LCEE (fruit) may also be inhibited by other components. Although we did not evaluate the effects of specific vitamins or minerals on streptococci, several reports have indicated that anthocyanin and phenolic acid are involved in the antibacterial effect of LCEE (*4-6,18*). Although we used cyanidin-3-glucoside as a representative component of LCEE when we performed 3D-HPLC analysis (*18*), we did not evaluate the effects of cyanidin-3-glucoside on streptococci. Future studies should focus on the effects of individual components of LCEE on streptococci. The hydrophobic properties of bacterial cell surfaces play important roles in host cell-bacterium interactions (*21*). A previous study showed that plant extracts altered bacterial hydrophobicity by suppressing the formation of biofilms (*22*). Similarly, LCEE (fruit) decreased the cell surface hydrophobicity of *S. pyogenes* to approximately 2/3 of the hydrophobicity of untreated cells. Thus, LCEE (fruit) may exhibit anti-

biofilm activity. Moreover, reduced hydrophobicity may increase exposure of bacteria to antibiotics due to elimination of biofilms.

Several investigations have demonstrated the antibacterial effects of fruits on *S. pyogenes in vitro*. A previous study showed that crude extracts of *C. fistula* fruit exhibited moderate to strong antibacterial activity against *S. pyogenes* (*23*). Another study showed that a novel anti-bacterial peptide, brucin, which is specific to S. pyogenes was produced from the dried fruit protein of *Brucea javanica* (*24*). A mixture of active peptides was prepared from the fruit protein *in vitro* by pepsin hydrolysis, and its inhibitory activity toward gram-positive bacteria was higher than that of penicillin G and chloramphenicol (*24*). Other studies showed that 80% ethanol extracts of *Moringa oleifera*, *Limnophila aromatica*, *Terminalia chebula*, and *Phyllanthus emblica* had anti-bacterial activities against human virulent bacteria, including *S. pyogenes* (*25*). Our study was the first to show that that LCEE (fruit) may be effective against *S. pyogenes*.

Several reports have demonstrated the antibacterial effects of polyphenol compounds contained in LCEE (fruit) (*26*). DNA repair mutant gram-negative bacteria were significantly affected by phenolic compounds (*26*). This strain lacks a DNA repair mechanism, and was therefore expected to be more sensitive than the wild-type strain to damage caused by mutagenic agents (*26*). The chemical group of anthocyanidins, and the individual compounds quercetin and chlorogenic acid, suppressed the growth of the DNA repair mutant, but did not suppress growth of the wild-type (*26*). These results suggested that the anti-bacterial activities of these compounds occurred through interactions with DNA (*26*). Furthermore, antimicrobial action may also occur through genotoxicity. Small phenolic compounds such as carvacrol and thymol exhibited bacterial inhibitory effects by disrupting outer membranes (*27*). The flavonoid myricetin clearly inhibited growth of the *Lactococcus* and *Enterococcus* species (*28*). Based on these results, the degree of hydroxylation might affect the antimicrobial activity of pure phenolic compounds (*29*).

The antimicrobial activities of naturally-occurring phenols from fermented fruit juices such as wine have been widely studied (*30*), but little is known about the anti-microbial capacity of phenols present in berries. Cranberry and blueberry extracts rich in anthocyanins inhibited gram-negative bacteria (*26*). The antibacterial properties of cranberry juice have been extensively demonstrated (*31*) and these effects may be associated with inhibition of *E. coli* adherence to mucosal surfaces (*32*). However, berry extracts mainly inhibited the growth of gram-negative bacteria but had no effects on gram-positive bacteria (*25*). The anti-bacterial effects of LCEE (fruit) against S. pyogenes, a gram-positive bacterium, may distinguish these extracts from other berries. Furthermore, the bacterial morphological changes induced by LCEE (fruit), as evaluated by electron microscopy, were similar to those observed with cranberries (*33*).

Phenolic compounds affected the growth of different bacterial species by different mechanisms, which are not well-understood. Anti-adhesion may also be a mechanism of antimicrobial activity of berry compounds. Future studies should be performed to improve the understanding of these antimicrobial mechanisms.

5. Conclusions

In summary, LCEE (fruit) exerted anti-bacterial and anti-biofilm effects on *S. pyogenes in vitro*. Based on these results, the direct antibacterial effects of LCEE (fruit) may be useful for topical therapies, such as gargling. We propose that LCEE (fruit) is a novel therapeutic candidate for treatment of diseases resulting from *S. pyogenes* infections.

Conflicts of Interest

This study was partly supported by JSPS KAKENHI Grant Number JP 16K09251, and academic donations from both the Research Foundation for Oriental Medicine, and Atsuma town. There has been no other financial support for this work that could have influenced its outcome.

Acknowledgements

The authors thank Mr. Masashi Ishihara and Ms. Miwako Fujimura for excellent support through this investigation. The authors are grateful for providing LCE samples from Astuma town.

References

1. Cunningham MW. Pathogenesis of group A streptococcal infections. Clinic Microbiol Rev. 2000; 13:470-511.
2. Minami M, Sakakibara R, Imura T, Watanabe M, Morita H, Kanemaki N, Ohta M. Clinical characteristics of respiratory tract-associated *Streptococcus pyogenes* at general Japanese hospital in 2014 .J Biosci Med. 2015; 3:26-31.
3. Minami M, Sakakibara R, Watanabe M, Morita H, Kanemaki N, Ohta M. Clinical characteristics of vaginal discharge associated *Streptococcus pyogenes* at general Japanese hospital. J Biosci Med. 2018; 6:9-16.
4. Svarcova I, Heinrich J, Valentova K. Berry fruits as a source of biologically active compounds: the case of *Lonicera caerulea*. Biomed Pap Med Fac Univ Palacky Olomouc Czech Repub. 2007; 151:163-174.
5. Chaovanalikit A, Thompson MM, and Wrolstad RE. Characterization and quantification of anthocyanins and polyphenolics in blue Honeysuckle (*Lonicera caerulea* L.). J Agric Food Chem. 2004; 52:848-852.

6. Rupasinghe HPV, Arumuggam N, Amararathna M. The potential health benefits of haskap (*Lonicera caerulea* L.): Role of cyanidin-3-*O*-glucoside. J Funct Foods. 2018; 44:24-39.
7. Inami Y, Matsui Y, Hoshino T, Murayama C, Norimoto H. Inhibitory activity of the flower buds of *Lonicera japonica Thunb*. against histamine production and L-histidine decarboxylase in human keratinocytes. Molecules. 2014; 19:8212-8219.
8. Kang M, Jung I, Hur J, Kim SH, Lee JH, Kang JY, Jung KC, Kim KS, Yoo MC, Park DS, Lee JD, Cho YB. The analgesic and anti-inflammatory effect of WIN-34B, a new herbal formula for osteoarthritis composed of *Lonicera japonica Thunb* and *Anemarrhena asphodeloides Bunge in vivo*. J Ethnopharmacol. 2010; 131:485-496.
9. Zhao YY, Yang QR, Hao JB, Li WD. Research progress on pharmacological effects and their differences among the flowers, stems and leaves of *Lonicera japonica*. Zhongguo Zhongyao Zazhi. 2016; 41:2422-2427.
10. Wang C, Cao B, Liu QQ, *et al*. Oseltamivir compared with the Chinese traditional therapy maxingshigan-yinqiaosan in the treatment of H1N1 influenza: a randomized trial. Ann Intern Med. 2011; 155:217-225.
11. Jurikova T, Rop O, Mlcek J, Sochor J, Balla S, Szekeres L, Hegedusova A, Hubalek J, Adam V, Kizek R. Phenolic profile of edible honeysuckle berries (genus lonicera) and their biological effects. Molecules. 2011; 17:61-79.
12. Wu S, Yano S, Chen J, Hisanaga A, Sakao K, He X, He J, Hou DX. Polyphenols from *Lonicera caerulea* L. berry inhibit LPS-induced inflammation through dual modulation of inflammatory and antioxidant mediators. J Agric Food Chem. 2017; 65:5133-5141.
13. Zhou L, Wang H, Yi J, Yang B, Li M, He D, Yang W, Zhang Y, Ni H. Anti-tumor properties of anthocyanins from *Lonicera caerulea* 'Beilei' fruit on human hepatocellular carcinoma: *In vitro* and in vivo study. Biomed Pharmacother. 2018; 104:520-529.
14. Liu S, You L, Zhao Y, Chang X. Wild *Lonicera caerulea* berry polyphenol extract reduces cholesterol accumulation and enhances antioxidant capacity *in vitro* and in vivo. Food Res Int. 2018; 107:73-83.
15. Minami M, Ichikawa M, Hata N, Hasegawa T. Protective effect of hainosankyuto, a traditional Japanese medicine, on *Streptococcus pyogenes* infection in murine model. PloS One. 2011; 6:e22188.
16. Minami M, Konishi T, Takase H, Makino T. Shin'iseihaito (Xinyiqingfeitang) suppresses the biofilm formation of *Streptococcus pneumoniae in vitro*. Biomed Res Int. 2017; 2017:4575709.
17. Minami M, Takase H. Comparative investigation of alternative negative staining reagents in bacterial morphological study. J Biosci Med. 2017; 5:17-24.
18. Palíková I, Heinrich J, Bednár P, Marhol P, Kren V, Cvak L, Valentová K, Růzicka F, Holá V, Kolár M, Simánek V, Ulrichová J. Constituents and antimicrobial properties of blue honeysuckle: a novel source for phenolic antioxidants. J Agric Food Chem. 2008; 56:11883-11889.
19. Gupta P, Song B, Neto C, Camesano TA. Atomic force microscopy-guided fractionation reveals the influence of cranberry phytochemicals on adhesion of *Escherichia coli*. Food Funct. 2016; 7:2655-2666.
20. Daglia M, Papetti A, Grisoli P, Aceti C, Dacarro C, Gazzani G. Antibacterial activity of red and white wine against oral streptococci. J Agric Food Chem. 2007; 27:5038-5042.
21. Swiatlo E, Champlin FR, Holman SC, Wilson WW, Watt JM. Contribution of choline-binding proteins to cell surface properties of *Streptococcus pneumoniae*. Infect Immun. 2002; 70:412-415.
22. Nostro A, Cannatelli MA, Crisafi G, Musolino AD, Procopio F, Alonzo V. Modifications of hydrophobicity, *in vitro* adherence and cellular aggregation of *Streptococcus mutans* by *Helichrysum italicum* extract. Lett Appl Microbiol. 2004; 38:423-427.
23. Bhalodia NR, Nariya PB, Acharya RN, Shukla VJ. *In vitro* antibacterial and antifungal activities of *Cassia fistula* Linn. fruit pulp extracts. Ayu. 2012; 33:123-129.
24. Sornwatana T, Roytrakul S, Wetprasit N, Ratanapo S. Brucin, an antibacterial peptide derived from fruit protein of Fructus Bruceae, *Bruceajavanica* (L.) *Merr.* Lett Appl Microbiol. 2013; 57:129-136.
25. Rattanasena P. Antioxidant and antibacterial activities of vegetables and fruits commonly consumed in Thailand. Pak J Biol Sci. 2012; 15:877-882.
26. Puupponen-Pimiä R, Nohynek L, Meier C, Kähkönen M, Heinonen M, Hopia A, Oksman-Caldentey KM. Antimicrobial properties of phenolic compounds from berries. J Appl Microbiol. 2001; 90:494-507.
27. Fadli M, Chevalier J, Hassani L, Mezrioui NE, Pagès JM. Natural extracts stimulate membrane-associated mechanisms of resistance in Gram-negative bacteria. Lett Appl Microbiol. 2014; 58:472-477.
28. Xu HX, Lee SF. Activity of plant flavonoids against antibiotic-resistant bacteria. Phytother Res. 2001; 15:39-43.
29. Sakauchi M, Narushima K, Sone H, Kamimaki Y, Yamazaki Y, Kato S, Takita T, Suzuki N, Moro K. Kinematic approach to gait analysis in patients with rheumatoid arthritis involving the knee joint. Arthritis Rheum. 2001; 45:35-41.
30. Vivas N, Lonvaud-Funel A, Glories Y. Effect of phenolic acids and anthocyanins on growth, viability and malolactic activity of a lactic acid bacterium. Food Microbiol. 1997; 14:291-299.
31. Howell AB. Cranberry proanthocyanidins and the maintenance of urinary tract health. Crit Rev Food Sci Nutr. 2002; 42:273-278.
32. Howell AB, Vorsa N, Der Marderosian A, Foo LY. Inhibition of the adherence of P-fimbriated *Escherichia coli* to uroepithelial-cell surfaces by proanthocyanidin extracts from cranberries. N Engl J Med. 1998; 339:1085-1086.
33. Lacombe A, Wu VC, Tyler S, Edwards K. Antimicrobial action of the American cranberry constituents; phenolics, anthocyanins, and organic acids, against *Escherichia coli* O157:H7. Int J Food Microbiol. 2010; 139:102-107.

(January 11, 2019; Revised February 24, 2019; Accepted March 24, 2019)

Original Article

DOI: 10.5582/bst.2018.01292

Sperm DNA fragmentation valued by SCSA and its correlation with conventional sperm parameters in male partner of recurrent spontaneous abortion couple

Minmin Yuan[1], Liqing Huang[2], Wing Ting Leung[3], Mingyan Wang[1], Yi Meng[1], Zengshu Huang[3], Xinyao Pan[3], Jing Zhou[3], Chuyu Li[3], Yizhen Sima[3], Lan Wang[3], Yanzhi Zhang[3], Chunmei Ying[1,*], Ling Wang[3,4,5,*]

[1] *Laboratory for Clinical Laboratory Testing, Hospital of Obstetrics and Gynecology, Fudan University Shanghai Medical College, Shanghai, China;*
[2] *Department of Statistics and Psychology, College of Letters and Science, University of California Davis, Davis, California, USA;*
[3] *Laboratory for Reproductive Immunology, Hospital & Institute of Obstetrics and Gynecology, Shanghai Medical College, Fudan University, Shanghai, China;*
[4] *The Academy of Integrative Medicine, Fudan University, Shanghai, China;*
[5] *Shanghai Key Laboratory of Female Reproductive Endocrine-related Diseases, Shanghai, China.*

Summary **The objective of this study is to evaluate the predictive value of sperm DNA fragmentation Index (DFI) in unexplained recurrent spontaneous abortion (RSA) and to investigate its correlation with conventional sperm parameters. Besides, we aimed to reveal the necessity of establishing a DFI clinical threshold of each laboratory for the prognostic diagnosis of RSA and establish our own DFI threshold. Semen samples were collected from male partners of RSA patients (n = 139) and healthy recent fathers (control, n = 200). DFI was tested using SCSA and conventional semen analysis was performed using an automatic semen analyzer. The DFI value and distribution were compared between the two groups using corresponding statistical software. The diagnostic threshold value was established by ROC curve. The correlation between DFI and the conventional semen parameters of the 139 cases was further analyzed using Student's t test and Mann-Whitney U test. Our result showed that DFI was significantly higher in RSA patients compared with normal donor controls. We established our own DFI threshold at 13.59%. There was only a weak partial correlation between DFI values and conventional sperm analysis parameters. Our present study suggested that DFI might be used as a valuable predictor for RSA independent of conventional sperm parameters. Additionally, we recommend that each laboratory should establish its own clinical DFI threshold for more precise prediction of RSA and we recommend that sperm DNA fragmentation test should be included in complete sperm quality assessment in addition to conventional semen analysis for RSA male partners.**

Keywords: Recurrent spontaneous abortion (RSA), sperm DNA fragmentation (SDF), DNA fragmentation index (DFI), Sperm Chromatin Structure Assay (SCSA), high DNA stainability (HDS), semen analysis

Released online in J-STAGE as advance publication April 11, 2019.

**Address correspondence to:*
Dr. Ling Wang, Obstetrics & Gynecology Hospital of Fudan University, 419 Fangxie Road, Shanghai 200011, China.
E-mail: Dr.wangling@fudan.edu.cn

Dr. Chunmei Ying, Obstetrics & Gynecology Hospital of Fudan University, 419 Fangxie Road, Shanghai 200011, China.
E-mail: ycmzh2012@163.com

1. Introduction

Recurrent spontaneous abortion (RSA) is a pregnancy complication whose etiology is still unclear. There have been many controversies regarding its diagnosis and treatment, but there is a general agreement that the incidence of RSA involves combined pathogenic factors from both males and females of the infertile

couples. For decades, the initial diagnostic investigation of male fertility relies only on conventional semen analysis, which mainly includes sperm count, vitality, motility, and morphology according to World Health Organization (WHO) manual. No doubt that these parameters are closely relevant and important for the diagnosis of subfertility, which might be the cause of RSA. However, these parameters addressed only a few aspects of sperm quality and function, while in fact, an estimated 15-40% of males with normal conventional semen analysis results are nonetheless associated with infertility (*1-3*), or still suffer from repeated abortions. Thus, new tests for RSA male partners would be clinically useful.

In the past few decades, the role of sperm DNA integrity on fertility, embryo development, embryo quality, implantation and pregnancy has gained a lot of attention. As reported, fertilization of oocytes with spermatozoa that have damaged DNA could potentially lead to reduced fertilization rates, poor embryo quality, as well as higher rates of spontaneous miscarriage (*4,5*). Also, the correlation between sperm DNA fragmentation (SDF) and recurrent pregnancy loss has been illustrated by many studies. Several studies have demonstrated a significantly higher DNA fragmentation index (DFI) in couples with RSA than in controls (*6-8*). However, although there are already considerable data supporting the clinical use of SDF tests, there are controversies regarding the exact value of DNA integrity in diagnostic and prognostic evaluation of RSA patients because some studies found no obvious differences in SDF level between RSA patients and healthy recent fathers (*9*). Some studies even denied that DNA fragmentation is one of the possible causes of RSA (*9,10*). Thus, so far in China, only a few laboratories have implemented sperm chromatin integrity testing and adopted SDF as a routine scanning item to evaluate male's fertile capability. Therefore, more studies verifying the value of SDF testing in RSA couples are needed.

Despite some opposition, SDF has been proposed as a useful indicator for demonstrating the underlying causes of RSA and adopted as a scanning item in a few laboratories for male infertility, low assisted reproduction technology (ART) pregnancy rate, recurrent miscarriage and even severe adverse outcomes of the offspring such as cancer or neurological disorders (*11-13*). A variety of SDF detecting assays have been developed in the past few decades (*14-16*) but are limited in widespread use due to the inconsistent DFI threshold among different assays, the lack of standardized operation procedures and the lack of quality control among laboratories (*17*). Sperm chromatin structure assay (SCSA), firstly described by Evenson and his coworkers in 1980 (*18*) and improved later (*19,20*), has been recommended as a relatively independent and reliable assay in China because of its better sensitivity, stability and accuracy. DFI clinical threshold values using SCSA with regard to fertility have been proposed and established in some laboratories (*20*). However, the DFI thresholds reported are inconsistent and conflicted (*8*). To our knowledge, for the laboratories in China that have implemented SDF testing for male fertility assessment, most of them just adopt the DFI cutoff value offered by the commercial kit producer which is usually 15%. We hold the opinion that to use SDF testing more precisely in clinical practice, it is essential to establish a reliable clinical threshold value for each laboratory, which may reduce possible diagnostic error.

We expect to better illustrate these problems through our present study. Our work was comprised of the following parts. Firstly, we intended to reveal the clinical significance of using SDF test as a tool in evaluation of male fertility in RSA couples. Secondly, we aimed to investigate and establish the DFI clinical cutoff value of our laboratory, hoping to be helpful in establishment of a reference value for RSA male patients in Chinese Han population. Lastly, we further analyzed the correlation between DFI values and conventional semen analysis parameters to investigate the possible value of its future integration into routine clinical practice.

2. Materials and Methods

2.1. *Patients and data collection*

Patient data collection was approved by the Ethics Committees of Obstetrics & Gynecology Hospital affiliated to Fudan University. A total of 139 RSA couples were enrolled in this study. Written informed consent was obtained from all cases. The 139 RSA couples were collected from the reproductive immunology clinic and recurrent miscarriage specialist clinic from October 2017 to March 2018. Patients inclusion criteria included a history of at least two unexplained first trimester recurrent spontaneous abortion and all the known female causes of recurrent pregnant loss were ruled out, and only idiopathic recurrent miscarriage cases were recruited. In brief, the female partner of couples enrolled was physically healthy with regular menstrual cycles, normal in hormonal profiles, and anatomically normal in uterus. Other causes of RSA like antiphospholipid syndrome or thrombophilia, metabolic disorders and genital infections were also screened and ruled out. Only male partner of each of these females was included in the following study. Both males and females of the couples had normal karyotype with no family history of physical diseases. Patients with other confounding factors such as varicocele, antioxidant intake, bad habits like excessive drinking and smoking, which may affect DNA damage levels were ruled out. The age of enrolled patients all ranged from 20 to 40 years old and

were age matched with normal controls.

2.2. *Sample Collection and analysis*

The 139 male's fresh semen samples were obtained by masturbation at our laboratory in a sterile plastic container after 3-7 days of sexual abstinence. After liquefaction at room temperature, conventional semen analysis was performed with Weili automatic semen analyzer 9000 following WHO guidelines (*21*). The remaining volume of the semen samples was cryopreserved until SCSA analysis was performed. The 200 frozen semen samples from normal control fertile men were collected and donated by the research department of Zhejiang Xingbo Biological Technology Company. All the males included in the control group had their new born babies within the recent two years and their sperm quality were qualified according to the fifth edition of WHO laboratory manual for examination and processing of human semen.

2.3. *SCSA*

SCSA is a sensitive technology based on a flow cytometric technique measuring the susceptibility of sperm DNA to acid which can induce DNA denaturation in situ (*21*). By using SCSA, we can evaluate sperm DNA fragmentation index (DFI) and detect spermatozoa with abnormal sperm chromatin structure consisting of abnormal nuclear proteins which is described as high DNA stainability (HDS). We performed SCSA by using a commercial kit produced by Zhejiang Xingbo Biological Technology Company according to standard procedure (*20,22,23*). The sperm count ($\times 10^6$/mL) was adjusted with buffer A (comprised of Tris-HCL, NaCl, EDTA) in the kit according to the requirements for SCSA. Briefly, the sperm count was adjusted to 1-2 $\times 10^6$/mL and was prepared in a total of 100 uL. Then, 200 uL buffer B (comprised of HCL, NaCl, Triton X-100) was added to the tube. After 30 seconds, sperm cells were stained by adding 600 uL acridine orange (AO) staining (including Na_2HPO_4, EDTA, NaCl). After 3 minutes staining, a total of 10,000 sperm cells were analyzed by flow cytometry (FACS Calibur, Becton Dickinson). By staining with the fluorescent dye acridine orange (AO), double stranded native DNA emits green fluorescence, while fragmented single stranded DNA emits red fluorescence. The data was obtained from a specific dedicated software offered by the Xingbo Corporation. The extent of DNA denaturation is indicated by the percentage of sperm containing fragmented DNA after acid treatment, that is, shifting from green fluorescence to red fluorescence after an acidic treatment (*7,18,22,24*). A scatter plot was created, DFI was expressed as ratio of red to total (red plus green) fluorescence, that is, the ratio of sperm with denatured DNA over total sperm. The percentage of sperm with high DNA stainability (HDS) in each sample was also recorded from the graph plot.

2.4. *Statistical analysis approach*

Statistical analysis was performed using the Statistics Package for the Social Sciences software (SPSS), version 23.0. The classification data was represented by frequency and percentage. Chi-square test was used for group comparisons. The normality test was firstly conducted for the measurement data. If the normal distribution was satisfied, the data was represented as X (Mean) ± S (standard deviation). The *t* test of independent sample data was used for comparison between the two groups. Where the normal distribution was not satisfied, the median and quartile numbers were used to represent it. Kruskal-wallis *H* test was used for comparison among multiple groups, and Mann-Whitney *U* test was used for pairwise comparisons. Receiver operating characteristic (ROC) curve analysis was applied to evaluate the ability of DFI to differentiate RSA patients from controls, by calculating the corresponding truncation value, sensitivity and specificity. In this study, a bilateral test was used, and $p < 0.05$ was considered statistically significant. The correlation between DFI and semen parameters was determined by using Pearson's correlation coefficient. The level of significance was established at 95% of the confidence interval in order to be considered statistically significant.

3. Results

DFI median and range values as well as its comparison between 139 RSA semen samples and 200 normal controls are shown in Table 1. The results showed that the DFI median of RSA male partner was 13.84% (ranged 10.38-23.57%), which was significantly higher

Table 1. Comparison of sperm DNA fragmentation (DFI) between fertile controls and RSA male partners and distribution percentage of different levels of DFI in both groups

Parameter Category	Normal controls (*n* = 200)	RSA male partners (*n* = 139)	Chi-square	*p*
DFI (%)	9.86 (8.45-11.11)	13.84 (10.38-23.57)*	56.389	< 0.001
< 15%	187 (93.5%)	74 (53.2%)*	83.354	< 0.001
15-30%	13 (6.5%)	47 (33.8%)*	95.635	< 0.001
> 30%	0 (0.0%)	18 (12.9%)		

DFI values are presented as median(range); *compared with normal controls, $p < 0.05$ and considered statistically significant.

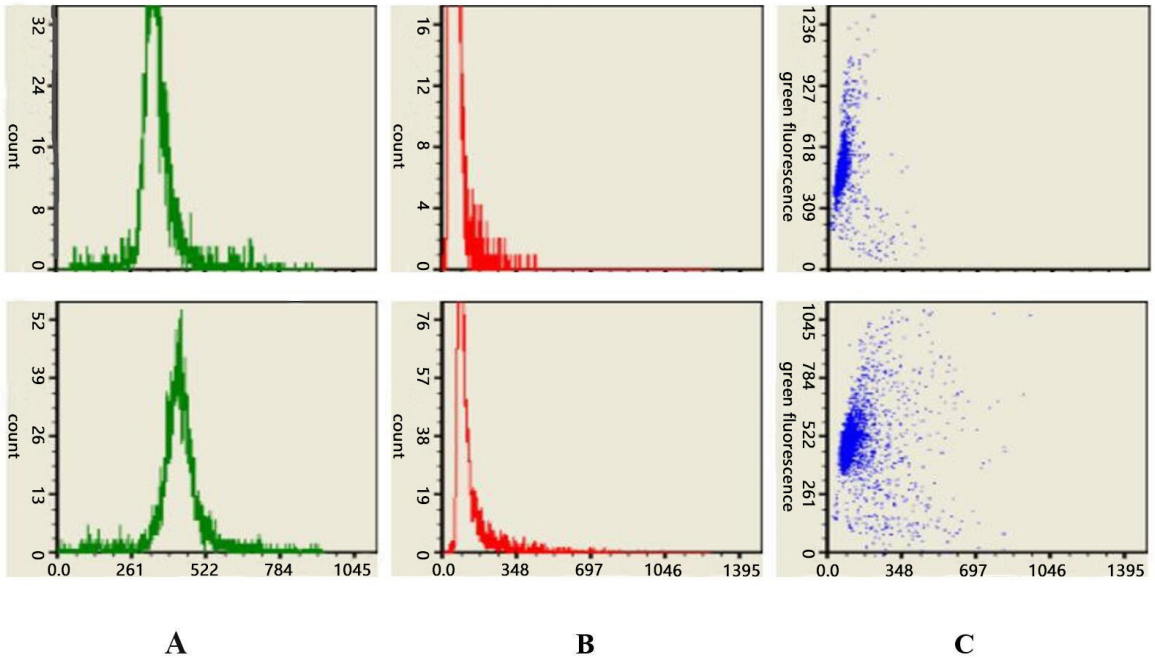

Figure 1. Florescent plots of two semen samples using SCSA. (A, B) Green fluorescence represents sperm with complete DNA, and red fluorescence represents sperm with fragmented DNA. X-axis: fluorescence intensity; Y-axis: sperm count; **(C)** Scatter diagram of sperm by SCSA, X-axis represents red fluorescence emitted from sperm with fragmented DNA and Y-axis represents green fluorescence emitted from sperm with complete DNA. Upper row: florescent plot of a semen sample from control group with DFI value of 5.7%; Lower row: florescent plot of a semen sample from RSA patient with DFI value of 17.1%.

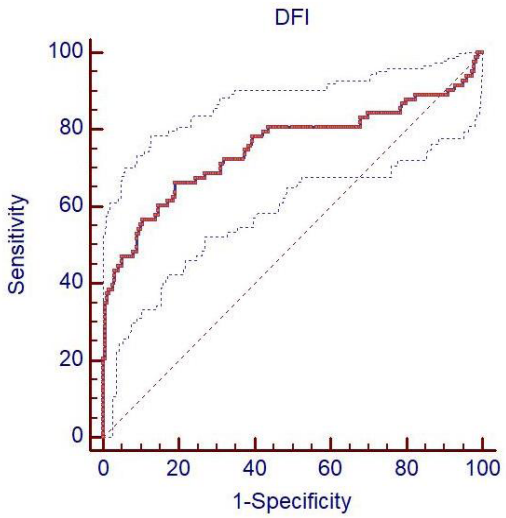

Figure 2. Receiver operating characteristics curve (ROC) analysis of DFI in RSA male patients to normal control group. ROC curve analysis of sperm DFI to diagnose male related RSA. DFI cutoff value: 13.59%; AUC (area under curve): 0.752; 95% CI (confidence interval): 0.697-0.801; sensitivity: 66.27%; specificity: 81.00%.

than that of normal controls, which was 9.86% (range 8.45-11.11%). Analysis of the three DFI level groups showed that the percentage of males with DFI < 15% was significantly higher ($p < 0.001$) in the control group (93.5%) than in RSA groups (53.2%). While on the contrary, for the other two DFI level groups (15-30% and > 30% respectively), RSA couples showed a significantly higher percentage than the fertile controls.

Figure 1 is a schematic diagram of a sperm fluorescent histogram plot from a normal male and a male patient by using SCSA and software fitting. The DFI was 5.7% and 17.1% respectively. Receiver operating characteristics curve (ROC) analysis of DFI in RSA patients compared to normal control group is shown in Figure 2. The DFI cut-off value with highest sensitivity and specificity for diagnosing RSA patients was found at 13.59%. When the threshold level 13.59% was used in RSA patients, the sensitivity and specificity was estimated as 66.27% and 81.00% respectively.

The correlation between DFI tested by SCSA and conventional seminal parameters was also analyzed. The 139 patients were divided into two groups, defined by the DFI threshold level of 13.59% (< 13.59% group *vs* ≥ 13.59% group). Student's *t*-test was applied to compare the two groups, and $p < 0.05$ was considered statistically significant. Non-normal distribution data is expressed as median (range). We found a significant difference in abstinence days and progressive motility ($p < 0.05$) but not sperm count, viability or normal morphology rate ($p > 0.05$) between the two groups (Table 2).

DFI and HDS were compared between different groups in four semen analysis parameters and are shown in Table 3. The parameters included abstinence days, sperm count, viability and progressive motility. Comparison of DFI and HDS levels among three groups classified by abstinence days showed that when comparing > 7 days of abstinence group with 3-7 days and < 3 days group, there was a tendency of decrement

Table 2. Comparison of conventional seminal parameters in RSA husbands with different DNA fragment levels divided by the threshold value (13.59%) of sperm DFI

Semen parameters	Sperm DFI < 13.59% group, *n* =76	Sperm DFI ≥ 13.59% group, *n* = 63	Z/t	*p*
Abstinence days	4.00 (3.00-5.00)	5.00 (4.00-7.00)	- 3.012	0.003*
Sperm count (× 10^6/mL)	52.22 (24.45-78.40)	65.05 (33.49-97.75)	- 1.658	0.097
Viability (%)	48.02 ± 18.76	42.97 ± 20.82	1.376	0.172
Progressive motility (%)	37.56 ± 14.31	32.01 ± 15.63	1.997	0.048*
Normal morphology (%)	80.00 (70.00-80.00)	75.00 (65.00-80.00)	- 1.686	0.092

*$p < 0.05$ was considered statistically significant.

Table 3. Comparison of DFI and HDS levels of groups classified by different situation of conventional parameters

Items	DFI (%)	*p* value	HDS (%)	*p* value
Abstinence days				
< 3 days	10.36 (5.62-13.66)		7.06 (4.58-8.75)	
3-7 days	12.29 (8.71-18.54)	0.043#	6.29 (4.62-8.96)	0.678
> 7 days	18.31 (12.54-25.99)	0.026*	4.44 (3.28-5.23)	0.052
Sperm count (× 10^6/mL)				
< 15	8.89 (7.61-13.29)		6.41 (4.45-9.51)	
≥ 15	13.19 (8.83-20.51)	0.038	5.91 (4.51-8.37)	0.618
Viability (%)				
< 58	10.38 (8.89-19.20)		6.30 (4.60-8.43)	
≥ 58	9.36 (8.30-17.43)	0.162	5.63 (3.88-8.28)	0.216
Progressive motility (%)				
< 32	15.41 (10.55-21.72)		6.41 (4.95-9.81)	
≥ 32	10.56 (8.30-15.76)	0.002	5.63 (4.36-7.59)	0.085

$p < 0.05$ was considered significant; *> 7 days group compared with < 3 days group, $p < 0.05$; #> 7 days group compared with 3-7 days group, $p < 0.05$.

in DFI and the differences were significant ($p < 0.05$), while comparison of HDS showed no significance (Table 3). To our surprise, sperm count < 15 × 10^6 group showed a significant lower median DFI level compared with ≥ 15 × 10^6 group, which was 8.89% (range 7.61%-13.29%) and 13.19% (range 8.83%-20.51%) respectively ($p < 0.05$), while there was no significant difference of HDS level between the two groups. We analyzed the possible relationship between sperm DNA fragmentation and conventional sperm parameters of sperm viability and progressive motility. Neither DFI nor HDS levels showed significant difference ($p > 0.05$) between two groups classified by 5th WHO standard of 58% for sperm viability (%) by using SCSA. As for the comparison of DFI and HDS levels between two groups classified by sperm progressive motility rate [PR(A + B)%] of 32%, the result showed a significant ($p < 0.05$) positive relationship between sperm DNA integrity and sperm progressive motility rate. However the result showed no significant difference ($p > 0.05$) in HDS level between the two groups.

Correlation between DFI and different WHO semen parameters was analyzed and calculated, as shown in Table 4. According to our results, abstinence days significantly positively correlated with DFI while sperm viability, progressive motility and normal morphology rate significantly negatively correlated with DFI ($p < 0.05$). There appeared to be no significant relation between DFI and sperm counts.

Table 4. Correlation analysis between semen parameters and DFI in 139 RSA group samples

Items	*r*	*p*
Abstinence days	0.332	0.000*
Sperm count (×10^6/mL)	0.157	0.092
Viability (%)	- 0.194	0.037*
Progressive motility (%)	- 0.266	0.004*
Normal morphology (%)	- 0.248	0.009*

*$p < 0.05$ was considered statistically significant; *r* = correlation coefficient.

4. Discussion

The etiology of reduced semen quality remains unexplained. Sperm DNA or chromatin damage has been reported as mainly linked to abnormal or incomplete chromatin packaging during spermatogenesis, abortive apoptosis and oxidative stress induced by releasing of reactive oxygen species (ROS) (*25,26*). The oxidative damage is associated with exposure to a variety of genotoxic risk agents including environmental exposure, diseases, life styles, and *et al*. (*1,27,28*). Sperm that lacks antioxidants and DNA repair systems, as well as DNA repair from oocytes or early embryo are vulnerable to DNA strand damage. Although their correlation was not always found statistically significant, numerous studies tended to believe that a high level of SDF is a deleterious factor

for achieving and sustaining term pregnancies (*1*).

A significant negative correlation between sperm DNA damage and embryo quality has been elucidated *in vitro* and *in vivo* (*29*) and high DFI has proven to be associated with increased miscarriage rate (*19,30*). The high degree of DNA fragmentation may not necessarily affect fertilization rates, but may result in subsequent miscarriage. From the present work we perceive that patients diagnosed with male caused RSA have a significantly higher level of DFI compared to normal controls (Table 1). Thus, our study further supports the value of SDF testing used in clinical investigation for male caused RSA.

According to the former report, when DFI is higher than 20%, the chance of obtaining a natural pregnancy is decreased, and close to zero when DFI is over 30-40% (*31*). It's now widely accepted that sperm with DFI > 15% (percentage offered by most commercial kits) is not ideal and patients with DFI > 30% are at higher risk of infertility regardless of whether they conceive via natural conception or ART. However, there is still no specific diagnostic threshold for specific infertility circumstances such as RSA. Besides, different ethnic population and different reagents or instruments used in different laboratories may be factors affecting the diagnostic accuracy of DFI results. Therefore, it is necessary for the laboratory to establish its own diagnostic threshold. According to our present work, we defined our own cutoff value as 13.59% using SCSA and its sensitivity and specificity was evaluated as 66.27% and 81.00%, respectively (Figure 1). Both the sensitivity and specificity of the DFI threshold were not very ideal, indicating that DFI is only one of the determinants which are important for the underlying causes of RSA.

It was shown that 25-40% of infertile men may have normal sperm characteristics according to WHO criteria, but with DFI > 20-30% (*32,33*). Thus, controversies regarding the correlations between DFI and conventional semen parameters exist. Several studies reported a weak-to-moderate inverse correlation between DFI and sperm count, motility, vitality and morphology (*19,34*). Our correlation study of 139 RSA cases showed a positive correlation between DFI level and abstinence days. This may be related to various adverse factors such as ROS on sperm DNA integrity during sperm's transmission to the epididymis. Our results also revealed an only weak negative correlation between DFI and viability, motility and normal morphological rate (Table 4). Since 'normal' sperm defined by conventional semen analysis may still carry fragmented DNA, we propose that sperm DNA integrity should be included in sperm quality tests and used as a parameter independent of conventional semen analysis.

HDS provides information on chromatin condensation associated with sperm cell immaturity. High HDS rate have negative effects on pregnancy and has been proven to be an effective indicator of possible spontaneous abortion in assisted reproduction, and the correlation between HDS > 15% and low fertilization rates in IVF was found (*19,31*). However, in our study, we found no significant difference of HDS between groups classified by routine semen parameters. In the future research, it is expected to enlarge the study sample size and further explore the relationship between HDS and fertility.

In summary, we conclude that DFI level of RSA males is significantly higher than that of normal controls which is accordance with some previous reports (*2,7,35*). We strongly recommend the use of SDF testing besides routine semen analysis to assess a male's fertility more comprehensively. We established a DFI threshold value of 13.59% for our own laboratory, which should be helpful for the establishment of a reference value of Chinese RSA patients. According to our work, lowering the DFI values to below the threshold of 13.59% through lifestyle management or medication is expected to increase the success rate of pregnancy in patients with repeated abortions. More investigations on the relation between DFI or HDS levels and pregnancy outcomes on a larger sample size are still waiting to be carried out. Understanding the precise mechanism of sperm DNA damage as well as exploring the corresponding clinical interventions that give the best chances of full term pregnancy are also of great importance.

Acknowledgements

This work was supported by grants from the National Natural Science Foundation of China (no. 31571196 to Ling Wang and no. 30801502 to Ling Wang), the Program to Guide Medicine ("Yixueyindao") of the Shanghai Municipal Science and Technology Commission (no. 18401902200 to Ling Wang and no. 15401932200 to Ling Wang), the Shanghai Program for Support of Leading Disciplines-Integrative Medicine (no. 20180101 and no. 20150407), the Research Foundation ("CR Sanjiu") of Obstetrics & Gynecology committee of Chinese Association of Integrated Traditional Chinese and Western Medicine (CR1901FC01 to Ling Wang), the Shanghai Committee of the China Democratic League (no. 02054 to Ling Wang), the FY2008 JSPS Postdoctoral Fellowship for Foreign Researchers (P08471 to Ling Wang), and the Shanghai Pujiang Program (no. 11PJ1401900 to Ling Wang). We also appreciate Huijing Tang and Jing Liu, laboratory technicians from the Department of Clinical Testing, for their support and assistance in data collection and analyzing the traditional semen parameters.

References

1. Evgeni E, Charalabopoulos K, Asimakopoulos B. Human

sperm DNA fragmentation and its correlation with conventional semen parameters. J Reprod Infertil. 2014; 15:2-14.
2. Lin MH, Kuo-Kuang Lee R, Li SH, Lu CH, Sun FJ, Hwu YM. Sperm chromatin structure assay parameters are not related to fertilization rates, embryo quality, and pregnancy rates in *in vitro* fertilization and intracytoplasmic sperm injection, but might be related to spontaneous abortion rates. Fertil Steril. 2008; 90:352-359.
3. van der Steeg JW, Steures P, Eijkemans MJ, JD FH, Hompes PG, Kremer JA, van der Leeuw-Harmsen L, Bossuyt PM, Repping S, Silber SJ, Mol BW, van der Veen F, Collaborative Effort for Clinical Evaluation in Reproductive Medicine Study G. Role of semen analysis in subfertile couples. Fertil Steril. 2011; 95:1013-1019.
4. Ahmadi A, Ng SC. Developmental capacity of damaged spermatozoa. Hum Reprod. 1999; 14:2279-2285.
5. Carrell DT, Liu L, Peterson CM, Jones KP, Hatasaka HH, Erickson L, Campbell B. Sperm DNA fragmentation is increased in couples with unexplained recurrent pregnancy loss. Arch Androl. 2003; 49:49-55.
6. Ford HB, Schust DJ. Recurrent pregnancy loss: Etiology, diagnosis, and therapy. Rev Obstet Gynecol. 2009; 2:76-83.
7. Absalan F, Ghannadi A, Kazerooni M, Parifar R, Jamalzadeh F, Amiri S. Value of sperm chromatin dispersion test in couples with unexplained recurrent abortion. J Assist Reprod Genet. 2012; 29:11-14.
8. Khadem N, Poorhoseyni A, Jalali M, Akbary A, Heydari ST. Sperm DNA fragmentation in couples with unexplained recurrent spontaneous abortions. Andrologia. 2014; 46:126-130.
9. Coughlan C, Clarke H, Cutting R, Saxton J, Waite S, Ledger W, Li T, Pacey AA. Sperm DNA fragmentation, recurrent implantation failure and recurrent miscarriage. Asian J Androl. 2015; 17:681-685.
10. Bellver J, Meseguer M, Muriel L, Garcia-Herrero S, Barreto MA, Garda AL, Remohi J, Pellicer A, Garrido N. Y chromosome microdeletions, sperm DNA fragmentation and sperm oxidative stress as causes of recurrent spontaneous abortion of unknown etiology. Hum Reprod. 2010; 25:1713-1721.
11. Basar MM, Kahraman S. Clinical utility of sperm DNA fragmentation testing: Practice recommendations based on clinical scenarios. Transl Androl Urol. 2017; 6:S574-S576.
12. Spanò M, Bonde JP, Hjøllund HI, Kolstad HA, Cordelli E, Leter G. Sperm chromatin damage impairs human fertility. The Danish First Pregnancy Planner Study Team. Fertil Steril. 2000; 73:43-50.
13. Ribas-Maynou J, Garcia-Peiro A, Fernandez-Encinas A, Amengual MJ, Prada E, Cortes P, Navarro J, Benet J. Double stranded sperm DNA breaks, measured by Comet assay, are associated with unexplained recurrent miscarriage in couples without a female factor. PLoS One. 2012; 7:e44679.
14. Tamburrino L, Marchiani S, Montoya M, Elia Marino F, Natali I, Cambi M, Forti G, Baldi E, Muratori M. Mechanisms and clinical correlates of sperm DNA damage. Asian J Androl. 2012; 14:24-31.
15. Bungum M, Bungum L, Giwercman A. Sperm chromatin structure assay (SCSA): A tool in diagnosis and treatment of infertility. Asian J Androl. 2011; 13:69-75.
16. Cho CL, Agarwal A, Majzoub A, Esteves SC. Clinical utility of sperm DNA fragmentation testing: Concise practice recommendations. Transl Androl Urol. 2017; 6:S366-S373.
17. Chi HJ, Chung DY, Choi SY, Kim JH, Kim GY, Lee JS, Lee HS, Kim MH, Roh SI. Integrity of human sperm DNA assessed by the neutral comet assay and its relationship to semen parameters and clinical outcomes for the IVF-ET program. Clin Exp Reprod Med. 2011; 38:10-17.
18. Evenson DP, Darzynkiewicz Z, Melamed MR. Relation of mammalian sperm chromatin heterogeneity to fertility. Science. 1980; 210:1131-1133.
19. Boe-Hansen GB, Fedder J, Ersbøll AK, Christensen P. The sperm chromatin structure assay as a diagnostic tool in the human fertility clinic. Human Reproduction. 2006; 21:1576-1582.
20. Evenson DP, Jost LK, Marshall D, Zinaman MJ, Clegg E, Purvis K, de Angelis P, Claussen OP. Utility of the sperm chromatin structure assay as a diagnostic and prognostic tool in the human fertility clinic. Human Reproduction. 1999; 14:1039-1049.
21. World Health Organization. WHO laboratory manual for the examination and processing of human semen. 5th ed. Geneva : World Health Organization, 2010; pp. 10-44.
22. Evenson DP, Larson KL, Jost LK. Sperm chromatin structure assay: its clinical use for detecting sperm DNA fragmentation in male infertility and comparisons with other techniques. J Androl. 2002; 23:25-43.
23. Jurewicz J, Radwan M, Wielgomas B, Sobala W, Piskunowicz M, Radwan P, Bochenek M, Hanke W. The effect of environmental exposure to pyrethroids and DNA damage in human sperm. Syst Biol Reprod Med. 2015; 61:37-43.
24. Imam SN, Shamsi MB, Kumar K, Deka D, Dada R. Idiopathic recurrent pregnancy loss: Role of paternal factors; a pilot study. J Reprod Infertil. 2011; 12:267-276.
25. Moustafa MH, Sharma RK, Thornton J, Mascha E, Abdel-Hafez MA, Thomas AJ, Jr., Agarwal A. Relationship between ROS production, apoptosis and DNA denaturation in spermatozoa from patients examined for infertility. Hum Reprod. 2004; 19:129-138.
26. Talebi AR, Fesahat F, Mangoli E, Ghasemzadeh J, Nayeri M, Sadeghian-Nodoshan F. Relationship between sperm protamine deficiency and apoptosis in couples with unexplained repeated spontaneous abortions. Int J Reprod Biomed (Yazd). 2016; 14:199-204.
27. Aitken RJ, De Iuliis GN. On the possible origins of DNA damage in human spermatozoa. Mol Hum Reprod. 2010; 16:3-13.
28. Sakkas D, Alvarez JG. Sperm DNA fragmentation: Mechanisms of origin, impact on reproductive outcome, and analysis. Fertil Steril. 2010; 93:1027-1036.
29. Erenpreiss J, Spano M, Erenpreisa J, Bungum M, Giwercman A. Sperm chromatin structure and male fertility: Biological and clinical aspects. Asian J Androl. 2006; 8:11-29.
30. Zhao J, Zhang Q, Wang Y, Li Y. Whether sperm deoxyribonucleic acid fragmentation has an effect on pregnancy and miscarriage after *in vitro* fertilization/ intracytoplasmic sperm injection: A systematic review and meta-analysis. Fertil Steril. 2014; 102:998-1005 e1008.
31. Kennedy C, Ahlering P, Rodriguez H, Levy S, Sutovsky P. Sperm chromatin structure correlates with spontaneous abortion and multiple pregnancy rates in assisted

reproduction. Reprod Biomed Online. 2011; 22:272-276.
32. Erenpreiss J, Elzanaty S, Giwercman A. Sperm DNA damage in men from infertile couples. Asian J Androl. 2008; 10:786-790.
33. Zini A, Sigman M. Are tests of sperm DNA damage clinically useful? Pros and cons. J Androl. 2009; 30:219-229.
34. Giwercman A, Richthoff J, Hjøllund H, Bonde JP, Jepson K, Frohm B, Spano M. Correlation between sperm motility and sperm chromatin structure assay parameters. Fertil Steril. 2003; 80:1404-1412.
35. Brahem S, Mehdi M, Landolsi H, Mougou S, Elghezal H, Saad A. Semen Parameters and Sperm DNA Fragmentation as Causes of Recurrent Pregnancy Loss. Urology. 2011; 78:792-796.

(Received December 7, 2018; Revised March 16, 2019; Accepted March 26, 2019)

Original Article

DOI: 10.5582/bst.2018.01293

Daucosterol induces autophagic-dependent apoptosis in prostate cancer *via* JNK activation

Ping Gao[1,§], Xiaopeng Huang[2,§], Tingting Liao[3], Guangsen Li[2], Xujun Yu[4], Yaodong You[2,*], Yuxing Huang[5]

[1] *Department of Urology, Hospital of Chengdu University of Traditional Chinese Medicine, Chengdu, China;*
[2] *Department of Andrology, Hospital of Chengdu University of Traditional Chinese Medicine, Chengdu, China;*
[3] *Department of Endocrinology, Hospital of Chengdu University of Traditional Chinese Medicine, Chengdu, China;*
[4] *Medicine and Life Sciences College, Chengdu University of Traditional Chinese Medicine, Chengdu, China;*
[5] *Department of Neurosurgery, Hospital of Chengdu University of Traditional Chinese Medicine, Chengdu, China.*

Summary **Plant sterols (phytosterols) have been widely accepted as a natural anti-cancer agent in multiple malignant tumors. This study was designed to investigate the functions of daucosterol in prostate cancer progression and its possible molecular mechanisms. Our results showed that daucosterol inhibited cell proliferation and induced cell cycle arrest. Moreover, daucosterol treatment obviously promoted apoptosis and autophagy. An autophagy inhibitor, 3-methyladenine (3-MA) was proved to counteract daucosterol-triggered autophagy, growth inhibition, and apoptosis, indicating that daucosterol-induced apoptotic response was dependent on autophagy. Additionally, treatment with daucosterol resulted in increased phosphorylation of c-Jun N-terminal kinase (JNK). Furthermore, pre-treatment with a JNK-specific inhibitor SP600125 abated daucosterol-elicited autophagy and apoptotic cell death. Taken together, our findings demonstrated that daucosterol blocked prostate cancer growth at least partly through inducing autophagic-dependent apoptosis *via* activating JNK signaling, providing a promising candidate for the development of antitumor drugs in prostate cancer treatment.**

Keywords: Prostate cancer, daucosterol, cell cycle, apoptosis, autophagy, JNK

1. Introduction

Prostate cancer, the most common non-cutaneous malignancy in male, ranks second in cancer-related death among men in the United States in 2016 (*1*). Chemoprevention has been generally used as a main therapy for prostate cancer patients (*2*). However, high cytotoxicity and drug resistance greatly limited its application (*3*). Hence, it is necessary to identify more effective therapeutic targets for prostate cancer treatment.

Natural compounds, multi-targeted and less toxic, have been found to be involved in the prevention and therapy of multiple cancers (*4,5*). Plant sterols (phytosterols), with similar structural and biological functions to cholesterol, are able to exert anti-cancer effects in different tumors through modulation of cell growth, invasion, metastasis, cell cycle arrest and apoptosis (*6,7*). Daucosterol, a β-sitosterol glycoside, is one of the major phytosterols in higher plants and extracted from an endemic medicinal plant of Iran, Salvia sahendica (*8*). Daucosterol was previously reported to display anti-inflammatory and immunomodulatory activities (*9-11*). Additionally, daucosterol showed neuroprotective action in *in vitro* model of ischemia by activating IGF1 signaling (*12*). Moreover, daucosterol could promote neural stem cells proliferation through regulating multiple genes, especially increasing insulin-like growth factor I (IGF1) expression (*13*).

In recent years, daucosterol is also proved as

Released online in J-STAGE as advance publication April 2, 2019.

[§]These authors contributed equally to this work.

**Address correspondence to:*
Dr. Yaodong You, Hospital of Chengdu University of Traditional Chinese Medicine. No. 39, Shi-er-qiao Road, Chengdu 610072, China.
E-mail: yaodong_youu@163.com

important regulators in the occurrence and progression of cancers. A previous report delineated that daucosterol induced apoptosis in human breast cancer through regulating PTEN/PI3K/Akt pathway (*14*). Zeng *et al*. disclosed that daucosterol repressed proliferation, migration and invasion in hepatocellular carcinoma *via* Wnt/β-catenin signaling pathway (*15*). Zhao *et al*. discovered that daucosterol suppressed cancer cell proliferation by triggering autophagy through reactive oxygen species (ROS)-dependent manner (*16*). However, the exact roles and molecular mechanisms of daucosterol in prostate cancer deserve to be further investigated.

Apoptosis, type-I programmed cell death (PCD), is a common mechanism of cancer cell death for various anticancer drugs (*17*). Autophagy has a controversial role in cancer development. It could relieve tumor cell from nutrient and oxidative stress during the rapid expansion of cancer, while excessive and sustained autophagy may result in cell death and tumor shrinkage (*18*). Many researchers have highlighted the importance of autophagy in tumorigenesis and cancer therapy (*19,20*). Natural compounds and extracts have been documented as potential inducers of autophagy through diverse cellular mechanisms and pathways, thereby leading to cell senescence, apoptosis-independent death, and apoptotic death (*21,22*). Jun N-terminal kinase (JNK), a member of mitogen-activated protein kinase (MAPK) family, plays a vital part in many cellular events, including apoptosis and autophagy (*23*). JNK signaling has been found to be implicated in the process of natural product therapy in a variety of neoplasms (*24,25*).

In this current study, we elucidated that daucosterol suppressed cell proliferation, induced cell cycle arrest and enhanced apoptosis in prostate cancer. Furthermore, the anti-cancer effect of daucosterol was mediated by autophagy *via* JNK signaling.

2. Materials and Methods

2.1. *Cell culture*

Human prostate cancer cell lines (PC3 and LNCap) were purchased from Shanghai Institute of Biochemistry and Cell Biology (Shanghai, China). Cells were maintained in RPMI1640 medium (Invitrogen, Carlsbad, CA, USA) containing 10% fetal bovine serum (Invitrogen) and 1% penicillin-streptomycin (Sigma, St. Louis, MO, USA) at 37°C with an atmosphere of 5% CO_2.

2.2. *Reagents*

Daucosterol was obtained from extractsupplier Biotechnology (Xi'an, China) and dissolved in DMSO at 10 mM as stock. Autophagy inhibitor 3-methyladenine (3-MA) was purchased from Sigma and JNK-specific inhibitor (SP600125) was acquired from Santa Cruz Biotechnology (Santa Cruz, CA, USA).

2.3. *Cell Counting Kit-8 (CCK-8) assay*

PC3 and LNCap cells were seeded in 6-well plates (1×10^5 cells/well) and exposed to different concentrations of daucosterol (0, 5, 10, 20, 40, and 80 μM) for 48 h. Then, 10 μl of CCK-8 solution was added and incubated for another 2 h at 37°C. The absorbance at 450 nm was determined, and cell viability was normalized as the percentage of control.

2.4. *Cell cycle and apoptosis assay*

PC3 and LNCap cells were treated with various concentrations of daucosterol (0, 5, 10, 20, 40, and 80 μM) for 48 h. For cell cycle analysis, cells were collected, fixed in 75% ethanol, incubated with 50 μg/mL propidium iodide (PI) containing 40 μg/mL RNase for 30 min. Subsequently, cell cycle distribution was detected by a FACSCalibur flow cytometer (BD Biosciences, San Jose, CA, USA).

After treatment, apoptotic rate was measured using the annexin-V-FITC/PI apoptosis kit (BD Biosciences) by a flow cytometry (FACScan; BD Bioscience).

2.5. *Western blot analysis*

Following daucosterol treatment, cell lysates were separated on 10% sodium dodecylsulphate polyacrylamide gel electrophoresis (SDS-PAGE) gel and then electrophoretically transferred to polyvinylidene difluoride (PVDF) membranes. Then, the membranes were sequentially probed with primary antibodies and peroxidase-conjugated secondary antibody. Finally, the protein bands were detected by ECL Advance Detection System (Amersham Biosciences, Piscataway, NJ, USA). The primary antibodies against cleaved caspase 3, cleaved caspase 9, Bax, Bcl-2, LC3, Beclin 1, p62, were purchased from Cell Signaling Technology (Danvers, MA, USA), and antibodies against p-JNK, JNK and β-actin were obtained from Santa Cruz Biotechnology.

2.6. *Statistical analysis*

All experiments were performed at least 3 times and all data were displayed as mean ± SD. Student's *t* test or one-way ANOVA was used to evaluate statistical difference by GraphPad Prism (GraphPad Software Inc.). $P < 0.05$ is considered as statistically significant.

3. Results

3.1. *Daucosterol suppressed proliferation in prostate cancer cells*

To explore the effects of daucosterol on prostate

cancer, PC3 and LNCap cells were treated with various concentrations of daucosterol for 48 h. CCK-8 assay manifested that daucosterol inhibited PC3 and LNCap cell growth in a dose-dependent manner (Figure 1A and 1B). Moreover, flow cytometry analysis demonstrated that daucosterol treatment resulted in an obvious cell cycle arrest at G1 phase in both PC3 (Figure 1C) and LNCap (Figure 1D) cells. These data suggested that daucosterol impaired cell proliferation in prostate cancer.

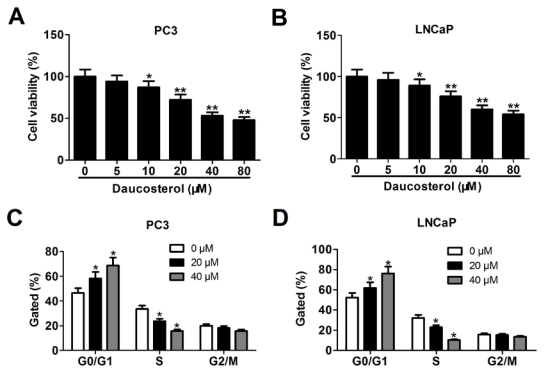

Figure 1. Daucosterol lowers the proliferation potential of prostate cancer cells. (A and **B)** PC3 and LNCap cells were treated with different concentrations of daucosterol (0, 5, 10, 20, 40, and 80 μM) for 48 h, then cell viability was assessed by CCK-8 assay; **(C** and **D)** Flow cytometry analysis was used to measure cell cycle distribution in PC3 and LNCap cells after treatment with various concentrations of daucosterol (0, 20, and 40 μM) for 48 h. *$p < 0.05$, **$p < 0.01$.

3.2. *Daucosterol promoted apoptosis in prostate cancer cells*

To further investigate whether the growth inhibition elicited by daucosterol was associated with apoptosis, we evaluated the apoptotic rate of PC3 and LNCap cells after treatment with different doses of daucosterol for 48 h. Flow cytometry assay displayed that the apoptotic rate was greatly enhanced in both PC3 and LNCap cells following daucosterol treatment (Figure 2A and 2B). Moreover, western blot analysis exhibited a dramatic increase of cleaved caspase 3, cleaved caspase 9 and Bax protein expressions, while a prominent decrease of Bcl-2 expression in PC3 and LNCap cells after treatment with daucosterol (Figure 2C and 2D). Together, these results indicated that daucosterol exerted anticancer activity at least partly by facilitating apoptosis in prostate cancer.

3.3. *Daucosterol induced autophagy in prostate cancer cells*

Autophagy, type-II PCD, is demonstrated to participate

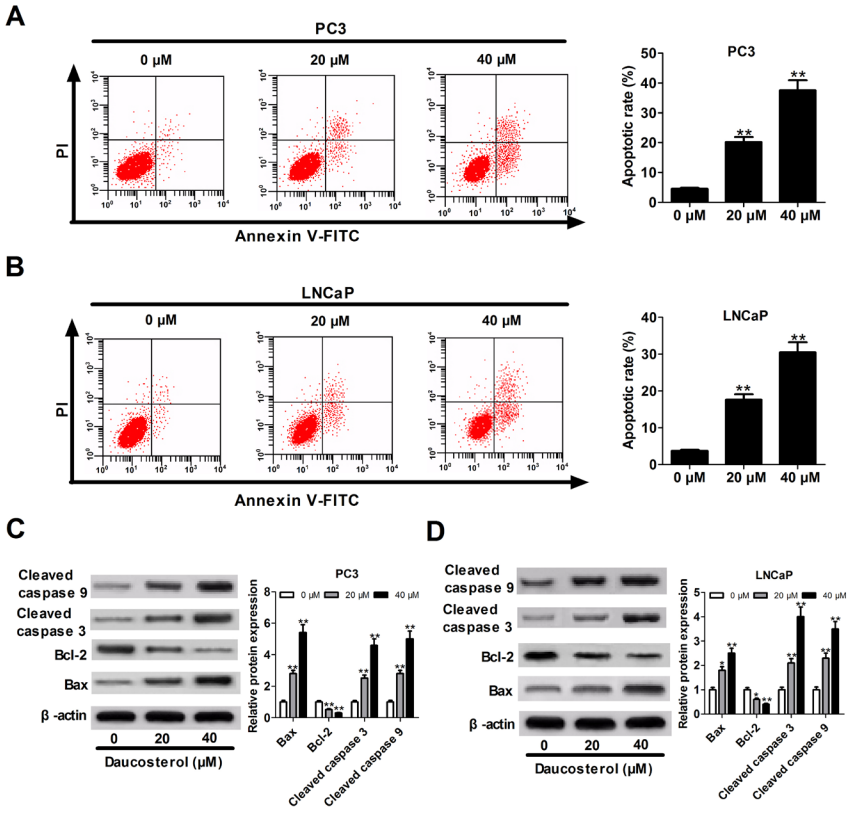

Figure 2. Daucosterol facilitates apoptosis in prostate cancer cells. (A and **B)** The apoptotic rate was detected in PC3 and LNCap cells after treatment with various concentrations of daucosterol (0, 20, and 40 μM) for 48 h; **(C** and **D)** Western blot analysis of cleaved caspase 3, cleaved caspase 3, Bax, and Bcl-1 in PC3 and LNCap cells treated with daucosterol for 48 h. *$p < 0.05$, **$p < 0.01$.

in the regulation of natural products in cancers (26). Thus, we determined the protein levels of autophagy markers (LC3, Beclin 1 and p62) in PC3 and LNCap cells after treatment with different doses of daucosterol for 48 h. Western blot analysis revealed that daucosterol treatment resulted in an increase of LC3II/LC3I ration and Beclin 1 expression, while a decline of p62 expression in PC3 and LNCap cells (Figure 3A and 3B), supporting the induction of autophagy by daucosterol in prostate cancer cells.

3.4. *Suppression of autophagy weakened daucosterol-elicited growth inhibition and apoptosis in prostate cancer cells*

To further analyze whether apoptosis and autophagy were related or independent events in response to daucosterol, we examined the effects of daucosterol on cell proliferation and apoptosis in the presence or absence of autophagy inhibitor 3-MA. As expected, 3-MA pre-treatment effectively attenuated daucosterol-

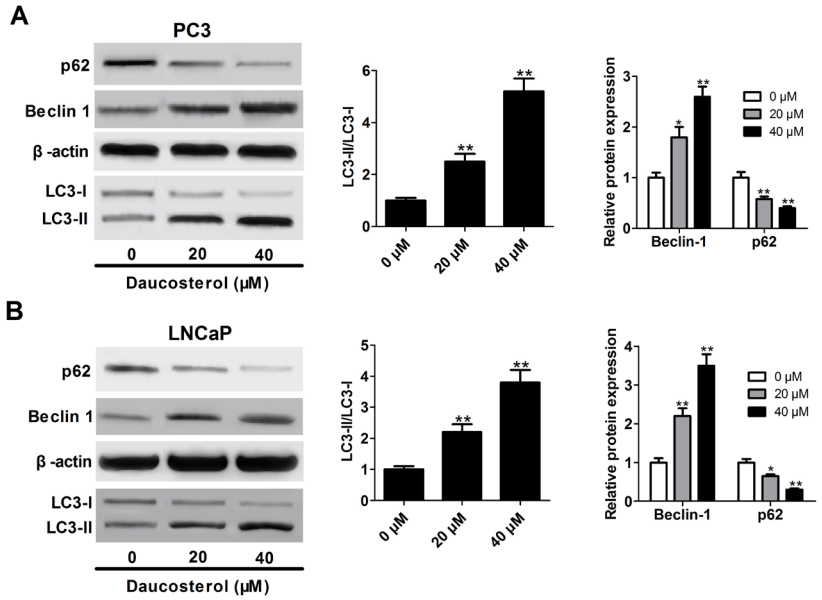

Figure 3. Daucosterol induces autophagy in prostate cancer cells. (A and **B)** The expression levels of LC3II, Beclin 1 and p62 were determined by Western blot in PC3 and LNCap cells following treatment with different concentrations of daucosterol for 48 h. *$p < 0.05$, **$p < 0.01$.

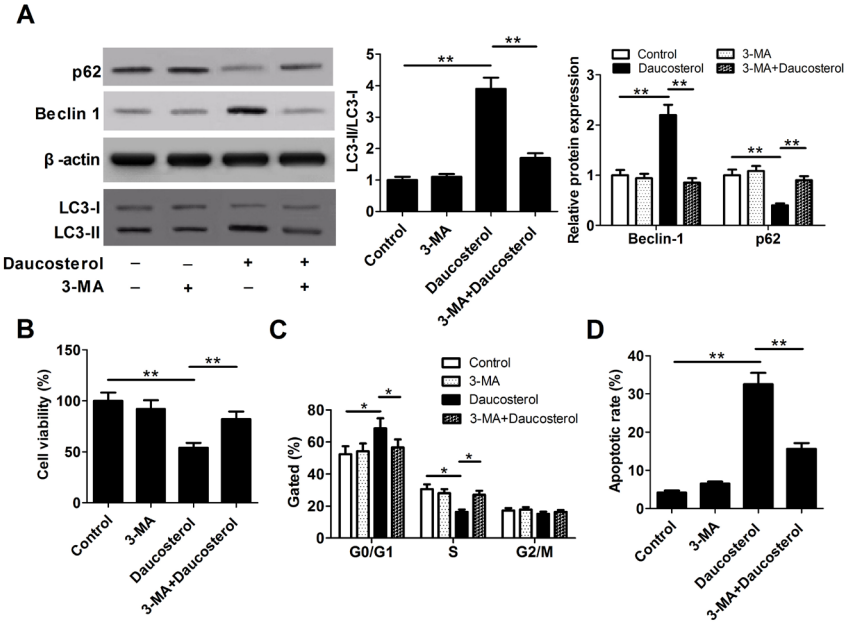

Figure 4. Daucosterol-triggered apoptosis depends on autophagy in prostate cancer cells. PC3 cells were pre-treated with or without 3-MA (5 mM) for 1 h prior to incubation with 40 μM daucosterol for 48 h, then **(A)** western blot was used to assess the protein expressions of LC3II, Beclin 1 and p62, **(B)** cell viability was detected by CCK-8 assay, **(C** and **D)** cell cycle distribution and apoptosis was examined by flow cytometry. *$p < 0.05$, **$p < 0.01$.

induced autophagy in PC3 cells, presented by reduced LC3II and Beclin 1 expressions, while enhanced p62 expression (Figure 4A). Moreover, the growth inhibition triggered by daucosterol was greatly reversed in PC3 cells following pre-treatment with 3-MA (Figure 4B and 4C). Further, treatment of PC3 cells with 3-MA abated daucosterol-induced apoptosis (Figure 4D). Collectively, the pro-apoptotic effect of daucosterol was modulated by autophagy.

3.5. *Daucosterol induced autophagy in prostate cancer cells*

JNK activation has been found to be involved in autophagy and apoptosis induced by natural compound (*27*). In order to explore the potential molecular basis of daucosterol in prostate cancer, we firstly determined the effects of daucosterol on JNK pathway in PC3 cells. As presented in Figure 5A, daucosterol treatment significantly increased the level of phosphorylated JNK. To further confirm whether daucosterol-induced apoptosis and autophagy require JNK activation, PC3 cells were pre-incubated with or without JNK-specific inhibitor (SP600125) prior to daucosterol treatment. The results demonstrated that SP600125 suppressed the conversion of LC3I to LC3II and Beclin 1 expression, while enhanced p62 expression in PC3 cells under daucosterol treatment (Figure 5B), suggesting the inhibitory effect of SP600125 on daucosterol-induced autophagy. Moreover, daucosterol-elicited growth inhibition (Figure 5C), cell cycle arrest (Figure 5D) and apoptosis (Figure 5E) were alleviated following SP600125 pre-treatment. From these data, we draw a conclusion that daucosterol induced autophagic-dependent apoptosis in prostate cancer by activating JNK signaling.

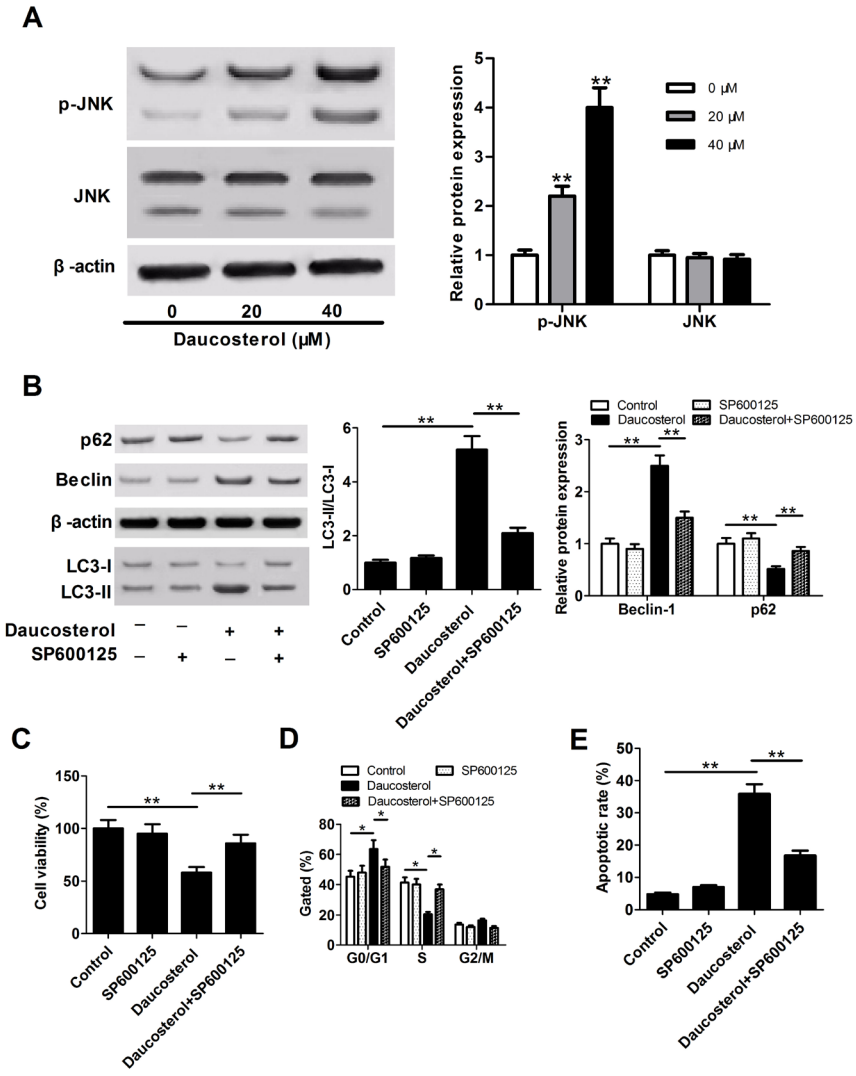

Figure 5. Daucosterol-triggered autophagic-dependent apoptosis by JNK activation in prostate cancer cells. (A) Western blot analysis of JNK and p-JNK expression in PC3 cells treated with daucosterol at indicated concentrations for 48 h; **(B)** PC3 cells were pre-incubated with SP600125 (10 μM) for 1 h prior to treatment with 40 μM daucosterol for 48 h, then (B) western blot was applied to evaluate the protein levels of LC3II, Beclin 1 and p62; (C) CCK-8 assay was performed to monitor cell viability; **(D** and **E)** flow cytometry analysis was conducted to analyze cell cycle distribution and apoptosis. *$p < 0.05$, **$p < 0.01$.

4. Discussion

Natural products have been discovered as a rich source for the discovery and development of cancer preventive and anticancer drugs (*28,29*). Daucosterol, a β-sitosterol glycoside, is one of the major phytosterols in higher plants (*30*). In this study, we found that daucosterol exerted tumor-suppressive function in prostate cancer by inducing autophagic-dependent apoptosis *via* activation of JNK.

Daucosterol are reported as an anti-cancer plant sterol in breast cancer (*14*), hepatic carcinoma (*15*) and gastric cancer (*16*) by various mechanisms and pathways. Rajavel *et al*. also revealed that the presence of phytosteols (β-sitosterol and daucosterol) significantly blocked the growth of lung cancer cells both alone and in combination (*31*). Wang *et al*. disclosed that daucosterol hindered proliferation, enhanced apoptosis, and inhibited migration and invasion in colon cancer *via* regulating caspase signaling (*32*). In this study, we firstly found that daucosterol suppressed prostate cancer cell viability in a dose-dependent manner. Deregulation of cell cycle progression has been regarded to be associated with cancer occurrence and development (*33*). Moreover, controlling or perturbing the cycle of tumor cells is an effective method for natural products to destroying malignant cell proliferation (*34*). Here, our results showed that daucosterol treatment resulted in a dramatic cell cycle arrest.

Apoptosis has been considered as a major mechanism to exert anti-cancer roles for chemotherapeutic agents (*35*). It has been proved that numerous plant-derived chemotherapy drugs kill cancer cells *via* inducting apoptotic cell death (*36,37*). In the present study, we demonstrated that daucosterol repressed cell apoptosis by flow cytometry. Moreover, daucosterol activated the mitochondria-dependent apoptotic signaling pathway, leading to increased expression of pro-apoptotic protein (Cleaved caspase 3, Cleaved caspase 9, Bax) and decrease expression of anti-apoptotic protein Bcl-2. These data suggested that daucosterol was cytotoxic to cells in prostate cancer through facilitating apoptosis.

Autophagy is a homeostatic cellular degradation process for eliminating damaged or unnecessary intracellular organelles and proteins in lysome (*38*). Autophagy is able to suppress early cancer development while contribute to advanced tumor progression (*39*). Numerous natural compounds have been discovered to induce cell apoptosis through modulating autophagy in cancers. For example, natural product peiminine repressed cell growth in colorectal cancer by enhancing autophagic cell death (*40*). Marchantin M promoted apoptosis in prostate cancer through induction of autophagy (*41*). Our results manifested that daucosterol treatment effectively enhanced autophagy in prostate cancer cells, indicated by up-regulated LC3II and Beclin 1 expression, while down-regulated p62 expression. Moreover, autophagy inhibitor 3-MA attenuated daucosterol-triggered growth inhibition and apoptosis in prostate cancer cells. These data confirmed that daucosterol impaired cell growth by contributing to autophagic-dependent cell death.

It is well known that JNKs are master protein kinases that modulate a variety of physiological events, such as inflammatory responses, morphogenesis, cell proliferation, differentiation, survival and death (*42*). Aberrant activation of JNK signaling has been reported to be associated with tumor progression (*43*). Our data exhibited that daucosterol increased the phosphorylation level of JNK in prostate cancer cells. Moreover, JNK-specific inhibitor (SP600125) inhibited daucosterol-induced autophagy. Furthermore, daucosterol-elicited growth inhibition, cell cycle arrest and apoptosis were abated by pre-treatment with SP600125. Together, daucosterol exerted anti-proliferation effect by inducing autophagic-dependent apoptosis *via* activation of JNK signaling. Consistent with our finding, JNK activation has been reported to be participate in apoptosis and autophagy mediated by multiple natural products (*44,45*).

In conclusion, our present study demonstrated that daucosterol inhibited cell proliferation, induced cell cycle arrest, and promoted autophagic-dependent apoptosis in prostate cancer. Moreover, the tumor-suppressive effect of daucosterol was at least partly mediated by JNK activation. Our findings indicated that daucosterol may be developed as a potential anti-cancer agent.

Acknowledgements

This work was supported by National Natural Science Foundation of China (No. 81503589) and Education Department of Sichuan Provincial of China (No.14ZB0089)

References

1. Siegel RL, Miller KD, Jemal A. Cancer statistics, 2016. CA Cancer J Clin. 2016; 66:7-30.
2. Halabi S, Lin CY, Kelly WK, Fizazi KS, Moul JW, Kaplan EB, Morris MJ, Small EJ. Updated Prognostic Model for Predicting Overall Survival in First-Line Chemotherapy for Patients With Metastatic Castration-Resistant Prostate Cancer. J Clin Oncol. 2014; 32:671-677.
3. Zhang W, Meng Y, Liu N, Wen XF, Yang T. Insights into Chemoresistance of Prostate Cancer. Int J Biol Sci. 2015; 11:1160-1170.
4. Shanmugam MK, Lee JH, Chai EZ, Kanchi MM, Kar S, Arfuso F, Dharmarajan A, Kumar AP, Ramar PS, Looi CY. Cancer prevention and therapy through the modulation of transcription factors by bioactive natural compounds. Semin Cancer Biol. 2016; 40-41:35-47.
5. Safarzadeh E, Shotorbani SS, Baradaran B. Herbal Medicine as Inducers of Apoptosis in Cancer Treatment.

Adv Pharm Bull. 2014; 4:421-427.
6. Ramprasath VR, Awad AB. Role of Phytosterols in Cancer Prevention and Treatment. J Aoac Int. 2015; 98:735-738.
7. Shahzad N, Khan W, Md S, Ali A, Saluja SS, Sharma S, Al-Allaf FA, Abduljaleel Z, Ibrahim IAA, Abdel-Wahab AF, Afify MA, Al-Ghamdi SS. Phytosterols as a natural anticancer agent: Current status and future perspective. Biomed Pharmacother. 2017; 88:786-794.
8. Mozafarian V. A Dictionary of Iranian Plant Names. Farhang Mosafer Publication, Tehran, Iran. 1996; pp. 90-91.
9. Bouic PJ, Etsebeth S, Liebenberg RW, Albrecht CF, Pegel K, Van Jaarsveld PP. beta-Sitosterol and beta-sitosterol glucoside stimulate human peripheral blood lymphocyte proliferation: Implications for their use as an immunomodulatory vitamin combination. Int J Immunopharmacol. 1996; 18:693-700.
10. Choi JN, Choi YH, Lee JM, Noh IC, Park JW, Choi WS, Choi JH. Anti-inflammatory effects of beta-sitosterol-beta-D-glucoside from Trachelospermum jasminoides (Apocynaceae) in lipopolysaccharide-stimulated RAW 264.7 murine macrophages. Nat Prod Res. 2016; 26:2340-2343.
11. Lee JH, Lee JY, Park JH, Jung HS, Kim JS, Kang SS, Kim YS, Han Y. Immunoregulatory activity by daucosterol, a beta-sitosterol glycoside, induces protective Th1 immune response against disseminated Candidiasis in mice. Vaccine. 2007; 25:3834-3840.
12. Jiang LH, Yuan XL, Yang NY, Ren L, Zhao FM, Luo BX, Bian YY, Xu JY, Lu DX, Zheng YY. Daucosterol protects neurons against oxygen-glucose deprivation/reperfusion-mediated injury by activating IGF1 signaling pathway. J Steroid Biochem Mol Biol. 2015; 152:45-52.
13. Jiang LH, Yang NY, Yuan XL, Zou YJ, Zhao FM, Chen JP, Wang MY, Lu DX. Daucosterol promotes the proliferation of neural stem cells. J Steroid Biochem Mol Biol. 2014; 140:90-99.
14. Esmaeili MA, Farimani MM. Inactivation of PI3K/Akt pathway and upregulation of PTEN gene are involved in daucosterol, isolated from Salvia sahendica , induced apoptosis in human breast adenocarcinoma cells. South Afri J Botany. 2014; 93:37-47.
15. Zeng J, Liu X, Li X, Zheng Y, Liu B, Xiao Y. Daucosterol Inhibits the Proliferation, Migration, and Invasion of Hepatocellular Carcinoma Cells *via* Wnt/β-Catenin Signaling. Molecules 2017; 22:E862.
16. Zhao C, She T, Wang L, Su Y, Qu L, Gao Y, Xu S, Cai S, Shou C. Daucosterol inhibits cancer cell proliferation by inducing autophagy through reactive oxygen species-dependent manner. Life Sci. 2015; 137:37-43.
17. Croce CM, Reed JC. Finally, An Apoptosis-Targeting Therapeutic for Cancer. Cancer Res. 2016; 76:5914-5920.
18. Jiang X, Overholtzer M, Thompson CB. Autophagy in cellular metabolism and cancer. J Clin Invest. 2015; 125:47-54.
19. Fulda S, Kögel D. Cell death by autophagy: Emerging molecular mechanisms and implications for cancer therapy. Oncogene. 2015; 34:5105-5113.
20. Rebecca VW, Amaravadi RK. Emerging strategies to effectively target autophagy in cancer. Oncogene. 2016; 35:1-11.
21. Wang N, Feng Y. Elaborating the role of natural products-induced autophagy in cancer treatment: Achievements and artifacts in the state of the art. Biomed Res Int. 2015; 2015:934207.
22. Naponelli V, Modernelli A, Bettuzzi S, Rizzi F. Roles of autophagy induced by natural compounds in prostate cancer. Biomed Res Int. 2015; 2015:121826.
23. Hao H, Zhang D, Shi J, Wang Y, Chen L, Guo Y, Ma J, Jiang X, Jiang H. Sorafenib induces autophagic cell death and apoptosis in hepatic stellate cell through the JNK and Akt signaling pathways. Anticancer Drugs. 2016; 27:192-203.
24. Zhong F, Tong ZT, Fan LL, Zha LX, Wang F, Yao MQ, Gu KS, Cao YX. Guggulsterone-induced apoptosis in cholangiocarcinoma cells through ROS/JNK signaling pathway. Am J Cancer Res. 2015; 6:226-237.
25. Peng F, Wang X, Shu M, Yang M, Wang L, Ouyang Z, Shen C, Hou X, Zhao B, Wang X. Raddeanin a Suppresses Glioblastoma Growth by Inducing ROS Generation and Subsequent JNK Activation to Promote Cell Apoptosis. Cell Physiol Biochem. 2018; 47:1108-1121.
26. Hua F, Shang S, Hu Z. Seeking new anti-cancer agents from autophagy-regulating natural products. J Asian Nat Prod Res. 2017; 19:305-313.
27. Zhao Y, Li ETS, Wang M. Alisol B 23-acetate induces autophagic-dependent apoptosis in human colon cancer cells *via* ROS generation and JNK activation. Oncotarget. 2017; 8:70239-70249.
28. Bishayee A, Sethi G. Bioactive natural products in cancer prevention and therapy: Progress and promise. Semin Cancer Biol. 2016; 40-41:1-3.
29. Cragg G, Pezzuto J. Natural Products as a Vital Source for the Discovery of Cancer Chemotherapeutic and Chemopreventive Agents. Med Princ Pract. 2016; 25:41-59.
30. Pegel K. The importance of sitosterol and sitosterolin in human and animal nutrition. South Afri J Sci. 1997; 93:263-268.
31. Rajavel T, Mohankumar R, Archunan G, Ruckmani K, Devi K. Beta sitosterol and Daucosterol (phytosterols identified in Grewia tiliaefolia) perturbs cell cycle and induces apoptotic cell death in A549 cells. Sci Rep. 2017; 7:3418.
32. Wang GQ, Gu JF, Gao YC, Dai YJ. Daucosterol inhibits colon cancer growth by inducing apoptosis, inhibiting cell migration and invasion and targeting caspase signalling pathway. Bangl J Pharmacol. 2016; 11:395.
33. Schwartz GK, Shah MA. Targeting the Cell Cycle: A New Approach to Cancer Therapy. J Clin Oncol. 2005; 23:9408-9421.
34. Newman DJ, Cragg GM, Holbeck S, Sausville EA. Natural Products and Derivatives as Leads to Cell Cycle Pathway Targets in Cancer Chemotherapy. Curr Cancer Drug Targets. 2002; 2:279-308.
35. Kaufmann SH, Earnshaw WC. Induction of Apoptosis by Cancer Chemotherapy. Exp Cell Res. 2000; 256:42-49.
36. Bosio C, Tomasoni G, Martínez R, Olea AF, Carrasco H, Villena J. Cytotoxic and apoptotic effects of leptocarpin, a plant-derived sesquiterpene lactone, on human cancer cell lines. Chem-Biol Interact. 2015; 242:415-421.
37. Firempong CK, Zhang HY, Wang Y, Chen J, Cao X, Deng W, Zhou J, Wang Q, Tong SS, Yu J. Segetoside I, a plant-derived bisdesmosidic saponin, induces apoptosis in human hepatoma cells *in vitro* and inhibits tumor growth *in vivo*. Pharmacol Res. 2016; 110:101-110.
38. Amaravadi R, Kimmelman AC, White E. Recent insights into the function of autophagy in cancer. Genes Dev.

2016; 30:1913-1930.
39. Kenific CM, Debnath J. Cellular and metabolic functions for autophagy in cancer cells. Trends Cell Biol. 2015; 25:37-45.
40. Lyu Q, Tou F, Su H, Wu X, Chen X, Zheng Z. The natural product peiminine represses colorectal carcinoma tumor growth by inducing autophagic cell death. Biochem Biophys Res Commun. 2015; 462:38-45.
41. Jiang H, Sun J, Xu Q, Liu Y, Wei J, Young C, Yuan H, Lou H. Marchantin M: A novel inhibitor of proteasome induces autophagic cell death in prostate cancer cells. Cell Death Dis. 2013; 4:e761.
42. Bubici C, Papa S. JNK signalling in cancer: In need of new, smarter therapeutic targets. Br J Pharmacol. 2014; 171:24-37.
43. Cicenas J, Zalyte E, Rimkus A, Dapkus D, Noreika R, Urbonavicius S. JNK, p38, ERK, and SGK1 Inhibitors in Cancer. Cancers (Basel). 2017; 10:E1.
44. Li HY, Zhang J, Sun LL, Li BH, Gao HL, Xie T, Zhang N, Ye ZM. Celastrol induces apoptosis and autophagy *via* the ROS/JNK signaling pathway in human osteosarcoma cells: An *in vitro* and *in vivo* study. Cell Death Dis. 2015; 6:e1604.
45. Sun ZL, Dong JL, Wu J. Juglanin induces apoptosis and autophagy in human breast cancer progression *via* ROS/JNK promotion. Biomed Pharmacother. 2017; 85:303-312.

(Received December 7, 2018; Revised March 14, 2019; Accepted March 21, 2019)

Original Article

DOI: 10.5582/bst.2019.01020

Predictive value of some pro-oxidants in type 2 diabetes mellitus with vascular complications

Petia Goycheva[1,*], Galina Nikolova[2], Mariana Ivanova[3], Todor Kundurdzhiev[4], Veselina Gadjeva[2]

[1] *Clinic of Endocrinology, University Hospital "Prof. Dr. Stoyan Kirkovich", Medical Faculty, Trakia University, Stara Zagora, Bulgaria;*
[2] *Department of Chemistry and Biochemistry, Medical Faculty, Trakia University, Stara Zagora, Bulgaria;*
[3] *Clinic of Rheumatology, University Hospital "St. Ivan Rilski", Medical Faculty, Medical University, Sofia, Bulgaria;*
[4] *Faculty of Public Health, Medical University, Sofia, Bulgaria.*

Summary **The study aims to analyze oxidative stress levels in circulation of some reactive molecules and products of biomolecular modification in type 2 diabetes mellitus (T2DM) with diabetes-specific vascular complications in order to determine their predictive value. Also, the alterations of their serum concentration with reference to disease characteristics were assessed. Reactive oxygen species (ROS), nitric oxide radicals (•NO), malondialdehyde (MDA), protein carbonyl (CO) and 8-hydroxydeoxyguanosin (8-OHdG) in serum were measured in 93 patients with T2DM with vascular complications, 94 control subjects and 16 diabetic patients who had no evidence of vascular disease. T2DM patients with clinically manifest vascular disease exhibit significantly elevated concentrations of all pro-oxidants in comparison to healthy subjects, with the highest degree of increase of •NO radicals. The levels of carbonylated proteins, ROS and 8-OHdG were significantly increased in insufficiently compensated diabetes as compared to good glycemic control state. Also, serum MDA, protein CO and 8-OHdG showed an association with glycemic control parameters. MDA, ROS and 8-OHdG correlated mostly with microvascular complications. Significant area under the curve (AUC) from plotted receiver operating characteristic (ROC) curves were obtained for all studied biomarkers, as for nitric oxide it was substantially bigger compared to those for the other pro-oxidants. Correspondingly, positive and negative predictive values related to the disease were in favor of the •NO radicals. The cutoff values of oxidative biomarkers may serve as an indicator of clinical reference for detecting T2DM with associated vascular complications, as nitric oxide radicals were the most reliable indicator.**

Keywords: Type 2 diabetes mellitus, diabetes-specific vascular complications, oxidative stress, pro-oxidants

1. Introduction

Type 2 diabetes mellitus (T2DM) is a metabolic disease characterized by hyperglycemia and dyslipidemia due to pancreatic β-cell dysfunction and insulin resistance. Usually, insulin resistance of target tissues such as the liver, muscles and fat stores precedes the onset of T2DM by many years, resulting in an initial hyperinsulinemia and followed by a consequent deficiency of insulin secretion by pancreatic beta cells. Impaired insulin secretion by the islet cells and impaired insulin action through insulin resistance are the hallmarks in type 2 diabetes (*1*). The disease is largely responsible to macrovascular (coronary heart disease, peripheral vascular disease and stroke), microvascular (neuropathy, retinopathy and nephropathy) and both micro- and

Released online in J-STAGE as advance publication April 8, 2019.

**Address correspondence to:*
Dr. Petia Goycheva, Clinic of Endocrinology, University Hospital "Prof. Dr. St. Kirkovich", 11 Armeyska Str., Stara Zagora 6003, Bulgaria.
E-mail: petya_goicheva@yahoo.com

macrovascular (diabetic foot) complications, which are the main reason for the mortality and morbidity (*2*).

It has been shown that oxidative stress *via* the production of larger amounts of reactive oxygen species (ROS) is implicated in the progression of insulin resistance, pancreatic β-cell dysfunction as well as in vascular degeneration processes and the accelerated atherosclerosis in T2DM (*3,4*). The metabolic abnormalities of diabetes cause mitochondrial superoxide overproduction in endothelial cells of both large and small vessels (*5*). It is considered that not only constant chronic hyperglycemia but also fluctuating blood glucose concentrations (*6,7*) mediates oxidative stress mechanisms through various pathways under diabetic condition, namely the nonenzymatic glycosylation reaction (*8*), the electron transport chain in mitochondria and membrane-bound nicotinamide adenine dinucleotide phosphate oxidase (NADPH oxidase) (*9*). Once formed, free radicals – ROS, reactive nitrogen species (RNS), which are short lived, but highly reactive species trigger cells damage through interaction with a broad range of cell components and biological molecules such as lipids (*10*), proteins (*11*) and nucleic acids (*12*), thus involving in the pathogenesis of distinct pathological conditions.

The aim of this study was to investigate serum levels of various biomarkers of oxidative stress: ROS, nitric oxide radicals (•NO), and those reflecting oxidative damages to proteins, lipids, and deoxyribonucleic acid (protein carbonyl groups, malondialdehyde and 8-hydroxy-2'-deoxyguanosine) in T2DM with vascular complications as compared to healthy subjects, and to determine their predictive value. Further, we have explored their alterations and relationships to disease characteristics.

2. Materials and Methods

2.1. *Study subjects*

T2DM patients referred to Endocrinology Clinic of University Hospital "Prof. Dr. St. Kirkovich" in Stara Zagora, Bulgaria, all fulfilled the WHO criteria (*13*) were included. The study population consisted of 93 type 2 diabetic patients with diabetes-specific complications, 94 healthy controls with normal glucose tolerance tests and absence of a history of either vascular disease or dyslipidemia and 16 newly diagnosed T2DM patients without manifestations of vascular disease.

Clinical and medical history data including obesity based on body mass index (BMI) > 30 kg/m^2; therapy for diabetes, were recorded for each patient. Patients were defined as having suffered a cardiovascular event if they had coronary heart disease, cerebrovascular disease, and/or peripheral artery disease. Diabetic microangiopathy complications (neuropathy, retinopathy and nephropathy) were based on physician diagnosis and/or microalbuminuria, the earliest marker of renal damage, for the latter. A venous blood of patients and controls was collected in the morning after an overnight fasting for lipid profile analysis. Fasting plasma glucose concentrations (FPG) and glycated hemoglobin (HbA1c %), representing an average measure of glycemic exposure over time, were measured as parameters for glycemic control. Poor glycemic control was taken at HbA1c values > 7% and FPG > 6.1 mmol/L. Subjects were excluded if they had a history of malignancy, exacerbated cardiac and renal failure, any other hormonal illness, diabetic ketoacidosis, antioxidant supplement intake and/or current active infection. A written informed consent was obtained from each participant and the study was approved by the Ethics Committee.

2.2. *Measurement of oxidative markers*

2.2.1. *Ex vivo electron paramagnetic resonance (EPR) study*

All EPR measurements were performed at room temperature on an X-band EMXmicro, spectrometer Bruker, Germany, equipped with standard Resonator. All EPR experiments were carried out in triplicate and repeated thrice. Spectral processing was performed using Bruker WIN-EPR and Sinfonia software.

2.2.2. *Ex vivo evaluation the levels of ROS products*

The levels of ROS were determined according Shi *et al*. (*14*) with some modification. To investigate in real time formation of ROS in the sera of patients and controls was used *ex vivo* EPR spectroscopy combined with N-tert-butyl-alpha-phenylnitrone (PBN) as a spin trapping agent. PBN, upon reaction with unstable radical such as ROS, forms a relatively stable spin adducts that can be subsequently detected by EPR spectroscopy. Briefly, to 100 μL serum was added 900 μL 50 mM PBN dissolved in dimethyl sulfoxide (DMSO) and after centrifugation at 4,000 rpm for 10 min at 4ºC the EPR spectra were immediately recorded in the supernatant. The levels of ROS products were calculated as double integrated plots of EPR spectra and results were expressed in arbitrary units (arb. units). EPR setting were as follows: 3503.73 G center field, 20.00 mW microwave power, 5 G modulation amplitude, 50 G sweep width, 1×10^5 gain, 81.92 ms time constant, 125.95 s sweep time, 5 scans per sample.

2.2.3. *Ex vivo evaluation the levels of •NO radicals*

Based on the methods published by Yoshioka *et al*. (*15*) and Yokoyama *et al*. (*16*) we developed and adapted the EPR method for estimation the levels of •NO radicals in serum. Briefly, to 50 μM solution of Carboxy.

2-(4-Carboxyphenyl)-4,4,5,5-tetramethylimidazoline-1-oxyl-3-oxide . potassium salt (PTIO.K) dissolved in a mixture of 50 mMTris (pH 7.5) and DMSO in a ratio 9:1. To 100 µL serum was added 900 µL Tris buffer dissolved in DMSO (9:1) after that the mixture is centrifuged at 4000 rpm for 10 min at 4ºC. 100 µL of sample and 100 µL 50 mM solution of Carboxy. PTIO were mixed and EPR spectra of spin adduct formed between the spin trap Carboxy. PTIO and generated •NO radicals was recorded. The levels of •NO radicals were calculated as double integrated plots of EPR spectra and results were expressed in arbitrary units. The EPR settings were as follows: 3505 G centerfield, 6.42 mW microwave power, 5 G modulation amplitude, 75 G sweep width, 2.5×10^2 gain, 40.96 ms time constant, 60.42 s sweep time, 1 scan per sample.

2.2.4. *Determination of Lipid Peroxidation Products (malondialdehyde)*

Total amount of lipid peroxidation products in the plasma of healthy volunteers and patients was estimated using the thiobarbituric acid (TBA) method of Plaser *et al*. (*17*) which measures the malondialdehyde (MDA) reactive products at 532 nm, and results were expressed in µmol/L.

2.2.5. *Protein Carbonyl Content (PCC)*

PCC (nmol/mg) was measured by using a commercial enzyme-linked immunosorbent assay (ELISA) kit followed manufacturer's instructions. The protein carbonyls present in the serum sample or standard are derivatized to 2,4-dinitrophenyl (DNP)hydrazone and probed with an anti-DNP antibody, followed by a horseradish peroxidase (HRP) conjugated secondary antibody. The protein carbonyl content in the serum sample is determined by comparing with a standard curve that is prepared from predetermined reduced and oxidized bovine serum albumin (BSA) standards.

2.2.6. *Quantity of 8-Hydroxy-2'-Deoxyguanosine (8-OHdG)*

The measurement of 8-OHdG was carried out using commercial ELISA kit, followed manufacturer's instructions. The ELISA kit is a competitive enzyme immunoassay developed for rapid detection and quantitation of 8-OHdG in serum. The serum 8-OHdG samples or 8-OHdG standards are coated with BSA conjugated 8-hydroxyguanine (8-OHG) on a preabsorbed microplate. After a brief incubation, an anti-8-OHdG monoclonal antibody is added, followed by a HRP conjugated secondary antibody. The 8-OHdG content in serum samples is determined by comparison with a predetermined 8-OHdG standard curve. The kit has an 8-OHdG detection sensitivity range of 100 pg/mL to 20 ng/mL.

2.3. *Statistical analysis*

Data were analyzed using SPSS version 13.0 (SPSS Inc., Chicago, IL, USA). Means with SDs and percentages were calculated to describe clinical and laboratory characteristics of the study subjects. Intergroup comparisons were performed by an analysis of variance (ANOVA), Kruskal-Wallis and Mann-Whitney *U* tests. Proportional differences were tested using the chi-square (χ^2)/ Fisher's exact tests. Pearson's correlation coefficients were calculated to assess univariate correlations between the continuous parameters. In the cases, where one of the samples is measured as dichotomous, the associations were estimated using the biserial correlation coefficient. Receiver operating characteristic (ROC) analysis was carried out for the evaluation of the diagnostic potential of pro-oxidants for T2DM, associated with vascular complications. The area under the curve (AUC) was calculated, as the diagnostic test that approaches 1 indicates a perfect discrimination. Sensitivity, specificity, positive and negative predictive values according to the cutoff values of the oxidative stress parameters related to diabetes with induced by it vascular changes were calculated. A 2-tailed p values of < 0.05 were considered statistically significant

3. Results

3.1. *Cohort description*

In total, 93 patients with T2DM with diabetes-specific vascular complications (male: female subjects 1: 1.3) aged 30 to 88 years, mean age 64.2 ± 9.8 years were studied. The mean disease duration was 12.7 ± 8.6 years with a range from 1 to 40. Approximately half of the diabetics (58.1%) were obese. Ninety of all patients (96.8%) had diabetic neuropathy, 24 (25.8%) had retinopathy and 7 (7.5%) had nephropathy. The proportion of patients suffering from coronary heart disease was 37.6%. Eleven of the patients (11.8%) had a medical history of cerebrovascular disease. None of the diabetics was presented with symptomatic lower extremity arterial disease. The diabetics with good glycemic control (39 patients) were taking oral hypoglycemic agents (sulphonylureas and biguanides) (n =32), as in 6 patient biguanides were combined with insulin; and 7 patients were on therapy with insulin alone. In the subgroup of diabetic patients with poor glycemic control (n =54), 15 were being treated with oral hypoglycemic agents (sulphonylureas plus biguanides); 39 were insulin-treated; 21 from which with the combination of oral drugs (insulin plus biguanides). Comparison was done with 94 healthy volunteers, 41 men and 53 women, age range from 35 to 83 years, mean age 56.6 ± 11.2 years. Only 7 (7.4%) from the non-diabetic controls had slightly increased bogy weight (BMI 31 - 33). Participants were

Table 1. General characteristic of the study subjects with T2DM with vascular complications *versus* healthy controls

Variable	Diabetic patients with vascular complications (n = 93)	Controls (n = 94)	p value
Age (years), mean ± SD	64.24 ± 9.76	56.57 ± 11.19	< 0.001
Sex: male/female	41/52	41/53	0.948
Disease duration (years), mean ± SD	12.70 ± 8.65	–	–
BMI (kg/m²), mean ± SD	31.52 ± 5.89	25.23 ± 3.52	< 0.001
BMI > 30 kg/m², *n* (%)	54 (58.1)	7 (7.4)	< 0.001
FPG (mmol/l), mean ± SD	9.52 ± 5.18	4.97 ± 0.32	< 0.001
FPG > 6.1 mmol/L, *n* (%)	62 (66.7)	0 (0)	–
HbA1c (%), mean ± SD	8.20 ± 2.06	5.06 ± 0.27	< 0.001
HbA1c > 7%, *n* (%)	53 (57.0)	0 (0)	–
Cholesterol (mmol/L), mean ± SD	5.12 ± 1.38	4.43 ± 0.76	< 0.001
Triglycerides (mmol/L), mean ± SD	2.43 ± 1.27	1.52 ± 0.44	< 0.001
HDL cholesterol (mmol/L), mean ± SD	1.25 ± 0.38	1.01 ± 0.28	< 0.001
LDL cholesterol (mmol/L), mean ± SD	2.86 ± 1.10	2.32 ± 0.62	< 0.001
Microvascular complications, *n* (%)			
Neuropathy	90 (96.8)	–	–
Retinopathy	24 (25.8)	–	–
Nephropathy	7 (7.5)	–	–
Macrovascular complications, *n* (%)			
Coronary heart disease	35 (37.6)	–	–
Cerebrovascular disease	11 (11.8)	–	–
Therapy, *n* (%)			
Insulin	25 (26.9)	–	–
Insulin + oral hypoglycemic agents	27 (29.0)	–	–
Oral hypoglycemic agents	41 (44.1)	–	–
ROS [arb. unit], mean ± SD	2.01 ± 0.76	1.19 ± 1.28	< 0.001
MDA [μmol/L], mean ± SD	3.27 ± 1.01	2.12 ± 0.55	< 0.001
Protein CO groups [nmol/mg], mean ±SD	8.06 ± 3.81	3.23 ± 2.58	< 0.001
8-OHdG [ng/mL], mean ± SD	2.34 ± 1.19	1.24 ± 0.51	< 0.001
•NO radicals [arb. unit], mean ± SD	31.22 ± 3.98	4.30 ± 5.01	< 0.001

BMI = body mass index; FPG = fasting plasma glucose; HbA1c = glycated hemoglobin; HDL = high density lipids; LDL = low density lipids; ROS = reactive oxygen species; arb. unit = arbitrary unit; MDA = malondialdehyde; 8-OHdG = 8-hydroxy-2'-deoxyguanosine; •NO radicals = nitric oxide radicals.

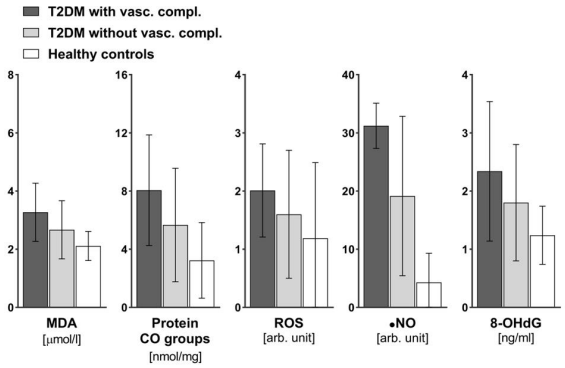

Figure 1. Comparison of the mean serum concentrations of the oxidative markers in T2DM patients with and without vascular complications versus healthy individuals. Shown is increased oxidative capacity in T2DM patients regardless of the presence or absence of vascular disease versus healthy controls. The oxidant profiles among both T2DM subsets demonstrated significantly higher MDA (p = 0.001) and •NO radicals (p < 0.001), a tendency of higher protein carbonyl content (p = 0.09) in diabetes with evidence of related vascular involvement and similar levels of ROS and 8-OHdG (p = 0.147; p = 0.109, respectively).

comparable for sex. Also, for comparison purposes, pro-oxidant profiles were examined in a small subset (n = 16) of newly diagnosed T2DM patients who had no evidence of complications. Table 1 presents key characteristics of diabetic patients with related vascular disease versus healthy controls.

3.2. *Comparisons of serum levels of pro-oxidants among study subjects*

Oxidative stress levels in circulation, expressed by the 5 biochemical markers, were considerably higher in both T2DM subsets as compared to healthy subjects with numerically higher values in those with signs of vascular damage (Figure 1, Table 1). No difference in serum concentration of all oxidative markers was found among obese and non-obese diabetics with vascular disease (p > 0.05). The levels of carbonylated proteins, ROS and 8-OHdG were significantly increased in insufficiently compensated diabetes compared to good glycemic control state (8.84 ± 3.95 nmol/mg *vs*. 6.98 ± 3.35 nmol/mg, p = 0.019; 2.14 ± 0.76 arb. unit *vs*. 1.81 ± 0.73 arb. unit, p = 0.031; 3.25 ± 0.65 ng/mL *vs*. 1.07 ± 0.13 ng/mL, p < 0.001, respectively), while MDA and •NO free radicals were estimated equal in these settings.

3.3. *Relationship between serum concentration of oxidative markers and disease characteristics in T2DM patients with associated vascular complications*

Serum MDA showed a weak association with fasting glucose ($r = 0.298$, $p = 0.004$). Calculation of the biserial correlation revealed an inverse correlation of MDA with diagnosed diabetic neuropathy ($r = -0.391$, $p < 0.001$) and a weak positive correlation of this pro-oxidant with diabetic nephropathy ($r = 0.235$, $p = 0.023$). Protein CO concentrations in the serum correlated weakly with both parameters for glycemic control, fasting plasma glucose and glycated hemoglobin ($r = 0.231$, $p = 0.026$; $r = 0.260$, $p = 0.012$, respectively). Likewise, systemic levels of the 8-OHdG showed a good significant correlation with parameters of blood glucose control; with fasting glucose ($r = 0.585$, $p < 0.001$) and with HbA1c ($r = 0.697$, $p < 0.001$). Plasma 8-OHdG levels correlated inversely with the diabetic neuropathy ($r = -0.548$, $p < 0.001$) and positively with diabetic retinopathy ($r = 0.269$, $p = 0.009$) and history of brain stroke ($r = 0.306$, $p = 0.003$). We also found a significant relation between ROS and diabetic retinopathy ($r = 0.307$, $p = 0.003$). No association was established for •NO radicals with any vascular complication or compensation state of diabetes. Most of the tested pro-oxidants correlated with serum levels of lipids (data not shown).

3.4. *Receiver operating characteristic curves with the cutoff values of pro-oxidants for detecting T2DM associated with complications*

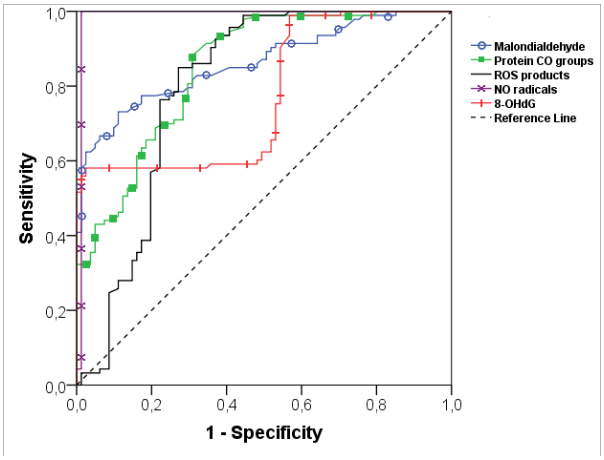

Figure 2. Receiver operating characteristic curves of oxidative biomarkers for detecting T2DM with diabetic-induced vascular damages. The model was performed to distinguish between above-mentioned disease and no disease.

To analyze the predictive accuracy of pro-oxidants for detecting the disease with the best combination of sensitivity and specificity values we calculated ROC. Figure 2 shows the ROC of various pro-oxidants against diabetic condition, with high cutoff values for all biochemical parameters. Significant AUC were obtained for all studied biomarkers ($p < 0.001$). AUC for nitric oxide was very large and substantially bigger compared to those for the other pro-oxidants, approaching a value of 1, suggesting the greater diagnostic accuracy of this biochemical test (Figure 2, Table 2).

4. Discussion

Pro-oxidants generated by chronic exposure to a high glucose concentration or increased glycemic variability and other metabolic abnormalities are important to the development of diabetes with its impairments by modifying biomolecules and cellular damage. Increased free radical generation and subsequent oxidative stress has been implicated as underlying cause of both long-term macrovascular and microvascular complications of diabetes (*4,18*). In the normal physiological conditions these chemical substances are counterbalanced with the cellular antioxidants, such as superoxide dismutases, catalases and glutathione peroxidases (*19*). The state of imbalance between pro-oxidants and antioxidants in favor of the former is known as "oxidative stress" (*20*). Since the vascular damage may begin to develop before the diagnosis and a great proportion of patients with T2DM may already have vascular disease at the time they are diagnosed with diabetes, the main focus of our investigation concerns such a population of patients. In the present study, we have attempted to test which of oxidative stress parameters would improve identification of T2DM with manifested diabetic vascular complications. We analyzed the systemic levels of ROS, •NO radicals, MDA, protein CO groups and 8-OHdG basing on the proven role of these reactive molecules and products of biomolecular modification as key tags in the oxidative damage, also on the consideration for the usage of some of them as biomarkers in the diagnosis of diabetes (*21*).

ROS are chemically reactive molecules, strong oxidants, which by the transfer of their free unpaired

Table 2. Results from ROC analysis

Pro-oxidants	Cut-off	AUC	Sensitivity (%)	Specificity (%)	PPV (%)	NPV (%)
MDA [μmol/L]	2.49	0.863	77.4	77.7	77.4	77.7
Protein CO groups [nmol/mg]	5.29	0.849	71.0	72.5	72.5	71.0
ROS products [arb. unit]	1.33	0.799	77.4	74.5	75.0	76.9
•NO radicals [arb. unit]	17.68	0.988	100.0	98.8	98.9	100.0
8-OHdG [ng/mL]	1.44	0.773	59.1	63.0	64.7	57.3

AUC = area under the curve; PPV = positive predictive value; NPV = negative predictive value; MDA = malondialdehyde; Protein CO groups = protein carbonyl groups; ROS = reactive oxygen species; arb. unit = arbitrary unit; •NO radicals = nitric oxide radicals; 8-OHdG = 8-hydroxy-2'-deoxyguanosine.

electron cause the oxidation of cellular macromolecules - polyunsaturated fatty acids (PUFAs) in lipids, amino acids in proteins and DNA, resulting in cell structures damage, with subsequent function disruption or cell death (*22*).

Lipids in cell membrane are among the most susceptible to oxidative damage macro molecules due to the presence of multiple bonds (*23*). Free radical attack of PUFAs, in particular reaction of oxygen with unsaturated lipids *via* enzymatic and/or non-enzymatic mechanisms is known as lipid peroxidation. Malondialdehyde (MDA) is one of the final products of lipid peroxidation generated by decomposition of arachidonic acid and larger PUFAs. Evidence now exists to suggest that along with primary dyslipidemia, oxidative damage and irreversible chemical lipoprotein modifications causing a production of oxidized low-density lipoproteins (oxLDL) is involved in an accelerated rate of atherosclerosis in T2DM (*24,25*). Furthermore, this aldehyde (MDA) is also a highly toxic and potentially mutagenic molecule, which exerts these capabilities through its high reactivity with proteins and deoxyribonucleic acids (DNA) (*26,27*). It is a convenient biomarker for lipid peroxidation and one of the most commonly used in clinical studies (*28*).

Oxidative modification of proteins is another event of oxidative stress. This oxidative damage often leads to loss in specific protein function and thus might play a significant role in the etiology of diseases. An accumulation and increase in protein carbonyls has been observed in several human pathologies including diabetes mellitus. At present, the measurement of protein CO groups after their derivatisation with 2,4-dinitrophenylhydrazine (DNPH) is the most widely utilized measure of protein oxidation (*29,30*). The usage of protein carbonyl CO groups (aldehydes and ketones) as biomarkers of oxidative stress has some advantages in comparison with the measurement of other oxidation products because of the relative early formation and the relative chemical stability of carbonylated proteins within hours and days (*31*), whereas lipid peroxidation products undergo detoxification within minutes (*32*).

A great deal of evidence support the role of oxidative DNA damage affecting tissue function and integrity as a common pathogenic factor in diabetes, as well in the onset and progression of diabetic complications (*33,34*). 8-hydroxy-2'-deoxyguanosine (8-OHdG), an oxidized nucleoside of nuclear and mitochondrial DNA, is a sensitive DNA damage biomarker of cellular oxidative stress. Diverse pathologies affect 8-OHdG level, but it is considered to be a measurable risk factor for cancer, atherosclerosis, and diabetes (*34*), such that its use as a biomarker in the diagnosis of diabetes has been considered (*21*).

•NO is a common gaseous free radical, which plays a role in vascular physiology and is also, known as endothelium derived relaxing factor. Therefore reduction of NO production, release or decreased bioavailability to the endothelium leads to endothelial cell dysfunction (*35*). Endothelial dysfunction plays an important role in the early stages of development of atherosclerosis, which is often observed as a macroangiopathic event in T2DM (*36*).

The results from our analysis showed a considerable overproduction of the 5 studied oxidative markers in T2DM patients, more distinctly in the presence of diabetes-associated vascular manifestations. These results are in agreement with the majority of publications, which demonstrate a significant rise in oxidative damage in the diabetic state (*3,4,37-39*). Notably, our T2DM patients with vascular involvement significantly exhibit approximately 7-fold elevated •NO levels than healthy controls, unlike the other biochemical markers which were increased only by 1.5 to 2.5 times, suggesting, that •NO free radical overproduction may be considered crucial in the generation of diabetes and vascular disease. The glycemic control status was significantly correlated to the level of oxidation of the lipids, proteins and DNAs (MDA, carbonyl values and 8-OHdG), which confirms the influence of elevated blood glucose on the damage of all types of biological molecules. The strongest degrees of correlation were apparent for the oxidized guanine of DNA, showing that hyperglycemia promotes DNA oxidation. ROS and 8-OHdG generated by high glucose were causally linked to diabetic retinopathy. Correspondingly, a positive correlation of the systemic 8-OHdG content with the brain stoke, a macrovascular manifestation attributable to diabetes was found. However, deoxyribonucleic acid base modification produced by the oxidation of deoxyguanosine was inversely correlated with diabetic neuropathy. MDA was associated with various locations of microvascular damage (neuro- and nephropathy) with a divergent link orientation. We further demonstrated the lack of difference in the systemic oxidative stress among obese and non-obese diabetics, despite the opposite findings of the other authors for the increase oxidative stress on accumulated fat in obesity (*40*).

ROC analysis revealed that •NO values in the circulation discriminated the presence of T2DM with diabetes-specific vascular complications better than the other oxidative stress parameters. The cutoff values based on the ROC were higher and outside the normal range for all of them. 8-OHdG had lower sensitivity (0.59) and specificity (0.63) compared with the other biomarkers and showed a reduced AUC, while the •NO gives the highest returns for detecting diabetes with induces vascular damage. In general, the test characteristics positive and negative predictive values were in favor of the •NO radicals (98.9% and 100%, respectively) while the positive predictive value of 8-OHdG variable was low (only 64.7 percent). Overall the positive predictive values – a relevant characteristic

in clinical practice – for MDA, carbonylated proteins and ROS were uniformly reasonable.

In conclusion, the chronic excess of carbohydrates present in T2DM and poor metabolic control result in creation of an abundance of reactive intermediates, leading to increase chemical modification of proteins, lipids and DNAs. Oxidative stress affects vascular function and ultimately contributes to vascular disease. The cutoff value for the studied oxidative biomarkers obtained from plotted ROC curves may serve as an indicator of clinical reference for detecting T2DM with associated vascular complications. The most efficient indicator is •NO, which may have the added ability to account for the disease and may strengthen the accuracy of clinical diagnosis.

Acknowledgement

This study was supported by scientific projects 6/2016 of Medical Faculty, Trakia University, Stara Zagora, Bulgaria.

References

1. DeFronzo RA. The Triumvirate: β-Cell, Muscle, Liver: A Collusion Responsible for NIDDM. Diabetes. 1988; 37:667-687.
2. Wallace JI. Management of Diabetes in the Elderly. Clin Diabetes. 1999; 17:1-26.
3. Evans JL, Goldfine ID, Maddux BA, Grodsky GM. Oxidative stress and stress-activated signaling pathways: A unifying hypothesis of type 2 diabetes. Endocr Rev. 2002; 23:599-622.
4. Rösen P, Nawroth PP, King G, Möller W, Tritschler HJ, Packer L. The role of oxidative stress in the onset and progression of diabetes and its complications: A summary of a Congress Series sponsored by UNESCO-MCBN, the American Diabetes Association and the German Diabetes Society. Diabetes Metab Res Rev. 2001; 17:189-212.
5. Giacco F, Brownlee M. Oxidative stress and diabetic complications. Circ Res. 2010; 107:1058-1070.
6. Hirsch IB, Brownlee M. Should minimal blood glucose variability become the gold standard of glycemic control? J Diabetes Complications. 2005; 19:178-181.
7. Wright E Jr, Scism-Bacon JL, Glass LC. Oxidative stress in type 2 diabetes: The role of fasting and postprandial glycaemia. Int J Clin Pract. 2006; 60:308-314.
8. Sakurai T, Tsuchiya S. Superoxide production from nonenzymatically glycated protein. FEBS Lett. 1988; 236:406-410.
9. Harrison D, Griendling KK, Landmesser U, Hornig B, Drexler H. Role of oxidative stress in atherosclerosis. Am J Cardiol. 2003; 91:7-11.
10. Biliński T, Litwińska J, Błaszczyński M, Bajus A. Superoxide dismutase deficiency and the toxicity of the products of autooxidation of polyunsaturated fatty acids in yeast. Biochim et Biophys Acta. 1989; 1001:102-106.
11. Cabiscol E, Piulats E, Echave P, Herrero E, Ros J. Oxidative stress promotes specific protein damage in Saccharomyces cerevisiae. J Biol Chem. 2000; 275:27393-27398.
12. Yakes FM, Van Houten B. Mitochondrial DNA damage is more extensive and persists longer than nuclear DNA damage in human cells following oxidative stress. Proc Natl Acad Sci USA. 1997; 94:514-519.
13. World Health Organization & International Diabetes Federation. Definition and diagnosis of diabetes mellitus and intermediate hyperglycaemia: Report of a WHO/IDF consultation. Geneva, 2006: World Health Organization. *http://www.who.int/iris/handle/10665/43588*. (accessed January 5, 2019).
14. Shi H, Sui Y, Wang X, Luo Y, Ji L. Hydroxyl radical production and oxidative damage induced by cadmium and naphthalene in liver of Carassius auratus Comp. Biochem and Physiol. Part C: Toxicol and Pharmacol. 2005; 140:115-121.
15. Yoshioka T, Iwamoto N, Lto K. An applicationof Electron Paramagnetic Resonance to evaluate nitric oxide and its quenchers. J Am Soci Nephrol. 1996; 7:961-965.
16. Yokoyama K, Hashiba K, Wakabayashi H, Hashimoto K, Satoh K, Kurihara T, Motohashi N, Sakagami H. Inhibition of LPS-stimulated NO production in mouse macrophage-like cells by Tropolones. Anticans Res. 2004; 24:3917-3922.
17. Plaser ZA, Cushman LL, Jonson BC. Estimation of product of lipid peroxidation (malonyl dialdehyde) in biochemical systems. Analyt Biochem. 1966; 16:359-364.
18. Pham-Huy LA, He H., Pham-Huy C. Free radicals, antioxidants in disease and health. IJBS. 2008; 4:89-96.
19. Gutteridge JM, Halliwell B. Comments on review of Free Radicals in Biology and Medicine, by Barry Halliwell and John MC. Gutteridge. Free Radic Biol Med. 1992; 12:93-95.
20. Sies H. Oxidative stress: Oxidants and antioxidants. Exp Physiol. 1997; 82:291-295.
21. Lai CQ, Tucker KL, Parnell LD, Adiconis X, García-Bailo B, Griffith J, Meydani M, Ordovás JM. PPARGC1A variation associated with DNA damage, diabetes, and cardiovascular diseases. Diabetes. 2008; 57:809-816.
22. Halliwell B. Antioxidants in human health and disease. Ann Rev Nutr. 1996; 16:33-50.
23. Butterfield DA, Koppal T, Howard B, Subramaniam RA, Hall N, Hensley K, Yatin S, Allen K, Aksenov M, Aksenova M, Carney J. Structural and functional changes in proteins induced by free radical-mediated oxidative stress and protective action of the antioxidants N-tert-butyl-alpha-phenylnitrone and vitamin E. Ann N Y Acad Sci. 1998; 854:448-462.
24. Steinberg D, Parthasarathy S, Carew TE. Beyond cholesterol. Modifications of low-density lipoprotein that increases its atherogenicity. New Engl J Med. 1989; 320:915-924.
25. Jenkins AJ, Best JD, Klein RL, Lyons TJ. Lipoproteins, glycoxidation and diabetic angiopathy. Diabetes Metab Res Rev. 2004; 20:349-368.
26. Esterbauer H, Eckl P, and Ortner A. Possible mutagens derived from lipids and lipid precursors. Mutation Research. 1990; 238:223-233.
27. Del Rio D, Stewart AJ, Pellegrini N. A review of recent studies on malondialdehyde as toxic molecule and biological marker of oxidative stress. Nutr Metab Cardiovasc Dis. 2005; 15:316-328.
28. Giera M, Lingeman H, Niessen WMA. Recent Advancements in the LC- and GC-Based Analysis of Malondialdehyde (MDA): A Brief Overview. Chromatographia. 2012; 75:433-440.

29. Chevion M, Berenshtein E, Stadtman ER. Human studies related to protein oxidation: Protein carbonyl content as a marker of damage. Free Radic Res. 2000; 33:99-108.
30. Beal MF. Oxidatively modified proteins in aging and disease. Free Radic Biol Med. 2002; 32:797-803.
31. Grune T, Reinheckel T, Davies KJA. Degradation of oxidized proteins in K562 human hematopoietic cells by proteasome. J Biol Chem. 1996; 271:15504-15509.
32. Siems WG, Zollner H, Grune T, Esterbauer H. Metabolic fate of 4-hydroxynonenal in hepatocytes: 1,4-dihydroxynonene is not the main product. J Lipid Res. 1997; 38:612-622.
33. Ayepola OR, Brooks NL, Oguntibeju OO. Oxidative Stress and Diabetic Complications: The Role of Antioxidant Vitamins and Flavonoids. In: Antioxidant-Antidiabetic Agents and Human Health. InTech, Croatia, 2014; pp. 25-58.
34. Wu LL, Chiou CC, Chang PY, Wu JT. Urinary 8-OHdG: A marker of oxidative stress to DNA and a risk factor for cancer, atherosclerosis and diabetics. Clin Chim Acta. 2004; 339:1-9.
35. Liao JK. Endothelium and acute coronary syndromes. Clin Chem. 1998; 44:1799-1808.
36. Cai H, Harrison DG. Endothelial dysfunction in cardiovascular diseases: The role of oxidant stress. Circ Res. 2000; 87:840-844.
37. Nakhjavani M, Esteghamati A, Nowroozi S, Asgarani F, Rashidi A, Khalilzadeh O. Type 2 diabetes mellitus duration: An independent predictor of serum malondialdehyde levels. Singapore Med J. 2010; 51:582-585.
38. Bollineni RC, Fedorova M, Blüher M, Hoffmann R. Carbonylated plasma proteins as potential biomarkers of obesity induced type 2 diabetes mellitus. J Proteome Res. 2014; 13:5081-5093.
39. Pan HZ, Zhang H, Chang D, Li H, Sui H. The change of oxidative stress products in diabetes mellitus and diabetic retinopathy. Br J Ophthalmol. 2008; 92:548-551.
40. Furukawa S, Fujita T, Shimabukuro M, Iwaki M, Yamada Y, Nakajima Y, Nakayama O, Makishima M, Matsuda M, Shimomura I. Increased oxidative stress in obesity and its impact on metabolic syndrome. J Clin Invest. 2004; 114:1752-1761.

(Received January 25, 2019; Revised March 11, 2019; Accepted March 21, 2019)

Original Article

DOI: 10.5582/bst.2019.01088

Preoperative albumin-bilirubin grade combined with aspartate aminotransferase-to-platelet count ratio index predict outcomes of patients with hepatocellular carcinoma within Milan criteria after liver resection

Hongmei Luo[1], Chuan Li[2], Liping Chen[2,*]

[1] *Department of Nursing, West China Hospital of Sichuan University, Chengdu, Sichuan, China;*
[2] *Department of General Surgery, West China Hospital of Sichuan University, Chengdu Sichuan, China.*

Summary **There is little information concerning the prognostic significance of combined albumin-bilirubin (ALBI) grade and aspartate aminotransferase-to-platelet count ratio index (APRI) in hepatocellular carcinoma (HCC). Therefore, we performed this study to assess the prognostic utility of combining ALBI and APRI (ALBI-APRI score) for predicting the prognosis of patients with HCC within Milan criteria after liver resection. Two hundred thirty-nine patients were involved in this study. Patients with a high APRI score were allocated a score of 1, whereas patients with a low APRI score were allocated a score of 0. The ALBI-APRI score is the summation of APRI score and ALBI grade. The area under the receiver operating characteristic curve (AUC) was used to estimate the predictive accuracy of different models. During the study period, 132 patients experienced recurrence, and 52 patients died. Multivariate analysis revealed the ALBI-APRI score (HR = 1.753, 95% CI = 1.293-2.377, $p < 0.001$), presence of microvascular invasion (MVI, HR = 2.693, 95%CI = 1.832-3.960, $p < 0.001$) and multiple tumors (HR = 1.973, 95% CI = 1.300-2.995, $p = 0.001$) were all associated with recurrence. In addition, blood transfusion (HR = 3.113, 95% CI = 1.677-5.778, $p < 0.001$), high preoperative alpha-fetoprotein (AFP, HR = 2.272, 95% CI = 1.298-3.976, $p = 0.004$), ALBI-APRI score (HR = 2.046, 95% CI = 1.237-3.382, $p = 0.005$) and presence of MVI (HR = 4.524, 95% CI = 2.514-8.140, $p < 0.001$) were correlated with postoperative mortality. The AUCs of ALBI-APRI score were significantly higher than either ALBI or APRI alone for predicting both postoperative recurrence and mortality. ALBI-APRI score may be a predictor for the prognosis of patients with HCC within Milan criteria following liver resection. A more well-designed and large-scale study are warranted to prove our findings.**

Keywords: Albumin-bilirubin grade, aminotransferase-to-platelet count ratio index, hepatocellular carcinoma

1. Introduction

Hepatocellular carcinoma (HCC) is one of the most common malignancies and is ranked the third most frequent cancer-related mortality worldwide (*1*). Every year, more than 800,000 new cases are diagnosed, and mortality is high due to the poor prognosis of HCC (*2*). Liver resection is widely accepted as a curative treatment for HCC patients with well-compensated liver function. However, the 5-year overall survival for HCC patients after liver resection remains unsatisfactory due to the high incidence of postoperative recurrence (*3*). Some investigations suggest as many as 51.6-70.3% of patients with HCC within Milan criteria will suffer from recurrence after liver resection (*4,5*).

Liver function greatly influences the prognosis of HCC patients. Patients with poor liver function are at high risk for postoperative complications and tend to

Released online in J-STAGE as advance publication April 27, 2019.

*Address correspondence to:
Dr. Liping Chen, Department of General Surgery, West China Hospital of Sichuan University, Chengdu 610041, Sichuan, China.
E-mail: cdclp1979@163.com

experience poor long-term overall survival. Recently, albumin-bilirubin (ALBI) grade was identified as a simple tool to assess patient liver function (*6*). Compared to Child-Pugh score, ALBI only includes total bilirubin and albumin as the two objective parameters. ALBI measurements may avoid the adverse influence of subjective variables, such as ascites and hepatic encephalopathy. Some studies also demonstrated that ALBI could predict HCC patient prognosis following liver resection (*6-8*). In addition to patient liver function, liver fibrosis or cirrhosis also plays a key role in HCC patient outcomes after liver resection (*9,10*). However, ALBI only reflects patient liver function and cannot indicate the degree of liver fibrosis in HCC patients. Preoperative aspartate aminotransferase (AST)-to-platelet count ratio index (APRI) has been confirmed as a surrogate marker for histological fibrogenesis (*11*). It is unclear whether ALBI incorporated with APRI results could strengthen the prognostic power for HCC patients within Milan criteria following liver resection. To clarify this issue, we conducted this study.

2. Patients and Methods

Patients with HCC within Milan criteria who underwent liver resection between 2013 and 2018 at our center were included in this study. Exclusion criteria included re-resection, ruptured HCC, receipt of preoperative antitumor treatment, a positive surgical margin, and the presence of other types of tumors. HCC was confirmed by postoperative pathological examination. This study was approved by the ethics committee of West China Hospital (No. 2017062).

2.1. *Follow-up*

All preoperative blood tests were performed two days before liver resection. After surgery, patients were followed up regularly every 3 months. Before and after surgery, antiviral drugs (entecavir, lamivudine or tenofovir) were conventionally administered to patients with positive hepatitis B virus-DNA (HBV-DNA) load. During follow-up, blood cell tests, liver function tests, serum alpha-fetoprotein (AFP) measurements, HBV-DNA tests, and visceral ultrasonography, as well as computed tomography or magnetic resonance imaging and chest radiography, were performed for all patients. Bone scintigraphy was performed whenever HCC recurrence was suspected. Postoperative recurrence was defined as positive imaging findings compared to preoperative examination values or as confirmed by biopsy or resection.

2.2. *Definitions*

ALBI score = (log10 bilirubin × 0.66) + (albumin × −0.085). ALBI grades were defined as grade 1 (score ≤ –2.60), grade 2 (score > –2.60 and ≤ –1.39), and grade 3 (score > –1.39) (*12*). APRI was calculated as [(AST value/ULN)/platelet count (10^9/L)] × 100 (*13*). APRI less than 0.5 was considered low APRI, whereas APRI ≥ 0.5 was defined as high APRI (*13*). ALBI-APRI scores were the summation of APRI scores and ALBI grade. ALBI-APRI scores ranged from 1 to 4. A high preoperative AFP was defined as an AFP level greater than 400 ng/mL (*13*). Neutrophil to lymphocyte ratio (NLR) was defined as absolute neutrophil counts divided by the lymphocyte counts (*7*). Platelet to lymphocyte ratio (PLR) as platelet counts divided by the lymphocyte counts (*7*). The preoperative prognostic nutritional index (PNI) was calculated using the following formula: serum albumin (g/L) + 0.005 × total lymphocyte count (per mm^3) (*7*).

2.3. *Statistical analysis*

All statistical analyses were performed using SPSS 21.0 (SPSS Company, Chicago, IL) for Windows. All continuous variables were compared using one-way analysis of variance. Categorical variables were compared using the χ^2 test or Fisher's exact test. Recurrence-free survival (RFS) and overall survival (OS) were determined using the Kaplan-Meier method, and comparisons were made using the log-rank test. Multivariable analysis was performed using Cox regression analysis to identify independent risk factors for OS and RFS. All variables found to be significant ($P < 0.05$) by univariate analysis were included in the multivariate analysis. The area under the receiver operating characteristic curve (AUC) was used to estimate the predictive accuracy of ALBI grade, APRI and ALBI-APRI score. A P-value of < 0.05 was considered statistically significant.

3. Results

Two hundred thirty-nine patients were included in this study. Of these, 197 were male, and 42 were female. Mean patient age was 48.86 ± 11.35 years. High preoperative AFP levels were detected in 77 patients. Positive HBV-DNA was observed in 122 patients, and 36 patients received blood transfusions. Multiple tumors were detected in 37 patients, and microvascular invasion (MVI) was observed in 48 patients. High APRI was observed in 208 patients. According to ALBI grade, 165 patients were stratified as grade 1, whereas 74 patients were stratified as grade 2. There were no ALBI grade 3 patients. There were 23 patients with ABLI-APRI score 1, 151 patients with ALBI-APRI score 2, and 65 patients in ALBI-APRI score 3. There were no patients with ALBI-APRI score 4. With a mean of 29.51 ± 13.18 months follow-up, 132 patients suffered from recurrence and 51 patients died.

3.1. *Univariate and multivariate analysis for RFS*

Table 1. Factors associated with RFS

Variables	Univariate	Multivariate	
	P value	HR (95%CI)	*P* value
Age (years)	0.629		
Gender (male)	0.946		
Tumor size (cm)	0.637		
Tumor number > 1	0.002	1.973 (1.300-2.995)	0.001
Differentiation	0.474		
AFP > 400 ng/mL	0.072		
Positive HBV-DNA load	0.495		
Presence of MVI	< 0.001	2.693 (1.832-3.960)	< 0.001
Transfusion	0.003		
Preoperative platelet (10^9/L)	0.029		
High APRI	< 0.001		
ALBI grade	< 0.001		
ALBI-APRI score	< 0.001	1.753 (1.293-2.377)	< 0.001
Preoperative PLR	0.969		
Preoperative NLR	0.691		
Preoperative PNI	0.315		

AFP, alpha-fetoprotein; APRI, aspartate aminotransferase-to-platelet count ratio index; HR, hazard ratio; PLR, platelet to lymphocyte ratio; PNI, prognostic nutritional index; NLR, Neutrophil to lymphocyte ratio; MVI, microvascular invasion.

Table 2. Factors associated with OS

Variables	Univariate	Multivariate	
	P value	HR (95%CI)	*P* value
Age (years)	0.065		
Gender (male)	0.837		
Tumor size (cm)	0.820		
Tumor number > 1	0.829		
Differentiation	0.380		
AFP > 400 ng/mL	0.007	2.272 (1.298-3.976)	0.004
Positive HBV-DNA load	0.162		
Presence of MVI	< 0.001	4.524 (2.514-8.140)	< 0.001
Transfusion	0.001	3.113 (1.677-5.778)	< 0.001
Preoperative platelet (10^9/L)	0.175		
High APRI	0.033		
ALBI grade	< 0.001		
ALBI-APRI score	< 0.001	2.046 (1.237-3.382)	0.005
Preoperative PLR	0.711		
Preoperative NLR	0.741		
Preoperative PNI	0.395		

AFP, alpha-fetoprotein; APRI, aspartate aminotransferase-to-platelet count ratio index; HR, hazard ratio; PLR, platelet to lymphocyte ratio; PNI, prognostic nutritional index; NLR, Neutrophil to lymphocyte ratio; MVI, microvascular invasion.

As shown in Table 1, factors associated with postoperative recurrence included multiple tumors, presence of MVI, transfusion, high preoperative APRI, ALBI grade, platelet counts and ALBI-APRI score by univariate analysis. In multivariate analysis, only ALBI-APRI score (HR = 1.753, 95% CI = 1.293-2.377), presence of MVI (HR = 2.693, 95%CI = 1.832-3.960) and multiple tumors (HR = 1.973, 95% CI = 1.300-2.995) exhibited prognostic power.

3.2. *Univariate and multivariate analysis for OS*

As shown in Table 2, presence of MVI, transfusion, high preoperative APRI, ALBI grade, high preoperative AFP and ALBI-APRI score were significant predictors of OS by univariate analysis. In multivariate analysis, only transfusion (HR = 3.113, 95% CI = 1.677-5.778), high preoperative AFP (HR = 2.272, 95% CI = 1.298-3.976), ALBI-APRI score (HR = 2.046, 95% CI = 1.237-3.382) and presence of MVI (HR = 4.524, 95% CI = 2.514-8.140) remained significant independent predictors of OS.

3.3. *Comparison of RFS and OS of patients with different ALBI-APRI scores*

The 1-, 3-, and 5-year RFS were 100%, 65.1%, and 48.8% for patients with ALBI-APRI score 1; 95.4%, 52.6%, and 12.4% for patients with ALBI-APRI score 2; and 87.7%, 39.0%, and 3.9% for patients with ALBI-APRI score 3, respectively. Significant differences were observed (Figure 1A, $p = 0.005$). The 1-, 3-, and 5-year OS were 100%, 91.7%, and 61.1% for patients

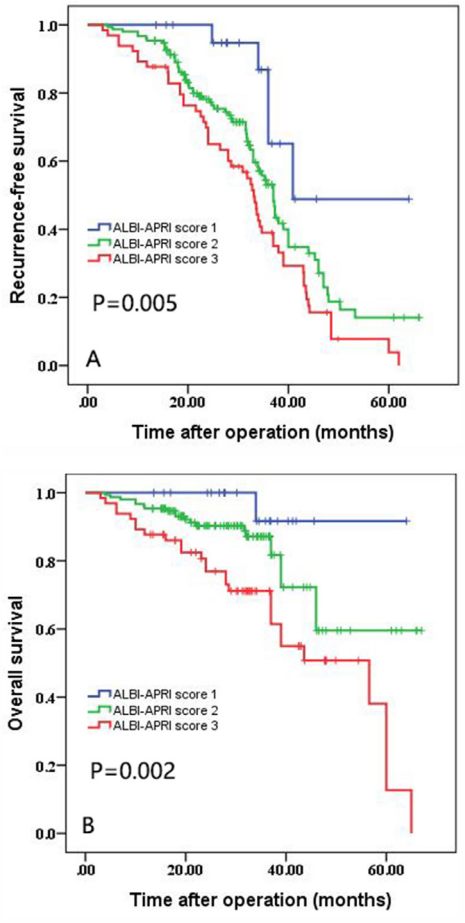

Figure 1. Comparison of recurrence-free (A) and overall (B) survival of patients with different ALBI-APRI scores.

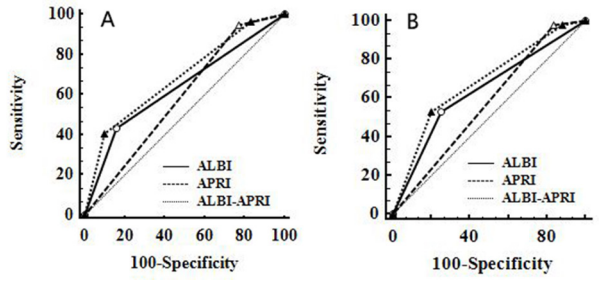

Figure 2. Comparison of the under the receiver operating characteristic curve of ALBI-APRI, ALBI, and APRI in predicting postoperative recurrence (A) and survival (B).

with ALBI-APRI score 1; 95.4%, 87.2% and 59.5% for patients with ALBI-APRI score 2; 87.7%, 71.1%, and 50.7% for patients with ALBI-APRI score 2, respectively (Figure 1B, p = 0.002).

3.4. *Comparison of the predictive abilities of ALBI-APRI, ALBI and APRI*

We compared the AUC of ALBI-APRI, ALBI and APRI, which were 0.686, 0.636 and 0.586, respectively, for predicting postoperative recurrence (Figure 2A). Significant differences were observed between ALBI-APRI versus ABLI ($P_{\text{ALBI-ALBI versus ABLI}} = 0.005$) and ALBI-APRI versus APRI ($P_{\text{ALBI-APRI versus APRI}} < 0.001$). As shown in Figure 2B, for predicting postoperative mortality, ALBI-APRI had the highest AUC (0.683), followed by ALBI (0.640) and APRI (0.570). Significant differences were also observed between ALBI-APRI versus ABLI ($P_{\text{ALBI-APRI versus ABLI}} < 0.001$) and ALBI-APRI versus APRI ($P_{\text{ALBI-APRI versus APRI}} < 0.001$).

4. Discussion

Liver resection is widely accepted as a curative treatment for patients with HCC. However, high postoperative recurrence rate remains an obstacle to long-term survival. Our study suggests that ALBI combined with APRI represent a surrogate marker to predict HCC patient prognosis after liver resection.

Recently, ABLI was confirmed as a superior tool to Child-Pugh score for assessing liver function (*14,15*). Child-Pugh score has some limitations because it includes two subjective variables: ascites and encephalopathy. Additionally, in Child-Pugh score, ascites and albumin may be confounded by their interrelationship. In our clinical practice, we perform liver resection in patients with Child-Pugh A grade. ALBI further discriminates patient liver function in the same Child-Pugh grade. ALBI not only evaluates patient liver function but also predicts HCC patient prognosis after liver resection. For example, Ho *et al*. (*16*) suggested that ALBI is a feasible marker for predicting patient recurrence after liver resection. Dong *et al*. (*7*) confirmed ALBI score significantly impacted both HCC patient RFS and OS after liver resection. However, though ABLI can assess patient liver function, it does not indicate the severity of patient fibrosis. Some patients with severe fibrosis may present with good liver function, and a number of investigations have revealed that severe fibrosis or cirrhosis has an adverse influence on HCC patient prognosis. In contrast, some patients without severe cirrhosis may also exhibit poor liver function, such as patients with malnutrition. The serum albumin level of patients with malnutrition may be very low. Accordingly, patients with malnutrition may have a high ALBI grade.

There are some potential mechanisms of poor ALBI grade contributing to poor prognosis of patients with HCC after liver resection. First, many studies have confirmed that patients with poor liver function may have increased surgical risk, a high incidence of postoperative complications, and a high recurrent rate. Ho *et al*. (*17*) compared the prognostic power of ten liver function models for predicting the prognosis of HCC patients after radiofrequency ablation. Only ALBI was an independent prognostic predictor by multivariate analysis (*17*). Second, some research has suggested that albumin may inhibit the growth of HCC (*18,19*). Carr and colleagues' study indicates that low serum albumin levels are associated with increased variables of HCC aggressiveness, such as larger maximum tumor diameters, increased portal vein thrombosis, higher α-fetoprotein levels and so on (*19*). Basic studies have also confirmed exogenous albumin at physiological concentrations can inhibit the growth of several HCC cell lines *in vitro* (*18*).

In contrast to ALBI, APRI is considered a promising noninvasive alterative to liver biopsy for assessing the stage of fibrosis (*20*). Previous studies have suggested liver fibrosis negatively affects HCC patient outcomes (*10,21*). Gon *et al*. (*22*) even suggested that liver fibrosis is an independent risk factor for rapid progression of portal vein tumor thrombus. Some investigators have also suggested that APRI could predict outcomes of patients with HCC after liver resection (*23,24*). Ichikawa *et al*. (*25*) confirmed that preoperative APRI independently predicts postoperative liver failure. In addition, Cheng *et al*. (*11*) suggested APRI could predict postoperative complications in HCC patients after liver resection. Further, some studies confirmed that postoperative complications may adversely influence both postoperative RFS and OS for patients with HCC after liver resection (*26-28*). Moreover, the preoperative platelet counts of patients with high APRI score may be low. Kaneko *et al*. (*29*) suggested HCC patients with low preoperative platelet counts may suffer from a high incidence of postoperative mortality. Maithel *et al*. (*30*) also confirmed low platelet count was associated with high postoperative mortality. Our study confirmed ALBI

combined with APRI score demonstrates superior predictive ability than either ALBI or APRI alone. ALBI plus APRI score reflect both patient liver function and stage of fibrosis. Recently, Pereya *et al*. (*31*) confirmed ALBI plus APRI score could predict the morbidity, liver dysfunction and mortality for patients who received liver resection for colorectal cancer liver metastases. They suggested ALBI plus APRI score was a good tool to dynamically reflect the chemotherapy-associated liver injury of patients with colorectal cancer liver metastases.

There are some limitations in this study. This is a small sample and single center's retrospective study. Moreover, in China, most HCC are hepatitis B virus-related HCC. Accordingly, whether ALBI+APRI score could predict the prognosis of other causes-related HCC needs further study. We believe that a multicenter prospective study is needed to further validate our conclusions.

In conclusion, our study suggests that ALBI plus APRI score predicts the prognosis of patients with HCC after liver resection. Patients with high ALBI+APRI score experience a high recurrence rate and poor long-term survival.

Acknowledgements

This study was supported by grants from the Science and Technology Department of Sichuan Province (2019YJ0149) as well as the Health and Family Planning Commission of Sichuan Province (17PJ393).

References

1. Wen T, Jin C, Facciorusso A, *et al*. Multidisciplinary management of recurrent and metastatic hepatocellular carcinoma after resection: An international expert consensus. Hepatobil Surg Nutr. 2018; 7:353-371.
2. Torre LA, Bray F, Siegel RL, Ferlay J, Lortet-Tieulent J, Jemal A. Global cancer statistics, 2012. CA Cancer J Clin. 2015; 65:87-108.
3. Li C, Shen JY, Zhang XY, Peng W, Wen TF, Yang JY, Yan LN. Predictors of Futile Liver Resection for Patients with Barcelona Clinic Liver Cancer Stage B/C Hepatocellular Carcinoma. J Gastrointest Surg. 2018; 22:496-502.
4. Liu H, Wang ZG, Fu SY, Li AJ, Pan ZY, Zhou WP, Lau WY, Wu MC. Randomized clinical trial of chemoembolization plus radiofrequency ablation versus partial hepatectomy for hepatocellular carcinoma within the Milan criteria. Brit J Surg. 2016; 103:348-356.
5. Sakaguchi T, Suzuki S, Morita Y, Oishi K, Suzuki A, Fukumoto K, Inaba K, Nakamura S, Konno H. Impact of the preoperative des-gamma-carboxy prothrombin level on prognosis after hepatectomy for hepatocellular carcinoma meeting the Milan criteria. Surg Today. 2010; 40:638-645.
6. Toyoda H, Lai PB, O'Beirne J, *et al*. Long-term impact of liver function on curative therapy for hepatocellular carcinoma: Application of the ALBI grade. Brit J Cancer. 2016; 114:744-750.
7. Yamamura K, Sugimoto H, Kanda M, Yamada S, Nomoto S, Nakayama G, Fujii T, Koike M, Fujiwara M, Kodera Y. Comparison of inflammation-based prognostic scores as predictors of tumor recurrence in patients with hepatocellular carcinoma after curative resection. J Hepatobiliary Pancreat Sci. 2014; 21:682-688.
8. Hiraoka A, Kumada T, Michitaka K, *et al*. Usefulness of albumin-bilirubin grade for evaluation of prognosis of 2584 Japanese patients with hepatocellular carcinoma. J Gastroenterol Hepatol. 2016; 31:1031-1036.
9. Kim JH, Lee M, Park SW, Kang M, Kim M, Lee SH, Kim TS, Park JM, Choi DH. Validation of modified fibrosis-4 index for predicting hepatocellular carcinoma in patients with compensated alcoholic liver cirrhosis. Medicine. 2018; 97:e13438.
10. Suh SW, Choi YS. Influence of liver fibrosis on prognosis after surgical resection for resectable single hepatocellular carcinoma. ANZ J Surg. 2019; 89:211-215.
11. Cheng J, Zhao P, Liu J, Liu X, Wu X. Preoperative aspartate aminotransferase-to-platelet ratio index (APRI) is a predictor on postoperative outcomes of hepatocellular carcinoma. Medicine. 2016; 95:e5486.
12. Fang KC, Kao WY, Su CW, Chen PC, Lee PC, Huang YH, Huo TI, Chang CC, Hou MC, Lin HC, Wu JC. The prognosis of single large hepatocellular carcinoma was distinct from barcelona clinic liver cancer stage A or B: The role of albumin-Bbilirubin grade. Liver Cancer. 2018; 7:335-358.
13. Wang H, Xue L, Yan R, Zhou Y, Wang MS, Cheng MJ, Huang HJ. Comparison of FIB-4 and APRI in Chinese HBV-infected patients with persistently normal ALT and mildly elevated ALT. J Viral Hepatitis. 2013; 20:e3-10.
14. Na SK, Yim SY, Suh SJ, Jung YK, Kim JH, Seo YS, Yim HJ, Yeon JE, Byun KS, Um SH. ALBI versus Child-Pugh grading systems for liver function in patients with hepatocellular carcinoma. J Surg Oncol. 2018; 117:912-921.
15. Li MX, Zhao H, Bi XY, Li ZY, Huang Z, Han Y, Zhou JG, Zhao JJ, Zhang YF, Cai JQ. Prognostic value of the albumin-bilirubin grade in patients with hepatocellular carcinoma: Validation in a Chinese cohort. Hepatol Res. 2017; 47:731-741.
16. Ho SY, Hsu CY, Liu PH, Hsia CY, Su CW, Huang YH, Hou MC, Huo TI. Albumin-bilirubin (ALBI) grade-based nomogram to predict tumor recurrence in patients with hepatocellular carcinoma. Eur J Surg Oncol. 2019; 45:776-781.
17. Ho SY, Liu PH, Hsu CY, Chiou YY, Su CW, Lee YH, Huang YH, Lee FY, Hou MC, Huo TI. Prognostic Performance of Ten Liver Function Models in Patients with Hepatocellular Carcinoma Undergoing Radiofrequency Ablation. Sci Rep. 2018; 8:843.
18. Bagirsakci E, Sahin E, Atabey N, Erdal E, Guerra V, Carr BI. Role of Albumin in Growth Inhibition in Hepatocellular Carcinoma. Oncology. 2017; 93:136-142.
19. Carr BI, Guerra V. Serum albumin levels in relation to tumor parameters in hepatocellular carcinoma patients. Int J Biol Markers. 2017; 32:e391-e396.
20. Lin ZH, Xin YN, Dong QJ, Wang Q, Jiang XJ, Zhan SH, Sun Y, Xuan SY. Performance of the aspartate aminotransferase-to-platelet ratio index for the staging of hepatitis C-related fibrosis: An updated meta-analysis. Hepatology. 2011; 53:726-736.

21. Kamarajah SK. Fibrosis score impacts survival following resection for hepatocellular carcinoma (HCC): A Surveillance, End Results and Epidemiology (SEER) database analysis. Asian J Surg. 2018; 41:551-561.
22. Gon H, Kido M, Tanaka M, Kinoshita H, Komatsu S, Tsugawa D, Awazu M, Toyama H, Matsumoto I, Itoh T, Fukumoto T. Growth velocity of the portal vein tumor thrombus accelerated by its progression, alpha-fetoprotein level, and liver fibrosis stage in patients with hepatocellular carcinoma. Surgery. 2018; 164:1014-1022.
23. Matsumoto M, Wakiyama S, Shiba H, Haruki K, Futagawa Y, Ishida Y, Misawa T, Yanaga K. Usefulness of aspartate aminotransferase to platelet ratio index as a prognostic factor following hepatic resection for hepatocellular carcinoma. Mol Clin Oncol. 2018; 9:369-376.
24. Shen SL, Fu SJ, Chen B, Kuang M, Li SQ, Hua YP, Liang LJ, Guo P, Hao Y, Peng BG. Preoperative aspartate aminotransferase to platelet ratio is an independent prognostic factor for hepatitis B-induced hepatocellular carcinoma after hepatic resection. Ann Surg Oncol. 2014; 21:3802-3809.
25. Ichikawa T, Uenishi T, Takemura S, Oba K, Ogawa M, Kodai S, Shinkawa H, Tanaka H, Yamamoto T, Tanaka S, Yamamoto S, Hai S, Shuto T, Hirohashi K, Kubo S. A simple, noninvasively determined index predicting hepatic failure following liver resection for hepatocellular carcinoma. J Hepatobiliary Pancreat Surg. 2009; 16:42-48.
26. Harimoto N, Shirabe K, Ikegami T, Yoshizumi T, Maeda T, Kajiyama K, Yamanaka T, Maehara Y. Postoperative complications are predictive of poor prognosis in hepatocellular carcinoma. J Surg Res. 2015; 199:470-477.
27. Zhou YM, Zhang XF, Li B, Sui CJ, Yang JM. Postoperative complications affect early recurrence of hepatocellular carcinoma after curative resection. BMC Cancer. 2015; 15:689.
28. Chok KS, Chan MM, Dai WC, Chan AC, Cheung TT, Wong TC, She WH, Lo CM. Survival outcomes of hepatocellular carcinoma resection with postoperative complications - a propensity-score-matched analysis. Medicine. 2017; 96:e6430.
29. Kaneko K, Shirai Y, Wakai T, Yokoyama N, Akazawa K, Hatakeyama K. Low preoperative platelet counts predict a high mortality after partial hepatectomy in patients with hepatocellular carcinoma. World J Gastroenterol. 2005; 11:5888-5892.
30. Maithel SK, Kneuertz PJ, Kooby DA, Scoggins CR, Weber SM, Martin RC, 2nd, McMasters KM, Cho CS, Winslow ER, Wood WC, Staley CA, 3rd. Importance of low preoperative platelet count in selecting patients for resection of hepatocellular carcinoma: A multi-institutional analysis. J Am Coll Surg. 2011; 212:638-648; discussion 648-650.
31. Pereyra D, Rumpf B, Ammann M, Perrodin SF, Tamandl D, Haselmann C, Stift J, Brostjan C, Laengle F, Beldi G, Gruenberger T, Starlinger P. The Combination of APRI and ALBI Facilitates Preoperative Risk Stratification for Patients Undergoing Liver Surgery After Neoadjuvant Chemotherapy. Ann Surg Oncol. 2019; 26:791-799.

(Received March 29, 2019; Revised April 16, 2019; Accepted April 23, 2019)

Original Article

DOI: 10.5582/bst.2019.01044

Treatment modalities and relative survival in patients with brain metastasis from colorectal cancer

Xingang Lu[1,2,§], Yibo Cai[2,§], Liang Xia[3], Haixing Ju[2,*], Xin Zhao[4,*]

[1] *The Second Clinical Medical College, Zhejiang Chinese Medical University, Hangzhou, Zhejiang, China;*
[2] *Department of Colorectal Surgery, Zhejiang Cancer Hospital, Hangzhou, Zhejiang, China;*
[3] *Department of Brain Surgery, Zhejiang Cancer Hospital, Hangzhou, Zhejiang, China;*
[4] *Department of Transplantation, The Third People's Hospital of Shenzhen, Shenzhen, Guangdong, China.*

Summary **Standard treatment options for brain metastases (BM) from colorectal cancer (CRC) are controversial. The purpose of this study was to evaluate the efficacy of multidisciplinary treatment modalities and provide optimal therapeutic strategies for selected patients with different clinical characteristics. All eligible patients diagnosed with BM from CRC during the past two decades (1997-2016) were identified in our center. Clinical characteristics, treatment modalities and relative survival were retrospectively analyzed. Median overall survival after the identification of BM was 6 months. The 1- and 2- year survival rates were 29.40% and 5.70%, respectively. On multivariate analysis, the number of BMs, Karnofsky performance score and the treatment modalities were found to be independent prognostic factors (the p-value was 0.006, 0.001 and < 0.001, respectively). In conclusion, multidisciplinary treatment is supported to be the optimal treatment for patients with BM from CRC. For patients with single brain metastases and KPS > 70, neurosurgery combined with chemotherapy could provide an additional survival benefit. For patients with multiple brain metastases or KPS ≤ 70, radiotherapy plus chemotherapy may be appropriate.**

Keywords: Brain metastases, colorectal cancer, treatment modalities, prognosis

1. Introduction

Colorectal cancer (CRC) metastatic to the brain occurs rarely and remains highly lethal in clinical practice. The crude incidence of brain metastases (BM) from CRC is 0.27%, while in metastatic colorectal cancer, it increases to 1.36% (*1*). Besides, the occurrence rate of asymptomatic BM has been observed to increase simultaneously in past decades (*2*), which has been attributed to the improvement of multimodality therapy to extend survival of CRC and novel diagnostic radiographic techniques to detect small brain lesions (*3,4*). Unfortunately, the prognosis for CRC patients developed to BM is rather poor. Patients without any therapeutic intervention will only have a survival period of about 4 weeks after the occurrence of BM (*5*). In the past, whole brain radiation therapy (WBRT) and neurosurgery were usually used for the treatment of brain metastases (*6*), but the effect of radiotherapy or neurosurgery alone was unsatisfactory. Patients who underwent WBRT alone had a median survival of only 3-6 months (*7,8*), and the ability of neurosurgery to improve survival in patients with BM is not as effective as clinicians expected. Currently, the concept of multidisciplinary treatment has been widely accepted in the clinical diagnosis and treatment of CRC liver metastasis and lung metastasis (*9,10*), and proved that multidisciplinary treatment could bring significant survival benefits to those patients. Nevertheless, in CRC patients with BM, the concept of multidisciplinary treatment was not universal. The decision-making for treatment modalities is still empirical in patients with

Released online in J-STAGE as advance publication April 27, 2019.

[§]These authors contributed equally to this work.
**Address correspondence to:*
Dr. Haixing Ju, Department of Colorectal Surgery, Zhejiang Cancer Hospital, 1 Banshan E. road, Hangzhou, Zhejiang 310011, China.
E-mail: juhx@zjcc.org.cn

Dr. Xin Zhao, Department of Transplantation, The Third People's Hospital of Shenzhen, No. 29, Buji Bulu Road, Longgang District, Shenzhen, Guangdong 510000, China.
E-mail: drzhaoxin@126.com

BM, and the selection criteria of candidates for various treatment models remains controversial. Therefore, the aim of this study is to compare different treatments for the patients with BM from CRC, then provide optimal treatment modalities for selected patients with different clinical characteristics.

2. Materials and Methods

2.1. *Patients*

We retrospectively analyzed 80 consecutive patients diagnosed with BM from CRC in the Zhejiang Cancer Hospital from Jan 1997 to Dec 2016. Brain metastatic lesions were diagnosed and assessed using radiologic imaging, such as brain CT or MRI scan. Clinical data regarding age, gender, location of the primary tumor, Karnofsky performance scale (KPS), and presence of extracranial metastasis, synchronous or metachronous metastasis, number of BM, location of BM, and treatment modalities was reviewed. Synchronous metastasis was defined as metastasis that occurred within 12 months of diagnosis of the primary CRC; Metachronous metastasis was defined as metastasis that was noted more than 12 months after diagnosis of the primary CRC. With regard to the location of BM, patients were divided into two groups according to bilobar distribution (unilateral and bilateral cerebral lesions groups) or tentorium of cerebellum (supratentorial lesions limited and infratentorial lesions involved groups).

2.2. *Treatment modalities*

The treatment options for BM from CRC included single treatment and multidisciplinary treatment. Single treatment included neurosurgery, radiotherapy (*i.e.* WBRT or SRS) or chemotherapy, and multidisciplinary treatment included neurosurgery plus chemotherapy or radiotherapy plus chemotherapy. Majority of patients (50 cases) were treated with WBRT in 30 Gy delivered at 3 Gy per fraction. The prescription isodose of SRS ranged from 12 to 22 Gy. Sequential chemotherapy with standard-dose of 5-fluorouracil-based regimens (Folfox or Folfori) was recommended in 55 patients. Sixteen metastatic CRC patients received additional molecular targeted therapy after diagnosis of BM, including cetuximab, bevacizumab, and regorafenib. All treatment decisions were made with coordination of experienced neurosurgeons, radiation and medical oncologists based on the comorbidities, performance status, availability of aggressive treatment and other tumor-specific parameters.

2.3. *Statistical analysis*

Overall survival (OS) after diagnosis of BM was measured from the date of dection of BM to the date of death or last follow-up. Kaplan-Meier method was performed to estimate OS curves. Potential predictors with p value less than 0.1 in the univariate analysis were entered into a backward stepwise Cox proportional hazards regression model. All statistical analysis was performed using SPSS statistical software version 19.0 (SPSS Inc., IBM Corporation, Chicago, IL). All two-sided P values less than 0.05 were considered statistically significant.

3. Results

3.1. *Patients characteristics and Treatment modalities*

A total of 80 patients with BM from CRC were enrolled in this retrospective study. Table 1 summarizes clinical and tumor characteristics of all included patients. The majority of BM were male (52 patients, 65.00%) and the average age at diagnosis of BM was 58.4 years. Half of BM (50%) had poor performance status (KPS ≤ 70). Synchronous colorectal BM occurred in only 6 patients, and rectum was the most common primary site for CRC metastatic to the brain. Majority of patients (83.75%) presented with extracranial metastases and the most common extracranial site was the lung, occupying 70.00% of all BM. Infratentorial metastatic lesions were observed in 27 (33.75%) patients. In terms of treatment, 38 patients received only a single treatment, of which 4

Table 1. Demographic and tumor characteristics of patients with colorectal brain metastases

Variable	Patients, *n* (%)
Age	
≤ 60	50 (62.50)
> 60	30 (37.50)
Gender	
Male	52 (65.00)
Female	28 (35.00)
Primary tumor location	
Right-sided	9 (11.25)
Left-sided	21 (26.25)
Rectum	50 (62.50)
KPS	
≤ 70	40 (50.00)
> 70	40 (50.00)
Metastases presentation	
Synchronous	6 (7.50)
Metachronous	74 (92.50)
Number of BM	
1	44 (55.00)
≥ 2	36 (45.00)
Site of BM lesion	
Supratentorial location limited	53 (66.25)
Infratentorial location involved	27 (33.75)
Extracranial metastases	
No	13 (16.25)
Lung metastases	56 (70.00)
Other organ metastases	11 (13.75)

Abbreviation: KPS, Karnofsky performance scale; BM, Brain metastases.

(5.00%) patients underwent neurosurgery, 16 (20.00%) patients received radiotherapy and 18 (22.50%) patients received chemotherapy. The remaining 42 patients received multidisciplinary treatment, including 15 patients who received neurosurgery plus chemotherapy and 27 patients received radiotherapy plus chemotherapy (Table 2).

3.2. *Survival analyses*

Four patients were lost to follow-up, 76 patients were eventually included in the survival analysis. The median overall survival (OS) was 6 months after diagnosis of BM (range, 1-33 months). The 1-year OS rate and 2-year OS rate were 29.40% and 5.70%, respectively. Patients who received monotherapy had a median OS of 4 months. Further analysis shows the median OS of patients who underwent only neurosurgery, radiotherapy and chemotherapy were 10 months, 3 months and 5 months respectively. Among the 16 patients who received targeted therapy, the median OS of 10 patients who used bevacizumab was 7.6 months. For patients who received multidisciplinary treatment, the median OS was 11 months. Univariate analysis showed KPS > 70 ($p < 0.001$), Synchronous metastasis ($p = 0.012$), Isolated BM lesions ($p = 0.011$) and multidisciplinary treatment ($p < 0.001$) were good prognostic factors. Multivariate analysis shows that KPS > 70 (hazard ratio (HR) = 2.75, $p < 0.001$), Isolated BM lesions (HR = 2.00, $p = 0.006$) and multidisciplinary treatment (HR = 0.37, $p < 0.001$) were independent predictors of good prognosis (Table 3, Figure 1).

The pattern of multidisciplinary treatment also led to significant differences in prognosis in different patient subgroups. Neurosurgery combined with chemotherapy achieved a better prognosis than radiotherapy plus chemotherapy ($p = 0.03$, Figure 2). In further subgroup analysis, we observed the exact survival benefit in single brain metastases group (neurosurgery plus chemotherapy vs radiotherapy plus chemotherapy, $p = 0.021$, Figure

Table 2. Treatment modalities for BM from CRC

Treatment modality	NO. (%)
Single treatment	38 (47.50)
Neurosurgery only	4 (5.00)
Radiotherapy only	16 (20.00)
Chemotherapy only	18 (22.50)
Multidisciplinary treatment	42 (52.50)
Neurosurgery + Chemotherapy	15 (18.75)
Radiotherapy + Chemotherapy	27 (33.75)

Abbreviation: BM, brain metastases; CRC, colorectal cancer.

Table 3. Potential predictors for overall survival in patients with colorectal brain metastases

Variable	Univariate		Multivariate	
	Median OS (95%CI, m)	*P*	Adjusted HR (95%CI)	*P*
Overall	6 (4.4-7.6)			
Age			NA	
≤ 60	6 (4.2-7.8)			
> 60	7 (4.2-9.8)	0.905		
Gender			NA	
Male	7 (5.4-8.6)			
Female	5 (3.4-6.6)	0.635		
Primary tumor location			NA	
Right-sided	3 (0.2-5.8)			
Left-sided	9 (3.9-14.1)			
Rectum	6 (4.4-7.6)	0.266		
KPS			1	
> 70	11 (5.2-16.8)		2.75 (1.60-4.74)	
≤ 70	4 (2.6-5.4)	< 0.001		< 0.001
Metastases presentation			1	
Synchronous	22 (0.5-43.5)		2.16 (0.71-6.63)	
Metachronous	6 (4.5-7.5)	0.012		0.177
Number of BM				
1	9 (5.8-12.2)		1	
≥ 2	5 (3.6-6.4)	0.011	2.00 (1.21-3.29)	0.006
Site of BM lesion				
Supratentorial location limited	6 (4.0-8.0)		NA	
Infratentorial location involved	6 (3.2-8.8)	0.608		
Extracranial metastasis				
No	7 (2.3-11.7)		NA	
Yes	6 (3.9-8.1)	0.278		
Treatment modalities				
Single treatment	4 (2.3-5.7)		1	
Multidisciplinary treatment	11 (6.8-15.2)	< 0.001	0.37 (0.22-0.64)	< 0.001

Abbreviation: OS, Overall survival; CI, Confidence interval; HR, Harzard ratio; BM, brain metastases; NA, Not available; KPS, Karnofsky performance score.

3) and in patients with KPS > 70 group (neurosurgery combined with chemotherapy achieved a therapeutic advantage, p = 0.029, Figure 4). For patients with multiple brain metastases (≥ 2) or KPS ≤ 70, there was no significant difference between neurosurgery combined with chemotherapy and radiotherapy plus chemotherapy (Figure 5 and Figure 6).

4. Discussion

Brain metastases is the most common type of intracranial tumors of adults and has a 10-fold increased incidence rate compared to primary brain tumors (*11*). Although metastasis to the brain rarely occurs to CRC patients with a prevalence rate of 0.60-3.20%, it occupies 71.90-79.90% of brain metastases originating from the gastrointestinal tract (*12,13*). The development of comprehensive treatment and the implementation of multidisciplinary team decision-making have improved the control of CRC (*14*). Extended survival in patients with liver or lung metastases may increase occurrence rate of BM. In addition, the developing radiological

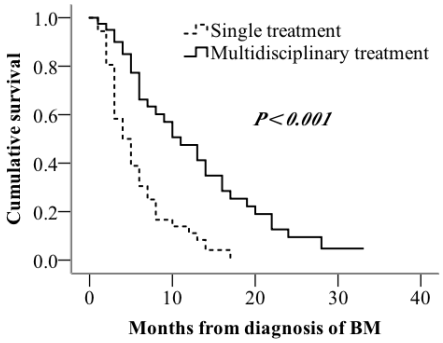

Figure 1. Comparison of survival curves of patients with BM from CRC receiving single treatment and multidisciplinary treatment.

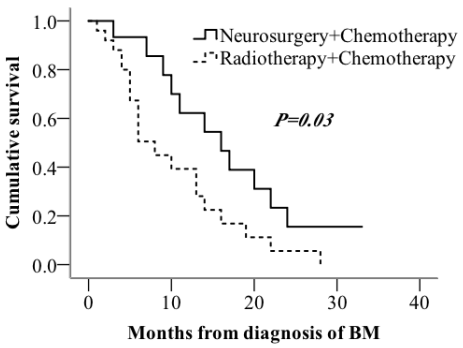

Figure 2. Comparison of survival curves of patients with BM from CRC receiving neurosurgery combined with chemotherapy and radiotherapy plus chemotherapy.

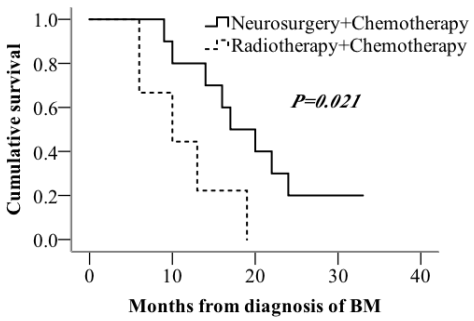

Figure 3. Comparison of survival curves of patients with isolated brain metastatic lesions receiving neurosurgery combined with chemotherapy and radiotherapy plus chemotherapy.

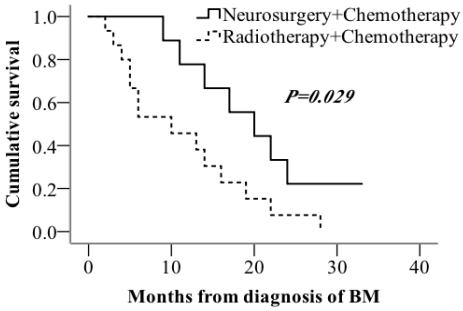

Figure 4. Comparison of survival curves of patients with KPS > 70 receiving neurosurgery combined with chemotherapy and radiotherapy plus chemotherapy.

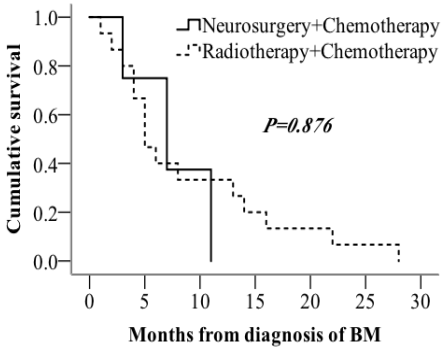

Figure 5. Comparison of survival curves of patients with multiple brain metastatic lesions (≥ 2) receiving neurosurgery combined with chemotherapy and radiotherapy plus chemotherapy.

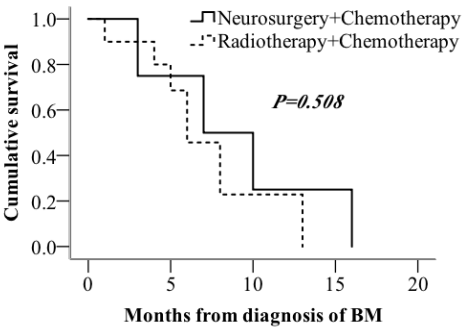

Figure 6. Comparison of survival curves of patients with KPS ≤ 70 receiving neurosurgery combined with chemotherapy and radiotherapy plus chemotherapy.

and metabolic imaging could also enhance the early detection of BM lesions, especially in asymptomatic patients (*8,15*).

We analyzed the clinical and pathological information of our colorectal cancer patients with BM, and found metachronous metastasis, lung metastasis and primary tumor from rectal cancer have a relationship with BM. As in previous reports (*16*), we found metachronous metastatic disease is one important risk factor for BM, however, despite the long survival until development of BM, survival after diagnosis of BM was only a median of 2.9 months (*17,18*). Our data also shows lung metastases and rectal cancer were associated with BM, and the location of the primary tumor may have a close relationship with the target organ of metastasis (*2,19*). These can be explained in part by the vascular anatomy of the colon and rectum. The colon drains mostly through the portal vein to the liver and from there to the lung and other organs. The rectum drains both through the portal and the cava vein and more often seeds the lung before the liver, and consequently the brain (*20*). Univariate analysis and multivariate analysis of our study shows KPS > 70, and isolated BM were regarded as independent prognostic factors associated with good prognosis which is consistent with previous studies (*2,19*). Song found females may have a longer survival time than males (*2,19*). In our study we found a male predominance for patients with BM (65.00%), but the gender was not an independent factor for BM.

CRC metastatic to the brain is a highly lethal condition warranting effective intervention (*21*), whereas the standard treatment modality for BM from CRC has not been established. Usually CRC-BM have been regarded as a terminal event which limited the development of treatment for colorectal cancer brain metastasis (*22,23*). Previous views hold that blood-brain barrier is considered to prevent most chemotherapy drugs from entering the brain and result in failure of chemotherapy in treatment of BM. Conversely, Butowski maintained that biological characteristics of BM tissue and its permeability kept pace with the primary tumor, illustrating the absence of essential conditions to form the blood-brain barrier around metastatic lesions (*24*). Besides, imaging examination showed that contrast agents could rapidly enter the brain and enhanced metastatic lesions that indicate CRC metastatic to the brain may change permeability of the blood-brain barrier (*25*). Recently, some studies show BM patients may benefit from target therapy (*26,27*). Our data found median survival of patients who received bevacizumab were 7.6 months, longer than those who did not receive target therapy (5 months), indicating that antiangiogenic therapy might be of value for BM patients.

Neurosurgery and radiotherapy (*e.g*. WBRT and SRS) usually form the cornerstone of brain metastasis treatment (*17,18,28*). WBRT, the most common treatment options for BM patients in past decades, can palliate nervous system symptoms, reduce recurrence risk and improve prognosis (*29*). External radiotherapy is a realistic method for patients with multiple intracranial lesions, poor performance status, contraindications for neurosurgery and extensive extracranial disease (*30*). WBRT only for patients still had poor prognosis, with survival ranging from 2.2 months to 4 months (*31,32*). Neurosurgery was considered as effective therapy by some clinicians. However, the survival of patients treated with neurosurgery alone was only 9 months even in the situation of patients with selective bias (*33*). Until recently, multidisciplinary treatment has been widely used for colorectal cancer liver metastasis and lung metastasis, and significantly improved patient prognosis. Our study showed a median survival time of 4 months for patients who underwent monotherapy, while for patients receiving multidisciplinary treatment, the median survival time was extended to 11 months. Chemotherapy may increase radiosensitivity, and radiotherapy or surgery may also increase intracranial vascular permeability which is more conducive to drugs entering brain metastases (*26*), this may explain to some extent that combined therapy is better than single therapy. Although this improvement in survival was not as pronounced in patients with liver metastases or lung metastases from CRC, it also significantly improved the prognosis of patients with colorectal cancer BM.

Under the multidisciplinary treatment model, we further compared the results of different subgroup patients. We found that for patients with isolated metastases and better physical status (KPS > 70), neurosurgery combined with chemotherapy can get better results than radiotherapy combined with chemotherapy. More specifically, Patients with isolated brain metastases had a median survival of 17 months after neurosurgery combined with chemotherapy, while after radiotherapy combined with chemotherapy, the survival was 10 months ($P = 0.021$). Simultaneously, we observed similar survival improvements in patients with KPS > 70 ($P = 0.029$). On the other hand, for patients with multiple BM lesions or poor physical status (KPS ≤ 70), we did not find significant differences between two treatment groups. Our results indicate that in patients with isolated metastases and better physical status, neurosurgery with chemotherapy should be recommended. But for patients with multiple BM lesions or poor physical status, we think radiotherapy plus chemotherapy maybe more appropriate.

5. Conclusions

CRC metastatic to the brain is a highly lethal condition warranting effective interventions. Multidisciplinary treatment of colorectal cancer BM is the general

trend. For patients with isolated metastases and KPS > 70, neurosurgery combined with chemotherapy is recommended. For patients with multiple brain metastases or KPS ≤ 70, radiotherapy plus chemotherapy may be more acceptable.

Acknowledgements

The present study was supported by the National Natural Science Foundation of China (Grant No. 81502147), the second term "New Medical Talents of Zhejiang Province" project.

References

1. Cagney DN, Martin AM, Catalano PJ, Redig AJ, Lin NU, Lee EQ, Wen PY, Dunn IF, Bi WL, Weiss SE, Haas-Kogan DA, Alexander BM, Aizer AA. Incidence and prognosis of patients with brain metastases at diagnosis of systemic malignancy: A population-based study. Neuro-oncology. 2017; 19:1511-1521.
2. Song WG, Wang YF, Wang RL, Qu YE, Zhang Z, Li GZ, Xiao Y, Fang F, Chen H. Therapeutic regimens and prognostic factors of brain metastatic cancers. Asian Pac J Cancer Prev. 2013; 14:923-927.
3. Kin DY, Ryu CG, Jung EJ, Paik JH, Hwang DY. Brain metastasis from colorectal cancer: A single center experience. Ann Surg Treat Res. 2018; 94:13-18.
4. Tanriverdi O, Kanytan-saglan E, Ulger S, *et al*. The clinical and pathological features of 133 colorectal cancer patients with brain metastasis: A multicenter retrospective analysis of the Gastrointestinal Tumors Working Committee of the Turkish Oncology Group (TOG). Med Oncol. 2014; 31:152-161.
5. Smith TR, Lall RR, Lall RR, Abecassis IJ, Arnaout OM, Marymont MH, Swanson KR, Chandler JP. Survival after surgery and stereotactic radiosurgery for patients with multiple intracranial metastases: Results of a single-center retrospective study. J Neurosurg. 2014; 121:839-845
6. Fabi A, Felici A, Metro G, *et al*. Brain metastases from solid tumors: Disease outcome according to type of treatment and therapeutic resources of the treating center. J Exp Clin Cancer Res. 2011; 30:10-16.
7. Kye BH, Kim HJ, Kang WK, Cho HM, Hong YK, Oh ST. Brain metastases from colorectal cancer: The role of surgical resection in selected patients. Colorectal Dis. 2012; 14:e378-e385.
8. Gu XD, Cai YT, Zhou YM, Li ZY, Xiang JB, Chen ZY. Prognostic factors and multidisciplinary treatment modalities for brain metastases from colorectal cancer: Analysis of 93 patients. BMC Cancer. 2015; 15:902-907.
9. Adam R, Kitano Y. Multidisciplinary approach of liver metastases from colorectal cancer. Ann Gastroenterol Surg. 2019; 3:50-56.
10. Lai HW, Wei JC, Hung HC, Lin CC. Impact of treatment modality on clinical outcome in metastatic colorectal cancer patients stratified by metastatic sites. Postgrad Med. 2019; 133:163-170.
11. Ekici K, Temelli O, Dikilitas M, Halil Dursun I, Bozdag Kaplan N, Kekilli E. Survival and prognostic factors in patients with brain metastasis: Single center experience. J BUON. 2016; 21:958-963.
12. Christensen TD, Spindler KL, Palshof JA, Nielsen DL. Systematic review: Brain metastases from colorectal cancer--Incidence and patient characteristics. BMC Cancer. 2016; 16:260-273.
13. Esmaeilzadeh M, Majlesara A, Faridar A, Hafezi M, Hong B, Esmaeilnia-Shirvani H, Neyazi B, Mehrabi A, Nakamura M. Brain metastasis from gastrointestinal cancers: A systematic review. Int J Clin Pract. 2014; 68:890-899.
14. Munro A, Brown M, Niblock P, Steele R, Carey F. Do Multidisciplinary Team (MDT) processes influence survival in patients with colorectal cancer? A population-based experience. BMC Cancer. 2015; 15:686-694
15. Yu C, Pan D, Mi B, Xu Y, Lang L, Niu G, Yang M, Wan W, Chen X. 18F-Alfatide II PET/CT in healthy human volunteers and patients with brain metastases. Eur J Nucl Med Mol Imaging. 2015; 42:2021-2028.
16. Sundermeyer ML, Meropol NJ, Rogatko A, Wang H, Cohen SJ. Changing patterns of bone and brain metastases in patients with colorectal cancer. Clin Colorectal Cancer. 2005; 5:108-113.
17. Noura S, Ohue M, Shingai T, Fujiwara A, Imada S, Sueda T, Yamada T, Fujiwara Y, Ohigashi H, Yano M, Ishikawa O. Brain metastasis from colorectal cancer: Prognostic factors and survival. J Surg Oncol. 2012; 106:144-148.
18. Michl M, Thurmaier J, Schubert-Fritschle G, *et al*. Brain Metastasis in Colorectal Cancer Patients: Survival and Analysis of Prognostic Factors. Clin Colorectal Cancer. 2015; 14:281-290.
19. Schuttrumpf LH, Niyazi M, Nachbichler SB, Manapov F, Jansen N, Siefert A, Belka C. Prognostic factors for survival and radiation necrosis after stereotactic radiosurgery alone or in combination with whole brain radiation therapy for 1–3 cerebral metastases. Radiat Oncol. 2014; 9:105-112.
20. Magni E, Santoro L, Ravenda PS, Leonardi MC, Bonomo G, Monfardini L, Nole F, Zampino MG. Brain metastases from colorectal cancer: Main clinical factors conditioning outcome. Int J Colorectal Dis. 2014; 29:201-208.
21. Kruser TJ, Chao ST, Elson P, Barnett GH, Vogelbaum M, Toms S, Angelov L, Suh JH. Multidisciplinary Management of Colorectal Cancer Brain Metastases: A Retrospective Study. Cancer. 2008; 113:158-165.
22. Nieder C, Hintz M, Grosu AL. Colorectal cancer metastatic to the brain: Analysis of prognostic factors and impact of KRAS mutations on presentation and outcome. Clin Transl Oncol. 2016; 18:88-92.
23. Del Carpio Huerta L, Virgili Manrique AC, Szafranska J, Martin-Richard M, Paez Lopez-Bravo D, Sebio Garcia A, Espinosa Mariscal I, Gomila Pons P, Andres Granyo M, Barba Joaquin A, Barnadas Molins A, Tobena Puyal M. Brain metastases in colorectal cancer: Prognostic factors and survival analysis. Int J Colorectal Dis. 2018; 33:1-7.
24. Butowski N. Medical Management of Brain Metastases. Neurosurg. Clin. N. Am. 2011; 22:27-36.
25. Kekelidze M, D'Errico L, Pansini M, Tyndall A, Hohmann J. Colorectal cancer: Current imaging methods and future perspectives for the diagnosis, staging and therapeutic response evaluation. World J Gastroenterol. 2013; 19:8502-8514.
26. Taofeek K. Owonikoko, Jack Arbiser, *et al*.Current approaches to the treatment of metastatic brain tumours. Nat Rev Clin Oncol. 2014;11:203-222.
27. Berghoff AS, Preusser M. The future of targeted

therapies for brain metastases. Future Oncol. 2015; 11:2315-2327.
28. Mege D, Sans A, Ouaissi M, Iannelli A, Sielezneff I. Brain metastases from colorectal cancer: Characteristics and management. Anz J Surg. 2017; 88:140-145.
29. Lamba N, Muskens IS, Dirisio AC, Meijer L, Briceno V, Edrees H, Aslam B, Minhas S, Verhoeff JJC, Kleynen CE, Smith TR, Mekary RA, Broekman ML. Stereotactic radiosurgery versus whole-brain radiotherapy after intracranial metastasis resection: A systematic review and meta-analysis. Radiat Oncol. 2017; 12:106-117.
30. Heisterkamp C, Haatanen T, Schild SE, Rades D. Dose Escalation in Patients Receiving Whole-Brain Radiotherapy for Brain Metastases from Colorectal Cancer. Strahlenther Onkol. 2010; 186:70-75.
31. Jung M, Ahn JB, Chang JH, Suh CO, Hong S, Roh JK, Shin SJ, Rha SY. Brain metastases from colorectal carcinoma: Prognostic factors and outcome. J Neurooncol. 2011; 101:49-55.
32. Lemke J, Scheele J, Kapapa T, von Karstedt S, Wirtz CR, Henne-Bruns D, Kornmann M. Brain metastases in gastrointestinal cancers: Is there a role for surgery? Int J Mol Sci. 2014; 15:16816-16830.
33. Damiens K, Ayoub JP, Lemieux B, Aubin F, Saliba W, Campeau MP, Tehfe M. Clinical features and course of brain metastases in colorectal cancer: An experience from a single institution. Curr Oncol. 2012; 19:254-258.

(Received February 23, 2019; Revised April 13, 2019; Accepted April 24, 2019)

Original Article

DOI: 10.5582/bst.2019.01072

A selective oral vasopressin V2-receptor antagonist for patients with end-stage liver disease awaiting liver transplantation: a preliminary study

Sho Kiritani[1], Junichi Kaneko[1], Yoichi Miyata[1], Masaru Matsumura[1], Nobuhisa Akamatsu[1], Takeaki Ishizawa[1], Junichi Arita[1], Sumihito Tamura[1], Norihiro Kokudo[2], Kiyoshi Hasegawa[1,*]

[1] *Hepato-Biliary-Pancreatic Surgery Division, and Artificial Organ and Transplantation Division, Department of Surgery, Graduate School of Medicine, The University of Tokyo, Tokyo, Japan;*
[2] *National Center for Global Health and Medicine, Tokyo, Japan.*

Summary **Administration of the selective arginine vasopressin V2 receptor antagonist tolvaptan to cirrhotic patients is controversial. There are no reports of tolvaptan use for patients with far-advanced end-stage liver disease (ESLD) and refractory ascites awaiting liver transplantation. Between 2013 and 2016, 64 patients awaiting adult-to-adult living donor liver transplantation (LDLT) were screened for enrollment. Patients with refractory ascites and on dual conventional diuretics (≥ 50 mg/day of spironolactone and ≥ 20 mg/day of a loop diuretic) were enrolled and assigned to the tolvaptan (TOL) group (n = 10), and low-dose tolvaptan, 3.75 mg/day, was started. The remaining patients who had no or little ascites on conventional diuretic therapy (CDT) were assigned to the CDT group (n = 23). The median model for end-stage liver disease and Child-Pugh scores were 16 (range 7-41) and 10 (7-15), respectively. The median dose of spironolactone in the TOL group was 88 mg (range 50-200) *vs*. 50 (0-100) in the CDT group ($p < 0.01$). The median dose of loop diuretics in the TOL group was 70 mg (20-120) *vs*. 20 (0-80) in the CDT group ($p = 0.03$). No significant liver damage was detected during tolvaptan therapy. Tolvaptan demonstrated favorable effects in 60% (6/10) of the patients, decreasing the body weight by at least 1.5 kg during the 7 day treatment. These findings suggest that low-dose of tolvaptan may be safe for patients having far-advanced ESLD patients with apparent and refractory ascites taking dual conventional diuretics for a short period before LDLT.**

Keywords: Tolvaptan, liver transplantation, end-stage liver disease

1. Introduction

Liver transplantation is a definitive treatment option for patients with end-stage liver disease (ESLD). A potentially serious major complication of cirrhosis is ascites, which occurs in 50% of patients over a 10-year observation period (*1*) and in approximately 90% of patients with ESLD (*2*). Management of ascites related to ESLD is a major challenge during the waiting period for liver transplantation.

Spironolactone and loop diuretics are key drugs used to manage cirrhotic patients with ascites (*3,4*). A new, recently approved diuretic, the selective arginine vasopressin V2 receptor antagonist tolvaptan, which acts at the V2 receptors in the renal collecting duct to inhibit water resorption, increases urine output volume, decreases body weight, increases serum sodium values (*5*), and helps to maintain renal function in patients with liver cirrhosis and ascites (*6,7*).

Tolvaptan was approved in the United States in 2009 for use in patients with hyponatremia due to heart failure, syndrome of inappropriate antidiuretic hormone secretion, and liver cirrhosis. In a randomized

Released online in J-STAGE as advance publication April 24, 2019.

*Address correspondence to:
Dr. Kiyoshi Hasegawa, Hepato-Biliary-Pancreatic Surgery Division, and Artificial Organ and Transplantation Division, Department of Surgery, Graduate School of Medicine, The University of Tokyo, 7-3-1 Hongo, Bunkyo-ku, Tokyo 113-8655, Japan.
E-mail: kihase-tky@umin.ac.jp

controlled trial of tolvaptan for patients with autosomal dominant polycystic kidney disease, however, 1.2% of patients in the tolvaptan group discontinued the trial due to liver-function abnormalities (*8*). In 2013, the United States Food and Drug Administration raised concerns regarding the potential risk of liver injury in patients taking tolvaptan (*9*). Therefore, tolvaptan is not yet approved for patients with liver cirrhosis in the United States. Sakaida and colleagues reported favorable results of a clinical trial of low-dose tolvaptan in cirrhotic patients with ascites without liver injury (*10*) , leading to its approval for cirrhotic patients by the Ministry of Health, Labour, and Welfare in Japan in 2013. A recent post-marketing surveillance report showed encouraging results for ascites control; three patients (0.7%, 3/473) had liver failure, however, and discontinued treatment.

Worldwide, tolvaptan administration for cirrhotic patients remains controversial. Currently, the American Association for the Study of Liver Diseases does not recommend tolvaptan for patients with cirrhosis (*11,12*). The clinical practice guidelines of the European Association for the Study of the Liver mention tolvaptan and its expected effects for cirrhotic patients with ascites and severe hypervolemic hyponatremia (*13*).

Despite the increasing number of studies of tolvaptan for patients with cirrhosis, there are no reports of tolvaptan for far-advanced ESLD patients with refractory ascites awaiting liver transplantation. In this preliminary study, we report the short-term results of tolvaptan use for patients scheduled to undergo living donor liver transplantation (LDLT).

2. Methods

Between May 2013 and January 2016, 64 consecutive adult-to-adult LDLTs were performed at the Tokyo University Hospital. The present preliminary, prospective study protocol was approved by the University of Tokyo Ethics Committee. The protocol was registered to the clinical trials registry managed by the university hospital medical information network in Japan (UMIN000027096, *http://www.umin.ac.jp/ctr/index.htm*).

Inclusion criteria were as follows: over 18 years of age, cirrhotic patients awaiting adult-to-adult LDLT, refractory ascites (*14*), and taking dual conventional diuretics (≥ 50 mg/day of spironolactone and ≥ 20 mg/day of a loop diuretic). The patients were enrolled and assigned to the tolvaptan (TOL) group during the preoperative evaluation period. The remaining patients who had no or little ascites on conventional diuretic therapy (CDT) were assigned to the CDT group, and the pre-and postoperative factors were compared between the TOL and CDT groups. Exclusion criteria were no apparent ascites without diuretics, patient already on tolvaptan, and acute liver failure. Preoperative factors, including Child-Pugh score, model for end-stage liver disease (MELD) score, total bilirubin, prothrombin time-international normalized ratio (PT-INR), serum creatinine, aspartate aminotransferase, alanine aminotransferase, serum albumin, serum sodium, and platelet counts, were recorded. Operation time, estimated blood loss, actual amount of ascites (all ascites was drained and measured just after starting the operation), amount of blood transfused, and Clavien-Dindo classification were compared between the TOL and CDT groups. Informed consent was obtained from all recipients.

In the TOL group, low-dose tolvaptan (Samsca; Otsuka Pharmaceutical Co., Ltd., Tokyo, Japan), 3.75 mg /day, was started. The dose was based on half the starting dose and clinical trial recommendation for hepatic edema (*10*) and the Japanese guidelines (*15*). If the patient's symptoms did not improve, the dose was increased to 7.5 mg. Tolvaptan administration was continued until the day before LDLT and discontinued immediately after LDLT. Body weight, daily urine output volume, total bilirubin, serum albumin, serum creatinine, sodium levels, PT-INR, Child-Pugh score, and MELD score were monitored on days 0, 1, 3, 7 after tolvaptan initiation. The serum creatinine level was also monitored on days 0, 1, 3, 7, and 30 after LDLT.

The primary endpoint was change in body weight: a 1.5-kg decrease from baseline to 7 days after tolvaptan initiation. The secondary endpoints were urine output volume on days 1, 3 and 7; whether or not the urine output volume was greater than that before tolvaptan initiation; and use of additional diuretics other than tolvaptan. Liver damage was defined as a two-fold increase in the levels of aspartate aminotransferase and alanine aminotransferase compared with the levels before tolvaptan initiation. Patients for whom tolvaptan was effective, defined as a greater than 1.5-kg decrease in body weight during the 7 days after tolvaptan initiation, were classified into the tolvaptan-effective group. The remaining patients were classified into the tolvaptan-ineffective group. Preoperative and postoperative factors were compared between the groups.

Statistical analysis The Mann-Whitney *U* test was used to compare the patient characteristics between groups. After tolvaptan initiation, variables were compared by the Wilcoxon signed-rank test. Changes in body weight and daily urine output volume in both groups were compared by two-way repeated measures analysis of variance using the JMP pro 12.2 statistical software package (SAS Institute Inc., Cary, NC, USA). Data are expressed as median and range. A $p < 0.05$ was considered statistically significant.

3. Results

A total of 64 patients were screened for enrollment. Of the 64, 31 patients were excluded from the study

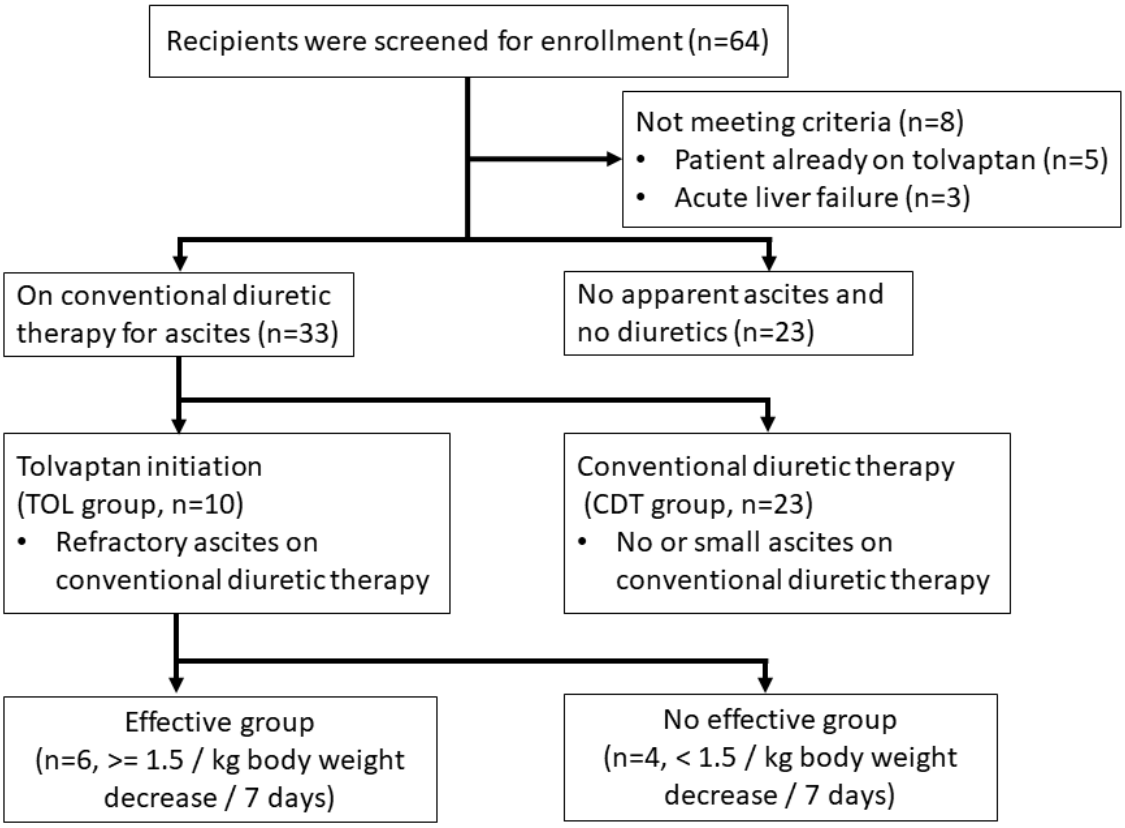

Figure 1. Flow chart summarizing subject enrollment for the present study.

because they did not meet the criteria, including no apparent ascites and no diuretics (n = 23), currently on tolvaptan prescribed during a previous hospital visit (n = 5), and acute liver failure (n = 3). Ten patients were assigned to the TOL group and tolvaptan was started. The remaining 23 patients, having no or little ascites on CDT, were assigned to the CDT group (Figure 1).

The subjects comprised 18 men and 15 women with a median age of 50 (range 18-67) years. Indications for transplantation included hepatitis B or C-related cirrhosis (n = 14), primary biliary cirrhosis (n = 6), alcoholic liver cirrhosis (n = 3), cryptogenic liver cirrhosis (n = 3), Budd-Chiari syndrome (n = 3), primary sclerosing cholangitis (n = 2), non-alcoholic steatohepatitis (n = 1), and Wilson's disease (n = 1). The median MELD and Child-Pugh scores were 16 (range 7-41) and 10 (7-15), respectively.

Characteristics of patients in the TOL and CDT groups are shown in Table 1. There was no significant difference between groups with respect to the Child-Pugh score, MELD score, total bilirubin, PT-INR, and serum creatinine, serum alanine transaminase, serum aspartate transaminase, or serum albumin levels. The median serum sodium concentration differed significantly between the TOL and CDT groups (130 mmol/L [122-139] *vs*. 136 [131-140], $p < 0.01$). The median dose of spironolactone in the TOL group was 88 mg (range 50-200) *vs*. 50 (0-100) in the CDT group ($p < 0.01$). The median dose of loop diuretics in the TOL group was 70 mg (20-120) *vs*. 20 (0-80) in the CDT group ($p = 0.03$).

In the TOL group, the median tolvaptan administration period was 18 (range 7-16) days before LDLT. Tolvaptan administration could continue for all patients. Changes in body weight, daily urine output volume, serum sodium concentration, and MELD score are shown in Figures 2A-D. The TOL and CDT groups differed significantly with respect to body weight between preadministration and 1 day after tolvaptan initiation (-1.1 kg, p = 0.02, 2A) and in daily urine output volume between preadministration (1475 mL/day) and 7 days (2675 mL/day, $p < 0.01$, 2B) after tolvaptan initiation. The change in the serum sodium concentration was not significant between preadministration and 1, 3, and 7 days after tolvaptan initiation (Figure 2C). The MELD score was relatively stable during the 7 days of treatment (Figure 2D). The change in the serum creatinine level was not significant between preadministration and 1, 3, and 7 days after tolvaptan initiation (Figure 2E). The remaining factors, including serum albumin level, PT-INR, and Child-Pugh score, did not change during the 7 days of treatment (data not shown).

The changes in the serum aspartate transaminase and alanine transaminase levels in the TOL group are shown in Figure 3. The median serum aspartate transaminase and alanine transaminase levels preadministration and 7 days after tolvaptan initiation were 57.5 and 58.0 U/L,

Table 1. Characteristics of patients in the tolvaptan (TOL) and conventional diuretic therapy (CDT) groups

Patient characteristics	TOL (n = 10)	CDT (n = 23)	P value
Age	58 (41-64)	57 (23-67)	0.75
Male/female	4/6	14/9	0.45
Liver disease			
Hepatitis B or C	2	12	0.09
Primary biliary cirrhosis	3	3	0.25
Alcoholic	1	2	0.9
Cryptogenic	2	1	0.15
Budd-Chiari syndrome	0	3	0.23
Primary sclerosing cholangitis	1	1	0.53
Non-alcoholic steatohepatitis	1	0	0.12
Wilson's disease	0	1	0.50
Preoperative factors			
Child-Pugh score	11 (8-13)	10 (8-13)	0.13
Model for end-stage liver disease score	16 (10-21)	14 (8-13)	1.00
Total bilirubin (mg/dL)	5.2 (1.7-19.3)	4.1 (0.8-27.1)	0.43
Prothrombin time-international normalized ratio	1.32 (1.15-1.78)	1.37 (1.12-1.92)	0.78
Serum creatinine (mg/dL)	0.83 (0.50-1.62)	0.75 (0.54-1.33)	0.35
Alanine transaminase (U/L)	58 (29-173)	49 (9-163)	0.47
Aspartate transaminase (U/L)	28 (12-63)	31 (6-89)	0.84
Serum albumin (g/dL)	2.9 (2.4-3.6)	2.7 (2.0-3.6)	0.13
Serum sodium (mEq/L)	130 (122-139)	136 (131-140)	< 0.01*
Platelet count (*10^4μL)	7.1 (4.0-32.2)	7.7 (2.6-18.5)	0.67
Conventional diuretics			
Spironolactone (mg)	88 (50-200)	50 (0-100)	< 0.01*
Loop diuretics (mg)	70 (20-120)	20 (0-80)	0.03*

The median serum sodium concentration differed significantly between the TOL and CDT groups (130 mmol/L [range 122-139] *vs*. 136 [131-140], $p < 0.01$). The dose of spironolactone was 88 mg (50-200) in the TOL group *vs*. 50 (0-100) in the CDT group ($p < 0.01$). The dose of loop diuretics was 70 mg (20-120) in the TOL group *vs*. 20 (0-80) in the CDT group ($p < 0.05$).

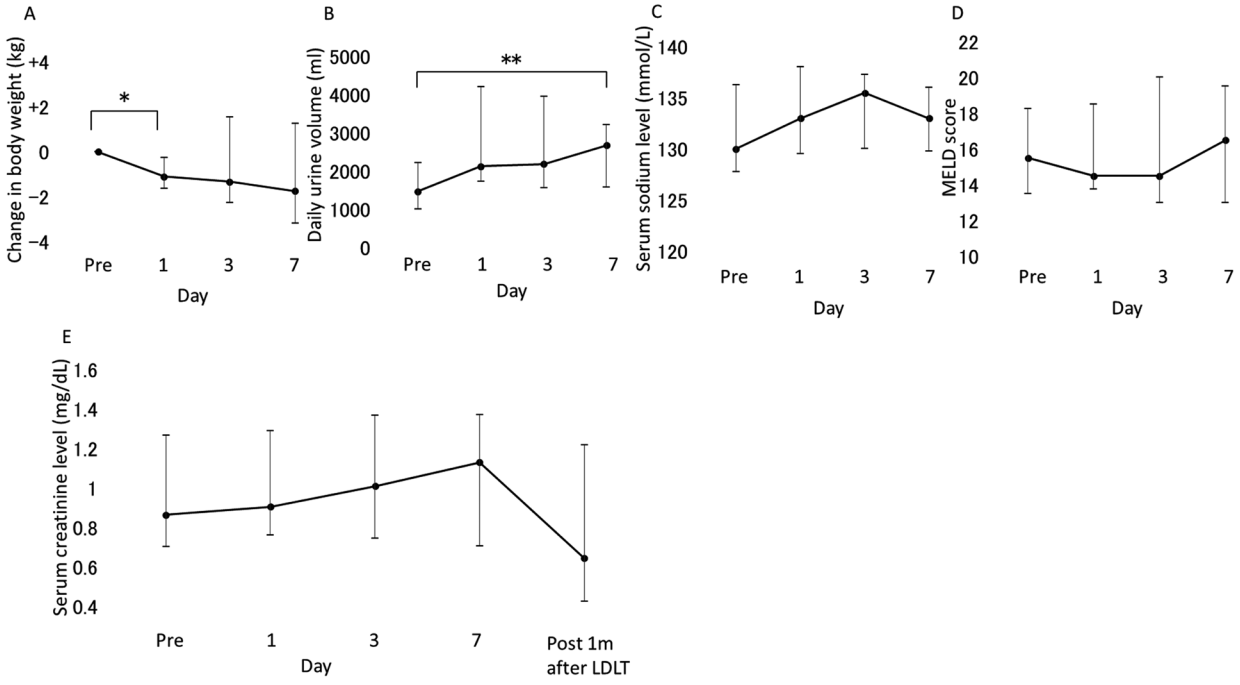

Figure 2. Changes in body weight (A), daily urine output volume (B), serum sodium concentration (C), model for end-stage liver disease (MELD) score (D) , and serum creatinine level (E) in the tolvaptan (TOL) group are shown. The groups differed significantly with respect to body weight between preadministration and 1 day after tolvaptan initiation (-1.1 kg, $p = 0.02$, **A**) and daily urine volume between preadministration and 7 days after tolvaptan initiation (1475 mL/day *vs*. 2675 mL/day, $p < 0.01$, **B**). The serum sodium concentration increased up to day 3, but the difference was not significant (**C**). The MELD score remained relatively stable over the 7 days (**D**). The serum creatinine level gradually increased up to day 7 and decreased within 1 month after LDLT. The difference, however, was not significant (**E**).

28 and 32 U/L, respectively. There was no significant difference between these values (Figure 3A, $p = 1.00$ and Figure 3B, $p = 0.89$) and no two-fold increase in the values.

A 1.5-kg body weight decrease during the 7 days of tolvaptan administration occurred in 60% (6/10) of the TOL patients in whom the drug was considered effective. The body weight did not decrease in 40% (4/10) of the TOL patients in whom the drug was considered ineffective. The median Child-Pugh score in the tolvaptan-effective and tolvaptan-ineffective groups was 10.5 (8-11) and 12.5 (11-13), respectively ($p < 0.01$; Table 2). The amount of ascites in the tolvaptan-effective and tolvaptan-ineffective groups was 1,450 mL (500-4,100) and 7,050 mL (4,000-13,550), respectively ($p = 0.04$). There were no significant differences between groups in the other related factors (Table 3). The change in body weight differed significantly ($p < 0.01$) between groups (Figure 4A). The groups did not differ significantly in the change in the daily urine output volume ($p = 0.88$, Figure 4B).

Operative factors of the TOL and CDT groups are shown in Table 3. The median amount of ascites was higher in the TOL group (3,450 mL [500-13,550]) than in the CDT group (250 mL [0-4,750], $p < 0.01$). There were no significant differences between groups in operation time, estimated blood loss, blood transfusion, or Clavien-Dindo classification. Changes in serum creatinine levels were not significant between preadministration of tolvaptan and 1 month after liver transplantation.

4. Discussion

The findings of this preliminary study demonstrated the safety of a low dose of tolvaptan for far-advanced ESLD patients with apparent and refractory ascites taking dual conventional diuretics for a short period before LDLT. Tolvaptan administration could be

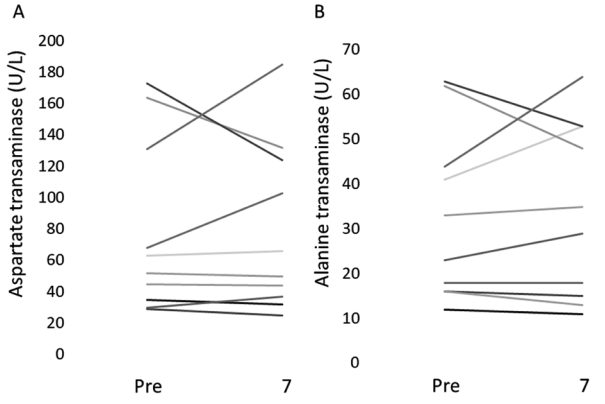

Figure 3. Changes in the serum aspartate transaminase (A) and alanine transaminase (B) levels in the tolvaptan (TOL) group are shown. There was no significant difference between preadministration and tolvaptan initiation ($p = 1.00$ and $p = 0.89$), and no 2-fold increase in the serum aspartate transaminase and serum alanine transaminase levels.

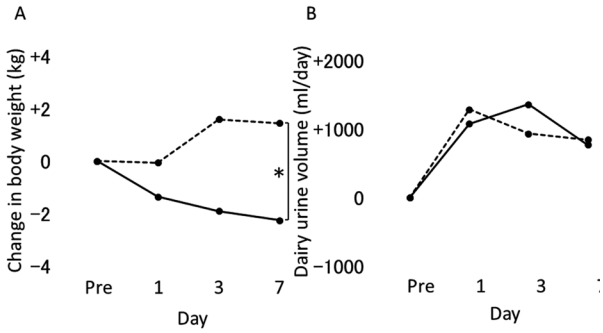

Figure 4. (A) Change in body weight in both groups. There was a significant difference between groups ($p < 0.01$). (B) Change in daily urine output volume in both groups. There was no significant difference between groups ($p = 0.88$).

Table 2. Tolvaptan was considered effective in 60% (6/10) of the patients

Relative factors	Effective ($n = 6$)	No effective ($n = 4$)	P value
Child-Pugh score	10.5 (8-11)	12.5 (11-13)	< 0.01*
Model for end-stage liver disease score	14.5 (10-19)	17 (14-21)	0.24
Total bilirubin (mg/dL)	3.7 (1.7-19.3)	7.9 (4.3-14.4)	0.39
Prothrombin time-international normalized ratio	1.20 (1.15-1.63)	1.59 (1.26-1.78)	0.05
Serum creatinine (mg/dL)	1.01 (0.50-1.62)	0.76 (0.75-0.98)	0.52
Serum sodium (mEq/L)	135 (122-139)	129 (127-131)	0.16
Operative factors			
Operation time (min)	657 (634-854)	639 (584-732)	0.39
Estimated blood loss (mL)	4,323 (1,640-6,690)	6,565 (4,770-7,740)	0.10
Amount of ascites (mL)	1,450 (500-4,100)	7,050 (4,000-13,550)	0.04*
Blood transfusion			
Red blood cells (unit)	8 (4-14)	10 (8-20)	0.26
Fresh frozen plasma (unit)	16 (12-28)	12 (12-28)	0.60
Platelet concentrate (unit)	15 (10-20)	20 (10-40)	0.61
Clavien-Dindo classification (> III)	3	4	0.09

The median Child-Pugh score in the tolvaptan-effective and tolvaptan-ineffective groups was 10.5 (range 8-11) and 12.5 (11-13), respectively ($p < 0.01$). The median amount of ascites in the tolvaptan-effective and tolvaptan-ineffective groups was 1,450 mL (500-4,100) and 7,050 mL (4,000-13,550), respectively ($p = 0.03$).

Table 3. Operative factors in the tolvaptan (TOL) and conventional diuretic therapy (CDT) groups

Operative factors	TOL (n = 10)	CDT (n = 23)	P value
Operation time (min)	657 (584-854)	697 (605-949)	0.18
Estimated blood loss (mL)	5,660 (1,640-7,740)	3,530 (1,520-13,520)	0.08
Amount of ascites (mL)	3,450 (500-13,550)	250 (0-4,750)	< 0.01*
Blood transfusion			
Red blood cells (unit)	10 (4-20)	6 (0-28)	0.20
Fresh frozen plasma (unit)	14 (12-28)	14 (8-28)	0.46
Platelet concentrate (unit)	20 (10-40)	20 (0-40)	0.61
Clavien-Dindo classification (>III)	6	12	0.40
Clavien-Dindo classification V	0	1	0.50

The median amount of ascites was significantly higher in the TOL group (3450 mL, range 500-13,550 than in the CDT group (250 mL, range 0-4,750; $p < 0.01$).

continued for all patients without a significant change in liver function, and discontinued immediately after LDLT without affecting renal function. Tolvaptan demonstrated favorable effects in 60% (6/10) of the patients, decreasing the body weight by at least 1.5 kg during the 7 day treatment.

Ascites is a crucial manifestation that occurs as a result of portal hypertension, the most common manifestation of decompensated cirrhosis and usually considered an important first sign (*16*). Proper treatment of ascites is thought to relate to an overall better outcome by reducing the likelihood of renal and electrolyte complications, decreasing hospital admissions, and providing a better quality of life for ESLD patients (*17*). Somsouk and colleagues reported that among patients awaiting liver transplantation, those with moderate ascites had a significantly higher mortality rate than those with little or no ascites (*18*). D'Amico and colleagues reported that mortality increases from 3% to 20% per year in the presence of ascites, and 5% to 7% of patients with compensated cirrhosis annually progress to a decompensated status (*19*). Ascites control is important for the management of ESLD patients awaiting liver transplantation.

To control ascites, spironolactone, an aldosterone antagonist, is started either alone or in combination with a loop diuretic, furosemide. Nevertheless, ascites may become refractory before LDLT. The International Ascites Club defines refractory ascites as ascites that cannot be mobilized or recurs early and cannot be satisfactorily prevented by medical therapy (*14*). Therapeutic abdominal paracentesis and a transjugular intrahepatic portosystemic shunt are recommended when these diuretics are not sufficiently effective or are poorly tolerated (*3*), but post-paracentesis circulatory dysfunction is a critical side effect (*20*). Tolvaptan, a new diuretic with a different mechanism of action (*5*), may have a role in the treatment of ESLD patients with refractory ascites who are on the waiting list for liver transplantation, but there have been no reports. The present study is the first report of the use of tolvaptan for ESLD patients awaiting liver transplantation.

Severe liver dysfunction is reported to be an adverse effect of tolvaptan (*12,21*). Safety remains a concern. According to one report published in 2015, tolvaptan was evaluated in a clinical trial of autosomal dominant polycystic kidney disease patients. A total of 1,445 subjects were randomized 2:1 (tolvaptan vs. placebo) (*12*). Significant increases in serum aminotransferase were detected in 16 patients on tolvaptan and in only 1 on placebo. The onset of hepatocellular injury occurred between 3 and 18 months after starting tolvaptan and gradually improved over the subsequent 1 to 4 months. Although hepatocellular injury was infrequent and reversible, there is a potential for serious irreversible injury. The authors recommended that transaminase levels be monitored regularly (*12*). Notably, however, in their study, the dose of tolvaptan was high, 60 mg to 120 mg/day. In the present study, a low dose tolvaptan was administered without significant alterations in liver function. The dose used in the present study was selected on the basis of a tolvaptan phase III trial in Japan (*10*).

In a Japanese clinical trial of cirrhotic patients, a dose of tolvaptan of 7.5 to 15 mg/day was selected as the optimal dose for liver cirrhosis patients (*22*). The details of that study are unknown, but there was no tolvaptan withdrawal from the study due to aminotransferase elevation and/or hepatocellular injury. In the present study, we selected a dose of 3.75 to 7.5 mg/day. No significant liver damage was detected during close follow-up after the initiation of tolvaptan therapy before liver transplantation. Thus, a low dose of tolvaptan may be safe for ESLD patients for a short period before LDLT.

In the non-transplant setting, a similar targeted patient population was reported (*23*). According to a report of post-marketing surveillance of tolvaptan for cirrhotic patients with edema or ascites, the mean decrease in body weight from baseline was -2.4 kg on day 7 (*23*). Surveillance focused on patients with better liver function. In their report, half of the cohort was classified as Child-Pugh A to B and the remaining patients were classified as Child-Pugh C. The total bilirubin level and mean platelet count were 2.4 mg/dl and 12.1 × 10^4 μL, resepctively. In the present

study, patients had far-advanced liver function. The median Child-Pugh score, total bilirubin level, and platelet count were 11, 5.2 mg/dL, and 7.1×10^4 μL, respectively. In the surveillance report, many details of changes in liver function remained to be clarified. The present study is the first to detail the changes in liver function during tolvaptan administration. Further studies are needed to clarify the effects of longer term use of tolvaptan in those patients.

On the basis of previous reports, we defined the tolvaptan-effective group as those patients on tolvaptan who lost more than 1.5 kg body weight within 7 days (*22*). Patients in the tolvaptan-ineffective group showed an increase in body weight despite an increase in the daily urine output volume. Although a low dose of tolvaptan was used, thirst was another problem for those in the tolvaptan-ineffective group, which led to difficulties in controlling their body weight. In the present study, the median Child-Pugh score of the tolvaptan-effective group was lower than that in the tolvaptan-ineffective group (10.5 *vs*. 12.5). The small number of patients and short administration period are limitations of the present study. In addition, the disease severity of patients in the TOL and CDT groups differed, resulting in a selection bias. Further, because the cohort size was not sufficient, there was also a statistical bias. The Child-Pugh score may be useful for selecting patients for tolvaptan administration, but studies of a larger patient cohort are needed to confirm this speculation. The findings of the present study demonstrate that tolvaptan administration may be a promising strategy for ESLD patients awaiting liver transplantation, but further evaluation is necessary.

In conclusion, administration of a low dose of tolvaptan may be safe for far-advanced ESLD patients for a short period before LDLT.

References

1. Gines P, Quintero E, Arroyo V, Teres J, Bruguera M, Rimola A, Caballeria J, Rodes J, Rozman C. Compensated cirrhosis: natural history and prognostic factors. Hepatology. 1987; 7:122-128.
2. Potts JR, Goubet S, Heneghan MA, Verma S. Determinants of long-term outcome in severe alcoholic hepatitis. Aliment Pharmacol Ther. 2013; 38:584-595.
3. Moore KP, Aithal GP. Guidelines on the management of ascites in cirrhosis. Gut. 2006; 55 Suppl 6:vi1-12.
4. Angeli P, Ginès P, Wong F, *et al*. Diagnosis and management of acute kidney injury in patients with cirrhosis: revised consensus recommendations of the International Club of Ascites. Gut. 2015; 64:531-537.
5. Decaux G, Soupart A, Vassart G. Non-peptide arginine-vasopressin antagonists: The vaptans. Lancet. 2008; 371:1624-1632.
6. Sakaida I, Yanase M, Kobayashi Y, Yasutake T, Okada M, Okita K; ASCITES Clinical Pharmacology Group. The pharmacokinetics and pharmacodynamics of tolvaptan in patients with liver cirrhosis with insufficient response to conventional diuretics: a multicentre, double-blind, parallel-group, phase III study. J Int Med Res. 2012; 40:2381-2393.
7. Okita K, Kawazoe S, Hasebe C, Kajimura K, Kaneko A, Okada M, Sakaida I; ASCITES Dose-Finding Trial Group. Dose-finding trial of tolvaptan in liver cirrhosis patients with hepatic edema: A randomized, double-blind, placebo-controlled trial. Hepatol Res. 2014; 44:83-91.
8. Torres VE, Chapman AB, Devuyst O, Gansevoort RT, Grantham JJ, Higashihara E, Perrone RD, Krasa HB, Ouyang J, Czerwiec FS. Tolvaptan in patients with autosomal dominant polycystic kidney disease. N Engl J Med. 2012; 367:2407-2418.
9. FDA limits duration and usage of Samsca (tolvaptan) due to possible liver injury leading to organ transplant or death. *https://www.fda.gov/Drugs/DrugSafety/ucm350062.htm* (accessd April 14, 2019)
10. Sakaida I, Kawazoe S, Kajimura K, Saito T, Okuse C, Takaguchi K, Okada M, Okita K; ASCITES-DOUBLEBLIND Study Group. Tolvaptan for improvement of hepatic edema: A phase 3, multicenter, randomized, double-blind, placebo-controlled trial. Hepatol Res. 2014; 44:73-82.
11. Runyon BA, AASLD. Introduction to the revised American Association for the Study of Liver Diseases Practice Guideline management of adult patients with ascites due to cirrhosis 2012. Hepatology. 2013; 57:1651-1653.
12. Watkins PB, Lewis JH, Kaplowitz N, Alpers DH, Blais JD, Smotzer DM, Krasa H, Ouyang J, Torres VE, Czerwiec FS, Zimmer CA. Clinical pattern of tolvaptan-associated liver injury in subjects with autosomal dominant polycystic kidney disease: Analysis of clinical trials database. Drug Saf. 2015; 38:1103-1113.
13. EASL clinical practice guidelines on the management of ascites, spontaneous bacterial peritonitis, and hepatorenal syndrome in cirrhosis. J Hepatol. 2010; 53:397-417.
14. Arroyo V, Gines P, Gerbes AL, Dudley FJ, Gentilini P, Laffi G, Reynolds TB, Ring-Larsen H, Scholmerich J. Definition and diagnostic criteria of refractory ascites and hepatorenal syndrome in cirrhosis. International Ascites Club. Hepatology. 1996; 23:164-176.
15. Fukui H, Saito H, Ueno Y, *et al*. Evidence-based clinical practice guidelines for liver cirrhosis 2015. J Gastroenterol. 2016; 51:629-650.
16. D'Amico G, Morabito A, Pagliaro L, Marubini E. Survival and prognostic indicators in compensated and decompensated cirrhosis. Dig Dis Sci. 1986; 31:468-475.
17. Cardenas A, Gines P. Management of patients with cirrhosis awaiting liver transplantation. Gut. 2011; 60:412-421.
18. Somsouk M, Kornfield R, Vittinghoff E, Inadomi JM, Biggins SW. Moderate ascites identifies patients with low model for end-stage liver disease scores awaiting liver transplantation who have a high mortality risk. Liver Transpl. 2011; 17:129-136.
19. D'Amico G, Garcia-Tsao G, Pagliaro L. Natural history and prognostic indicators of survival in cirrhosis: A systematic review of 118 studies. J Hepatol. 2006; 44:217-231.
20. Panos MZ, Moore K, Vlavianos P, Chambers JB, Anderson JV, Gimson AE, Slater JD, Rees LH, Westaby D, Williams R. Single, total paracentesis for tense ascites: sequential hemodynamic changes and right atrial

size. Hepatology. 1990; 11:662-667.
21. Hirai K, Shimomura T, Moriwaki H, Ishii H, Shimoshikiryo T, Tsuji D, Inoue K, Kadoiri T, Itoh K. Risk factors for hypernatremia in patients with short- and long-term tolvaptan treatment. Eur J Clin Pharmacol. 2016; 72:1177-1183.
22. Sakaida I, Yamashita S, Kobayashi T, Komatsu M, Sakai T, Komorizono Y, Okada M, Okita K. Efficacy and safety of a 14-day administration of tolvaptan in the treatment of patients with ascites in hepatic oedema. J Int Med Res. 2013; 41:835-847.
23. Sakaida I, Terai S, Kurosaki M, Yasuda M, Okada M, Bando K, Fukuta Y. Effectiveness and safety of tolvaptan in liver cirrhosis patients with edema: Interim results of post-marketing surveillance of tolvaptan in liver cirrhosis (START study). Hepatol Res. 2017; 47:1137-1146.

(Received March 18, 2019; Revised April 18, 2019; Accepted April 20, 2019)

Brief Report

DOI: 10.5582/bst.2019.01055

Design, synthesis and biological evaluation of 4-piperidin-4-yl-triazole derivatives as novel histone deacetylase inhibitors

He Miao[1,2,§], Jianjun Gao[2,§], Zishuo Mou[2], Baolei Wang[2], Li Zhang[1], Li Su[1], Yantao Han[3,*], Yepeng Luan[1,*]

[1] *Department of Medicinal Chemistry, School of Pharmacy, Qingdao University, Qingdao, Shandong, China;*
[2] *Department of Pharmacology, School of Pharmacy, Qingdao University, Qingdao, Shandong, China;*
[3] *Department of Pharmacology, College of Basic Medicine, Qingdao University, Qingdao, Shandong, China.*

Summary **Histone deacetylase is an important member of epigenetics and a well validated target for anti-cancer drug discovery. In this study, we designed and synthesized a series of twenty-one novel hydroxamic acid-based histone deacetylase inhibitors with 4-piperidin-4-yl-triazole as the core skeleton. Most target compounds displayed excellent inhibition rates toward histone deacetylases at the concentration of 1 μM. Among them, the inhibition rates of two compounds MH1-18 and MH1-21 exceeded 90%. Furthermore, these two compounds selectively inhibited the activity of histone deacetylase 6 with low IC_{50} values. The high potency of them toward histone deacetylase 6 was rationalized by molecular docking studies. We found that MH1-18 and MH1-21 moderately inhibited the proliferation of four human cancer cell lines SGC-7901, NCI-H226, MCF-7, and HL-60. However, MH1-21 showed potent efficacy in suppressing the migration of MCF-7 cells. Results obtained in the current study shed light on designing potent HDAC6 inhibitors as anti-cancer agents.**

Keywords: Histone deacetylase, isoform, selective, inhibitor, anti-tumor

1. Introduction

Acetylation as one of the most important covalent modification manners in the field of epigenetics, the level of it is taken control of by two families of enzymes with opposite mechanisms, histone acetyltransferases (HATs) and histone deacetylases (HDACs). HDACs are responsible for removal of the acetyl group from lysine residues in histones and non-histone substrates (*1*). Till now, 18 isoforms of HDACs have been discovered, and they are divided into four categories based on their sequence similarity and functions: class I (HDAC1, 2, 3 and 8), class II (class IIa (HDAC4, 5, 7 and 9) and class IIb (HDAC6 and 10)) and class IV (HDAC11) are all zinc-dependent HDACs, while class III HDACs are NAD^+-dependent (*2-4*). Studies demonstrated that HDACs are key enzymes regulating important cell processes such as cell-cycle progression and apoptosis (*2-4*).

Overexpression of HDAC is involved in many cancers, so HDAC has become an important target in the development of anti-cancer drugs (*5-9*). A large number of HDAC inhibitors (HDACis) have been reported and some of them have been approved by FDA such as vorinostat (SAHA), romidepsin, belinostat, panobinostat, and chidamide (*10-12*). Pan-HDACis as the majority of reported HDACis often cause some adverse effects, such as fatigue, nausea, vomiting, and cardiotoxicity (*13-15*) which greatly limit their application in cancer therapy. To avoid these adverse effects and enhance the efficacy against solid tumors, more and more researches are concentrating on the development of isoform selective HDACis, especially HDAC6 selective inhibitors which usually cause less toxicities. Different from other HDAC isoforms,

Released online in J-STAGE as advance publication April 25, 2019.

§These authors contributed equally to this work.
**Address correspondence to:*
Dr. Yantao Han, Department of Pharmacology, College of Basic Medicine, Qingdao University, Qingdao 266071, China.
E-mail: hanyt@qdu.edu.cn

Dr. Yepeng Luan, Department of Medicinal Chemistry, School of Pharmacy, Qingdao University, Qingdao 266021, Shandong, China.
E-mail: yluan@qdu.edu.cn

HDAC6 is located in the cytoplasm and mainly responsible for deacetylating non-histone substrates such as α-tubulin, cortactin, HSP90, and other proteins (*16,17*). HDAC6 is involved in many cellular processes such as misfolded protein degradation, cell adhesion, cell migration, cell growth, immune synapse formation and stress granule formation (*18,19*). Several selective HDAC6 inhibitors have been extensively explored due to their relatively low toxicity compared with pan-HDACis (*4,20*). ACY1215, a well-known and moderately selective HDAC6 inhibitor with 10- to 12-fold selectivity over class I HDACs, is now in phase I/II clinical trials in combination with dexamethasone and bortezomib, lenalidomide, or pomalidomide for the treatment of multiple myeloma (*21-23*).

In this work, we designed and synthesized novel HDAC6 selective inhibitors utilizing 4-piperidin-4-yl-triazole fragment as the backbone. Enzyme inhibition activity, antiproliferative activity, anti-migration activity and their proposed binding modes with HDAC6 were all investigated.

2. Materials and Methods

2.1. *Chemistry*

All chemical reagents and solvents were purchased from Energy Chemical (Shanghai, China), and used as received without any purification. Thin-layer chromatography was performed on 0.20 mm Silica Gel 60 F254 plates (Qingdao Haiyang Chemical, China). MS spectra were acquired on a Thermo Scientific LTQ Orbitrap XL mass spectrometer. 1H NMR spectra, and 13C NMR spectra were acquired on a Bruker DRX 400 NMR spectrometer using $CDCl_3$ or DMSO-d6 as solvent. Chemical shifts were reported in parts per million (ppm, δ) relative to the solvent peak (1H, $CDCl_3$ δ 7.26 ppm, DMSO-d6 δ 2.50 ppm; 13C, $CDCl_3$ δ 77.0 ppm, DMSO-d6 δ 39.6 ppm). Coupling constants (*J*) were measured in hertz (Hz).

2.2. *Cell line and cell culture*

Human cancer cell lines SGC-7901 (gastric cancer), NCI-H226 (lung squamous cell cancer), MCF-7 (breast cancer), and HL-60 (leukemia) were obtained from China Cell Bank (Shanghai, China) and maintained in RPMI-1640 supplemented with 10% fetal bovine serum (FBS; PAN Biotech) at 37°C in a humid atmosphere (5% CO_2-95% air).

2.3. *In vitro HDAC inhibition fluorescence assay*

In brief, 10 μL of enzyme solution (HeLa cell nuclear extract, HDAC1, or HDAC6) was mixed with different concentrations of tested compounds (50 μL). The mixture was incubated at 37°C for 5 min, followed by adding 40 μL fluorogenic substrate (Boc-Lys(acetyl)-AMC). After incubation at 37°C for 30 min, the mixture was quenched by addition of 100 μL of developer containing trypsin and trichostatin A (TSA). Over another incubation at 37°C for 20 min, fluorescence intensity was measured using a microplate reader at excitation and emission wavelengths of 390 and 460 nm, respectively. The inhibition rates were calculated from the fluorescence intensity readings of tested wells relative to those of control wells, and the IC_{50} values were calculated using a regression analysis of the concentration/inhibition data.

2.4. *In vitro antiproliferative activity assay*

The antiproliferative activities of the compounds were tested in four human cancer cell lines SGC-7901 (gastric cancer), NCI-H226 (lung squamous cell cancer), MCF-7 (breast cancer), and HL-60 (leukemia). Cells in logarithmic phase were seeded in 96-well plates and allowed to adhere (except for HL-60). Then the cells were incubated with indicated concentrations of the compounds for 72 h. 3-(4,5-Dimethylthiazol-2-yl)-2,5-diphenyltetrazolium bromide (MTT) was subsequently added for an extra 3 h of incubation. The MTT formazan precipitate was dissolved in DMSO, and the absorbance was measured at a wavelength of 570 nm by a Spectramax M5 microtiter plate luminometer (Molecular Devices, Sunnyvale, CA, USA) (*24-26*). Experiments were performed in triplicate and repeated for three times.

2.5. *Wound healing assay*

MCF-7 cells were seeded in 6-well plates at a density of 10^6 cells/well and allowed to reach 100% confluence. After treatment with mitomycin C (10 μg/mL, 12 h), a scratch wound was created on the cell surface using a 200-μL pipette tip. The detached cells were washed away with PBS. The medium was changed to serum free RPMI-1640 with the representative compound (at three concentrations), and the cells were continuously cultured for 48 h. The wound was photographed with an inverted phase contrast microscope (Nikon; magnification, 40×) at 0, 12, 24, 36, and 48 h. The migration distance and areas were calculated using ImageJ.

2.6. *Docking study*

Compounds were docked into the active site of HDAC6 (PDB entry: 5WGL) using Tripos SYBYL-X 2.1. Before docking process, the protein structure retrieved from PDB site was treated by deleting water molecules, FF99 charges. A 100-step minimization process was performed to further optimize the protein structure. The molecular structures were generated with Sybyl/Sketch

module and optimized using Powell's method with the Tripos force field with convergence criterion set at 0.05 kcal/(Å mol) and assigned charges with the Gasteiger_ Hückel method (*27*). Molecular docking was carried out via the Sybyl/SurflexDock module. Other docking parameters were kept to the default values.

2.7. *Statistical analysis*

Data were expressed as mean for at least three different determinations. Statistical significance was analyzed by one-way analysis of variance (ANOVA) followed by Dunnett's multiple range tests. The value of $p < 0.05$ was considered as statistically significant. Statistical analysis was performed using the SPSS/Win 16.0 software (SPSS, Inc, Chicago, IL, USA).

3. Results and Discussion

3.1. *Chemistry*

The structures of all 21 target compounds and the synthetic route were showed in Scheme 1. In general, the canonical pharmacophore of a HDACi is composed of three parts: a cap structure that can interact with the rim of the entrance of the active pocket of HDACs, a zinc ion (Zn^{2+}) binding group (ZBG), and a linker responsible for the connection of cap and ZBG and for interaction with the hydrophobic tunnel of the active site (*28*). In this work, we designed and synthesized novel HDAC6 selective inhibitors utilizing 4-piperidin-4-yl-triazole fragment as core skeleton and the cap part. Actually, many HDACis containing a triazole moiety were reported due to its structural stability. Triazole is relatively resistant to metabolic degradation and can perform as an bioisostere of esters and amides (*29*). Hydroxamic acid was selected as the ZBG due to its strong affinity with Zn^{2+}.

The organic synthesis work started with the commercially available 1-Boc-4-hydroxypiperidine which was allowed to react with methanesulfonyl chloride (MsCl) in presence of triethylamine (TEA) to give the methanesulfonyl ester **1**. And the methanesulfonyl ester was substituted by sodium azide (NaN_3) to give the azido intermediate **2**. In another hand, the methyl 6-propiolamidohexanoate **3** was obtained by the condensation of methyl 6-aminocaproate hydrochloride and propiolic acid in the presence TEA and dicyclohexylcarbodiimide (DCC). Then compound **3** was allowed to react with compound **2** through Click reaction to give the methyl ester compound **4**. After de-protection mediated by trifluoroacetic acid (TFA), the important derivative **5** was obtained and allowed to react with different aryl acid to give the compounds **6-1** to **6-21**. Finally, in the presence of NH_2OH in anhydrous methanol, the hydroxamic acid final products **MH1-1** to **MH1-21** possessing different substituent groups were obtained. Specific synthetic procedures and spectroscopy data of all compounds see supplementary data (*http://www.biosciencetrends.com/action/getSupplementalData.php?ID=42*).

3.2. *In vitro anti-HDACs activity*

We first screened the inhibitory activity of all 21 final products against Hela cell nucleus extracts whose main component is class I HDACs. Single concentration (1 μM) was used and the inhibition rate (%) was calculated. The results were showed in Figure 1. All 21 compounds displayed moderate to strong inhibitory activities against HDACs demonstrating that the 4-piperidin-4-yl-triazole fragment as the "cap" part and the linker length were desirable. Among all compounds, five ones (MH1-2, MH1-5, MH1-14, MH1-18, and MH1-21) displayed potent inhibitory activity against HDACs with the inhibition rate higher than 80% at 1 μM. The cap part structures of MH1-2, MH1-5, MH1-18, and MH1-21 all contained polar atoms such as oxygen, fluoride and nitrogen which may contribute to the interactions with HDACs. Notably, the inhibition rates of compounds MH1-18 and MH1-21 were 93.6% and 92.7%, respectively, comparable to that of SAHA (96.3%).

3.3. *HDAC isoform specificity of compounds MH1-18 and MH1-21*

With two potent compounds MH1-18 and MH1-21 in hand, the isoform selectivity of them was further evaluated. HDAC1 (class I) and HDAC6 (class IIb) were selected as the targets, SAHA and HDAC6 selective inhibitor ACY1215 were utilized as the positive controls. The result was showed in Table 1. Consistent with published data, SAHA as a pan HDACi was almost equipotent toward HDAC1 and 6 without conspicuous selectivity. While, ACY1215 as a well-studied HDAC6 selective inhibitor displayed high potency to HDAC6 with the IC_{50} value of 8.0 nM, and the SF (6/1) (selectivity factor for HDAC6 over HDAC1) was 9.1. Encouragingly, our two inhibitors MH1-18 and MH1-21 were also robust HDAC6 inhibitors with the IC_{50} values of 11.5 and 8.6 nM, respectively. And the SF (6/1) values were discernible (10.4 and 12.3, respectively), even slightly better than that of ACY1215.

3.4. *In vitro antiproliferative activity of compounds MH1-18 and MH1-21*

Since compounds MH1-18 and MH1-21 had the best HDACs inhibitory activity, they were evaluated in an MTT assay to determine their antiproliferative effect on human cancer cell line SGC-7901 (gastric cancer), NCI-H226 (lung squamous cell cancer), MCF-

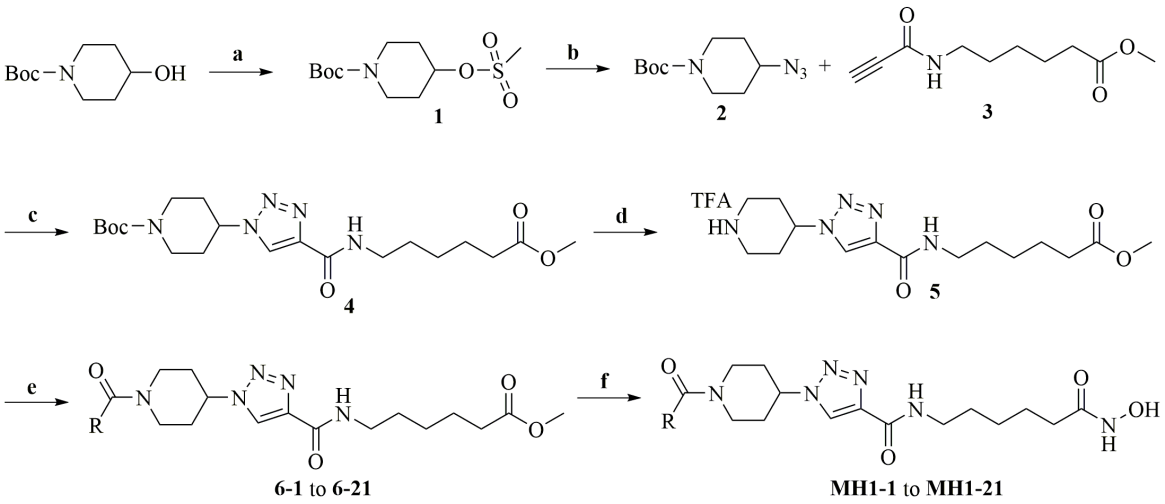

R=

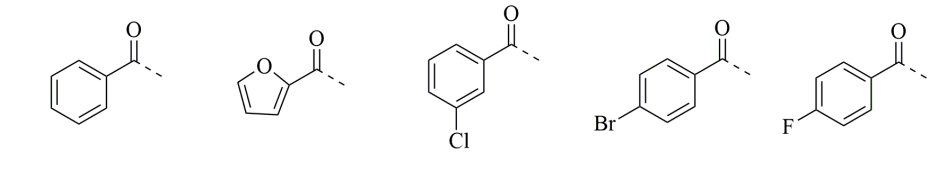

MH1-1 **MH1-2** **MH1-3** **MH1-4** **MH1-5**

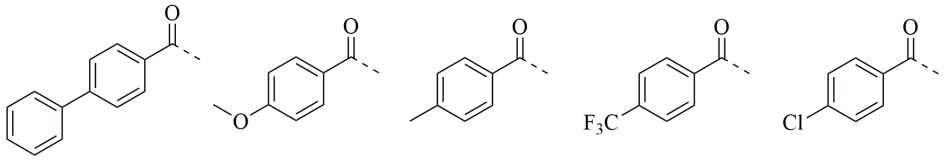

MH1-6 **MH1-7** **MH1-8** **MH1-9** **MH1-10**

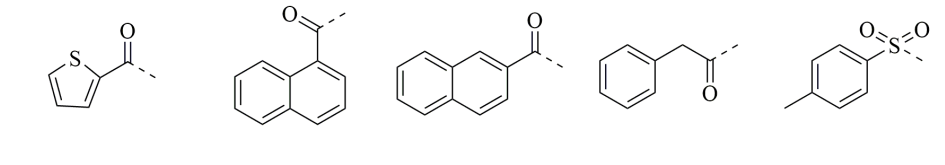

MH1-11 **MH1-12** **MH1-13** **MH1-14** **MH1-15**

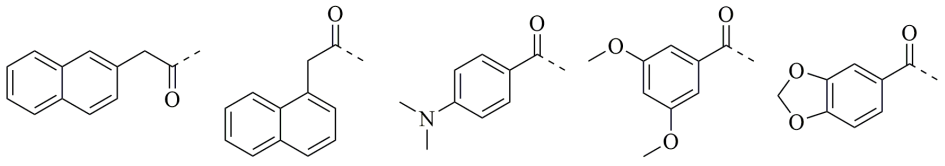

MH1-16 **MH1-17** **MH1-18** **MH1-19** **MH1-20**

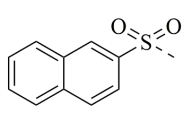

MH1-21

Scheme 1. Reagents and conditions: a. MsCl, TEA, DCM, 0°C; **b**. NaN_3, DMF, 80°C; **c**. CuI, anhydrous THF, nitrogen, r.t.; **d**. TFA:DCM = 1:5, r.t.; **e**. aromatic acid, HATU, N,N-diisopropylethylamine (DIPEA), dry DMF, r.t.; **f**. NH_2OH, KOH, MeOH, r.t..

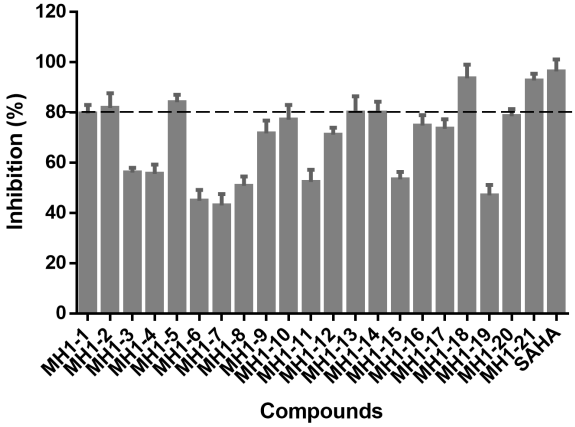

Figure 1. The inhibition rates of all 21 compounds against HDACs at 1 μM concentration.

Table 1. Inhibitory activity of four representative compounds toward HDAC1 and 6

Compound	IC_{50}[a], nM		SF(6/1)[b]
	HDAC1	HDAC6	
MH1-18	119.2	11.5	10.4
MH1-21	105.6	8.6	12.3
SAHA	43.2	20.7	2.1
ACY1215	73.0	8.0	9.1

[a]The IC_{50} values are the means of three experiments. [b]SF(6/1): selectivity factor for HDAC6 over HDAC1. SF(6/1) = IC_{50}(HDAC1)/ IC_{50}(HDAC6).

Table 2. Antiproliferative effects on four tumor cell lines

Compound	IC_{50}[a], nM			
	SGC-7901	NCI-H226	MCF-7	HL-60
MH1-18	N.D.	N.D.	N.D.	57.7
MH1-21	166.3	119.3	226.4	43.8
ACY1215	10.2	7.44	6.31	6.73
SAHA	5.8	5.41	7.10	3.87

[a]IC_{50} values are the mean of at least three experiments. N.D., not determined.

7 (breast cancer), and HL-60 (leukemia). Treatment with our two compounds as well as the positive control SAHA and ACY1215 for 72 h resulted in dose-dependent growth inhibition of all four cancer cell lines (Table 2). Contrast to the strong enzyme inhibitory activity, our two compounds MH1-18 and MH1-21 showed moderate activity in suppressing the cell proliferation, with IC_{50} values more than 40 μM for the four cancer lines. This result is consistent with the low antiproliferative activity of many known selective HDAC6 inhibitors (*20,30*). For example, in our previous work, we designed and synthesized three novel HDAC6 inhibitors LYP-2, -3, and -6 with the 4-aminopiperidine-1-carboxamide as the core structure which showed moderate efficacy in suppressing the proliferation of cancer cells (*20*). In another study, HDAC6 selective inhibitor 4-hydroxybenzoic acid failed to induce significant cell death in MCF-7 cells

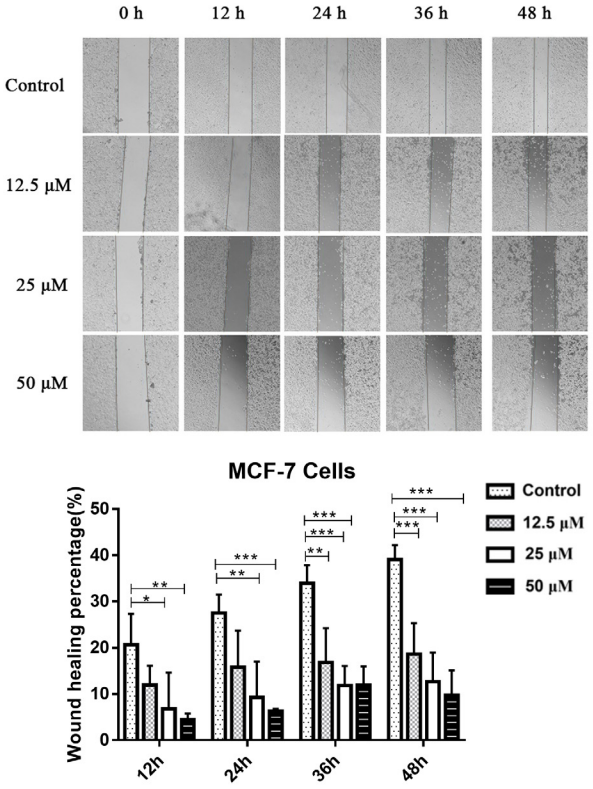

Figure 2. MH1-21 suppressed migration of MCF-7 cells. The effect of MH1-21 on MCF-7 tumor cell migration was determined using a wound healing assay. The cells were exposed to 12.5, 25, or 50 μM of MH1-21 for 12, 24, 36, and 48 h, respectively, and the wound areas were measured at each time point. *$p < 0.05$, **$p < 0.01$, ***$p < 0.001$ *vs*. control.

at concentrations below 20 μM (*30*). On the other hand, the relatively low antiproliferation activity of MH1-18 and MH1-21 may possibly be attributed to their high polarity, as the calculated LogP (cLogP) values of MH1-18 and MH1-21 were -1.03 and 0.40 (by ChemDraw 14.0), respectively. While the cLogP values of ACY1215 and SAHA were 3.38 and 0.989. The permeability across the cell membrane of our compounds might be further improved.

3.5. *Compound MH1-21 suppressed the migratory capability of MCF-7 tumor cells*

As reported, HDAC6 plays a significant role in migration of tumor cells (*31*), in this work, we tested the anti-migration activity of compound MH1-21 which displayed best inhibitory activity toward HDAC6 with good selective index. To investigate the anti-migration effect of MH1-21, an *in vitro* wound healing assay was performed using MCF-7 cells. Results were showed in Figure 2, which indicated that treatment with three concentrations of MH1-21 (12.5, 25 and 50 μM) all remarkably reduced the migratory capability of MCF-7 cells compared to that of the blank control group at 12, 24, 36 and 48 h after wound creation. This result suggested that compound MH1-21 possessing potent

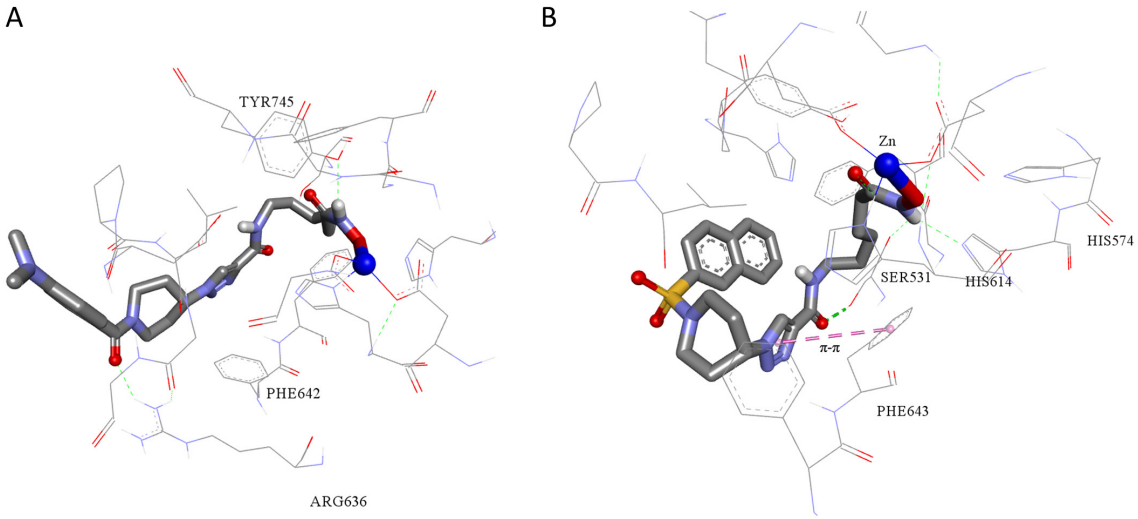

Figure 3. Proposed binding model of compounds MH1-18 (A) and MH1-21 (B) with HDAC6 (derived by modification of PDB code 5WGL using Tripos SYBYL-X 2.1). The Zn^{2+} is shown as a blue sphere. Hydrogen bonds are shown as green dashed lines. The figure was generated by Discovery Studio Visualizer.

inhibitory activity toward HDAC6 was able to inhibit the migration of MCF-7 cells.

3.6. *The docking results of compound MH1-18 and MH1-21 to HDAC6*

Considering that compound MH1-18 and MH1-21 displayed potent inhibitory activity toward HDAC6, we investigated the proposed binding modes of these two compounds with HDAC6 (Figure 3). The crystal structure of *Danio rerio* histone deacetylase 6 catalytic domain 2 in complex with ACY1215 was used as the template (PDB code: 5WGL). From the proposed binding mode, we can see that the hydroxamic acid group of both compounds can smoothly chelate with the Zn^{2+} which makes contribution for the HDAC6 inhibition. For compound MH1-18 (Figure 3A), the oxygen atom of the terminal carboxyl group forms a hydrogen bond with Arg636 residue of HDAC6. While for compound MH1-21 (Figure 3B), the oxygen atom of the carboxyl group forms an extra hydrogen bond with Ser531 residue of HDAC6, and a π-π stack interaction is predicted to be formed between the triazole and the phenyl group of Phe643 residue.

4. Conclusion

In this work, a series of 21 novel HDAC inhibitors possessing 4-piperidin-4-yl- triazole as the core skeleton were rationally designed based on the pharmacophore constituents of known HDACis. All of the target compounds displayed moderate to excellent inhibitory activity to HDACs. Out of them, compounds MH1-18 and MH1-21 with inhibition rate exceeding 90% toward HDACs at 1 μM exhibited potent inhibitory activity toward HDAC6 isoform, and MH1-21 displayed good selectivity to HDAC6 over HDAC1, better than ACY1215. In addition, compound MH1-21 showed potent efficacy in suppressing the migration of MCF-7 cells *in vitro*. Compounds obtained in the current study shed light on discovering novel HDAC6 inhibitors as anti-cancer agents.

Acknowledgements

We gratefully acknowledge the financial support from the National Science Foundation for Young Scientists of China to Y. L. (NSFC no. 81602947) and J. G. (NSFC no. 81503094), China Postdoctoral Science Foundation (no. 2016M600524), and Qingdao Postdoctoral Applied Research Project (no. 2016072; Jianjun Gao, Qingdao University).

References

1. Minucci S, Pelicci PG. Histone deacetylase inhibitors and the promise of epigenetic (and more) treatments for cancer. Nat Rev Cancer. 2006; 6:38-51.
2. de Ruijter AJ, van Gennip AH, Caron HN, Kemp S, van Kuilenburg AB. Histone deacetylases (HDACs): characterization of the classical HDAC family. Biochem J. 2003; 370:737-749.
3. Gregoretti IV, Lee YM, Goodson HV. Molecular evolution of the histone deacetylase family: functional implications of phylogenetic analysis. J Mol Biol. 2004; 338:17-31.
4. Kalin JH, Bergman JA. Development and therapeutic implications of selective histone deacetylase 6 inhibitors. J Med Chem. 2013; 56:6297-6313.
5. Falkenberg KJ, Johnstone RW. Histone deacetylases and their inhibitors in cancer, neurological diseases and immune disorders. Nat Rev Drug Discov. 2014; 13:673-691.
6. Khan O, La Thangue NB. HDAC inhibitors in cancer biology: emerging mechanisms and clinical applications. Immunol Cell Biol. 2012; 90:85-94.

7. Gammoh N, Lam D, Puente C, Ganley I, Marks PA, Jiang X. Role of autophagy in histone deacetylase inhibitor-induced apoptotic and nonapoptotic cell death. Proc Natl Acad Sci U S A. 2012; 109:6561-6565.
8. Weichert W. HDAC expression and clinical prognosis in human malignancies. Cancer Lett. 2009; 280:168-176.
9. Bolden JE, Peart MJ, Johnstone RW. Anticancer activities of histone deacetylase inhibitors. Nat Rev Drug Discov. 2006; 5:769-784.
10. Thaler F, Mercurio C. Towards selective inhibition of histone deacetylase isoforms: what has been achieved, where we are and what will be next. Chem Med Chem. 2014; 9:523-526.
11. Wagner JM, Hackanson B, Lubbert M, Jung M. Histone deacetylase (HDAC) inhibitors in recent clinical trials for cancer therapy. Clin Epigenetics. 2010; 1:117-136.
12. Lu X, Ning Z, Li Z, Cao H, Wang X. Development of chidamide for peripheral T-cell lymphoma, the first orphan drug approved in China. Intractable Rare Dis Res. 2016; 5:185-191.
13. Ramalingam SS, Belani CP, Ruel C, Frankel P, Gitlitz B, Koczywas M, Espinoza-Delgado I, Gandara D. Phase II study of belinostat (PXD101), a histone deacetylase inhibitor, for second line therapy of advanced malignant pleural mesothelioma. J Thorac Oncol. 2009; 4:97-101.
14. Boumber Y, Younes A, Garcia-Manero G. Mocetinostat (MGCD0103): a review of an isotype-specific histone deacetylase inhibitor. Expert Opin Investig Drugs. 2011; 20:823-829.
15. Fraczek J, Vanhaecke T, Rogiers V. Toxicological and metabolic considerations for histone deacetylase inhibitors. Expert Opin Drug Metab Toxicol. 2013; 9:441-457.
16. Dallavalle S, Pisano C, Zunino F. Development and therapeutic impact of HDAC6-selective inhibitors. Biochem Pharmacol. 2012; 84:756-765.
17. Zuo Q, Wu W, Li X, Zhao L, Chen W. HDAC6 and SIRT2 promote bladder cancer cell migration and invasion by targeting cortactin. Oncol Rep. 2012; 27:819-824.
18. Hideshima T, Bradner JE, Chauhan D, Anderson KC. Intracellular protein degradation and its therapeutic implications. Clin Cancer Res. 2005; 11:8530-8533.
19. Li Y, Shin D, Kwon SH. Histone deacetylase 6 plays a role as a distinct regulator of diverse cellular processes. FEBS J. 2013; 280:775-793.
20. Zhao C, Gao J, Zhang L, Su L, Luan Y. Novel HDAC6 selective inhibitors with 4-aminopiperidine-1-carboxamide as the core structure enhanced growth inhibitory activity of bortezomib in MCF-7 cells. Biosci Trends. 2019; 13:91-97.
21. Santo L, Hideshima T, Kung AL, *et al*. Preclinical activity, pharmacodynamic, and pharmacokinetic properties of a selective HDAC6 inhibitor, ACY-1215, in combination with bortezomib in multiple myeloma. Blood. 2012; 119:2579-2589.
22. Haggarty SJ, Koeller KM, Wong JC, Grozinger CM, Schreiber SL. Domain-selective small-molecule inhibitor of histone deacetylase 6 (HDAC6)-mediated tubulin deacetylation. Proc Natl Acad Sci U S A. 2003; 100:4389-4394.
23. Haggarty SJ, Koeller KM, Wong JC, Butcher RA, Schreiber SL. Multidimensional chemical genetic analysis of diversity-oriented synthesis-derived deacetylase inhibitors using cell-based assays. Chem Biol. 2003; 10:383-396.
24. Sun Z, Zhu Y, Aminbuhe, Fan Q, Peng J, Zhang N. Differential expression of APE1 in hepatocellular carcinoma and the effects on proliferation and apoptosis of cancer cells. Biosci Trends. 2018; 12:456-462.
25. Yang Z, Ji L, Jiang G, Liu R, Liu Z, Yang Y, Ma Q, Zhao H. FL118, a novel camptothecin analogue, suppressed migration and invasion of human breast cancer cells by inhibiting epithelial-mesenchymal transition via the Wnt/beta-catenin signaling pathway. Biosci Trends. 2018; 12:40-46.
26. Zhang X, Li P, Guo S, Wang S, Liu D. Quantitation of beta-carboline and quercetin in alligator weed (Alternanthera philoxeroides (Mart.) Griseb.) by LC-MS/MS and evaluation of cardioprotective effects of the methanol extracts. Drug Discov Ther. 2018; 12:341-346.
27. Zhang H, Li X, Wang X, Xu W, Zhang J. Sulfonyl phosphonic 1,4-dithia-7-azaspiro[4,4]nonane derivatives as matrix metalloproteinase inhibitors: Synthesis, a docking study, and biological evaluation. Drug Discov Ther. 2017; 11:118-125.
28. Marson CM. Histone deacetylase inhibitors: design, structure-activity relationships and therapeutic implications for cancer. Anticancer Agents Med Chem. 2009; 9:661-692.
29. Tron GC, Pirali T, Billington RA, Canonico PL, Sorba G, Genazzani AA. Click chemistry reactions in medicinal chemistry: applications of the 1,3-dipolar cycloaddition between azides and alkynes. Med Res Rev. 2008; 28:278-308.
30. Wang XN, Wang KY, Zhang XS, Yang C, Li XY. 4-Hydroxybenzoic acid (4-HBA) enhances the sensitivity of human breast cancer cells to adriamycin as a specific HDAC6 inhibitor by promoting HIPK2/p53 pathway. Biochem Biophys Res Commun. 2018; 504:812-819.
31. Hsieh YL, Tu HJ, Pan SL, Liou JP, Yang CR. Anti-metastatic activity of MPT0G211, a novel HDAC6 inhibitor, in human breast cancer cells *in vitro* and *in vivo*. Biochim Biophys Acta Mol Cell Res. 2019; 1866:992-1003.

(Received March 2, 2019; Revised April 17, 2019; Accepted April 21, 2019)

Brief Report

DOI: 10.5582/bst.2019.01021

Circular RNA profiling reveals circRNA1656 as a novel biomarker in high grade serous ovarian cancer

Yan Gao[1,2], Chuanqi Zhang[1], Yisi Liu[1], Min Wang[1,*]

[1] *Department of Gynecology and Obstetrics, Shengjing Hospital Affiliated of China Medical University, Shenyang, Liaoning, China;*
[2] *Department of Gynecology, Cancer Hospital of China Medical University, Liaoning Cancer Hospital & Institute, Shenyang, Liaoning, China.*

Summary **Circular RNA (circRNA) is a class of endogenous non-coding RNAs that are closely related to the pathogenesis of many human diseases, particularly cancer. However, the characterization of circRNAs in high-grade serous ovarian cancer (HGSOC) remains unknown. This study aimed to investigate the expression profile of circRNAs in HGSOC. Expression profiles of circRNAs differential expression based on circRNAs High-throughput sequencing were identified in 3 HGSOC specimens and 3 normal ovarian tissues. A total of 710 differentially expressed circRNAs were found (354 expressions up-regulated and 356 expressions down-regulated). CircRNA sequencing data were verified by qRT-PCR in HGSOC tissue and benign ovarian lesions. Differential expression of 7 circRNAs (circRNA385, circRNA2058, circRNA3336, circRNA2606, circRNA1656, circRNA1312 and circRNA7474) in HGSOC tissue was confirmed by qRT-PCR. Among them, circRNA1656 showed the highest fold change. qRT-PCR was used to verify the expression of circRNA1656 in ovarian cancer cell lines. In order to analyze the relationship between circRNA1656 expression and clinical pathological biological characteristics of HGSOC, qRT-PCR was used to verify the expression of circRNA1656 in 60 HGSOC tissues compared with 60 benign ovarian lesions. The expression of circRNA1656 was down-regulated in HGSOC tissues and ovarian cancer cell lines, and correlated with the FIGO stage of HGSOC. circRNA1656 has the potential to serve as a novel tumor marker for HGSOC.**

Keywords: HGSOC, circular RNA, ovarian cancer, High-throughput sequencing, circular RNA profile, circRNA1656

1. Introduction

Ovarian cancer has the second highest incidence of gynecological malignant tumors, and is the leading cause of cancer-related mortality in the female reproductive system (*1*). The 5-year survival rate of Stage III-IV ovarian cancer is only 30% (*2,3*). Epithelial ovarian cancer (EOC) is the most important pathological subtype of ovarian cancer, accounting for more than 90%. Among the pathological subtypes of EOC, high-grade ovarian serous carcinoma (HGSOC) accounts for 60-70% (*4*), the highest proportion. HGSOC often indicates a worse clinical outcome. Current studies have shown that HGSOC has a different pathogenesis from low-grade serous ovarian cancer. Despite the heterogeneity of HGSOC, the current treatment of clinical patients is not specific, further clarifying the pathogenesis of HGSOC and finding potential tumor markers or therapeutic targets are essential for improving the 5-year survival rate of HGSOC patients.

Circular RNAs (circRNAs) are characterized by a covalent closed-loop structure with no 5' cap or 3' polyadenylation tail (*5,6*), with the property of stable structure, good conservation, tissue specificity, and expression specificity at different developmental stages in different species (*7*). These unique features make circRNA a research hotspot.

To date, there is growing evidence that circRNAs

Released online in J-STAGE as advance publication April 24, 2019.

*Address correspondence to:
Dr. Min Wang, Department of Gynecology and Obstetrics, Shengjing Hospital Affiliated of China Medical University, No. 36 Sanhao Street, Heping District, Shenyang 110004, Liaoning, China.
E-mail: wm21st@126.com

are closely related to the pathogenesis of many human diseases, particularly cancer (*8*). So far, various types of cancer, including breast cancer (*9*), liver cancer (*10*), gastric cancer (*11*), colorectal cancer (*12*), and bladder cancer (*13,14*), have revealed abnormal expression levels of circRNA. However, ovarian cancer-based circRNAs research started late, with few studies. In a study by LINING *et al*. (*15*), circRNA sequencing analysis was performed in 4 matched EOCs and normal ovarian tissues. CircRNA sequencing data was verified by reverse transcription-quantitative polymerase chain reaction (qRT-PCR) in 54 EOC specimens and 54 normal ovarian tissues. In the subtype of EOC, existing studies have shown that HGSOC has a different pathogenesis from low-grade serous ovarian cancer. However, there has been no HGSOC-based circRNA study reported so far. So the aim of this study is to investigate the pathogenesis of HGSOC by high-throughput sequencing analysis of differential expression of circRNA in HGSOC specimens.

2. Materials and Methods

2.1. *Clinical samples*

A total of 120 cases were included. The postoperative pathology of all cases was confirmed by two chief physicians of the Department of Pathology of Liaoning Cancer Hospital & Institute, and all clinical data of the enrolled cases were collected. Among them, 60 cases of ovarian cancer cases were HGSOC; 60 cases in the control group were pathologically confirmed ovarian benign lesions. All cases had no history of tumors and radiochemotherapy. Among them, 3 cases of HGSOC and 3 cases of benign ovarian disease were chosen for High-throughput sequencing. The 6 selected cases were postmenopausal women with no endocrine diseases, metabolic diseases, infectious diseases and other medical history. This study was approved and supervised by The Ethics Committees of Liaoning Cancer Hospital& Institute, and written informed consent for participation was obtained from all subjects before sample collection.

2.2. *Cell lines and culture*

Ovarian cancer cells SKOV-3, HO 8910, and A2780 were purchased from Puno, Wuhan; OVCAR-3 was purchased from Zhongqiao Xinzhou, Shanghai; human ovarian epithelial cells were purchased from Saibai, Shanghai. All cells were cultured in a 37℃, 5% CO_2 incubator. SKOV3 was cultured in McCoy's 5A medium containing 10% fetal bovine serum; OVCAR-3 was cultured in RPMI-1640 medium containing 20% fetal bovine serum; A2780 was cultured in DMEM medium containing 10% fetal bovine serum; HO 8910, Human ovarian epithelial cells were cultured in RPMI-1640 medium containing 10% fetal bovine serum. The cells used in the experiments were all in the logarithmic growth phase.

2.3. *High-throughput sequencing*

The experimental procedure was performed according to standard procedures provided by Illumina, including preparative libraries and sequencing experiments. Total RNA was treated with Trizol reagent (Invitrogen, CA, USA) according to the manufacturer's protocol. The purified RNA was randomly broken into short fragments by Fragmentation Buffer, and the fragmented circular RNA was used as a template to synthesize a strand of cDNA with six-base random primers (Random hexamers), followed by buffer and dNTPs. RNaseH and DNA Polymerase I for double-stranded cDNA synthesis. AMPure XP beads purified double-stranded product, using T4 DNA polymerase and klenow DNA polymerase activity to repair the sticky end of DNA to blunt end, 3' end plus base A and linker, AMPure XP beads for fragment selection, then USER enzyme. The second strand of cDNA containing U was degraded, and finally the final sequencing library was obtained by PCR amplification. After the library was qualified, it was sequenced by Illumina Hiseq 4000, and the sequencing read length was double-ended 2 × 150 bp (PE150).

The circRNA sequence itself was predicted by CIRC Explorer, the expression of these expressed circRNAs was quantified by the results of the tophat comparison, and dealt with the difference statistics between the circRNAs. The data results were statistically analyzed and graphically displayed using R language.

2.4. *Quantitative real-time PCR (qRT-PCR)*

RNA was extracted from cells and tissues. After RNA extraction, cDNA was synthesized by reverse transcription using super M-MLV reverse transcriptase (BioTeke, Beijing, China). The expression level of circRNA was evaluated by fluorescence quantitative analysis using an SYBR Green assay (Solarbio, Beijing, China) by an ExicyclerTM 96 fluorescence meter (BIONEER, Korea). Primers designed to amplify circular transcripts are shown in Table 1. The relative levels of expression of selected circRNAs were measured using the $2^{-\Delta\Delta ct}$ method.

2.5. *GO and KEEG enrichment analysis*

Functional analysis of differential genes included GO (Gene Ontology) enrichment analysis and KEGG (Kyoto Encyclopedia of Genes and Genomes) signal pathway enrichment analysis.

2.6. *Statistical analysis*

qRT-PCR validation is expressed as mean ± standard

Table 1. The primers for qRT-PCR

Name	Forward (from 5' to 3'),	Reverse(from 5' to 3'),
circRNA385	TGGGTCGGCCAGTCATGTAT	ACACAACTGCTTGGCTCTACT
circRNA2606	ACCTCGATCTGTCCCAAGCA	GGTTTCTGCCCTGACACCTG
circRNA2058	TCAGGTGCTTTTCAGTGGGA	ACGCTTCAGCCTTTAAGACAGG
circRNA3336	AATGCTGCATTCCCCTCTCG	TCTCGAGACATGATGGCCCA
circRNA1656	CTGCGAGGTGGAGAAGGAGA	GACACACCCATGGCCATACG
circRNA2558	CGAAGTCGTTCAAGGGGTCG	AGAACTGCTCGAGGAGGACC
circRNA1312	GCTCAAGATCTTTGGCCAGAGC	GCATTGCCACTCCTCCAGAGA
circRNA7474	CCACAGCCTTGCACAGTGTG3	TCAACACCAGAGTCGTGATCATGT
GAPDH	CAGGAGGCATTGCTGATGAT	GAAGGCTGGGGCTCATTT

error of the mean. The comparison between HGSOC and benign ovarian lesions was performed by Student's *t* test (two-tailed). Chi-square test was used to analyze the correlation between circRNA1656 expression and clinical pathological biological characteristics. The *p* value < 0.05 was considered statistically significant.

3. Results and Discussion

3.1. *CircRNA expression profile differentially expressed by HGSOC*

12,291 different circRNA candidates were found in all samples. Then, we used *P* value < 0.05, with | log2fold change | ≥ 1 to define the statistical criteria for selecting aberrantly expressed circRNA. A total of 710 circRNAs were differentially expressed, of which 354 were up-regulated and 356 were down-regulated. Including 693 exonics, 7 intronics, and 3 antisenses. Differential expression of circRNA between HGSOC group and benign ovarian lesion group was demonstrated by cluster analysis of heat map, volcano map and scatter plot.

According to the similarity of gene expression profiles of the samples, the genes were clustered and the differential gene clustering analysis heat map visually showed the expression of the genes in different samples. We used Log (FPKM+1) for gene expression display. Each column represents a sample, and each row represents a circRNA. The color scale reflects the log2 signal strength, from green (low intensity) to black (medium intensity) to red (strong intensity). The hierarchical clustering map indicates the relative expression levels of circRNA in the HGSOC group and the normal ovarian group (Figure 1A).

The volcano map can be used to understand the overall distribution of differentially expressed circRNA. The volcano map was drawn for all genes in the differential expression analysis by using log2 (fold change) as the abscissa and -log10 (*p* value) as the ordinate. The abscissa represents the differential expression fold change of the gene in different samples; the ordinate represents the statistical significance of the difference in gene expression changes; the red dots represent significant differentially expressed transcripts, and the gray dots represent non-significant differentially expressed transcripts (Figure 1B).

The circRNA differential expression scatter plot can visually display the differential expression of circRNA in HGSOC and benign ovarian lesions. Among them, the horizontal and vertical coordinates represent log10 values of circRNA expression in tumor tissues and normal tissues, red represents differentially up-regulated circRNA, green represents differentially down-regulated circRNA, and blue represents non-differential circRNA (Figure 1C).

Studies have shown that circRNA plays an important role in the occurrence and development of tumors and has become a hot spot in cancer research. However, studies on the correlation between ovarian cancer and circRNA are rarely reported. Ahmed *et al*. (*16*) performed paired sequencing of the primary site, peritoneal and lymph node metastases in 3 patients with stage IIIC ovarian cancer, and analyzed the differential expression profiles of circRNA in the primary and metastatic sites of ovarian cancer. In the study of LINING *et al*. (*15*), circRNA sequencing analysis in 4 matched EOCs and normal ovarian tissues and qRT-PCR verification revealed that circEXOC6B and circN4BP2L2 are expected to be new markers of EOC. It is well known that EOC is rich in histopathological types, and the pathogenesis of HGSOC is different from that of low-grade serous ovarian cancer. Therefore, the circRNA expression profile of ovarian EOC differentially expressed by LINING *et al*. (*15*) has obvious limitations. Until now, the study of circRNA in HGSOC, the most common and poorly prognostic pathological subtype of ovarian cancer, has not been reported. This study analyzed the circRNA expression profile of HGSOC tissue for the first time, and found 354 up-regulated circRNAs, and 356 down-regulated CircRNAs.

3.2. *GO and KEEG enrichment analysis of differentially expressed circRNAs*

GO enrichment analysis is divided into three parts: biological process, molecular function and cell composition to interpret the function of differentially expressed circRNA. The results are shown in plot enriched GO DAG graph (Figure 2A) and histogram (Figure 2B). As shown, the top 5 rankings of biological

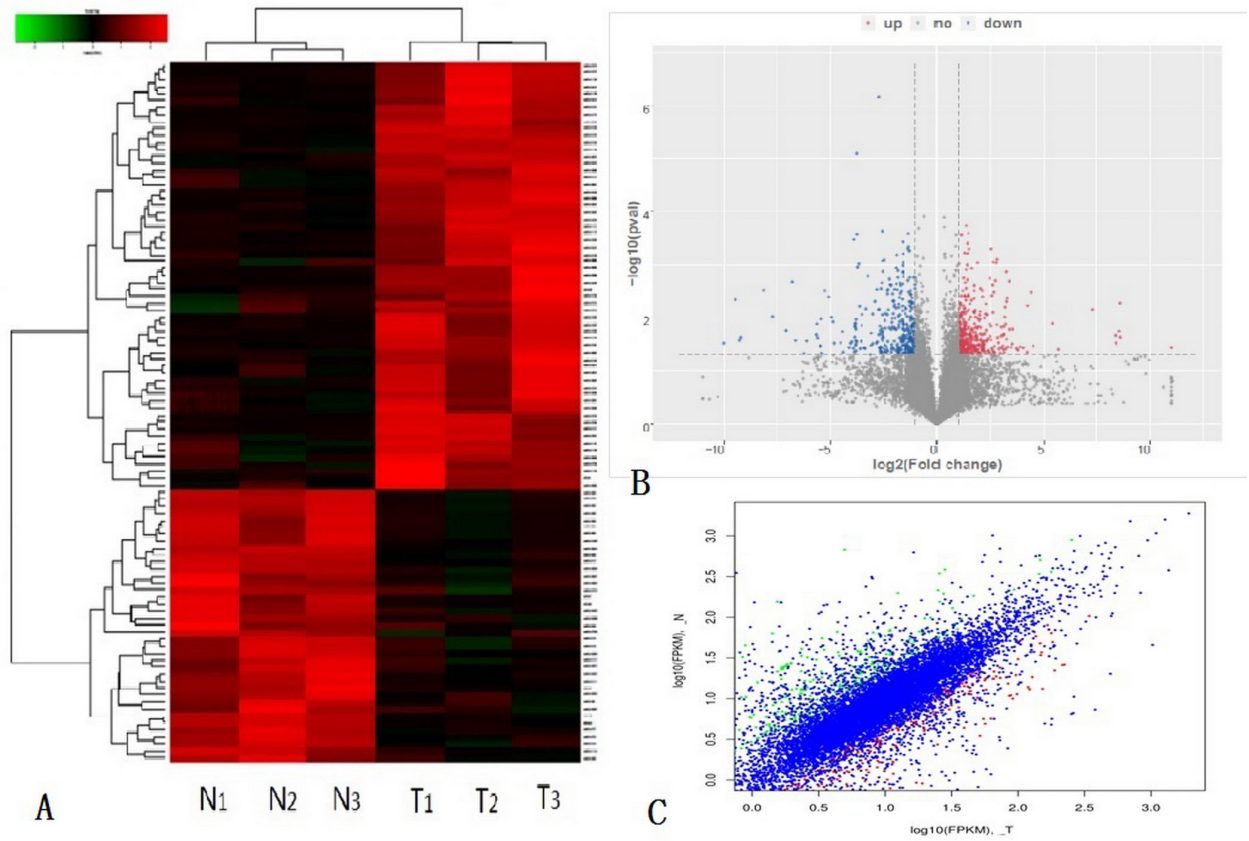

Figure 1. The differentially expressed circular RNAs (circRNAs). (A), Clustered heatmap. Each column represents a sample, and each row represents a circRNA. The color scale reflects the log2 signal strength, from green (low intensity) to black (medium intensity) to red (strong intensity). **(B)**, Volcano plots. The red points in plot denote the differentially up-regulated expressed circRNAs with statistical significance while the green points denote down-regulated. **(C)**, Scatter plot. Red represents differentially up-regulated cicRNA, green represents differentially down-regulated circRNA, and blue represents non-differential circRNA.

processes in which differentially expressed circRNAs are predominantly involved in HGSOC are (1) regulation of transcription, DNA-templated, (2) transcription, DNA-templated, (3) signal transduction, (4) transport, (5) positive regulation of GTP ase activity. The top 5 positions of the molecular functions of the differentially expressed circRNAs in HGSOC are (1) protein binding, (2) metal ion binding, (3) nucleotide binding, (4) DNA binding, and (5) ATP binding. The top 5 order of the cellular components involved in the differential expression of circRNA in HGSOC are (1) cytoplasm, (2) membrane, (3) nucleus, (4) cytosol, and (5) plasma membrane. The first cell component of the differentially expressed circRNAs in HGSOC was cytoplasm, and the vast majority of the differential expression in this study was exonic type, located in cytoplasm, consistent with the results of GO enrichment analysis.

KEEG enrichment analysis can present enrichment of possible pathways of action of differentially expressed circRNA in HGSOC. As shown, the pathways for differential expression of circRNA enrichment in HGSOC are (1) Pathways in cancer (2) Rap1 signaling pathway (3) PI3K-Akt signaling pathway (4) Tight junction (5) Proteoglycans in cancer (Figure 2C). Except for (4) tight junction, most pathways are closely related to the pathogenesis of tumors. Rap1 plays a key role in the development and progression of cancer. It inhibits the transformation of oncogene Ras-induced cells; it also induces malignant transformation of cells by a switch molecule on the cell signaling pathway through interaction with its downstream target molecules (*17*). The PI3K-Akt signaling pathway is involved in the regulation of various cellular functions such as cell proliferation, differentiation, apoptosis, and glucose transport, and is associated with a variety of tumors (*18*).

3.3. *qRT-PCR verification High-throughput sequencing results*

Based on differential expression of circRNA fold change, *p* value, FDR and fpkm, we selected 8 circRNAs for qRT-PCR validation (Table 2). Validation was performed in 40 HGSOC tissues and 40 ovarian benign lesions.

The results showed that the fold change of circRNA2558 was down-regulated in qRT-PCR, which was inconsistent with circRNA-seq results (up-regulated) ($p < 0.05$). circRNA385, circRNA2058, circRN3336, circRNA2606 and circRNA1656 expression were down-regulated and qRT-PCR results were consistent with circRNA-seq results ($p < 0.05$). The expression of

circRNA1312 and circRNA7474 were up-regulated, and the qRT-PCR results were consistent with the circRNA-seq results ($p < 0.05$). The results of qRT-PCR verified in the tissue were consistent with the circRNA-seq results, which further validated the reliability of our circRNA-seq results (Figure 3).

CircRNA has tissue-specific and developmental stage specificity (*19,20*). The unique closed-loop structure makes circRNA insensitive to ribonuclease and is highly stable, allowing it to be fully expressed in various

Table 2. The 8 circRNAs chosen to to validate High-throughput sequencing by qRT-PCR

CircRNA ID	Chrom	CircRNA Type	Gene symbol	Log2Fold change	*P* value
CircRNA385	Chr11	Exonic	HIPK3	-1.24	0.04
CircRNA2058	Chr5	Exonic	RHOBTB3	-3.85	0.01
CircRNA3336	Chr9	Exonic	BNC2	-2.30	0.00
CircRNA2606	Chr3	Exonic	LRCH3	-1.38	0.04
CircRNA2558	Chr3	Exonic	RSRC1	1.06	0.02
CircRNA1656	Chr7	Exonic	CLIP2	-1.09	0.03
CircRNA1312	Chr19	Exonic	ZNY208	2.26	0.01
CircRNA7474	Chr1	Exonic	STIL	2.53	0.00

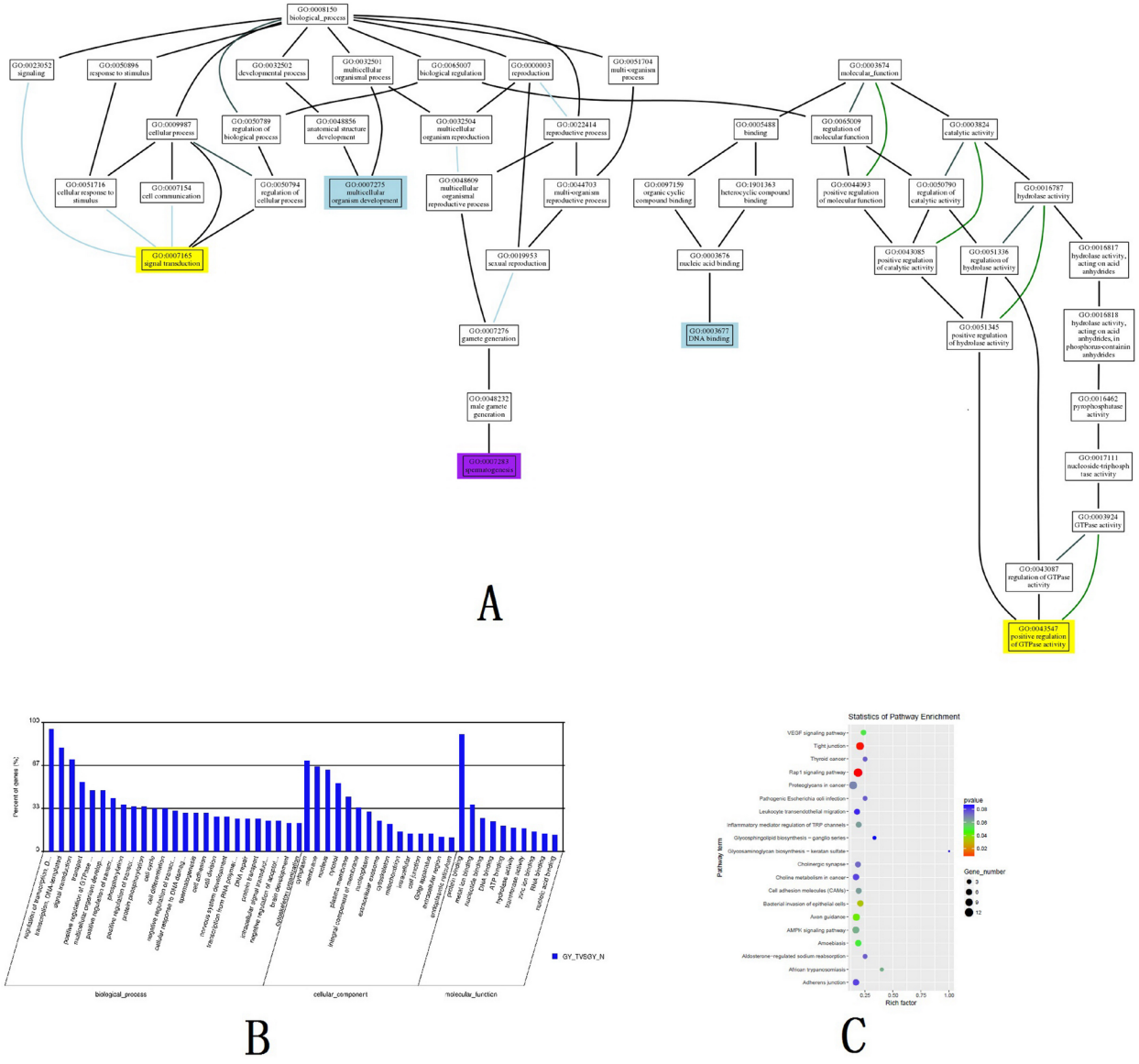

Figure 2. GO and KEEG enrichment analysis of differentially expressed circRNAs between HGSOC group and benign ovarian lesions group. (A), GO enrichment analysis showed by plot enriched GO DAG graph. **(B)**, GO enrichment analysis is divided into three parts: biological process, molecular function and cell composition, a list of differential gene expression shows abundances number for the function. **(C)**, Scatter plot of KEEG enrichment analysis. The vertical axis shows the annotated significantly enriched pathway of the significant differentially expressed gene. The horizontal axes shows the rich factor.

tissues and body fluids. Existing studies have shown that circRNA is stably expressed in human blood, saliva (*21*) and urine. These features give circRNA the potential to be a tumor marker for tumor diagnosis, treatment, and prognosis follow-up. In this study, circRNA385, circRNA2058, circRNA3336, circRNA2606, circRNA1656, circRNA1312 and circRNA7474 are expected to become a potential tumor marker, but further research is needed.

3.4. *KEEG analysis of circRNA1656*

According to the results of the qRT-PCR validation test, the differential expression of circRNA1656 was the highest and consistent with the high-throughput sequencing results, so circRNA1656 was selected for subsequent investigation of its potential as a tumor marker. CircRNA1656 (hsa-circ-0002755) is located at chr 7:74356410-74357477 and belongs to exon type circRNA. It is included in the authoritative database CircBase of circRNA, with the ID: hsa-circ-0002755. The gene signature of circRNA1656 is CLIP2, and there are few studies on its CLIP2. Some studies have shown that the loss of CLIP2 may be an important factor leading to the pathogenesis of Williams-Beuren syndrome (*22,23*). Studies on CLIP2 have focused on the mechanisms of papillary thyroid cancer caused by exposure to radioactive iodine after the Chernobyl nuclear leak (*24-26*) . Several studies have shown that CLIP2 is involved in basic carcinogenesis, including apoptosis, mitogen-activated protein kinase signaling, and genomic instability.

To further clarify the possible pathway of circRNA1656, we performed a KEEG metabolic pathway analysis of circRNA1656. Circ1656 has no annotation information in the KEGG database, so we draw the path map with the annotation of the host gene CLIP2 corresponding to circ1656 in the KEGG database. According to the analysis, circRNA1656 is mainly involved in the GPI-anchor biosynthesis metabolic pathway (Figure 4A). As can be seen from the figure, circRNA1656 inhibits the expression of PIG-U, thereby inhibiting GPI-anchor biosynthesis, affecting the binding

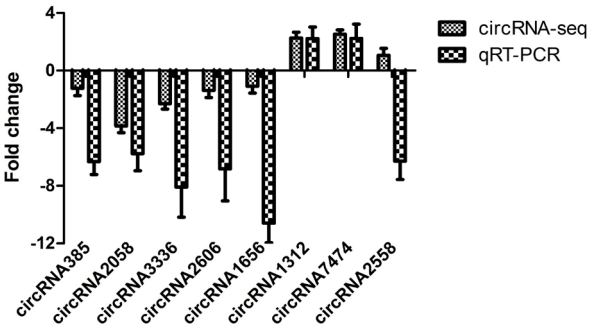

Figure 3. Validation of 8 differentially expressed circular RNAs according to circular sequencing.

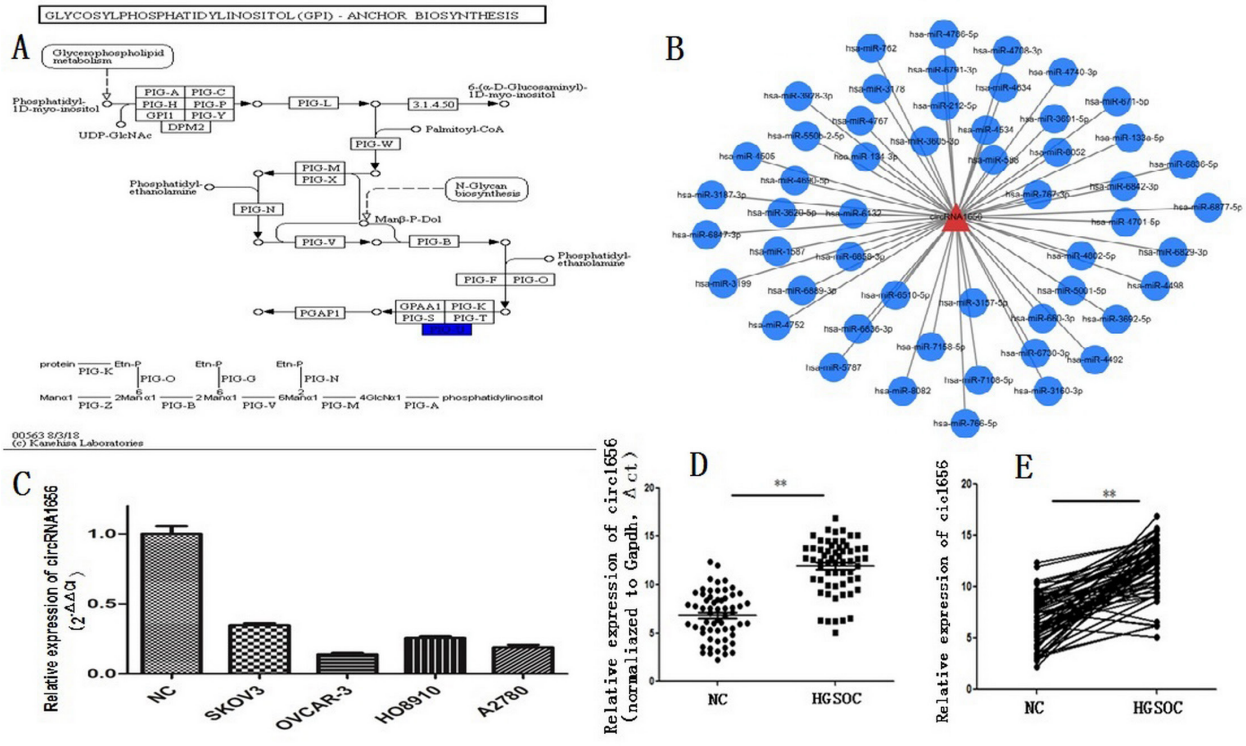

Figure 4. CircRNA1656 in HGSOC. (A), KEEG metabolic analysis of circRNA1656. CircRNA1656 is mainly involved in the GPI-anchor biosynthesis metabolic pathway, circRNA1656 inhibits the expression of PIG-U. **(B)**, CircRNA-miRNA network map of circ1656. The red triangle represents circRNA1656 and the blue dot represents the miRNA that may interact with circRNA1656. **(C)**, The qRT-PCR results of circRNA1656 expression in NC(human ovarian epithelial cells), ovarian cancer cells. **(D and E)**, The qRT-PCR results of circRNA1656 expression in NC (benign ovarian lesion group) and HGSOC tissue.

of proteins to cell membranes to play a biological role. GPI is the only way in which proteins bind to the cell membrane, and many receptors, antigens, and biologically active proteins have been shown to bind to cell membranes through GPI structures (*27*).

3.5. *CircRNA-miRNA network map of circRNA1656*

Current studies have shown that the competitive inhibition of molecular sponges as miRNAs is the most important mechanism of action of circRNA. To explore the possible mechanism of action of circRNA1656, based on bioinformatics and information mining, predict miRNAs that may interact with circRNA1656 and map circRNA-miRNA networks (Figure 4B).

3.6. *Detection of circRNA1656 expression in ovarian cancer cell lines by qRT-PCR*

qRT-PCR was used to detect the expression of circRNA1656 in human ovarian epithelial cells, ovarian cancer cells SKOV3, OVCAR-3, HO8910, and A2780 for the purpose of further verification of the circRNA-seq results. The expression of circRNA1656 ($2^{-\Delta\Delta Ct}$) in the ovarian cancer cells were compared with human ovarian epithelial cells (the average of $2^{-\Delta\Delta Ct}$ was 1.0). The results showed that circRNA1656 in the ovarian cancer cells were all significantly down-regulated. The p value was < 0.01 (Figure 4C). This result is consistent with the results of circRNA-seq.

3.7. *Detection of circRNA1656 expression in HGSOC tissue by qRT-PCR*

In order to further clarify the expression of circRNA1656 in HGSOC tissues, qRT-PCR was performed in 60 HGSOC tissues and 60 benign ovarian lesions. The results showed that the expression level and overall expression level of circRNA1656 in HGSOC tissues was lower than that in the ovarian benign lesion group, and the difference was statistically significant (Figure 4D and 4E).

3.8. *Relationship between circRNA1656 expression and clinical pathological biological characteristics of HGSOC*

In order to analyze the relationship between circRNA1656 expression and clinical pathological biological characteristics of HGSOC, 60 cases of HGSOC patients were divided into 2 groups (low expression group and high expression group) according to the the median of Δct expression of circRNA1656 (11.9). The results showed that the expression of circRNA1656 was correlated with the patient's FIGO stage (p = 0.012), and the difference was statistically significant. There was no correlation among menopause, ascites, LN metastasis and CA-125 level with the expression of circRNA (p > 0.05) (Table 3).

Table 3. Relationship between circRNA1656 expression and clinical pathological biological characteristics of HGSOC

clinical characteristics	cases (n = 60)	circRNA1656 expression		*P* value
		low	high	
menopause				0.475
yes	27	14	13	
no	33	18	15	
ascites				0.0641
yes	22	9	13	
no	38	23	15	
FIGO stage				0.012
I-II	15	4	11	
III-IV	45	28	17	
LN metastasis				0.392
Positive	36	19	17	
negative	24	13	11	
CA-125				0.285
Normal	12	6	6	
Increasing	48	26	22	

In conclusion, this study is the high-throughput sequencing study of HGSOC to find differential expression profiles of circRNA for the first time. A total of 354 circRNA expressions were up-regulated and 356 circRNA expression was down-regulated. qRT-PCR confirmed circRNA385, circRNA2058, circRNA3336, circRNA2606, and circRNA1656 were all down-regulated in HGSOC tissues, while circRNA1312 and circRNA7474 were up-regulated in HGSOC tissues (p < 0.05), consistent with circRNA-seq results. circRNA1656 was down-regulated in both HGSOC tissue and ovarian cancer cell lines, and was significantly associated with HGSOC FIGO stage, and is expected to become a novel tumor marker for HGSOC.

Acknowledgements

This work was supported by Research Foundation of Science and Technology Bureau, Shenyang city (18-014-4-61).And this work was also supported by the Outstanding Scientific Fund of Shengjing Hospital (Grant No. 201705).

References

1. Torre LA, Bray F, Siegel RL, Ferlay J, Lortet-Tieulent J, Jemal A. Global cancer statistics, 2012. CA Cancer J Clin. 2015; 65:87-108.
2. Siegel RL, Miller KD, Jemal A. Cancer statistics, 2016. CA Cancer J Clin. 2016; 66:7-30.
3. Kim JH, Park CW, Um D, Baek KH, Jo Y, An H, Kim Y, Kim TJ. Mass spectrometric screening of ovarian cancer with serum glycans. Dis Markers. 2014; 2014:634289.
4. Bachmayr-Heyda A, Auer K, Sukhbaatar N, Aust S, Deycmar S, Reiner AT, Polterauer S, Dekan S, Pils

D. Small RNAs and the competing endogenous RNA network in high grade serous ovarian cancer tumor spread. Oncotarget. 2016; 7:39640-39653.
5. Lasda E, Parker R. Circular RNAs: Diversity of form and function. RNA. 2014; 20:1829-1842.
6. Cortes-Lopez M, Miura P. Emerging functions of circular RNAs. Yale J Biol Med. 2016; 89:527-537.
7. Wang Y, Lu T, Wang Q, Liu J, Jiao W. Circular RNAs: Crucial regulators in the human body (Review). Oncol Rep. 2018; 40:3119-3135.
8. Chen Y, Li C, Tan C, Liu X. Circular RNAs: A new frontier in the study of human diseases. J Med Genet. 2016; 53:359-365.
9. Kristensen LS, Hansen TB, Veno MT, Kjems J. Circular RNAs in cancer: Opportunities and challenges in the field. Oncogene. 2018; 37:555-565.
10. Qin M, Liu G, Huo X, Tao X, Sun X, Ge Z, Yang J, Fan J, Liu L, Qin W. Hsa_circ_0001649: A circular RNA and potential novel biomarker for hepatocellular carcinoma. Cancer Biomark. 2016; 16:161-169.
11. Li P, Chen H, Chen S, Mo X, Li T, Xiao B, Yu R, Guo J. Circular RNA 0000096 affects cell growth and migration in gastric cancer. Br J Cancer. 2017; 116:626-633.
12. Huang G, Zhu H, Shi Y, Wu W, Cai H, Chen X. *cir-ITCH* plays an inhibitory role in colorectal cancer by regulating the Wnt/beta-catenin pathway. PloS One. 2015; 10:e0131225.
13. Zhong Z, Lv M, Chen J. Screening differential circular RNA expression profiles reveals the regulatory role of circTCF25-miR-103a-3p/miR-107-CDK6 pathway in bladder carcinoma. Sci Rep. 2016; 6:30919.
14. Yang X, Yuan W, Tao J, Li P, Yang C, Deng X, Zhang X, Tang J, Han J, Wang J, Li P, Lu Q, Gu M. Identification of circular RNA signature in bladder cancer. J Cancer. 2017; 8:3456-3463.
15. Ning L, Long B, Zhang W, Yu M, Wang S, Cao D, Yang J, Shen K, Huang Y, Lang J. Circular RNA profiling reveals circEXOC6B and circN4BP2L2 as novel prognostic biomarkers in epithelial ovarian cancer. Int J Oncol. 2018; 53:2637-2646.
16. Ahmed I, Karedath T, Andrews SS, Al-Azwani IK, Mohamoud YA, Querleu D, Rafii A, Malek JA. Altered expression pattern of circular RNAs in primary and metastatic sites of epithelial ovarian carcinoma. Oncotarget. 2016; 7:36366-36381.
17. Chrzanowska-Wodnicka M. Rap1 in endothelial biology. Curr Opin Hematol. 2017; 24:248-255.
18. Haddadi N, Lin Y, Travis G, Simpson AM, Nassif NT, McGowan EM. PTEN/PTENP1: 'Regulating the regulator of RTK-dependent PI3K/Akt signalling', new targets for cancer therapy. Mol Cancer. 2018; 17:37.
19. Salzman J, Chen RE, Olsen MN, Wang PL, Brown PO. Cell-type specific features of circular RNA expression. PLoS Genet. 2013; 9:e1003777.
20. Memczak S, Jens M, Elefsinioti A, *et al*. Circular RNAs are a large class of animal RNAs with regulatory potency. Nature. 2013; 495:333-338.
21. Bahn JH, Zhang Q, Li F, Chan TM, Lin X, Kim Y, Wong DT, Xiao X. The landscape of microRNA, Piwi-interacting RNA, and circular RNA in human saliva. Clinical chemistry. 2015; 61:221-230.
22. Vandeweyer G, Van der Aa N, Reyniers E, Kooy RF. The contribution of CLIP2 haploinsufficiency to the clinical manifestations of the Williams-Beuren syndrome. Am J Hum Genet. 2012; 90:1071-1078.
23. Delgado LM, Gutierrez M, Augello B, Fusco C, Micale L, Merla G, Pastene EA. A 1.3-mb 7q11.23 atypical deletion identified in a cohort of patients with williams-beuren syndrome. Mol Syndromol. 2013; 4:143-147.
24. Selmansberger M, Kaiser JC, Hess J, Guthlin D, Likhtarev I, Shpak V, Tronko M, Brenner A, Abend M, Blettner M, Unger K, Jacob P, Zitzelsberger H. Dose-dependent expression of CLIP2 in post-Chernobyl papillary thyroid carcinomas. Carcinogenesis. 2015; 36:748-756.
25. Hess J, Thomas G, Braselmann H, Bauer V, Bogdanova T, Wienberg J, Zitzelsberger H, Unger K. Gain of chromosome band 7q11 in papillary thyroid carcinomas of young patients is associated with exposure to low-dose irradiation. Proc Natl Acad Sci U S A. 2011; 108:9595-9600.
26. Kaiser JC, Meckbach R, Eidemuller M, Selmansberger M, Unger K, Shpak V, Blettner M, Zitzelsberger H, Jacob P. Integration of a radiation biomarker into modeling of thyroid carcinogenesis and post-Chernobyl risk assessment. Carcinogenesis. 2016; 37:1152-1160.
27. Muniz M, Riezman H. Trafficking of glycosylphosphatidylinositol anchored proteins from the endoplasmic reticulum to the cell surface. J Lipid Res. 2016; 57:352-360.

(Received January 27, 2019; Revised March 29, 2019; Accepted April 5, 2019)

Brief Report

DOI: 10.5582/bst.2019.01037

Living donor liver transplantation for a patient with a history of total gastrectomy

Keita Shimata, Tomoaki Irie, Masashi Kadohisa, Seiichi Kawabata, Sho Ibuki, Yasuko Narita, Hidekazu Yamamoto, Yasuhiko Sugawara*, Taizo Hibi

Department of Transplantation and Pediatric Surgery, Kumamoto University Graduate School of Medical Sciences, Kumamoto, Japan.

Summary **Adhesions due to previous upper abdominal surgery may complicate later liver transplantation. Here we report successful living donor liver transplantation (LDLT) in a patient with a history of total gastrectomy. A 32-year-old Japanese woman developed end-stage liver failure due to alcoholic cirrhosis. She had undergone total gastrectomy, pancreato-splenectomy, and partial colectomy due to rupture of a pancreatic cyst. LDLT was performed using a right lobe graft from her sister. To minimize blood loss and injury to the jejunum, adhesions between the left lobe and nearby organs were dissected without blood flow in or out of the liver. The right liver graft was implanted uneventfully. She was extubated on postoperative day (POD) 1, but then developed septic shock due to aspiration pneumonia on POD 2. She was reintubated and antibiotics and antifungal agents were administered. Administration of tacrolimus was changed to an intravenous route on POD 3. Her condition improved and she was re-extubated on POD 9. On POD 14, tacrolimus was administered orally. She was discharged from our hospital on POD 30 without any other events and is doing well 6 months after LDLT. We believe that careful planning, such as mobilizing the left lobe with the blood flow blocked just before liver explantation, elevating the head of the bed during tube-feeding, and calculating the area under the curve after drug administration will enable liver transplantation for patients with a history of total gastrectomy.**

Keywords: Total gastrectomy, adhesion, LDLT, aspiration pneumonia, tacrolimus

1. Introduction

The indications for liver transplantation (LT) in high-risk patients have been cautiously expanded due to improvements in LT techniques, including surgical techniques, perioperative management, immunosuppressive agents, and effective management of secondary complications. As a result, LT may be indicated in patients with significant comorbidities (*1*). In patients with a history of abdominal surgery, the operative procedures and postoperative management for LT are often difficult due to intra-abdominal adhesions and distortion of bowel continuity, which may complicate liver explantation and biliary reconstruction (*2-5*). In addition, poor drug absorption in patients that have undergone gastric resection or a Roux-en-Y procedure may make immunosuppressive management difficult (*6,7*). Although there are previous reports of LT after distal gastrectomy or sleeve gastrectomy as bariatric surgery (*5,8*), there are no published reports describing LT in a patient with a history of total gastrectomy. Here we report successful living donor liver transplantation (LDLT) in a patient with a history of total gastrectomy, pancreato-splenectomy, and partial colectomy to treat a large pancreatic cyst rupture.

Released online in J-STAGE as advance publication April 15, 2019.

**Address correspondence to:*
Dr. Yasuhiko Sugawara, Department of Transplantation and Pediatric Surgery, Kumamoto University Graduate School of Medical Sciences, Kumamoto, Japan.
E-mail: yasusuga-tky@umin.ac.jp

2. Patients and Methods

A 32-year-old Japanese woman developed end-stage

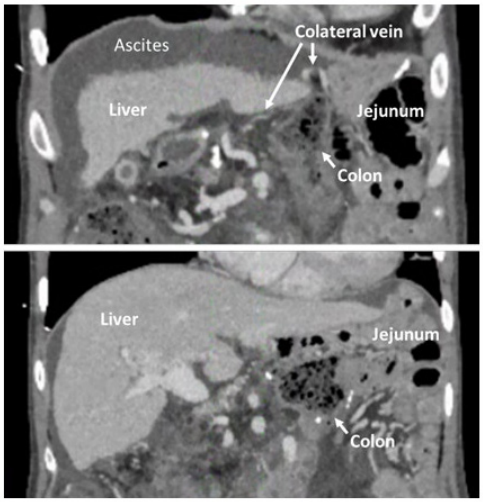

Figure 1. Preoperative angiographic computed tomography. These are coronal sections in the portal phase of preoperative angiographic computed tomography. These images showed severe adhesions between the left lobe and the Roux-Y jejunum or transverse colon, and collateral blood vessels around the left lateral segment.

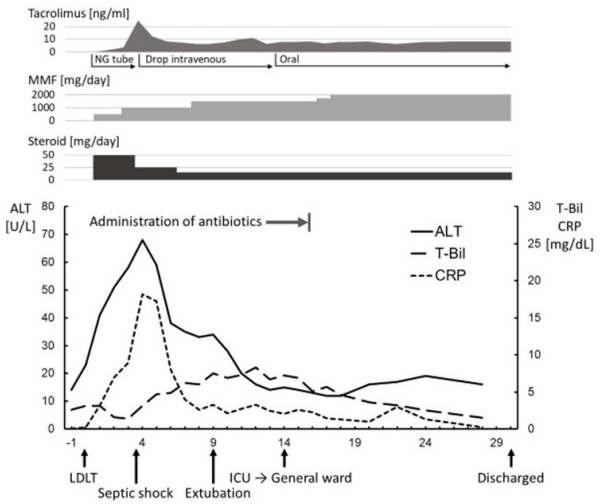

Figure 2. Postoperative clinical course. NG, nasogastric; MMF, mycophenolate mofetil; LDLT, living donor liver transplantation; ICU, intensive care unit

liver failure due to alcoholic cirrhosis. She had a history of total gastrectomy, pancreato-splenectomy, and partial colectomy due to rupture of a pancreatic cyst. LDLT was indicated and a right lobe graft was obtained from her sister. Preoperative angiographic computed tomography showed severe adhesions between the left lobe and the Roux-en-Y jejunum, and collateral blood vessels at the portal vein and around the left lateral segment (Figure 1). Due to ABO blood-type incompatibility between the donor and recipient, rituximab (400 mg/body, body weight: 50 kg) was administered daily for 14 days before LDLT for B cell desensitization.

3. Results and Discussion

3.1. *Surgical procedure, and clinical course of the patient*

A reverse T-shaped incision was made with a longer midline incision to avoid the adhesions. At the upper left abdominal cavity, severe adhesions were observed between the liver and transverse colon. The hepatoduodenal ligament was dissected first, and then the hepatic arteries were divided and the portal vein dissected. Next, the right lobe of the liver was mobilized with the portal vein clamped. The short hepatic veins were separated from the right side by transecting the right hepatic vein because it was impossible to approach the site from left side due to adhesions between the jejunum and the left lobe of the liver. The middle and left hepatic vein were transected after clamping for subsequent anastomosis, followed by transection of the portal vein. Without blood flow in or out of the liver, adhesions between the left lobe and the Roux-Y jejunum were dissected. In some areas with the tough adhesions, the liver parenchyma was resected using a vessel sealing system (Ligasure™ Small Jaw, Covidien, Japan) to prevent injuring the liver parenchyma covering the jejunum during surgery. Dissection of all adhesions around the liver was completed and the whole liver was explanted. A right liver graft (weight: 665 g, graft to recipient body weight ratio: 1.33%) with reconstruction of V5+V8 from the patient's sister was implanted in our regular fashion. No other events occurred throughout the LDLT procedure. The total blood loss was 15,780 mL and the operative time was 782 min, including 204 min of functional anhepatic time after clumping the portal vein until reperfusion of the graft. After the operation, the patient was transferred to the intensive care unit on mechanical ventilation.

The postoperative course of the patient is shown in Figure 2. Immunosuppression was initiated with the administration of tacrolimus, steroids, and mycophenolate mofetil (MMF) using a nasogastric tube on postoperative day (POD) 1. This is our usual protocol for ABO blood type-incompatible LT. After extubating on POD 1, her respiratory condition worsened and she developed septic shock due to aspiration pneumonia. She was re-intubated on POD 2 and administered antibiotics (meropenem + vancomycin) and antifungal (micafungin) agents, as well as vasopressors and continuous hemodiafiltration with endotoxin absorption. To minimize the risk of aspiration and maintain the blood concentration of tacrolimus, administration of tacrolimus was changed to an intravenous route on POD 3. The target trough value was set to 8~10 ng/mL. Her condition improved gradually, and she was re-extubated on POD 9. On POD 14, she was moved from the ICU to the general

Table 1. Recommendations for liver transplantation in patients with a history of total gastrectomy

1) Mobilize the left lobe with the blood flow blocked just before liver explanation.
2) Place patients with a history of total gastrectomy in a head-up position while administering medicines or enteral nutrients.
3) Administer tacrolimus intravenously immediately after liver transplantation.

ward and tacrolimus was administered orally. She was discharged from the hospital on POD 30 and is doing well 6 months after LDLT.

She was administered 4 mg of tacrolimus every 12 h and the blood concentration of tacrolimus was checked to determine the trough level at, 2 h, 3 h, and 4 h after administration (4.5 ng/mL, 25.1 ng/mL, 13.6 ng/mL, and 9.8 ng/mL, respectively). The area under the curve (AUC) for the blood concentration of tacrolimus revealed a trough level of 200 ng hour/mL; the trough level in patients with a total stomach is 5~7 ng/mL. The trough level of MMF ranged from less than 0.4 to 1.83 ng/mL when the patient was administered 1,000 mg of MMF every 12 h.

3.2. *Surgical technique in patients with severe adhesions*

LT for patients with a history of partial gastrectomy, especially sleeve gastrectomy, was recently reported (*2-5,8*), but there are no reports of LT for patients with a history of total gastrectomy. Therefore, to our knowledge this is the first case of LDLT for a patient with a history of total gastrectomy. The successful outcome of the present case demonstrates the feasibility of LDLT as a treatment option for such patients.

With respect to the surgical techniques, mobilizing the left lobe with the blood flow blocked just before liver explantation effectively minimized blood loss during surgery. During LT, hyperfibrinolysis occurs at the anhepatic phase and immediately after reperfusion (*9*), when bleeding tends to increase. As such, minimizing bleeding before liver explantation is crucial. When performing LT in a patient with cirrhosis and a history of upper abdominal surgery, collateral vessel and adhesions around the liver may cause a large amount of intraoperative bleeding. A previous report described an intraoperative demise during LT after distal pancreatectomy (*10*). In the present case, dissection of adhesions around the left lateral lobe was performed just before explantation without blood flow in or out of the liver. Retrograde liver explantation, in which the transection of hepatic veins is performed before transection of all structures in the hepatoduodenal ligament, is effective in cases with shortening of the hepatoduodenal structure due to adhesions and sufficient collateral venous formation (*8*).

Intraoperative injuries to the intestine and colon when dissecting adhesions around the liver may cause severe complications in immunosuppressed patients after surgery. For this reason, when tough adhesions were dissected, the liver parenchyma was resected using a vessel sealing system and the jejunum was not injured due to the remnant liver parenchyma covering the jejunum.

Even if severe adhesions between the left lobe and the organ around the left lobe are predicted, elaborating on a surgical plan in advance can make LT possible for a patient with a history of upper abdominal surgery.

3.3. *Postoperative management of patients with total gastrectomy*

In the present case, aspiration pneumonia led to septic shock, likely due to absence of the gastric cardia and a strong immunosuppressive state were considered to be the reasons. Kaneda *et al*. reported that previous gastrectomy is a risk factor for postoperative pneumonia and recommended preoperative administration of ranitidine and antibiotics with a broader spectrum than that of cefazolin to prevent postoperative pneumonia (*11*). Elevating the head of the bed head during tube-feeding may also be effective for preventing aspiration (*12*). In light of our experience, patients with a history of total gastrectomy should be in a head-up position for a longer time and the injection rate should be decreased to avoid aspiration during administration of medicines or enteral nutrients.

Regarding immunosuppressive agents, drug absorption in patients without a stomach is unclear (*6*). The majority of oral tacrolimus absorption occurs in the proximal duodenum; however, it has been shown that the drug is absorbed from the intestine to the colon (*7*). In the present case, to keep the drug concentration high enough to prevent acute cellular rejection and to prevent aspiration, tacrolimus was administrated intravenously beginning on POD 3. After changing to oral administration of the drug, a higher dose of tacrolimus than usual was required in the present case to maintain an appropriate AUC of tacrolimus. MMF is primarily absorbed in the stomach (*7*), so the trough level of MMF was lower than expected in this case on the basis of other cases. Intravenous administration of tacrolimus and calculating the AUC by measuring the drug concentration at more than three points after administration is important for confirming the pharmacokinetics of immunosuppressive agents in patients with a history of total gastrectomy.

In conclusion, we believe that the three recommendations described in Table 1 enable LT in a patient with a history of total gastrectomy.

References

1. Stauffer JA, Steers JL, Bonatti H, Dougherty MK, Aranda-Michel J, Dickson RC, Harnois DM, Nguyen JH. Liver transplantation and pancreatic resection: a single-center experience and a review of the literature. Liver Transpl. 2009; 15:1728-1737.
2. Taneja S, Gupta S, Wadhawan M, Goyal N. Single-lobe living donor liver transplant in a morbidly obese cirrhotic patient preceded by laparoscopic sleeve gastrectomy. Case Rep Transplant. 2013; 2013:279651.
3. Lin MY, Tavakol MM, Sarin A, Amirkiai SM, Rogers SJ, Carter JT, Posselt AM. Laparoscopic sleeve gastrectomy is safe and efficacious for pretransplant candidates. Surg Obes Relat Dis. 2013; 9:653-658.
4. Heimbach JK, Watt KD, Poterucha JJ, Ziller NF, Cecco SD, Charlton MR, Hay JE, Wiesner RH, Sanchez W, Rosen CB, Swain JM. Combined liver transplantation and gastric sleeve resection for patients with medically complicated obesity and end-stage liver disease. Am J Transplant. 2013; 13:363-368.
5. Safwan M, Collins KM, Abouljoud MS, Salgia R. Outcome of liver transplantation in patients with prior bariatric surgery. Liver Transpl. 2017; 23:1415-1421.
6. Chen L, Liberatore L, Chin T, Walker S, Fanous H, Nash MM, Rapi L, Huckle J, Zaltzman JS, Prasad GVR. The Impact of Total Gastrectomy on Pharmacokinetics in Kidney Transplant Immunosuppressive Drug Regimes: A Case Study. Transplantation. 2017; 101:2213-2217.
7. Rogers CC, Alloway RR, Alexander JW, Cardi M, Trofe J, Vinks AA. Pharmacokinetics of mycophenolic acid, tacrolimus and sirolimus after gastric bypass surgery in end-stage renal disease and transplant patients: a pilot study. Clin Transplant. 2008; 22:281-291.
8. Eguchi S, Soyama A, Takatsuki M, Hidaka M, Adachi T, Kitasato A, Baimakhanov Z, Kuroki T. How to explant a diseased liver for living donor liver transplantation after previous gastrectomy with severe adhesion (with video). J Hepatobiliary Pancreat Sci. 2014; 21:E62-64.
9. Kim EH, Ko JS, Gwak MS, Lee SK, Kim GS. Incidence and clinical significance of hyperfibrinolysis during living donor liver transplantation. Blood Coagul Fibrinolysis. 2018; 29:322-326.
10. Van Vilsteren FG, Baskin-Bey ES, Nagorney DM, Sanderson SO, Kremers WK, Rosen CB, Gores GJ, Hobday TJ. Liver transplantation for gastroenteropancreatic neuroendocrine cancers: Defining selection criteria to improve survival. Liver Transpl. 2006; 12:448-456.
11. Kaneda H, Nakano T, Taniguchi Y, Saito T, Konobu T, Saito Y. Impact of previous gastrectomy on postoperative pneumonia after pulmonary resection in lung cancer patients. Interact Cardiovasc Thorac Surg. 2012; 14:750-753.
12. Scolapio JS. Decreasing aspiration risk with enteral feeding. Gastrointest Endosc Clin N Am. 2007; 17:711-716.

(Received February 19, 2019; Revised April 7, 2019; Accepted April 9, 2019)

BST
BioScience Trends

Guide for Authors

1. Scope of Articles

BioScience Trends is an international peer-reviewed journal. BioScience Trends devotes to publishing the latest and most exciting advances in scientific research. Articles cover fields of life science such as biochemistry, molecular biology, clinical research, public health, medical care system, and social science in order to encourage cooperation and exchange among scientists and clinical researchers.

2. Submission Types

Original Articles should be well-documented, novel, and significant to the field as a whole. An Original Article should be arranged into the following sections: Title page, Abstract, Introduction, Materials and Methods, Results, Discussion, Acknowledgments, and References. Original articles should not exceed 5,000 words in length (excluding references) and should be limited to a maximum of 50 references. Articles may contain a maximum of 10 figures and/or tables.

Brief Reports definitively documenting either experimental results or informative clinical observations will be considered for publication in this category. Brief Reports are not intended for publication of incomplete or preliminary findings. Brief Reports should not exceed 3,000 words in length (excluding references) and should be limited to a maximum of 4 figures and/or tables and 30 references. A Brief Report contains the same sections as an Original Article, but the Results and Discussion sections should be combined.

Reviews should present a full and up-to-date account of recent developments within an area of research. Normally, reviews should not exceed 8,000 words in length (excluding references) and should be limited to a maximum of 100 references. Mini reviews are also accepted.

Policy Forum articles discuss research and policy issues in areas related to life science such as public health, the medical care system, and social science and may address governmental issues at district, national, and international levels of discourse. Policy Forum articles should not exceed 2,000 words in length (excluding references).

Case Reports should be detailed reports of the symptoms, signs, diagnosis, treatment, and follow-up of an individual patient. Case reports may contain a demographic profile of the patient but usually describe an unusual or novel occurrence. Unreported or unusual side effects or adverse interactions involving medications will also be considered. Case Reports should not exceed 3,000 words in length (excluding references).

News articles should report the latest events in health sciences and medical research from around the world. News should not exceed 500 words in length.

Letters should present considered opinions in response to articles published in BioScience Trends in the last 6 months or issues of general interest. Letters should not exceed 800 words in length and may contain a maximum of 10 references.

3. Editorial Policies

Ethics: BioScience Trends requires that authors of reports of investigations in humans or animals indicate that those studies were formally approved by a relevant ethics committee or review board.

Conflict of Interest: All authors are required to disclose any actual or potential conflict of interest including financial interests or relationships with other people or organizations that might raise questions of bias in the work reported. If no conflict of interest exists for each author, please state "There is no conflict of interest to disclose".

Submission Declaration: When a manuscript is considered for submission to BioScience Trends, the authors should confirm that 1) no part of this manuscript is currently under consideration for publication elsewhere; 2) this manuscript does not contain the same information in whole or in part as manuscripts that have been published, accepted, or are under review elsewhere, except in the form of an abstract, a letter to the editor, or part of a published lecture or academic thesis; 3) authorization for publication has been obtained from the authors' employer or institution; and 4) all contributing authors have agreed to submit this manuscript.

Cover Letter: The manuscript must be accompanied by a cover letter signed by the corresponding author on behalf of all authors. The letter should indicate the basic findings of the work and their significance. The letter should also include a statement affirming that all authors concur with the submission and that the material submitted for publication has not been published previously or is not under consideration for publication elsewhere. The cover letter should be submitted in PDF format. For example of Cover Letter, please visit http://www.biosciencetrends.com/downcentre.php (Download Centre).

Copyright: A signed JOURNAL PUBLISHING AGREEMENT (JPA) form must be provided by post, fax, or as a scanned file before acceptance of the article. Only forms with a hand-written signature are accepted. This copyright will ensure the widest possible dissemination of information. A form facilitating transfer of copyright can be downloaded by clicking the appropriate link and can be returned to the e-mail address or fax number noted on the form (Please visit Download Centre). Please note that your manuscript will not proceed to the next step in publication until the JPA Form is received. In addition, if excerpts from other copyrighted works are included, the author(s) must obtain written permission from the copyright owners and credit the source(s) in the article.

Suggested Reviewers: A list of up to 3 reviewers who are qualified to assess the scientific merit of the study is welcomed. Reviewer information including names, affiliations, addresses, and e-mail should be provided at the same time the manuscript is submitted online. Please do not suggest reviewers with known conflicts of interest, including participants or anyone with a stake in the proposed research; anyone from the same institution; former students, advisors, or research collaborators (within the last three years); or close personal contacts. Please note that the Editor-in-Chief may accept one or more of the proposed reviewers or may request a review by other qualified persons.

Language Editing: Manuscripts prepared by authors whose native language is not English should have their work proofread by a native English speaker before submission. If not, this might delay the publication of your manuscript in BioScience Trends.

The Editing Support Organization can provide English proofreading, Japanese-English translation, and Chinese-English translation services to authors who want to publish in BioScience Trends and need assistance before submitting a manuscript. Authors can visit this organization directly at http://www.iacmhr.com/iac-eso/support.php?lang=en. IAC-ESO was established to facilitate manuscript preparation by researchers whose native language is not English and to help edit works intended for international academic journals.

4. Manuscript Preparation

Manuscripts should be written in clear, grammatically correct English and submitted as a Microsoft Word file in a single-column format. Manuscripts must be paginated and typed in 12-point Times New Roman font with 24-point line spacing. Please do not embed figures in the text. Abbreviations should be used as little as possible and should be explained at first mention unless the term is a well-known abbreviation (*e.g.* DNA). Single words should not be abbreviated.

Title Page: The title page must include 1) the title of the paper (Please note the title should be short, informative, and contain the major key words); 2) full name(s) and affiliation(s) of the author(s), 3) abbreviated names of the author(s), 4) full name, mailing address, telephone/fax numbers, and e-mail address of the corresponding author; and 5) conflicts of interest (if you have an actual or potential conflict of interest to disclose, it must be included as a footnote on the title page of the manuscript; if no conflict of

interest exists for each author, please state "There is no conflict of interest to disclose"). Please visit Download Centre and refer to the title page of the manuscript sample.

Abstract: The abstract should briefly state the purpose of the study, methods, main findings, and conclusions. For article types including Original Article, Brief Report, Review, Policy Forum, and Case Report, a one-paragraph abstract consisting of no more than 250 words must be included in the manuscript. For News and Letters, a brief summary of main content in 150 words or fewer should be included in the manuscript. Abbreviations must be kept to a minimum and non-standard abbreviations explained in brackets at first mention. References should be avoided in the abstract. Key words or phrases that do not occur in the title should be included in the Abstract page.

Introduction: The introduction should be a concise statement of the basis for the study and its scientific context.

Materials and Methods: The description should be brief but with sufficient detail to enable others to reproduce the experiments. Procedures that have been published previously should not be described in detail but appropriate references should simply be cited. Only new and significant modifications of previously published procedures require complete description. Names of products and manufacturers with their locations (city and state/country) should be given and sources of animals and cell lines should always be indicated. All clinical investigations must have been conducted in accordance with Declaration of Helsinki principles. All human and animal studies must have been approved by the appropriate institutional review board(s) and a specific declaration of approval must be made within this section.

Results: The description of the experimental results should be succinct but in sufficient detail to allow the experiments to be analyzed and interpreted by an independent reader. If necessary, subheadings may be used for an orderly presentation. All figures and tables must be referred to in the text.

Discussion: The data should be interpreted concisely without repeating material already presented in the Results section. Speculation is permissible, but it must be well-founded, and discussion of the wider implications of the findings is encouraged. Conclusions derived from the study should be included in this section.

Acknowledgments: All funding sources should be credited in the Acknowledgments section. In addition, people who contributed to the work but who do not meet the criteria for authors should be listed along with their contributions.

References: References should be numbered in the order in which they appear in the text. Citing of unpublished results, personal communications, conference abstracts, and theses in the reference list is not recommended but these sources may be mentioned in the text. In the reference list, cite the names of all authors when there are fifteen or fewer authors; if there are sixteen or more authors, list the first three followed by *et al.* Names of journals should be abbreviated in the style used in PubMed. Authors are responsible for the accuracy of the references. Examples are given below:

Example 1 (Sample journal reference):
Inagaki Y, Tang W, Zhang L, Du GH, Xu WF, Kokudo N. Novel aminopeptidase N (APN/CD13) inhibitor 24F can suppress invasion of hepatocellular carcinoma cells as well as angiogenesis. Biosci Trends. 2010; 4:56-60.

Example 2 (Sample journal reference with more than 15 authors):
Darby S, Hill D, Auvinen A, *et al.* Radon in homes and risk of lung cancer: Collaborative analysis of individual data from 13 European case-control studies. BMJ. 2005; 330:223.

Example 3 (Sample book reference):
Shalev AY. Post-traumatic stress disorder: diagnosis, history and life course. In: Post-traumatic Stress Disorder, Diagnosis, Management and Treatment (Nutt DJ, Davidson JR, Zohar J, eds.). Martin Dunitz, London, UK, 2000; pp. 1-15.

Example 4 (Sample web page reference):
Ministry of Health, Labour and Welfare of Japan. Dietary reference intakes for Japanese. *http://www.mhlw.go.jp/houdou/2004/11/h1122-2a.html* (accessed June 14, 2010).

Tables: All tables should be prepared in Microsoft Word or Excel and should be arranged at the end of the manuscript after the References section. Please note that tables should not in image format. All tables should have a concise title and should be numbered consecutively with Arabic numerals. If necessary, additional information should be given below the table.

Figure Legend: The figure legend should be typed on a separate page of the main manuscript and should include a short title and explanation. The legend should be concise but comprehensive and should be understood without referring to the text. Symbols used in figures must be explained.

Figure Preparation: All figures should be clear and cited in numerical order in the text. Figures must fit a one- or two-column format on the journal page: 8.3 cm (3.3 in.) wide for a single column, 17.3 cm (6.8 in.) wide for a double column; maximum height: 24.0 cm (9.5 in.). Please make sure that the symbols and numbers appeared in the figures should be clear. Please make sure that artwork files are in an acceptable format (TIFF or JPEG) at minimum resolution (600 dpi for illustrations, graphs, and annotated artwork, and 300 dpi for micrographs and photographs). Please provide all figures as separate files. Please note that low-resolution images are one of the leading causes of article resubmission and schedule delays. All color figures will be reproduced in full color in the online edition of the journal at no cost to authors.

Units and Symbols: Units and symbols conforming to the International System of Units (SI) should be used for physicochemical quantities. Solidus notation (*e.g.* mg/kg, mg/mL, mol/mm^2/min) should be used. Please refer to the SI Guide www.bipm.org/en/si/ for standard units.

Supplemental data: Supplemental data might be useful for supporting and enhancing your scientific research and BioScience Trends accepts the submission of these materials which will be only published online alongside the electronic version of your article. Supplemental files (figures, tables, and other text materials) should be prepared according to the above guidelines, numbered in Arabic numerals (*e.g.*, Figure S1, Figure S2, and Table S1, Table S2) and referred to in the text. All figures and tables should have titles and legends. All figure legends, tables and supplemental text materials should be placed at the end of the paper. Please note all of these supplemental data should be provided at the time of initial submission and note that the editors reserve the right to limit the size and length of Supplemental Data.

5. Submission Checklist

The Submission Checklist will be useful during the final checking of a manuscript prior to sending it to BioScience Trends for review. Please visit Download Centre and download the Submission Checklist file.

6. Online Submission

Manuscripts should be submitted to BioScience Trends online at http://www.biosciencetrends.com. The manuscript file should be smaller than 5 MB in size. If for any reason you are unable to submit a file online, please contact the Editorial Office by e-mail at office@biosciencetrends.com.

7. Accepted Manuscripts

Proofs: Galley proofs in PDF format will be sent to the corresponding author via e-mail. Corrections must be returned to the editor (proof-editing@biosciencetrends.com) within 3 working days.

Offprints: Authors will be provided with electronic offprints of their article. Paper offprints can be ordered at prices quoted on the order form that accompanies the proofs.

Page Charge: Page charges will be levied on all manuscripts accepted for publication in BioScience Trends ($140 per page for black white pages; $340 per page for color pages). Under exceptional circumstances, the author(s) may apply to the editorial office for a waiver of the publication charges at the time of submission.

(*Revised February 2013*)

Editorial and Head Office:
Pearl City Koishikawa 603
2-4-5 Kasuga, Bunkyo-ku
Tokyo 112-0003 Japan
Tel: +81-3-5840-8764
Fax: +81-3-5840-8765
E-mail: office@biosciencetrends.com

BST
BioScience Trends

JOURNAL PUBLISHING AGREEMENT (JPA)

Manuscript No.:

Title:

Corresponding Author:

The International Advancement Center for Medicine & Health Research Co., Ltd. (IACMHR Co., Ltd.) is pleased to accept the above article for publication in BioScience Trends. The International Research and Cooperation Association for Bio & Socio-Sciences Advancement (IRCA-BSSA) reserves all rights to the published article. Your written acceptance of this JOURNAL PUBLISHING AGREEMENT is required before the article can be published. Please read this form carefully and sign it if you agree to its terms. The signed JOURNAL PUBLISHING AGREEMENT should be sent to the BioScience Trends office (Pearl City Koishikawa 603, 2-4-5 Kasuga, Bunkyo-ku, Tokyo 112-0003, Japan; E-mail: **office@biosciencetrends.com**; Tel: **+81-3-5840-8764**; Fax: **+81-3-5840-8765**).

1. Authorship Criteria

As the corresponding author, I certify on behalf of all of the authors that:
1) The article is an original work and does not involve fraud, fabrication, or plagiarism.
2) The article has not been published previously and is not currently under consideration for publication elsewhere. If accepted by BioScience Trends, the article will not be submitted for publication to any other journal.
3) The article contains no libelous or other unlawful statements and does not contain any materials that infringes upon individual privacy or proprietary rights or any statutory copyright.
4) I have obtained written permission from copyright owners for any excerpts from copyrighted works that are included and have credited the sources in my article.
5) All authors have made significant contributions to the study including the conception and design of this work, the analysis of the data, and the writing of the manuscript.
6) All authors have reviewed this manuscript and take responsibility for its content and approve its publication.
7) I have informed all of the authors of the terms of this publishing agreement and I am signing on their behalf as their agent.

2. Copyright Transfer Agreement

I hereby assign and transfer to IACMHR Co., Ltd. all exclusive rights of copyright ownership to the above work in the journal BioScience Trends, including but not limited to the right 1) to publish, republish, derivate, distribute, transmit, sell, and otherwise use the work and other related material worldwide, in whole or in part, in all languages, in electronic, printed, or any other forms of media now known or hereafter developed and the right 2) to authorize or license third parties to do any of the above.

I understand that these exclusive rights will become the property of IACMHR Co., Ltd., from the date the article is accepted for publication in the journal BioScience Trends. I also understand that IACMHR Co., Ltd. as a copyright owner has sole authority to license and permit reproductions of the article.

I understand that except for copyright, other proprietary rights related to the Work (*e.g.* patent or other rights to any process or procedure) shall be retained by the authors. To reproduce any text, figures, tables, or illustrations from this Work in future works of their own, the authors must obtain written permission from IACMHR Co., Ltd.; such permission cannot be unreasonably withheld by IACMHR Co., Ltd.

3. Conflict of Interest Disclosure

I confirm that all funding sources supporting the work and all institutions or people who contributed to the work but who do not meet the criteria for authors are acknowledged. I also confirm that all commercial affiliations, stock ownership, equity interests, or patent-licensing arrangements that could be considered to pose a financial conflict of interest in connection with the article have been disclosed.

Corresponding Author's Name (Signature):

Date: